



Ghent University
Faculty of Science
Department of Molecular Genetics

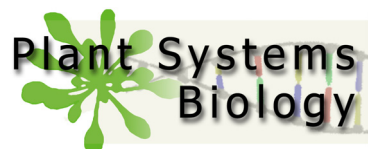
Walking with plant specific kinesins during cell division

Marleen Vanstraelen

Thesis submitted in partial fulfillment of the requirements for the degree
of Doctor (Ph.D.) in Science: Biotechnology
Academic year 2004-2005

Promotor: Prof. Dr. Dirk Inzé

Co-promotor: Dr. D. Geelen



Promotor

Prof. Dr. Dirk Inzé (secretary)
Dept. Plant Systems Biology
Flanders Interuniversity Institute for Biotechnology (VIB)
Ghent University

Co-promotor

Dr. Danny Geelen
Dept. Plant Systems Biology
Flanders Interuniversity Institute for Biotechnology (VIB)
Ghent University

Promotion commission

Prof. Dr. Erik Remaut (chairman)
Dept. Molecular Biomedical Research
Flanders Interuniversity Institute for Biotechnology (VIB)
Ghent University

Prof. Dr. Godelieve Gheysen
Dept. Molecular Biotechnology
Ghent University

Dr. Marylin Vantard
Département Réponse et Dynamique Cellulaires
PCV UMR 5168 CNRS/CEA/INRA/UJF
France

Prof. Dr. Peter Vandenabeele
Dept. Molecular Biomedical Research
Flanders Interuniversity Institute for Biotechnology (VIB)
Ghent University

Prof. Dr. Marcelle Holsters
Dept. Plant Systems Biology
Flanders Interuniversity Institute for Biotechnology (VIB)
Ghent University

Dr. Tom Beeckman
Dept. Plant Systems Biology
Flanders Interuniversity Institute for Biotechnology (VIB)
Ghent University

Dr. Lieven De Veylder
Dept. Plant Systems Biology
Flanders Interuniversity Institute for Biotechnology (VIB)
Ghent University

Table of contents

Scope

| | | |
|----------------------------------|--|-----|
| Chapter 1 | Introduction | 1 |
| Chapter 2 | Mitotic kinesins in Arabidopsis | 43 |
| Chapter 3 | A plant-specific subclass of C-terminal kinesins contains a conserved A-type cyclin-dependent kinase site implicated in folding and dimerization | 65 |
| Chapter 4 | The kinesin KCA1 defines a plasma membrane region for cell plate guidance | 93 |
| Chapter 5 | Arabidopsis trehalose-6-P synthase AtTPS1 forms a high molecular weight protein complex, together with cell cycle proteins CDKA;1 and the kinesin KCA1 | 123 |
| Chapter 6 | Functional analysis of KCA1 and KCA2 in plant growth and development | 147 |
| Chapter 7 | Conclusions and future perspectives | 165 |
| Summary/ Samenvatting | | 177 |

Frequently used abbreviations

| | |
|-------------|--|
| aa | amino acid |
| ABA | abscisic acid |
| ABD | actin binding domain |
| ACC | 1-amino-cyclopropane-1-carboxylic acid |
| ADZ | actin depleted zone |
| APM | amiprophos-methyl |
| 3AT | 3-amino-1,2,4-triazole |
| bp | base pairs |
| BFA | Brefeldin A |
| <i>Bot1</i> | <i>Botero1</i> |
| BY-2 | Bright Yellow-2 |
| CDK | cyclin dependent kinase |
| D-box | destruction box |
| Dex | dexamethasone |
| DIC | differential interference contrast |
| ER | endoplasmic reticulum |
| ET | ethylene |
| <i>Erh3</i> | ectopic root hair 3 |
| FL | full length |
| FM4-64 | <i>N</i> -(3-triethylammoniumpropyl)-4-(6-(4-(diethylamino)phenyl)hexatrienyl)pyridinium dibromide |
| FPLC | fast performance liquid chromatography |
| <i>Fra2</i> | <i>fragile fiber 2</i> |
| FRAP | fluorescence recovery after photobleaching |
| GA | gibberellin |
| GFP | green fluorescent protein |
| His | histidine |
| kb | kilo base |
| KCA | kinesin CDKA;1 associated |
| KDZ | KCA depleted zone |
| kDa | kilo dalton |
| LatB | latrunculin B |
| LB | left border |
| MALDI TOF | matrix assisted laser desorption ionization time-of-flight |
| MAP | microtubule associated protein |

| | |
|----------|---|
| MBD | microtubule binding domain |
| MI | mitotic index |
| MSA site | mitosis specific activation site |
| MT | microtubule |
| MTOC | microtubule organizing center |
| MTCC | microtubule converging center |
| MW | molecular weight |
| NLS | nuclear localization signal |
| ORF | open reading frame |
| PAGE | poly acrylamide gel electrophoresis |
| PPB | preprophase band |
| PM | plasma membrane |
| PTGS | post transcriptional gene silencing |
| RB | right border |
| RFP | red fluorescent protein |
| RT-PCR | reverse transcription polymerase chain reaction |
| SDS PAGE | sodium dodecyl sulfate polyacrylamide gel electrophoresis |
| SPB | spindle pole body |
| T-DNA | transfer DNA |
| T6P | trehalose-6-phosphate |
| TPP | trehalose-6-phosphate phosphatase |
| TPS | trehalose-6-phosphate synthase |
| WT | wild type |
| YFP | yellow fluorescent protein |

Scope

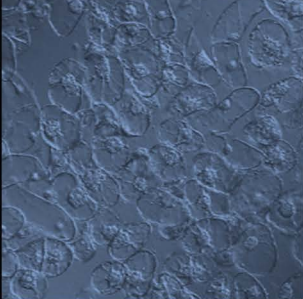
The complexity and dynamicity of the plant microtubule (MT) cytoskeleton and the presence of plant specific MT structures require the cooperation of many MT-associated proteins (MAP) of which some are specific to plants. The goal of this research was to characterize kinesins that function in plant specific MT related processes during cell division. Kinesin candidates for these functions are listed in chapter 2, where the publicly available Affymetrix microarray of synchronized Arabidopsis suspension cells was searched for mitotically regulated kinesins. These include members from subfamilies present in animal cells and members of plant specific kinesin groups.

Cell cycle regulation also includes post-translational modifications like protein phosphorylation by cyclin-dependent kinases (CDK). CDKA;1 associates with MTs both in dividing and interphase cells and in animal cells, it regulates MT organization by phosphorylation of MT associated proteins. Initially, KCA1 was identified as a CDKA;1 interacting protein in a yeast two hybrid screen and later, evidence for CDK dependent phosphorylation was provided in insect cells. KCA1 and its homolog are plant specific kinesins that belong to the C-terminal/Kinesin-14 subfamily of kinesins, members of which have functions related to cell division. For these reasons we anticipated that KCA1 and KCA2 were potential candidates to function in MT related processes unique for plant cell division.

In Chapter 3, we analyzed the interaction between the KCA proteins and CDKA;1 in more detail and show evidence for the implication of CDKA;1 phosphorylation in the folding configurations of KCA. These structural aspects of KCA may be important for protein function. A study of the intracellular localization of KCA1, presented in Chapter 4, illustrates how different protein domains contribute to the differential subcellular localization of KCA. Detailed analysis of the distribution of GFP tagged KCA1 revealed a region in the plasma membrane that is modified during cell division to define the division site in plant cells.

Kinesin motors often associate with other proteins that regulate their function, activity and cargo binding. In Chapter 5, KCA1 was identified as an interactor of trehalose-6-synthase AtTPS1. Here, we investigate the occurrence of a protein complex consisting of KCA1, AtTPS1, CDKA;1 and tubulin and propose a function for this complex at the start of cell division.

A genetic analysis of the KCA proteins in plant development is presented in Chapter 6. Plants disrupted in the KCA genes, were identified and subjected to a phenotypic analysis.



Chapter 1

Introduction

Chapter page: Tobacco BY-2 cells, viewed using confocal microscopy (transmission light).

Sessile but not senile; Fixed cells within fixed bodies

Imagine us as sessile organisms: not able to go searching for water when thirsty, no shelter if it starts raining, and no hideaway from hungry predators. Despite these threats, plants were very successful throughout evolution. The sessile lifestyle of plants has challenged these organisms to become masters in adaptation. Because they can't run, plants have learnt to deal with a whole range of environmental stresses, like drought, pathogens and predators. This is accomplished by a battery of defense response mechanisms and most important of all, their regenerative capability. Unlike animals, plants can grow new organs throughout their lifespan. The way organ morphogenesis in plants depends on the presence of a wall that determines the final shape of the plant cell.

Plant cells are encased by a semi-rigid cell wall that is a complex amalgam of cellulose microfibrils bonded non-covalently to a matrix of hemicelluloses, pectins, and structural proteins (Carpita and Gibeaut, 1993; Cosgrove, 1997). Cellulose is probably the single most abundant organic molecule in the biosphere. The microfibrils they produce have a per weight tensile strength equivalent to steel (Wainwright, 1976), thereby providing mechanical support for each cell and the whole plant body. However, it also renders plant cells immobile and this fixed nature of plant cells requires that morphological and developmental diversity in plants is determined by 2 processes; the orientation of cell division planes and the direction of cell expansion (Traas et al., 1995). Spatial regulation of division plane alignment allows plants to organize cells in files and layers that are typically observed in plant tissues (Lloyd, 1995; Smith et al., 1996). After cells have divided, cell expansion determines the final shape of every cell and at the end, of each plant organ. The MT cytoskeleton organizes into various arrays to govern these processes.

Microtubule basis of plant morphology

Cell expansion in developing tissues; the microtubule-microfibril enigma

After leaving the cell cycle, differentiating cells expand dramatically and this expansion is driven by turgor pressure. The cross-linked cellulose microfibrils in the wall of growing cells are arranged in parallel to one another and perpendicular to the direction of cell elongation. Because this microfibrillar network resists radial expansion much more than longitudinal expansion, the cells react to turgor pressure by elongating perpendicularly to the microfibril orientation. In elongating cells, cortical MT align transversely to the axis of cell elongation and parallel the alignment of cellulose microfibrils (Ledbetter, 1981). This observation, along with data showing that MT depolymerization leads to isotropic cell growth (Green, 1980; Akashi et al., 1988; Baskin et al., 1994) has led to the idea that cortical MTs relay spatial information to the cellulose microfibrils to

mediate cell expansion. The theory is supported by evidence that plant hormones, such as ethylene and gibberellins, exert their effects on the expansion of stem cells via the control of cortical MT orientation (Shibaoka, 1994). Although this hypothesis has been generally accepted, the mechanism by which cortical MTs influence cellulose microfibril deposition remains unclear. The cellulose-synthase-constraint hypothesis states that MTs, through their close interaction with the plasma membrane, form barriers that constrain the paths of cellulose synthase complexes as they deposit cellulose chains in the cell wall (Fig. 1.1) (Giddings and Staehelin, 1991).

However, new drug experiments on elongating cells in a variety of experimental systems showed that well organized microfibrils could be produced in the absence of cortical MTs (Baskin, 2001). As a result, the hypothesis was adjusted in that MTs deposit a directional scaffold in which established microfibrils can continue to grow in absence of MTs (Baskin, 2001). This theory was referred to as the 'template-incorporation theory' and was supported by later observations in the sensitive mutant *mor1-1*. This mutant shows a loss of growth anisotropy when grown at the restrictive temperature, accompanied with cortical MT disorganization (Whittington et al., 2001). However, cellulose microfibrils are deposited transverse to the elongation axis even after prolonged disruption of cortical MT arrays, supporting the template-incorporation model (Sugimoto et al., 2003). To further test this hypothesis, cellulose microfibrils were disrupted in the *mor1-1* mutant, then plants were shifted to *mor1-1*'s restrictive temperature and finally, cellulose synthesis was allowed to recover. Surprisingly, microfibrils not only recovered a parallel order, their net orientation was perpendicular to the elongation axis (Himmelspach et al., 2003).

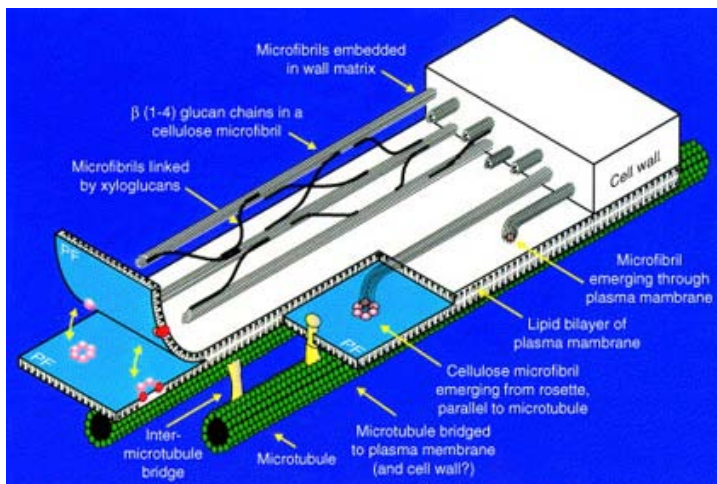


Figure 1.1 The cellulose-synthase constraint hypothesis. Relationships between cellulose-synthesizing complexes (rosette type), wall microfibrils, plasma membrane and MTs. Figure taken from Wasteneys (2004).

Recently, the microfibril-length-regulation hypothesis was proposed by Wasteneys (2004). Here, MTs ensure the synthesis and integrity of long microfibrils by forming parallel cortical arrays in the same direction as cellulose microfibril deposition. This model predicts that intact transverse cortical MTs allow the formation/maintenance of long microfibrils resulting in perfect growth anisotropy or cell elongation. Altering the MT polymer status, results in short microfibrils. This induces a weakness in the cellulose chains, allowing turgor driven separation of microfibrils in two directions, while maintaining microfibrils in a transverse orientation (Fig. 1.2).

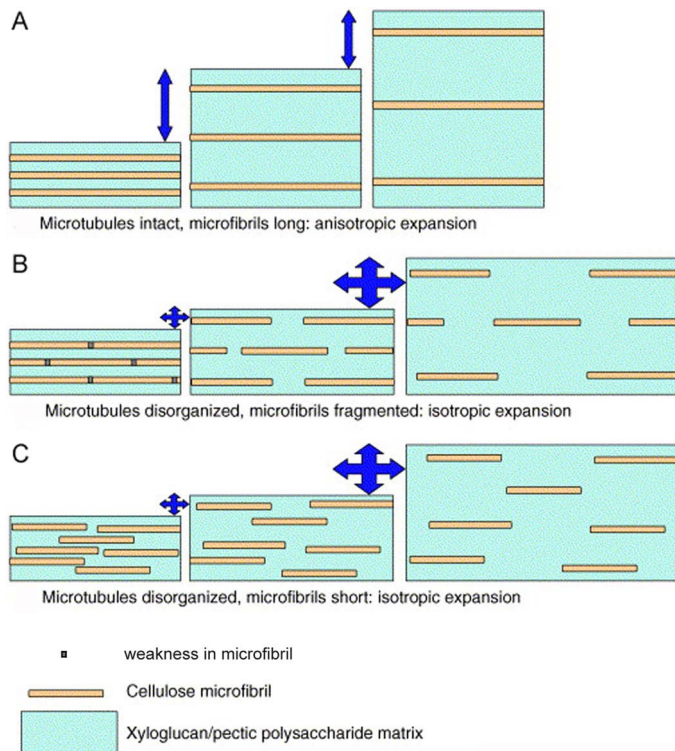


Figure 1.2 The microfibril-length-hypothesis. MT activity at the plasma membrane influences the length of cellulose microfibrils, whose separation, which is mediated by the activity of enzymes on inter-microfibril polysaccharide tethers, determines the direction of cell-surface expansion (arrows). A, Under normal conditions, in which MTs (not shown) are plentiful and oriented in the direction of microfibril synthesis, long microfibrils are produced and their separation is only at right angles to their orientation. B, Loss of cortical MTs or their mis-orientation generates periodic weaknesses in microfibrils, which are prone to breakage, allowing separation of microfibrils in the lateral as well as longitudinal direction. C, The loss of well-organized MTs affects the longevity or activity of cellulose synthase complexes, resulting in shorter microfibrils. This model explains how cells can undergo radial expansion while microfibril orientation remains transverse. Figure taken from Wasteneys (2004).

Several mutants stress the importance of MTs in cell expansion and tissue morphology. For example, AtKSS is a MT severing protein with an important role in cortical MT organization (McClinton et al., 2001; Wasteneys, 2002). Mutant alleles affected in the katanin AtKSS gene show defects in cell elongation which has been attributed to an aberrant cortical MT array (Bichet et al., 2001; Burk et al., 2001; Webb et al., 2002; Bouquin et al., 2003). In one of the mutant alleles, *fra2*, these defects were accompanied with a decrease of cellulose content in cell walls, thereby linking the transverse organization of cortical MTs in elongating cells to cellulose biosynthesis (Burk et al., 2001). The occurrence of organ twisting phenotypes has been attributed repeatedly to defects in MT organization. Recessive mutations in either of two Arabidopsis thaliana SPIRAL loci, SPR1/SKU6 or SPR2, reduce anisotropic growth of cells in roots and etiolated hypocotyls, and induce right-handed helical growth in epidermal cell files of these organs (Furutani et al., 2000; Sedbrook et al., 2004). Cortical MTs in these cells are arranged in left-handed helical arrays. Recently, the SPR1/SKU6 has been identified as a novel plant specific MT associated protein that associates with the plus-ends of MTs (Nakajima et al., 2004; Sedbrook et al., 2004). Similarly, the temperature sensitive alleles of MOR1 and the semi-dominant tubulin mutants *lefty1* and *lefty2*, generate left-handed twisting in most organs (Whittington et al., 2001; Thitamadee et al., 2002; Konishi and Sugiyama, 2003). In these mutants, MTs are respectively abnormally shortened or are right-handed obliquely oriented. Together these mutants show how MT organization is important for cell expansion, growth anisotropy and finally plant morphogenesis.

Cell expansion during single cell morphogenesis

Certain types of plant cells with highly specialized functions undergo dramatic cellular morphogenesis during differentiation. This group of cells includes pollen tubes, root hairs and trichomes, which are extremely elongated cells that are either un-branched in the case of pollen tubes and root hairs, or branched in the case of trichomes. Pharmacological studies suggest that turgor-driven, MT and cell wall controlled growth mediates the initial outgrowth of root hairs and trichomes while at later stages, MTs seem to determine growth directionality (Bibikova et al., 1999; Kost et al., 1999). This hypothesis is supported by mutants that have an altered morphology in these single cell structures. *Tip1* mutants display short, branched root hairs and reduced fertility, which is caused by a moderate inhibition of the elongation of morphologically normal pollen tubes. The *Tip1* defects are strongly reminiscent of the effects observed after treating root hairs and pollen tubes with drugs that affect MT organization. The *Tip1* gene product may therefore be required for MT functions specifically during tip growth (Schiefelbein et al., 1993). The *Zwichel* mutant exhibits a decreased trichome branching, a defect that can be corrected by a short treatment with the MT stabilizing drug taxol. This mutant is affected in a MT based motor protein, KCBP and shows that MTs in trichomes dictate the branching pattern (Oppenheimer et al., 1997; Mathur and Chua, 2000).

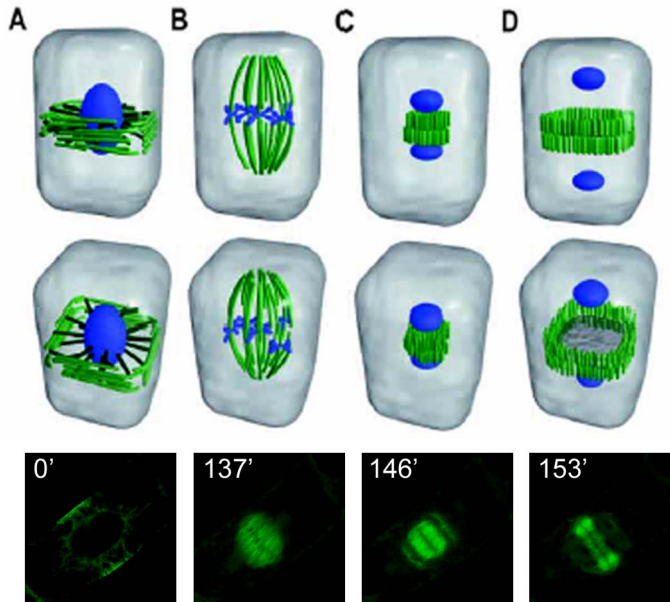


Figure 1.3 MT arrays during plant cell division. Schematic illustrations in 3D are pictured at two aspects in the upper panels (taken from Wasteneys, 2002). MTs are visualized in green and DNA in blue. 2D confocal sections of a GFP-tubulin expressing cell at different phases during cell division. Time points are indicated in minutes at the top left corner. A, A PPB connected to the nucleus by MTs marks the future division plane. B, Metaphase spindle with a dispersed polar region. C, During cytokinesis, the phragmoplast forms a dense cylinder of MTs between daughter nuclei. D, The phragmoplast expands centrifugally, guiding the cell plate towards attachment sites previously established by the PPB.

Division plane alignment

The preprophase band and the phragmoplast

The role of MTs in plant morphogenesis is not limited to cell expansion. Plants have developed unique MT arrays that contribute to the positioning of the division plane during cytokinesis (Goddard et al., 1994; Mineyuki, 1999; Smith, 1999; Sylvester, 2000; Mayer and Jurgens, 2004). Cell plate positioning involves two major steps, first the establishment of the division site early in mitosis and guidance of the cell plate during cytokinesis. In the G2 phase of the cell cycle, the first sign of the approaching mitosis is the preprophase band (PPB) (Fig. 1.3), which gradually replaces the cortical MT array in G2 phase. This ring of transverse MTs and actin filaments encircles the cell at the cortex surrounding the prophase nucleus. It first appears as a broad ring-like structure that narrows as G2 progresses, and simultaneously perinuclear MTs increase in number and organize into a bipolar spindle. As the nuclear envelope disintegrates, the PPB disappears leaving behind a

hallmark to guide the phragmoplast to the division site (Palevitz and Hepler, 1974; Wick and Duniec, 1983; Wick, 1991; Mineyuki, 1999). This is supported by data showing that when PPBs are experimentally perturbed, the cell plate is either mispositioned or misoriented (Mineyuki et al., 1991b).

Although the division site is established at the start of mitosis, it is during cytokinesis that its information becomes critical. During cytokinesis, Golgi derived vesicles containing cell wall components, are transported along the phragmoplast MTs to form a new cell plate (Verma, 2001). Like spindles, phragmoplasts are bipolar MT complexes with their plus-ends meeting at the midplane (Fig. 1.3). This structure is thought to be formed from the remnants of spindle MTs (Staehein and Hepler, 1996) that centripetally coalesce at the division plane (Zhang et al., 1993; Granger and Cyr, 2000). It first appears as a compact cylindrical bundle, but gradually forms a ring-like structure that increases in circumference in pace with the cell plate as it expands towards the parent wall.

The cell plate will fuse to the parent cell wall at a site previously demarcated by the PPB; thus some form of spatial information must be guiding the phragmoplast to this predetermined site. It has been hypothesized that the PPB guides the local deposition of molecules in the plasma membrane and/or cell wall that serve as landmarks for phragmoplast guidance (Young et al., 1994; Smith, 1999). Indeed, kinases and phosphatases (Mineyuki et al., 1991c; Young et al., 1994; Weingartner et al., 2001), cyclins (Mews et al., 1997), γ -tubulin (Liu et al., 1993), wall maturation factors (Mineyuki and Gunning, 1990), localized wall thickenings (Galatis et al., 1982) and actin filaments (Palevitz, 1987) have been shown to associate with or accumulate at the PPB site. The sighting of Golgi stacks at the division site during metaphase also supports this idea (Nebenfuhr et al., 2000).

The PPB offers spatial cues for division plane establishment in multicellular tissues

Throughout the landplants, the PPB is absent in cells of reproductive lineages; meiotic microsporogenesis and pollen mitosis (Hogan, 1987; Palevitz, 1993), megasporogenesis and megagametogenesis (Webb and Gunning, 1990, 1991, 1994) and endosperm development (Vanlammeren, 1988; Brown et al., 1994). The PPB is absent from cells entering a developmental pathway where they are no longer part of an organized tissue. For example, compare the development of the embryo and endosperm in flowering plants. Both originate from fertilization, yet the zygote displays a PPB in the first division (Webb and Gunning, 1991). In contrast, endosperm develops as a coenocyte (at least in cereals and *Arabidopsis thaliana*) before becoming cellular and does not exhibit a PPB until later when divisions occur in the aleurone layer (Brown et al., 1994). Thus the PPB appears in cells inserting spatially predetermined new walls within the pattern of neighboring cells during organogenesis.

Genes required for cell plate orientation

The importance of the PPB in division plane establishment and plant morphology is strengthened by the analysis of plant mutants impaired in their ability to orient cell walls. The Arabidopsis *fass* and *tonneau2* (*ton2*) mutants, as well as the *tangled1* mutants of maize are characterized by misoriented cell walls. Whereas *ton2/fass* mutants altogether lack PPBs, these rings of cortical MTs are often misoriented in *tangled* mutants (for review, see Nacry et al., 2000).

In *ton2/fass* mutants, both cell expansion as the pattern of cell division are affected (Torresruiz and Jurgens, 1994; Traas et al., 1995). This is accompanied by a disorganization of the interphase transverse MT array and lack of a preprophase band before mitosis. The mutants grow as short, thick misshapen plants with irregular radial swollen cells and in roots and hypocotyls, the ordered cell files and layers observed in wild-type plants are completely absent. However, mutants develop into tiny adult plants with all parts including floral organs present. These mutants are a perfect example of how MTs, through their importance in cell expansion and control of division plane alignment, determine the morphology of a plant, without interfering with differentiation patterns.

Tangled mutants do not perturb overall plant morphology, but illustrate the importance of the PPB in division site establishment and phragmoplast guidance. In *tan-1* mutant leaves, longitudinal divisions that result in leaf widening, are largely substituted by a variety of aberrantly oriented divisions, leading to a perturbed cell pattern and more narrow leaves. Accordingly, a 10-fold decrease in the proportion of longitudinal PPBs was observed when compared to WT plants and in addition phragmoplasts were not guided to sites formerly occupied by PPBs (Smith et al., 1996). The *TANGLED* gene was cloned and shown to bind MTs *in vitro*. Moreover, anti-TAN1 antibodies localize to the PPB, spindle and phragmoplast (Smith et al., 2001). In addition to orienting the PPB, *TANGLED* may be implicated in the establishment of the division site during preprophase and/or guide the leading edges of the phragmoplast to this site during cytokinesis.

The role of the nucleus and spindle in division plane alignment

A number of studies point to a role of premitotic nuclei in PPB positioning (Mineyuki et al., 1991b; Mineyuki et al., 1991a; Murata and Wada, 1991). Here, cells with premitotic nuclei and a PPB were centrifuged and the nucleus was displaced. Remarkably, a new PPB was formed at the new position of the nucleus and accordingly a cell plate was formed at the new division site. In addition, when binucleate cells were induced upon caffeine treatment, two PPBs were formed, one at each nucleus (Murata and Wada, 1993; Gimenez-Abian et al., 1998). These experiments point to a function of nuclear positioning in PPB formation and division site establishment. On the other hand, fine positioning of the premitotic nucleus relative to the PPB position has also been reported with MTs connecting the PPB and the nucleus (Granger and Cyr, 2001). The data suggest that cross-communication between the nucleus and PPB is important in division plane establishment.

After disintegration of the nuclear envelope, the spindle invades the nuclear region to catch and align the chromosomes. This bipolar structure, which is composed mainly of MTs and associated proteins, assembles first as an unorganized perinuclear MT array with MTs radiating to the broad PPB (Mineyuki et al., 1991a). As the PPB narrows, this array is organized into a bipolar spindle with MTs only emanating from the poles. Remarkably, inhibition of PPB narrowing using actin depolymerizing drugs also prevents formation of the bipolar spindle. These data indicate that the PPB not only establishes the division sites at the cell cortex, but also determines the division plane by organizing the bipolar spindle relative to the division sites.

The bipolar plant spindle, like other eukaryotic spindles is composed of an anti-parallel array of MTs, whereby slower-growing MT minus-ends are anchored at the spindle poles and the faster growing plus-ends are facing the spindle equator (Fig. 1.3) (Euteneuer and McIntosh, 1980). Within this structure, there are two different sub-populations of MTs; the kinetochore MTs, which attach to the kinetochore and thereby connect chromosomes to the spindle poles, and interpolar MTs, which stabilize the spindle by originating at opposite poles and interdigitate at the spindle midzone. This MT configuration is found in most eukaryotic spindles, however, plant spindles are unique because they lack highly focused MT organizing centers (MTOC) at the spindle poles. Most animal MTOCs are defined by the presence of centriole-containing centrosomes, which nucleate MTs at the spindle poles (Doxsey, 2001).

Although plants lack the nucleating activating of centrosomes, bipolar spindles still form in plant mitosis. In plants, during spindle pole formation MTs are nucleated off the nuclear envelope (Lambert, 1993; Smirnova and Bajer, 1994; Stoppin et al., 1994; Azimzadeh et al., 2001) and form MT converging centers (MTCC) (Smirnova and Bajer, 1994, 1998). These MTCCs cluster by an unknown mechanism and develop into the spindle poles during prophase. Similar MT patterning is also observed in acentrosomal *Allium* cells (Wick and Duniec, 1983), and this pathway of bipolar spindle assembly might be universal among somatic cells of higher plants (Baskin and Cande, 1990).

The proper positioning of the spindle is critical to karyokinesis, however, the spindle also plays a supportive role in cell plate guidance. In cells treated with the actin inhibiting drug Latrunculin-B, some spindles fail to position near the PPB site and as a result phragmoplasts in these cells do not fuse at the site predetermined by the PPB (Granger and Cyr, 2001). Thus, the maintenance of spatial positioning of the spindle influences the trajectory of the phragmoplast during cytokinesis.

Properties of the microtubular cytoskeleton

MT nucleation

Although the major cytoskeletal components are common to plant and animal cells, plants do not possess the centrosome-like organelles found in animal cells (MTOC) and yeast (spindle pole body; SPB). In animal and yeast cells, MT nucleation requires the activity of protein complexes containing

γ -tubulin, Spc98p and Spc97p (Geissler et al., 1996; Knop and Schiebel, 1997; Murphy et al., 1998; Tassin et al., 1998; Moritz and Agard, 2001). These proteins form γ -tubulin ring complexes, γ -TuRC (animal) and γ -TuSc (yeast), which are recruited at the structured MT organizing centers. Homologues of these proteins are also present in Arabidopsis. γ -tubulin has been localized all over the plant nuclear surface and along all MT arrays suggesting the presence of multiple, dispersed nucleating sites in plants (Fig. 1.4) (Liu et al., 1993; Joshi and Palevitz, 1996; Panteris et al., 2000). Till now, MT nucleating activity has only been characterized at the nuclear surface (Mizuno, 1993; Stoppin et al., 1994), which was then considered as the major MTOC in plants (Fig. 1.5). Using antibodies against γ -tubulin, the nucleation activity of purified nuclei was inhibited by 70-90%, proving that plant γ -tubulin is essential for MT nucleation (Seltzer et al., 2003). The presence of plant γ -tubulin has been found along whole MTs length of all plant MT arrays, in different cell types and at all stages of the cell cycle led to the idea that plant γ -tubulin is not only involved in MT nucleation, but may have a function in MT dynamics (Schmit, 2002). This idea was supported by the isolation of γ -tubulin from the cytosol as a single molecule and in association with various soluble complexes (Stoppin-Mellet et al., 2000).

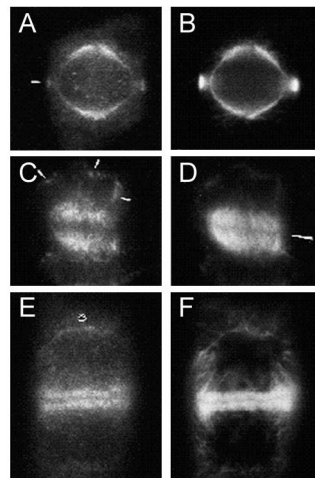


Figure 1.4 Distribution of γ -tubulin along MTs in dividing plant cells. Immunolocalisation of γ -tubulin (A, C and E) and β -tubulin (B, D and F) in soybean cells. Anti γ -tubulin staining is associated with MTs of the PPB and perinuclear spindle (A and B), the metaphase spindle (C and D) and the phragmoplast (E and F). Images are taken from Liu et al. (1993).

Homologues of the two γ -tubulin interacting proteins Spc98p and Spc97p have also been found in the Arabidopsis genome. The plant Spc98p orthologue codistributed with γ -tubulin around the nuclear surface of higher plant cells (Erhardt et al., 2002). Accordingly, Spc98p has been shown to be essential for MT nucleation activity at purified nuclei (Fig. 1.5) (Erhardt et al., 2002; Seltzer et al., 2003). Together these data reinforce the view that γ -TuSC-like components are functional as MT-nucleating factors at the perinuclear surface of higher plants, where they initiate minus-end MT assembly.

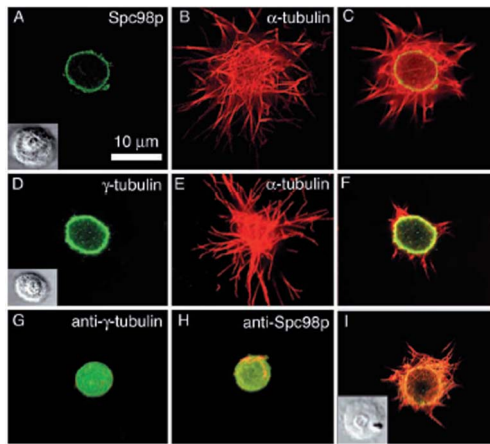


Figure 1.5 Plant Spc98p and γ -tubulin localization at the surface of isolated tobacco BY-2 nuclei after *in vitro* MT nucleation. A and D, Confocal images of nuclei labeled either with anti-Spc98pB (A) or anti- γ -tubulin (D). B and E, Confocal section at the surface of the respective nuclei labeled with anti- α -tubulin. C and F, Merged image showing MT nucleation from perinuclear sites. G and H, Inhibition of MT nucleation by preincubation with either anti- γ -tubulin (G) or anti-Spc98pB (H) antibodies. I, Following a competition assay for 1 hour with preincubation using anti-Spc98pB antibodies and Spc98pB peptide, nucleation was not inhibited. Insets, Nomarski images of the isolated nuclei. Bar = 10 μ m. Figure taken from Erhardt et al. (2002).

MT dynamics

MTs in plant cells were discovered in the early 1960s by Ledbetter and Porter (1963). They form anisotropic polymers of α - and β -tubulin heterodimers (each with a molecular mass of 50,000 Daltons). In cells, these are normally organized by a head-to-tail fashion to form a linear protofilament (Fig. 1.6). Typically, 13 protofilaments align laterally to form a hollow, cylindrical polymer with a diameter of ~ 25 nm (Evans et al., 1985). Once assembled, the MT polymer forms an asymmetric structure; within each protofilament α - and β -tubulin heterodimers orient such that the β -tubulin is exposed on one end of the MT and the α -tubulin is exposed on the other end

(Valiron et al., 2001). This results in a kinetic polarity within the MT polymer, creating a faster-growing end (termed the plus-end) and a slower-growing end (termed the minus-end).

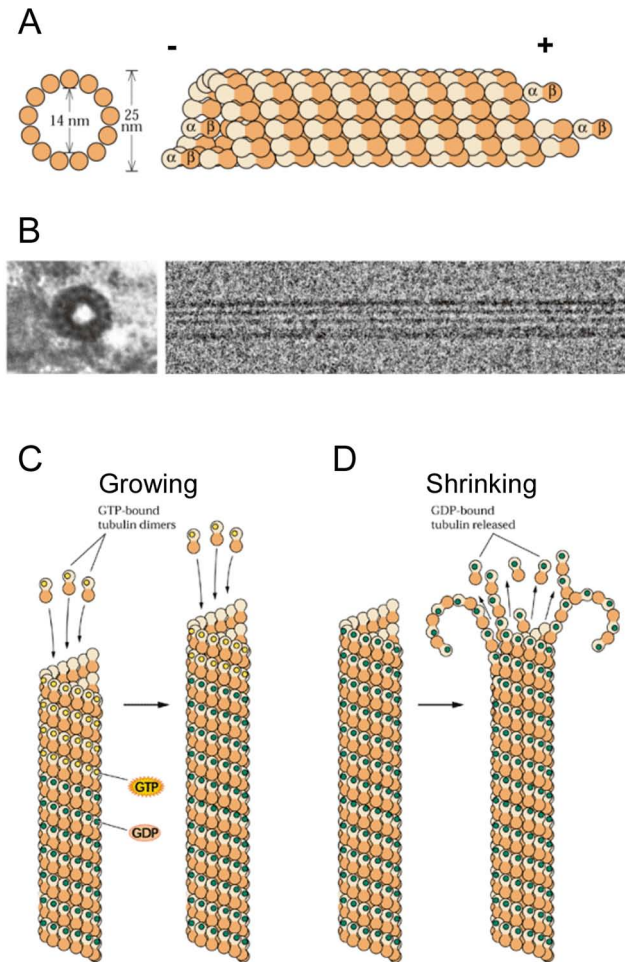


Figure 1.6 Structure of MTs and model for MT dynamic instability. A, Diagrams of a MT in cross-section and side view. The subunits of the MT, dimers of α - and β -tubulin, align head to tail in long parallel columns called protofilaments. 13 protofilaments are displaced longitudinally from one another, forming the MT. The dimers assemble head to tail, giving MTs a structural polarity; α -tubulin is exposed at the minus-end of the polymer and β -tubulin at the plus-end. B, Electron micrograph of a MT from a plant cell in cross-section and side view. C and D, Model for MT dynamic instability. C, Since hydrolysis of GTP usually lags behind polymerization of new subunits, the growing ends of MTs are rich in subunits in which β -tubulin monomers bind GTP. Such MTs are said to have a 'GTP cap'. Hydrolysis of GTP causes a conformational change that tends to bend the protofilament outward, weakening lateral contacts between dimers in adjacent protofilaments. In an intact MT, the GDP-subunits in a protofilament are held in straight alignment by numerous lateral bonds to adjacent subunits and by the stability of the GTP cap. D, However, if the rate of polymerization decreases relative to the rate of hydrolysis, the GTP cap is lost and the GDP-subunits can more readily assume their bent conformation. In this situation, the destabilized MTs can undergo catastrophic depolymerization, during which subunits are released at a rate that far exceeds both the growth rate and the normal rate of subunit loss. Figure taken from Baskin (2000).

MTs undergo random stages of rapid shortening and slow elongation, along with pauses and rescues (Mitchison and Kirschner, 1984; Cassimeris et al., 1988; Cassimeris, 1993). This innate dynamic character, termed dynamic instability, allows MTs to rapidly assemble, disassemble, and linger for various periods of time. Experiments done in mammalian cells have quantified this dynamic behavior by measuring the MT elongation velocity, shortening velocity, catastrophic frequency (transition from polymerization to depolymerization), and rescue frequency (transition from depolymerization to polymerization) (Mitchison and Kirschner, 1984; Cassimeris et al., 1988; Walker et al., 1988; Gelfand and Bershadsky, 1991). These studies, along with data showing that MT dynamics is GTP-dependent (Macneal and Purich, 1978), have led to the formation of a GTP cap model of MT dynamics (Fig. 1.6) (Mitchison and Kirschner, 1984; Nogales, 1999). This model proposes that during MT assembly, GTP-tubulin subunits add to the growing end of the MT but are subsequently hydrolyzed to GDP. As a result, the MT body is composed of GDP, which energetically favors depolymerization, whereas the MT plus-end has a stable GTP cap. If hydrolysis overtakes the addition of GTP-tubulin, the cap is removed and MTs quickly depolymerize.

In living plant cells, injection of fluorescently-labeled brain tubulin, which incorporates into the plant MT array, has allowed kinematic analysis of MT dynamics (Zhang et al., 1990). Specifically, by using Fluorescence Recovery After Photobleaching (FRAP, Saxton et al., 1984) in injected cells, measurements of interphase MT turnover rate can be made by measuring the length of time it takes for a photobleached polymer to recover its fluorescence. Data obtained from these studies show that the rate of MT turnover in the spindle of *Tradescantia* stamen hair cells is similar to that of mammalian spindles (31s) and twice as fast as the turnover rates found in the PPB, phragmoplast, and interphase cortical array (60-67s) (Hush et al., 1994). Notably, the turnover rate in the plant cortical MT array was 3.4 fold higher than mammalian interphase MTs, thus implying that plant MTs are more dynamic than animal MTs. Further supporting this data are *in vitro* measurements of plant MT dynamics, which show that although the elongation velocity of plant and animal MTs is similar, the shortening velocity of plant MTs is about 10 fold higher and plant MTs undergo more catastrophes and exhibit no rescues (Moore et al., 1997). Overall, these differences in dynamic behavior have been attributed to sequence divergence between plant and animal tubulin (Moore et al., 1997) as well as functional differences between plant and animal MTs (Hush et al., 1994).

In vivo studies on individual cortical MTs using green fluorescent protein (GFP) fused to tubulin led to new insights on cortical MT behavior in plants (Shaw et al., 2003). Using GFP-tubulin in *Arabidopsis* seedlings, Shaw et al. showed that cortical MTs arise *de novo* at the cell cortex both in absence and in association with existing MTs. The leading (plus-) ends of these MTs exhibited polymerization biased dynamic instability and the lagging (minus-) ends were found to depolymerize slowly. The net effects of these dynamics were that MTs migrated across the cell cortex by a so-called hybrid treadmilling mechanism. Motile MTs were observed to cross over other MTs or incorporate into bundles of MTs, which remained dynamic through polymerization and depolymerization. They also observed that individual MTs rarely detached from the cell cortex,

implying that they are securely fastened to the plasma membrane by linker proteins. However, in rare cases single MTs detached at their leading end from the cortex, resulting in complete depolymerization or re-association accompanied with a reorientation of the MTs. This implies that attachment of MTs to cell cortex may be important for array organization.

In recent studies, MT-associated proteins (MAP) have been adopted to study the behavior of MTs. Donukshe and Gadella (2003) used yellow fluorescent protein (YFP) fused to the mammalian plus-end tracking MAP CLIP-170 to track MT dynamics in transfected cowpea protoplasts and stably transformed tobacco cells. They found that PPB MTs were shorter and more dynamic compared to interphase MTs. Using MAP4 fused to GFP in Bright Yellow-2 cells (BY-2), Vos et al. (2004) confirmed that dynamic instability of MTs increased during PPB formation, however, they argued that MTs possibly become longer at this stage. This discrepancy might be explained by the fact that the two studies used different MAPs that might interfere differentially with MT stability. Indeed, a recent study on cortical MTs in BY-2 cells showed that MT dynamics differ depending on the MAP used to track the MTs. Here, MT polymerization and depolymerization rates differed between experiments using AtMAP65, MAP4 and EB1 GFP tagged fusions, reflecting stabilizing or destabilizing character of the particular MAP (Van Damme et al., 2004b).

Building different MT arrays

Throughout the cell cycle, plant cells reorganize their cytoskeleton into different MT arrays. The origin of the MTs that construct these arrays is still under debate. In living cells, the highest nucleating activity of the nuclear surface is observed in G2 phase. At that time, the PPB forms and the bipolar spindle progressively assembles around the nucleus. In telophase, when sister nuclei are reconstructed, a dramatic nucleation of MTs occurs on their nuclear surface and takes part in phragmoplast formation and later in the construction of the cortical array (Schmit, 2002). These data suggest that the nuclear surface generates the MTs that will constitute the different MT arrays after translocation of individual MTs. This is supported by studies done in BY-2 protoplasts. Here, MT stabilization by taxol did not prevent MT reorganization during cell wall regeneration, and therefore, it was inferred that MT reorganization occurs by the translocation of intact MT polymers (Wymer et al., 1996).

However, indications for MT nucleation within the different MT arrays exist. Fluorescent tubulin incorporation in the cortical array (Cyr and Palevitz, 1995) and the co-distribution of γ -tubulin and Spc98p in the cell cortex suggests that γ -tubulin complexes are recruited close to the cell membrane, where they may act as nucleation sites (Erhardt et al., 2002). Using a marker for MT plus- and minus-ends, Chan et al. (2003) were able to affirm that MT nucleation occurs simultaneously at numerous sites in the plant cortex, supporting the hypothesis of multiple nucleation sites in plants. Furthermore, Panteris et al. (1995) showed that taxol, which impedes MT turnover, prevents PPB formation in wheat roots and studies done in *Tradescantia*, show that the PPB predominantly arises from new MT assembly (Cleary et al., 1992; Panteris et al., 1995).

Microinjection (Hush et al., 1994) or incorporation of exogenous tubulin in phragmoplasts (Vantard et al., 1990) shows an intense MT assembly in the equatorial region, which increases during lateral expansion of the phragmoplast, suggesting the existence of phragmoplast-located MTCC in plants. The localization of γ -tubulin and Spc98p at plant kinetochores (Binarova et al., 1998) also indicates that the spindle does not only originate from a reorganization of perinuclear MTs during prophase, but also by de novo assembly at kinetochore MTCCs.

MT regulation

To form complex MT arrays, cells must regulate whether a MT elongates, shortens or maintains a steady-state. The mechanism guiding this regulation could come from within the structure of the MT polymer itself. In most eukaryotic cells, a variety of α - and β -tubulin isoforms are present in the cytosol, and it is hypothesized that cells selectively utilize specific isoforms to regulate MT dynamics (Joshi and Cleveland, 1989). Biochemical data support this idea by showing that the various isotypes have different dynamic behaviors (Rothwell et al., 1986; Savage et al., 1989). In particular, the Arabidopsis plant genome consists of six α - and nine β -tubulins (Kopczak et al., 1992), therefore plants, like other eukaryotic cells, could incorporate various isoforms into the MT polymer to regulate dynamics (Eun and Wick, 1998).

MT dynamics might also be regulated by post-translational modification of the α - and β -tubulin heterodimers. Tubulins can be detyrosinated/tyrosinated (Barra et al., 1973), acetylated (Piperno et al., 1987), glutamated (Edde et al., 1990) and phosphorylated (Lockerbie et al., 1989). These post-translational modifications, which mainly occur on the C-terminal site of the β -tubulin dimer, could alter MT dynamics by regulating tubulins interactions with MAPs (Kierszenbaum, 2002).

Soluble, unpolymerized tubulin by itself has the ability to assemble onto, or disassemble from a MT. A group of auxiliary proteins, termed MAPs, give MTs their biochemical diversity by influencing MT dynamicity. MAPs can be divided into two classes- structural MAPs and mechanochemical MAPs. Structural MAPs bind to MTs and affect MT organization by stabilizing, destabilizing, cross-linking and anchoring MTs (Chapin and Bulinski, 1992; Lee, 1993; Wick, 2000; Wasteneys, 2002). Alternatively, mechanochemical MAPs generate force along the MT that propels the MAP, as well as any cargo it may carry, forward. These MAPs have been implicated in intracellular transport, MT organization and MT dynamics.

Structural MAPs

The initiation, stabilization, cross-linking, anchoring and removal of MTs is mediated by structural MAPs. The identity of these MAPs remained elusive for some time in plant cells despite evidence for their presence in early electron micrographs (Hardham and Gunning, 1978). Extracting and identifying MAPs is hindered by the recalcitrance of plant material to biochemical approaches. Whereas MAPs are relatively easy to purify from brain tissue that is teeming with MTs, plant tissues

have modest concentrations of tubulins. Plant cells are usually cytoplasm-poor, most cell volume being occupied by vacuoles, whose rupture releases proteolytic enzymes that hamper purification strategies. Homology searches for plant structural MAPs were at first largely unsuccessful, although some candidates, isolated by MT affinity, cross-reacted with antibodies to the animal MAPs tau (Vantard et al., 1991) and MAP4 (Maekawa et al., 1990), which are probably one of the best documented MAPs in animals (Mandelkow and Mandelkow, 1995).

Problems encountered with biochemical isolation of plant MAPs were overcome by Cyr and Palevitz (1989), who isolated several carrot polypeptides that bound taxol stabilized neuronal MTs. Later, Jiang and Sonobe (1993) made protoplasts from tobacco BY-2 suspension culture cells and removed the vacuoles to generate 'miniprotoplasts'. Cycling of MTs from these preparations through multiple rounds of MT assembly/disassembly led to the identification of the MAP65, a plant specific MAP family of 3 or 4 electrophoretically separable proteins all around 65 kDA in size. Later, immunological equivalents of the tobacco MAP65 family were found in cytoskeletal preparations from carrot suspension cells (Chan et al., 1996) and a complete Arabidopsis family of nine MAP65 proteins (AtMAP65-1 to AtMAP65-9) was discovered in the Arabidopsis genome sequence (Hussey et al., 2002). MAP65 from tobacco, carrot and the members of the *Arabidopsis* MAP65 family have been expressed in bacteria and shown to bind and bundle plant MTs (Fig.1.7) (Smertenko et al., 2000; Hussey et al., 2002; Smertenko et al., 2004). However, not all MAP65 proteins show bundling *in vitro*, like the tobacco NtMAP65-1a and NtMAP65-1b that were shown to respectively enhance MT polymerization or protect MTs from cold-induced depolymerization (Wicker-Planquart et al., 2004). A role in MT stabilization has also been suggested for AtMAP65-1 and -5 (Van Damme et al., 2004b). As GFP-fusions, these MAPs only associated to co-aligned MTs in elongated BY-2 cells. Moreover, AtMAP65-1 and -5 labeled MTs were protected against MT destabilizing drugs and displayed reduced depolymerization.

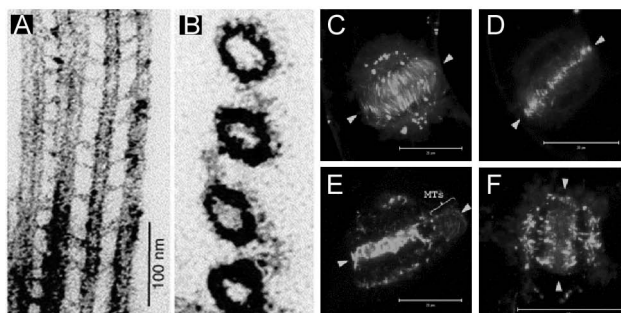


Figure 1.7 Function and differential localization of MAP65 family members. A, Longitudinal and B, transverse electron micrograph sections of MTs cross-linked *in vitro* by purified carrot MAP65. MAP65 can be seen as the evenly spaced filamentous cross-bridges. Image taken from Sedbrook (2004). C-F, Differential localization of AtMAP65-1 (C), AtMAP65-3 (D), AtMAP65-5 (E) and AtMAP65-8 (F) at the phragmoplast MTs. Images taken from Van Damme et al. (2004a).

Different members of the MAP65 family have been localized at the subcellular level (Smertenko et al., 2000; Muller et al., 2004; Van Damme et al., 2004b; Van Damme et al., 2004a). Although they all label MTs, they associate differentially to plant MT arrays, indicating that different MAPs have different MT-binding activities and are differentially regulated (Fig. 1.7). For instance, a destruction box (short sequence present in cell cycle regulated proteins that targets proteins to the ubiquitin degradation pathway (Juang et al., 1997) is present in AtMAP65-4, which displays a mitotic specific expression during cell cycle. Accordingly, AtMAP65-4-GFP only labels MTs of the spindle. On the other hand, AtMAP65-1 and -5, which are selectively targeted to distinct mitotic configurations, are expressed throughout the cell cycle, indicating that MT binding is differentially controlled throughout the cell cycle, probably through posttranslational modification (Van Damme et al., 2004b). The importance of MAP65 proteins in MT organization and cell division is illustrated by the mutant *pleiade*. Pleiade was identified as AtMAP65-3 and has a C-terminal truncation abolishing MT binding. This mutant has distorted phragmoplasts and accordingly, cytokinesis is disrupted, leading to multinucleated cells and incomplete cell walls (Muller et al., 2004).

Another well characterized MAP is MOR1, which is the Arabidopsis homologue of Xenopus XMAP215 (Tournéze et al., 2000; Whittington et al., 2001). XMAP215 as stabilizing factor, and the destabilizing factor XKCM1 (a MCAK/Kinesin-13 motor protein) have been shown to regulate MT dynamics in Xenopus extracts (Vasquez et al., 1994; Walczak et al., 1996). The sequence of XMAP215 contains a CDK phosphorylation site and phosphorylation of the CDK1 site inhibits the ability of XMAP215 to promote polymerization of pure tubulin (Vasquez et al., 1999). Based on these data, a model was proposed for XMAP215/XKCM1 controlled regulation of MT dynamics during cell cycle. During interphase, XMAP215 is unphosphorylated and its activity predominates over that of XKCM1 leading to long MTs. In mitosis, CDK1 activity is high and XMAP215 is hyperphosphorylated, its activity reduced and the activity of XKCM1 predominates leading to short MTs. In Arabidopsis, mutations in the *MOR1* gene lead to severely stunted plants, with radial swollen and left-handed twisted organs (Whittington et al., 2001). MTs in the cortical array are disorganized and abnormally shortened. MCAK/Kinesin-13 members are present in the Arabidopsis genome and AtMOR1 contains a CDK phosphorylation site. Possibly, MOR1 regulates MT dynamics in plants in a similar way as in Xenopus (Hussey and Hawkins, 2001). In Arabidopsis, MOR1 localizes to the cortical array during interphase and in addition, to the midline of spindle and phragmoplast. Another mutant *gem1*, which is allelic to *mor1*, affects cytokinesis in pollen mitosis I, leading to binucleate pollen. This indicates that MOR1/GEM1, like in animal cells, also functions during cell division during which it might stabilize the growing ends at the phragmoplast midline (Twell et al., 2002).

A distinct class of MAPs in animals have been called the 'plus-end-tracking proteins' or +TIPs (Schuyler and Pellman, 2001). They mark the growing plus-ends of MTs and thus give the appearance of tracking. To this class belong the interacting proteins EB1 and CLIP170 subfamilies which are conserved in animal and yeast. Although Clip170 is absent in plants, it has been used as a marker to study MT dynamics in plants (Dhonukshe and Gadella, 2003). Arabidopsis contains 3

isoforms of EB1. AtEB1a has been shown to localize to the growing plus-ends of cortical MTs, but also marks the minus-end as a site from which MTs can grow and shrink (Chan et al., 2003). In contrast, MT minus-end labeling was not observed by Mathur et al. (2003). They found that GFP-AtEB1a associated to motile membrane networks, which resembles the behavior of CLIP170 in animal cells (Pierre et al., 1992). In addition, GFP-AtEB1a was present on the growing plus-ends of MTs, from which it disappeared upon MT shrinking, as observed for animal EB1 (Tirnauer et al., 2002). However, AtEB1a associated to already stabilized MTs, whereas EB1 proteins in animal cells and yeast are shown to induce MT stabilization (Mimori-Kiyosue et al., 2000; Tirnauer et al., 2002). Another MT plus-end tracking protein is the plant-specific SPIRAL1 (SPR1) (Nakajima et al., 2004; Sedbrook et al., 2004). SPR1 may not be a traditional MAP because it does not co-purify *in vitro* with taxol stabilized MTs. However, SPR1 GFP fusions label all four MT arrays with preferential MT plus-end labeling in the cortical array. Plus-end label occurred as MTs were growing, but vanished upon depolymerization, comparable to the EB1 proteins. Mutations in SPR1 caused axial twisting of roots and etiolated hypocotyls as well as reduced anisotropic growth in endodermal and cortical cells. Organ twisting and anisotropic growth has been observed in mutants affected in specific MAPs. The secondary structure of the 12 kDa SPR1 protein suggests that it might be a structural protein that links other proteins, like for instance traditional MAPs.

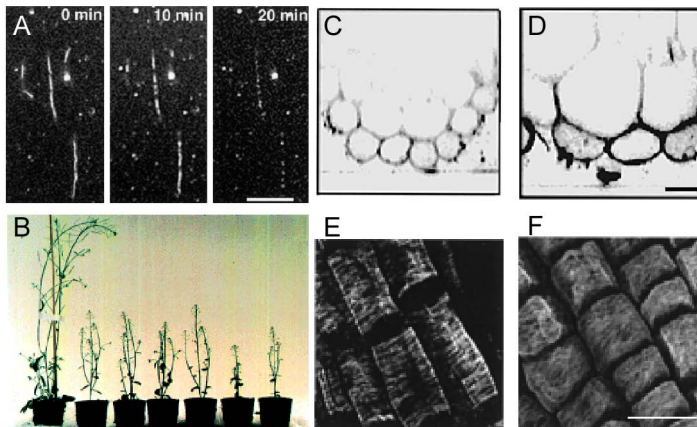


Figure 1.8 Katanin function and mutant phenotype. A, Time-lapse video microscopy of fluorescent taxol-stabilized MTs. After addition of the katanin p60 subunit and ATP, the MTs are fragmented. Bar = $5\mu\text{m}$. B, katanin mutant *bot1-1* allelic plants (right) are stunted compared to wild type plants (left). C and D, Confocal image of a transverse section of a wild type (C) and the katanin mutant *bot1-1* (D), showing isodiametrically swollen cells in roots. E and F, Cortical MTs in elongating cells of roots of *bot1-1* plants (F) are less transverse than in wild type plants (E). As a result, cells are shorter. Bar = $20\mu\text{m}$. Images taken from Bichet et al. (2001).

Among the many actions of MAPs, is MT severing by katanins. In animal cells, katanins form heterodimers, consisting of a catalytic p60 and a regulatory p80 subunit. They sever MTs from the

centrosome, thereby regulating spindle MT dynamics and/or restricting MT lengths (McNally and Thomas, 1998; McNally et al., 2000). Katanin p60 and p80 subunits are both present in *Arabidopsis* and were shown to interact in a yeast two-hybrid screen (McClinton et al., 2001; Bouquin et al., 2003). In addition, the p60 subunit severs MTs *in vitro* (Fig. 1.8) (Stoppin-Mellet et al., 2002, 2003). Mutants in the p60 subunit have been characterized as smaller plants with defects in cell elongation (Bichet et al., 2001; Burk et al., 2001; Webb et al., 2002; Bouquin et al., 2003). Accordingly, katanin mutants exhibit a delayed transition from the perinuclear array to a transverse orientation after cell division, resulting in isodiametric swollen cells.

Mechanochemical MAPs

Mechanochemical MAPs also called motor proteins, possess the special capability to convert chemical energy in the form of ATP into force and movement. During these movements, motor proteins transport different kinds of cargo such as vesicles, organelles, chromosomes or other MT polymers. Mechanochemical MAPs are divided into two superfamilies: kinesins and dyneins. Dynein was first discovered in cilia and flagella as a high molecular weight protein with ATPase activity (Gibbons, 1963; Gibbons and Rowe, 1965). Cytoplasmic dynein acts as a MT dependent, minus-end directed motor and functions in ciliary/flagellar beating, vesicular transport, spindle assembly and chromosome movement. It is activated by dynactin that is believed to couple dynein to its cargos. The dynein superfamily has not evolutionarily diverged and the yeast genome consists of only 1 dynein, *Drosophila* 1-2, mammals 3-5 (Goldstein, 2001) and no dynein homologs exist in *Arabidopsis* (Lawrence et al., 2001). In contrast, kinesins, which were originally isolated from squid axoplasm due to their ability to bind MTs in an ATP-dependent manner (Brady, 1985; Vale et al., 1985), are evolutionary and functionally divergent (Goldstein, 2001). Kinesins share sequence homology in a conserved region of about 340 amino acids within the motor domain (Bloom and Endow, 1994). The conserved motor domain, with highly diverged non-motor flanking regions, is consistent with an evolutionary model in which the ancestral motor function is retained by all kinesins, but a variety of more derived functions have evolved outside this region.

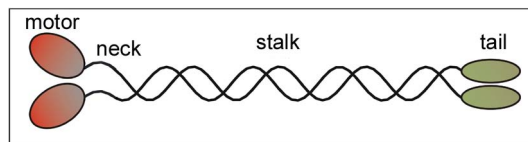


Figure 1.9 Structure of conventional kinesin. Conventional kinesin is a homodimeric motor protein. The motor heads bind to the MT and ATP. Each head is connected to a flexible neck that enables motor stepping. The neck is connected to a long coiled-coil stalk that holds two heads together. At the end of the stalk, kinesin has a cargo-binding domain, called the tail domain.

The kinesin superfamily

Kinesins occur in a variety of quaternary structures, depending on the subfamily. Although some kinesins operate as monomers, many form homo- or heterodimers, heterotrimers or bipolar homotetramers (Reilein et al., 2001). Conventional kinesin consists of two heavy chains and two light chains (Vale et al., 1985). Within most kinesin heavy chains are four domains arranged in a modular fashion; the motor domain, neck, stalk and tail (Fig. 1.9). Each domain of the kinesin heavy chain has a defined function. The motor (frequently called the head domain) binds MTs in a ATP dependent manner (Scholey et al., 1989; Yang et al., 1989; Yang et al., 1990). Together with the neck region that attaches the motor domain to the rest of the protein, it is required for kinesin movement (Case et al., 2000). Kinesin stalks are comprised of α -helical coiled-coils and are highly variable in both sequence and length. In some kinesins, a terminal portion of the stalk is referred to as the tail. It is this tail domain which interacts with the two light chains or other kinesin-associated proteins (KAP) to bind the cargo that a particular kinesin carries (Reddy, 2001).

Budding yeast has 6 kinesins, humans have 45 kinesins (Miki et al., 2001), *C. elegans* and *Drosophila* 20-25 (Goldstein, 2001), mice 30 (Miki et al., 2001) and over 60 kinesins are present in *Arabidopsis* (Reddy and Day, 2001). Several kinesin family trees have been generated in the past, based upon sequence similarity among the various kinesins in their motor domains (Moore and Endow, 1996; Kim and Endow, 2000; Reddy and Day, 2001; Lawrence et al., 2002; Dagenbach and Endow, 2004). These include nine basic kinesin subfamilies together with several unclassified kinesins. Recently, a standardized nomenclature has been proposed that unifies all previous phylogenies and nomenclature proposals and that allocates unclassified kinesins to defined groups (Lawrence et al., 2004). This nomenclature identifies 14 recognized kinesin groups, each with unique structural and functional characteristics.

Kinesin directionality

A property intrinsic to molecular motors is their ability to move unidirectionally along cytoskeletal filaments. Motor domains can be positioned either N-terminal, C-terminal or internal to the polypeptide chain (Vale and Fletterick, 1997). To date, all studies regarding kinesin movement have shown that kinesins with an N-terminal motor domain move towards the plus-end of MTs, while kinesins with a C-terminal motor are minus-end directed (Higuchi and Endow, 2002). This suggests that domain organization, particularly the position of the motor domain, is important for polarity of force generation. Indeed, replacement of the motor domain of a plus-end motor (conventional kinesin) with the motor domain of a minus-end directed kinesin (Ncd) did not change the directionality of the chimeric kinesin (Higuchi and Endow, 2002), also suggesting that the other determinants of directionality lie in the neck outside the motor domain (Case et al., 1997). This neck domain is located N-terminal to the motor domain in minus-end directed kinesins, and is situated C-terminal to the motor domain in plus-end directed kinesins (Vale and Fletterick, 1997).

Moreover, neck sequences are conserved within the N- and C-terminal kinesins and Endow and Wagilora (1998) determined that the GN residues at the neck/motor core junction are necessary for minus-end directed movement. In addition, there is also a difference at the structural level. Whereas plus-end kinesins have neck domains consisting of a coiled-coil and a β -sheet, the latter called neck linker, minus-end kinesins do not have a neck linker (Higuchi and Endow, 2002). In *Arabidopsis*, 21 out of the 61 kinesins belong to the C-terminal/Kinesin-14 subfamily and minus-end directed movement has been demonstrated *in vitro* for three members of this subfamily (Song et al., 1997; Marcus et al., 2002; Ambrose et al., 2005). It is remarkable that structurally, 11 members of the *Arabidopsis* C-terminal subfamily have internal motor domains and five have N-terminal motor domains (Reddy and Day, 2001). Although the directionality of these structurally divergent kinesins remains to be determined experimentally, all kinesins belonging to this subfamily have a typical neck for minus-end kinesins (including the GN residues) that is located N-terminally to the motor domain. Thus it seems that the position of the neck relative to the motor domain is the main determinant for directionality.

Despite the differences in neck structure and sequence, analysis of chimeric motors implicates both the conventional kinesin and Ncd stalk/neck in determination of motor directionality. Fusing the conventional kinesin stalk/neck, including the neck linker, to the motor core of the minus-end directed kinesin Ncd resulted in a plus-end directed chimeric motor (Case et al., 1997; Henningsen et al., 1997), whereas fusing the Ncd stalk/neck to the motor core of plus-end kinesin resulted in minus-end directed chimeric motor (Endow and Waligora, 1998).

How does the stalk/neck region determine directionality? Single motor laser trap assays show that a conformation or angle change of the stalk/neck region relative to the motor domain occurs when Ncd binds to the MT. In wild type Ncd motors, the final stalk/neck position is biased to the minus-end. Ncd mutants with point mutations in the stalk/neck region reveal a bi-directional movement, and the stalk/neck position is not biased to the minus-end, but appears to be ad random (Endow and Higuchi, 2000). Thus, it comes out that the directionality of minus-end motors is due to the position of the stalk/neck region relative to the motor domain. In plus-end motors, the neck linker undergoes nucleotide-dependent conformational changes, thereby causing the neck linker to be docked pointing towards the plus end of MTs. This conformation mediates plus-end directed movement by pulling the other head forward. Thus plus-end directed motors cannot orient towards the minus-end, thereby making plus-end directionality the default mode (Endow, 1999).

Kinesin processivity

One molecule of ATP provides kinesin with the energy to take 8 nm steps between adjacent tubulin dimers (Coy et al., 1999). Some kinesins step processively and hydrolyze hundreds of ATP molecules without disassociating from the MT (Howard et al., 1989; Block et al., 1990). To do this, it is predicted that the two kinesin heads act in a coordinated manner, such that the binding and hydrolysis of ATP by one head, promotes ADP release in the other head (Lohman et al., 1998).

Thus, in this hand-over-hand model of kinesin movement, there is an alternation of head catalysis, whereby at least one head always remains bound to the MT substrate, preventing the disassociation of the kinesin from the MT in between steps (Block et al., 1990; Schnapp et al., 1990; Hackney, 1994).

For this model to hold true, a transient two-heads-bound state must exist. This has been seen in a structurally similar actin-binding motor protein, myosin (Walker et al., 2000). Cryoelectron micrograph reconstructions of a two-heads bound state for kinesins have not been reproducible (Hoenger et al., 2000). Nonetheless, support for this model comes from data obtained using single-headed kinesins, most of which cannot retain attached to the MT for long distances (Berliner et al., 1995; Hancock and Howard, 1998; Higuchi and Endow, 2002). This implies that two heads are required for processive movement and is therefore consistent with the hand over hand model for kinesin movement.

The simplest example of the hand-over-hand model is a 'symmetric model', meaning that the motor reverts to exactly the same 3D conformation after each step (Howard, 1996). This would enable each head to repeat the ATPase cycle starting from the same physical condition and to create identical steps. However, it also implies that the stalk rotates 180° every step. Because the tail region is fixed when attached to cargo, rotation along one direction would overwind the stalk and prevent the kinesin from walking after several steps. To test the rotation of the stalk, tail regions of kinesin motors were fixed on a glass surface (Hua et al., 2002). When a single kinesin translates the MT, the torsion would rotate the MT instead of twisting the stalk. MTs did not show 180° rotation and a new mechanism was proposed as the 'inchworm model'. This model suggests that only one head is catalytically active. One head always leads and the other head follows. However, motility assays and fluorescence imaging with one-nanometer accuracy (FIONA) experiments rejected the inchworm model and the results directly showed that kinesin walks in a hand-over-hand manner (Asbury et al., 2003; Kaseda et al., 2003; Yildiz et al., 2003).

To avoid twisting of the stalk in the symmetric hand-over-hand model, Hoenger et al (2000) proposed an asymmetric model. It suggests that the trailing head can move forward alternately from the right and the left side of the stalk, without stalk rotation. In other words, the kinesin moves in much the same way as humans walk.

Notably, some two headed kinesins are non-processive and disassociate from the MT without taking successive steps. Biochemical data obtained with one non-processive motor, Ncd, show that it releases its bound head from the MT before binding its second head, and therefore, diffuses away from the MT after one step (Pechatnikova and Taylor, 1999; Mackey and Gilbert, 2000). Though it would seem that non-processive motors are functionally inefficient, they are predicted to generate a productive movement by working cooperatively (Howard, 1997). Motility data shows that the non-processive kinesin, Ncd, requires at least four kinesin molecules bound to the MT to generate a continuous force on the MT (deCastro et al., 1999). The mechanism by which non-processive kinesins orchestrate these cooperative movements is not known, however, it is hypothesized that a

second motor must bind to the MT before the first motor releases to generate a continuous force (Endow and Higuchi, 2000).

In order for all kinesins to exhibit motility they must be able to translate the chemical energy stored in ATP into mechanical energy. Studies investigating the crystal structure of plus-end directed conventional kinesins propose that two structural elements, switch I and II, which flank the nucleotide binding sites, are critical to this process (Vale and Milligan, 2000; Schliwa and Woehlke, 2001). These regions are thought to act as relays and transfer ATP hydrolysis information to the rest of the kinesin molecule. In particular, it is thought that a subdomain of the kinesin head, termed the switch II cluster, transduces the energy into a conformational change that increases its length and rotates it 20° relative to the kinesin molecule (Kikkawa et al., 2001). These reconfigurations are subsequently translated to the neck linker region (a 15 amino acid stretch found within the kinesin neck region), which becomes docked onto the motor domain and acts as a mechanical amplifier to drive the kinesin forward (Rice et al., 1999; Case et al., 2000). Notably, this scheme of events is only true for plus-end directed motors, because minus-end motors lack a neck linker region. As stated previously, the basis of minus-end directed movement is thought to lie in the position of the neck/stalk region relative to the motor domain (Endow and Higuchi, 2000).

Kinesin function

The first kinesin, conventional kinesin, was identified in squid giant axons as a protein involved in transport of vesicles (Vale et al., 1985). Since then, many more kinesins were identified and their roles in intracellular transport expanded. To date, kinesins have been shown to transport a multitude of cellular elements including: lysosomes (Hollenbeck and Swanson, 1990), melanosomes (Rogers et al., 1997), vesicles (Hall and Hedgecock, 1991), mitochondria (Tanaka et al., 1998), cargo bearing rafts (Cole et al., 1998) and possibly RNA (Carson et al., 1998). In addition, kinesins are also involved in various aspects of mitotic and meiotic spindle assembly and maintenance, and are proposed to generate sufficient force to assemble and maintain spindles as well as drive chromosome movement to and from the spindle equator (Sharp et al., 2000b; Scholey et al., 2003; Kline-Smith and Walczak, 2004).

In animals, the mechanisms by which kinesins operate in mitotic spindle functioning are well understood. It appears that mitotic motors use at least three distinct mechanisms: (1) cross-bridging and sliding MTs relative to adjacent MTs (2) transporting specific mitotic cargoes along the spindle MTs and (3) regulating MT assembly dynamics and coupling movement to MT growth and shrinkage. In addition, analysis of the functional inter-relationships between multiple mitotic motors have revealed that specific mitotic movements are not driven by individual motors but, instead, result from shifts in a dynamic balance of complementary and antagonistic forces generated by multiple motors functioning co-operatively. Below, examples are given from the animal field of how different kinesins from the same or different subfamilies cooperate to control functioning of the mitotic spindle and chromosome movement (Sharp et al., 2000a).

At the start of mitosis, a spindle is formed around the still intact nucleus. This involves the establishment of a bipolar array with MT plus-ends overlapping at the centre and the organization of the MT minus-ends into spindle poles that are separated along with the duplicated centrosomes towards opposing sides of the nucleus. Cytoplasmic dynein focuses MT minus-ends by forming a multi-protein complex with dynactin to transport the MT cross-linking protein NuMA to the spindle poles (Merdes et al., 2000). In addition, the minus-end directed kinesin Ncd (C-terminal/Kinesin-14 subfamily) cross-links MTs *in vitro* and localizes to spindle poles during mitosis (Endow and Komma, 1996). Mutants of this motor have multipolar spindles with broad or splayed poles, indicating that Ncd functions cooperatively with dynein to organize spindle poles (Hatsumi and Endow, 1992). In *Drosophila*, these motors collaborate along with KLP61F to establish the bipolar spindle (Sharp et al., 2000a). KLP61F belongs to the BimC/Kinesin-5 subfamily of plus-end directed motors that form bipolar homotetramers, with two motor domains positioned at opposite ends of a central stalk. At the central spindle, these motors bind, cross-link and slide antiparallel MTs, thereby generating poleward-directed forces. In this way, they organize MTs of opposite polarity into a bipolar structure and push spindle poles apart during mitosis (Sharp et al., 2000a). This is supported by studies showing that when KLP61F or other BimC kinesins are mutated, spindles are monopolar and collapse inwards (Saunders and Hoyt, 1992; O'Connell et al., 1993; Blangy et al., 1995). Spindle pole separation by KLP61F is reinforced by dynein that pulls on spindle poles via astral MTs, but counterbalanced by Ncd (Fig. 1.10) (Sharp et al., 2000a). In addition to a spindle pole association, Ncd also localizes to the inter-polar MTs (Endow and Komma, 1996). As this kinesin moves towards the minus-end of MTs, it pulls spindle poles together thus providing opposite forces to the plus-end directed BimC kinesins. The idea that a balance of forces from BimC and minus-end directed kinesins is important for spindle functioning is supported by data showing that mutations in minus-end directed kinesins, such as Ncd, can suppress the monopolar spindle phenotype of BimC mutants (such as KLP61F) (Wilson et al., 2004). Similar results were obtained in yeast and fungi (Saunders and Hoyt, 1992; O'Connell et al., 1993), suggesting that this mechanism is conserved among eukaryotes. In addition, it is noteworthy that during anaphase, Ncd appears to have no effect on spindle pole movements, suggesting that its activity is down-regulated at this time, allowing dynein and KLP61F to drive spindle elongation during anaphase B (Sharp et al., 2000a). During metaphase, paired chromosomes oscillate until they are aligned at the metaphase plate with sister chromatids attached to opposite poles. A specialized subfamily of kinesins, the MCAK/Kinesin-13 subfamily, have internal motor domains and contribute to various aspects of chromosome movement (reviewed in Moore and Wordeman, 2004). Remarkably, these motors do not move along MTs as other kinesins do, but instead destabilize MTs at their plus- or minus-ends (Desai et al., 1999). Members of this subfamily, among which the mammalian MCAK, are enriched on centrosomes, centromeres and the spindle midzone during mitosis. Accordingly, they are involved in bipolar spindle formation, correcting improper kinetochore-MT attachments before anaphase, suppressing the oscillating behavior of chromatids once they have aligned at the metaphase plate and the segregation of chromosomes towards their respective poles. A nice example of functional

cooperation is illustrated by two members of this subfamily in *Drosophila* (Rogers et al., 2004). One of them, KLP59C, localizes to the centromeric regions of chromosomes during anaphase and is required to depolymerize kinetochore MTs at their plus-ends. This allows chromatids to move towards the pole by 'chewing up' MTs tracks, a mechanism called the 'Pac-Man' model (Fig. 1.10). Contrary, KLP10A labels the spindle poles during anaphase and is required to depolymerize MTs at their minus ends. In this 'pole ward flux' model, chromatids are pulled towards the poles through depolymerization at the minus-ends (Fig. 1.10).

Another kinetochore-associated kinesin is CENP-E. This motor is required for stability of kinetochore-MT attachments during chromosome congression and segregation. Accordingly, depletion of CENP-E results in unaligned chromosomes during mitosis and missegregation due to a reduced kinetochore MT binding at aligned and unaligned chromosomes (Schaar et al., 1997; McEwen et al., 2001; Tanudji et al., 2004). It is hypothesized that CENP-E uses its plus-end directed transport properties in two ways; to transport kinetochores toward the plus-ends through metaphase and subsequently anchor kinetochores to the plus-ends of MTs that are depolymerized through the action of depolymerizing kinesins as MCAK during anaphase (Sharp et al., 2000b).

Another subfamily of kinesins involved in chromosome movement is the chromokinesin/Kinesin-4 subfamily, which contain MT- and DNA-binding domains and localize to the chromosome arms. These kinesins are thought to push chromosomes away from spindle poles, thus creating polar-ejection forces (Fig. 1.10) (Mountain and Compton, 2000).

In animal cells, cytokinesis does not involve the formation of a MT-based phragmoplast that laterally expands simultaneously guiding vesicle trafficking to the midline for cell plate construction. Instead, an actomyosin ring is formed at the division plane that constricts the cell resulting in the partitioning of the cytoplasm. Ingression continues until the contractile ring compresses the central spindle into a compact midbody. It is proposed that midbody MTs serve as tracks for motor-mediated transport of Golgi derived vesicles and signaling molecules to the furrow during cell-cell abscission (Finger and White, 2002; Shuster and Burgess, 2002). Such a motor function has been suggested for the kinesin Rab6-KIFL, which functions in membrane traffic within the Golgi apparatus during interphase. Introduction of anti-Rab6-KIFL antibodies into dividing cells blocks cytokinesis, suggesting that this motor is involved in transporting Golgi-derived vesicles during cytokinesis in animal cells (Echard et al., 1998; Hill et al., 2000). Two other kinesins, Borsin (a BimC kinesin) and Pavarotti (also called MKLP1, CHO1 and ZEN4) are essential for the completion of cytokinesis. These motors are crucial in organizing the arrays of anti-parallel MTs that form the compressed central spindle during cytokinesis (Glotzer, 2001; Touitou et al., 2001).

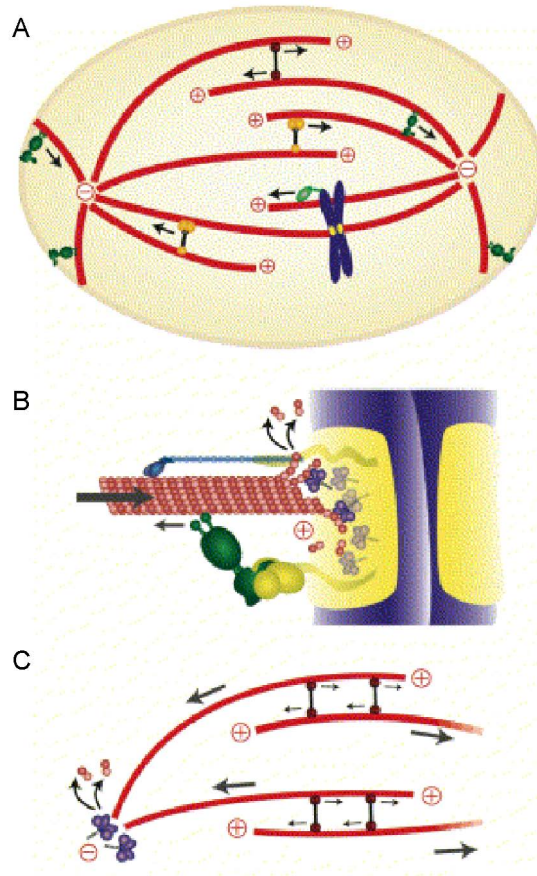


Figure 1.10 Diverse activities of motors in the spindle. A, Plus- (red) and minus-end (yellow) directed cross-linking motors that increase or decrease the overlap of antiparallel MTs determine spindle pole separation. Cytoplasmic dynein (dark green) in the cortex pulls on astral MTs or focus MT minus-ends into poles. Chromokinesins (light green) push chromosomes away from the spindle poles. B, Pac-Man model. Dynein (green) helps in the delivery of MTs to depolymerizing kinesins (purple) by moving MTs with their plus-ends leading. The plus-end directed motor CENP-E (light blue) assures the attachment of the MT with the kinetochore. C, Pole-ward flux model. Minus-end directed movement of MTs driven by the flux motor Eg5 (red) is coordinated with minus-end depolymerization by a depolymerizing kinesin (purple). Figure taken from Gadde and Heald (2004).

Plant kinesins

Like in animal cells, plant kinesins have been found that function in mitosis and cytokinesis, although the information is less elaborate compared to the animal field. In cells of higher plants which do not have centrosomes, bipolar spindle formation does not involve the separation of spindle poles, but requires the premitotic organization of a perinuclear bipolar array of MTs (Wick and Duniec, 1983). The tobacco TKRP125 kinesin belongs to the BimC/Kinesin-5 subfamily (Asada et al., 1997). It localizes to the perinuclear bipolar MTs at prophase and at the spindle MTs during metaphase with enrichment at the midzone. These data suggest that TKRP125, like BimC kinesins in animals and yeast, binds and slides anti-parallel MTs in the spindle midzone to establish the bipolar spindle structure. In addition, it localizes to the anaphase spindle mainly at the midzone, indicating that sliding of anti-parallel MTs by TKRP125 during anaphase B might result in spindle elongation. Homologues of this protein are present in carrot and *Arabidopsis* (Barroso et al., 2000; Liu and Lee, 2001). The latter contains four BimC/Kinesin-5 kinesins, which might explain why molecular genetic approaches supporting the proposed function for TKRP125 homologues have not yet been reported.

Minus-end directed kinesins counterbalance the outward force of BimC kinesins to construct a bipolar spindle. The *Arabidopsis* kinesins ATK1/2/3 and ATK5 (C-terminal/Kinesin-14 subfamily) are closely related to Ncd from *Drosophila* (Lee and Liu, 2004). Similar to Ncd, ATK1 behaves as a non-processive MT minus-end directed motor (Marcus et al., 2002). During mitosis, it concentrates to the midzone of the metaphase and anaphase spindle, suggesting that ATK1 works antagonistically to BimC-like kinesins, establishing a balance of forces necessary for spindle bipolarity (Liu et al., 1996). This is supported by mutant *atk1-1* plants that are defective in male meiosis. Meiotic spindles were abnormally broad with unfocused poles during metaphase I (Chen et al., 2002). Defects in spindle pole formation and reduced spindle bipolarity were also observed in somatic cells. However by anaphase, spindle abnormalities were rectified resulting in normal somatic cell division (Marcus et al., 2003). In animal and yeast, the minus-end directed motors Ncd and Kar3 respectively, are involved in focusing the minus-end of MTs into spindle poles. As spindle poles in both male meiotic and mitotic *atk1-1* cells were unfocussed, it is likely that ATK1 is needed to organize MTs at the two poles. A function in spindle pole formation has also been proposed for ATK5, which is 83% identical (91% similar) to ATK1 (Ambrose et al., 2005). This minus-end directed motor localizes to the spindle midzone by a plus-end tracking mechanism that does not involve the motor domain. Mitotic spindles in *atk5-1* null mutants are abnormally broad with unfocussed poles. Perhaps ATK5 cross-links MTs of the same polarity at the midzone and the poles of the spindle. The authors also suggested a role for ATK5 in cross-linking interdigitating anti-parallel MTs to construct a bipolar spindle. However no defects in spindle bipolarity were observed in the *atk5-1* mutant.

TKRP125, ATK1 and ATK5 also localize to the phragmoplast MTs during cytokinesis, suggesting that the same balance of forces that construct the bipolar spindle is involved in the construction of the

bipolar phragmoplast. Using plasma membrane-permeabilized BY-2 cells, Asada et al (1991) showed that fluorescein-labeled tubulin, applied together with GTP was incorporated into the equatorial region of phragmoplasts and this fluorescent band separated towards the poles when labeled tubulin was replaced with unlabeled tubulin. When an antibody raised against TKRP125 was added together with GTP, the translocation of phragmoplast MTs reduced in a dose dependent manner (Asada et al., 1997). This illustrated that TKRP125 addresses its BimC function to construct the bipolar phragmoplast, where it slides anti-parallel MTs apart. In contrast, *atk1-1* and *atk5-1* mutants did not reveal any defects in phragmoplast formation and cytokinesis occurred normally in mitotic cells suggesting that other minus-end directed kinesins balance the forces of TKRP125 during cytokinesis.

Another minus-end directed motor which localizes to the phragmoplast is KCBP (Bowser and Reddy, 1997; Smirnova et al., 1998). This kinesin is unique in that its motor activity and MT binding is inhibited upon Ca²⁺/calmodulin binding (Deavours et al., 1998). KCBP's association with anaphase spindle poles and minus-ends of phragmoplast MTs suggests that it may be involved in organizing MT minus-ends. An antibody was raised against the calmodulin binding domain, which constitutively activates the motor activity of KCBP (Vos et al., 2000). Microinjection experiments resulted in the formation of aberrant phragmoplasts and delayed the completion of cytokinesis significantly. Therefore it was proposed that KCBP's activity is down-regulated in the phragmoplast by a rise of Ca²⁺ concentration in the phragmoplast region. However, earlier in mitosis, KCBP might be activated and contribute to converging MT minus-ends in the spindle poles.

AtPAKRP1/AtKinesin-12A specifically associates with the plus-end of phragmoplast MTs (Lee and Liu, 2000). This localization pattern was dependent on the integrity of the MTs. The homologues AtPAKRP1L/AtKinesin-12B behaves similar to AtPAKRP1 (Pan et al., 2004). It is proposed that both motors are required to maintain the bipolar structure of the phragmoplast once BimC/Kinesin-5 motors, like TKRP125 have established bipolarity. AtPAKRP1 bears neck sequences conserved among plus-end directed kinesins, suggesting that this motor maintains the integrity of phragmoplast MTs by keeping MTs plus-ends in position while new MT segments are added to the ends (Liu and Lee, 2001). Such a function would require a second MT binding domain outside the motor domain, however, co-sedimentation with MTs only occurred with the motor domain of AtPAKRP1 and not with regions outside the motor domain (Lee and Liu, 2000).

During plant cytokinesis, Golgi-derived vesicles are transported to the phragmoplast midline and fuse there to form a cell plate (Verma, 2001). AtPAKRP2 appears in a punctuate pattern along phragmoplast MTs and is enriched in the midline (Lee et al., 2001). This localization pattern is dependent on both MTs and an intact vesicle trafficking system. In addition, AtPAKRP2 is proposed to be a plus-end directed kinesin that follows the centrifugal expansion of the phragmoplast and disappears where MTs have depolymerized. AtPAKRP2 is thus a likely motor candidate that transports Golgi-derived vesicles to the phragmoplast midline (Lee and Liu, 2004).

Following the initial formation of the cell plate in the centre of the cell, phragmoplast MTs reorganize to the cell plate edges and depolymerize in the centre. Expansion of these MTs results in

delivery of additional vesicles to the growing margin of the cell plate (Staehein and Hepler, 1996; Heese et al., 1998; Otegui and Staehein, 2000). AtNACK1/HIK was independently identified to be essential for phragmoplast expansion during vegetative cytokinesis (Nishihama et al., 2002; Strompen et al., 2002). The corresponding *Arabidopsis* mutants *nack1-1* and *hinkel* cease growth at respectively the vegetative and seedling stage, and embryos in both cases contain multinucleate cells with incomplete cell walls. Tubulin staining in *hinkel* embryos revealed that phragmoplast MTs are not depolymerized at the centre when the initial cell plate is already formed (Strompen et al., 2002). Initially, cell plate/phragmoplast expansion occurred, but ceased afterwards (Nishihama et al., 2002). These data suggest that NACK1/HIK function in the reorganization of phragmoplast MTs during cytokinesis. It is noteworthy that NACK1 interacts with NPK1, which is a MAPKKK required for phragmoplast expansion. Both NPK1 and NACK1 localize to the phragmoplast midline. Moreover, NACK1 is required for the correct localization of NPK1 during cytokinesis and activates the kinase activity of NPK1 (Nishihama et al., 2002).

NACK2 is the closest homologue of NACK1 and was identified as an interactor of NPK1 (Nishihama et al., 2002). Whether NACK2 also localizes to the phragmoplast midline is not reported. Similar to NACK1, its expression is up-regulated during mitosis. Vegetative cytokinesis is not disrupted in *tetraspore/stud* mutants, which are allelic to NACK2. However cytokinesis is disrupted during male meiosis due to a failure to establish the radial MT array associated with cytokinesis of tetrads (Hulskamp et al., 1997; Yang et al., 2003). Thus, whereas NACK1 functions in phragmoplast MT organization in somatic tissues, its homologue NACK2 is required to organize the MT arrays to separate microspores in male meiosis. Surprisingly, double heterozygous *atnack1/atnack2* mutants affected cellularization (cytokinesis) synergistically during megagametogenesis, indicating that these motors function redundantly to some extent (Tanaka et al., 2004).

In addition to functions during cell division, plant kinesins have been found at mitochondria (Itoh et al., 2001), Golgi (Lu et al., 2004), pollen organelles (Cai et al., 1993; Romagnoli et al., 2003), actin (Preuss et al., 2004) and MTs (Preuss et al., 2003) during interphase. They have been shown to function in trichome morphogenesis through either MT stabilization resulting in trichome branching (Zwichel/KCBP) (Oppenheimer et al., 1997) or by organizing Golgi stacks (AtKinesin-13A) (Lu et al., 2004). AtKinesin-13A contains an internal motor domain, which shares a high degree of similarity to the motor domain of internal motor kinesin in animals, like MCAK. However, their functions are unrelated as internal kinesins in animals are involved in spindle functioning and chromosome movements during mitosis (Moore and Wordeman, 2004). Another kinesin, AtFRA1 belongs to the chromokinesins/Kinesin-4 subfamily (Zhong et al., 2002). Animal kinesins in this subfamily typically play roles in chromatid motility and chromosome condensation, activities associated with mitosis (Mountain and Compton, 2000). The *fra1* mutant, however, does not show defects in cell division, but the orientation of cellulose microfibrils is altered in fiber walls which resulted in a reduced mechanical strength of cell walls in *fra1* mutants (Zhong et al., 2002).

References

- Akashi T, Izumi K, Nagano E, Enomoto M, Mizuno K, Shibaoka H** (1988) Effects of Propyzamide on Tobacco Cell Microtubules In vivo and In vitro. *Plant and Cell Physiology* **29**: 1053-1062
- Ambrose JC, Li W, Marcus A, Ma H, Cyr R** (2005) A Minus-End Directed Kinesin with +TIP Activity Is Involved in Spindle Morphogenesis. *Mol Biol Cell*
- Asada T, Kuriyama R, Shibaoka H** (1997) TKRP125, a kinesin-related protein involved in the centrosome-independent organization of the cytokinetic apparatus in tobacco BY-2 cells. *Journal of Cell Science* **110**: 179-189
- Asada T, Sonobe S, Shibaoka H** (1991) Microtubule Translocation in the Cytokinetic Apparatus of Cultured Tobacco Cells. *Nature* **350**: 238-241
- Asbury CL, Fehr AN, Block SM** (2003) Kinesin moves by an asymmetric hand-over-hand mechanism. *Science* **302**: 2130-2134
- Azimzadeh J, Traas J, Pastuglia M** (2001) Molecular aspects of microtubule dynamics in plants. *Curr Opin Plant Biol* **4**: 513-519
- Barra HS, Arce CA, Rodrigue Ja, Caputto R** (1973) Incorporation of Phenylalanine as a Single Unit into Rat-Brain Protein - Reciprocal Inhibition by Phenylalanine and Tyrosine of Their Respective Incorporations. *Journal of Neurochemistry* **21**: 1241-1251
- Barroso C, Chan J, Allan V, Doonan J, Hussey P, Lloyd C** (2000) Two kinesin-related proteins associated with the cold-stable cytoskeleton of carrot cells: characterization of a novel kinesin, DcKRP120-2. *Plant Journal* **24**: 859-868
- Baskin TI** (2000) The cytoskeleton. In *Biochemistry and Molecular Biology of Plants*, B.B. Buchanan, W. Gruissem, and R.L. Jones (Eds.). Rockville, American Society of Plant Physiologists: 202- 258
- Baskin TI** (2001) On the alignment of cellulose microfibrils by cortical microtubules: a review and a model. *Protoplasma* **215**: 150-171
- Baskin TI, Cande WZ** (1990) The Structure and Function of the Mitotic Spindle in Flowering Plants. *Annual Review of Plant Physiology and Plant Molecular Biology* **41**: 277-315
- Baskin TI, Wilson JE, Cork A, Williamson RE** (1994) Morphology and Microtubule Organization in Arabidopsis Roots Exposed to Oryzalin or Taxol. *Plant and Cell Physiology* **35**: 935-942
- Berliner E, Young EC, Anderson K, Mahtani HK, Gelles J** (1995) Failure of a Single-Headed Kinesin to Track Parallel to Microtubule Protofilaments. *Nature* **373**: 718-721
- Bibikova TN, Blancaflor EB, Gilroy S** (1999) Microtubules regulate tip growth and orientation in root hairs of Arabidopsis thaliana. *Plant J* **17**: 657-665
- Bichet A, Desnos T, Turner S, Grandjean O, Hofte H** (2001) BOTERO1 is required for normal orientation of cortical microtubules and anisotropic cell expansion in Arabidopsis. *Plant J* **25**: 137-148
- Binarova P, Hause B, Dolezel J, Draber P** (1998) Association of gamma-tubulin with kinetochore/centromeric region of plant chromosomes. *Plant Journal* **14**: 751-757
- Blangy A, Lane HA, dHerin P, Harper M, Kress M, Nigg EA** (1995) Phosphorylation by p34(cdc2) regulates spindle association of human Eg5, a kinesin-related motor essential for bipolar spindle formation in vivo. *Cell* **83**: 1159-1169
- Block SM, Goldstein LSB, Schnapp BJ** (1990) Bead Movement by Single Kinesin Molecules Studied with Optical Tweezers. *Nature* **348**: 348-352
- Bloom GS, Endow SA** (1994) Motor Proteins .1. Kinesins. *Protein Profile* **1**: 1059-1116
- Bouquin T, Mattsson O, Naested H, Foster R, Mundy J** (2003) The Arabidopsis lue1 mutant defines a katanin p60 ortholog involved in hormonal control of microtubule orientation during cell growth. *J Cell Sci* **116**: 791-801
- Bowser J, Reddy AS** (1997) Localization of a kinesin-like calmodulin-binding protein in dividing cells of Arabidopsis and tobacco. *Plant J* **12**: 1429-1437
- Brady ST** (1985) A Novel Brain Atpase with Properties Expected for the Fast Axonal-Transport Motor. *Nature* **317**: 73-75
- Brown RC, Lemmon BE, Olsen OA** (1994) Endosperm Development in Barley - Microtubule Involvement in the Morphogenetic Pathway. *Plant Cell* **6**: 1241-1252
- Burk DH, Liu B, Zhong R, Morrison WH, Ye ZH** (2001) A katanin-like protein regulates normal cell wall biosynthesis and cell elongation. *Plant Cell* **13**: 807-827

- Cai G, Bartalesi A, Delcasino C, Moscatelli A, Tiezzi A, Cresti M** (1993) The Kinesin-Immunoreactive Homolog from Nicotiana-Tabacum Pollen Tubes - Biochemical-Properties and Subcellular-Localization. *Planta* **191**: 496-506
- Carpita NC, Gibeaut DM** (1993) Structural models of primary cell walls in flowering plants: consistency of molecular structure with the physical properties of the walls during growth. *Plant J* **3**: 1-30
- Carson JH, Kwon SJ, Barbarese E** (1998) RNA trafficking in myelinating cells. *Current Opinion in Neurobiology* **8**: 607-612
- Case RB, Pierce DW, HomBooher N, Hart CL, Vale RD** (1997) The directional preference of kinesin motors is specified by an element outside of the motor catalytic domain. *Cell* **90**: 959-966
- Case RB, Rice S, Hart CL, Ly B, Vale RD** (2000) Role of the kinesin neck linker and catalytic core in microtubule-based motility. *Current Biology* **10**: 157-160
- Cassimeris L** (1993) Regulation of microtubule dynamic instability. *Cell Motil Cytoskeleton* **26**: 275-281
- Cassimeris L, Pryer NK, Salmon ED** (1988) Real-time observations of microtubule dynamic instability in living cells. *J Cell Biol* **107**: 2223-2231
- Chan J, Calder GM, Doonan JH, Lloyd CW** (2003) EB1 reveals mobile microtubule nucleation sites in Arabidopsis. *Nature Cell Biology* **5**: 967-971
- Chan J, Rutten T, Lloyd C** (1996) Isolation of microtubule-associated proteins from carrot cytoskeletons: A 120 kDa map decorates all four microtubule arrays and the nucleus. *Plant Journal* **10**: 251-259
- Chapin SJ, Bulinski JC** (1992) Microtubule Stabilization by Assembly-Promoting Microtubule-Associated Proteins - a Repeat Performance. *Cell Motility and the Cytoskeleton* **23**: 236-243
- Chen C, Marcus A, Li W, Hu Y, Calzada JP, Grossniklaus U, Cyr RJ, Ma H** (2002) The Arabidopsis ATK1 gene is required for spindle morphogenesis in male meiosis. *Development* **129**: 2401-2409
- Cleary AL, Gunning BES, Wasteneys GO, Hepler PK** (1992) Microtubule and F-Actin Dynamics at the Division Site in Living Tradescantia Stamen Hair-Cells. *Journal of Cell Science* **103**: 977-988
- Cole DG, Diener DR, Himelblau AL, Beech PL, Fuster JC, Rosenbaum JL** (1998) Chlamydomonas kinesin-II-dependent intraflagellar transport (IFT): IFT particles contain proteins required for ciliary assembly in *Caenorhabditis elegans* sensory neurons. *Journal of Cell Biology* **141**: 993-1008
- Cosgrove DJ** (1997) Assembly and enlargement of the primary cell wall in plants. *Annu Rev Cell Dev Biol* **13**: 171-201
- Coy DL, Wagenbach M, Howard J** (1999) Kinesin takes one 8-nm step for each ATP that it hydrolyzes. *Journal of Biological Chemistry* **274**: 3667-3671
- Cyr RJ, Palevitz BA** (1989) Microtubule-Binding Proteins from Carrot .1. Initial Characterization and Microtubule Bundling. *Planta* **177**: 245-260
- Cyr RJ, Palevitz BA** (1995) Organization of cortical microtubules in plant cells. *Curr Opin Cell Biol* **7**: 65-71
- Dagenbach EM, Endow SA** (2004) A new kinesin tree. *Journal of Cell Science* **117**: 3-7
- Deavours BE, Reddy ASN, Walker RA** (1998) Ca²⁺/calmodulin regulation of the Arabidopsis kinesin-like calmodulin-binding protein. *Cell Motility and the Cytoskeleton* **40**: 408-416
- deCastro MJ, Ho CH, Stewart RJ** (1999) Motility of dimeric ncd on a metal-chelating surfactant: Evidence that ncd is not processive. *Biochemistry* **38**: 5076-5081
- Desai A, Verma S, Mitchison TJ, Walczak CE** (1999) Kin I kinesins are microtubule-destabilizing enzymes. *Cell* **96**: 69-78
- Dhonukshe P, Gadella TWJ** (2003) Alteration of microtubule dynamic instability during preprophase band formation revealed by yellow fluorescent protein-CLIP170 microtubule plus-end labeling. *Plant Cell* **15**: 597-611
- Doxsey S** (2001) Re-evaluating centrosome function. *Nat Rev Mol Cell Biol* **2**: 688-698
- Echard A, Jollivet F, Martinez O, Lacapere JJ, Rousselet A, Janoueix-Lerosey I, Goud B** (1998) Interaction of a Golgi-associated kinesin-like protein with Rab6. *Science* **279**: 580-585
- Edde B, Rossier J, Lecaer JP, Desbroyeres E, Gros F, Denoulet P** (1990) Posttranslational Glutamylation of Alpha-Tubulin. *Science* **247**: 83-85
- Endow SA** (1999) Determinants of molecular motor directionality. *Nature Cell Biology* **1**: E163-E167
- Endow SA, Higuchi H** (2000) A mutant of the motor protein kinesin that moves in both directions on microtubules. *Nature* **406**: 913-916
- Endow SA, Komma DJ** (1996) Centrosome and spindle function of the *Drosophila* Ncd microtubule motor visualized in live embryos using Ncd-GFP fusion proteins. *Journal of Cell Science* **109**: 2429-2442
- Endow SA, Waligora KW** (1998) Determinants of kinesin motor polarity. *Science* **281**: 1200-1202

- Erhardt M, Stoppin-Mellet V, Campagne S, Canaday J, Mutterer J, Fabian T, Sauter M, Muller T, Peter C, Lambert AM, Schmit AC** (2002) The plant Spc98p homologue colocalizes with gamma-tubulin at microtubule nucleation sites and is required for microtubule nucleation. *Journal of Cell Science* **115**: 2423-2431
- Eun SO, Wick SM** (1998) Tubulin isoform usage in maize microtubules. *Protoplasma* **204**: 235-244
- Euteneuer U, McIntosh JR** (1980) Polarity of midbody and phragmoplast microtubules. *J Cell Biol* **87**: 509-515
- Evans L, Mitchison T, Kirschner M** (1985) Influence of the centrosome on the structure of nucleated microtubules. *J Cell Biol* **100**: 1185-1191
- Finger FP, White JG** (2002) Fusion and fission: Membrane trafficking in animal cytokinesis. *Cell* **108**: 727-730
- Furutani I, Watanabe Y, Prieto R, Masukawa M, Suzuki K, Naoi K, Thitamadee S, Shikanai T, Hashimoto T** (2000) The SPIRAL genes are required for directional control of cell elongation in *Arabidopsis thaliana*. *Development* **127**: 4443-4453
- Gadde S, Heald R** (2004) Mechanisms and molecules of the mitotic spindle. *Current Biology* **14**: R797-R805
- Galatis B, Apostolakos P, Katsaros C, Loukari H** (1982) Pre-Prophase Microtubule Band and Local Wall Thickening in Guard-Cell Mother Cells of Some Leguminosae. *Annals of Botany* **50**: 779-791
- Geissler S, Pereira G, Spang A, Knop M, Soues S, Kilmartin J, Schiebel E** (1996) The spindle pole body component Spc98p interacts with the gamma-tubulin-like Tub4p of *Saccharomyces cerevisiae* at the sites of microtubule attachment. *Embo J* **15**: 3899-3911
- Gelfand VI, Bershadsky AD** (1991) Microtubule dynamics: mechanism, regulation, and function. *Annu Rev Cell Biol* **7**: 93-116
- Gibbons IR** (1963) Studies in the protein components of cilia from *Tetrahymena*. *Proceedings of the National Academy of Sciences of the United States of America* **50**: 1002- 1010
- Gibbons IR, Rowe AJ** (1965) Dynein: a protein with adenosine triphosphatase. *Science* **149**
- Giddings TH, Staehelin LA** (1991) Microtubule-mediated control of microfibril deposition; a re-examination of the hypothesis. In *The Cytoskeletal Basis of Plant Growth and Form*. Edited by Lloyd C.W. London: Academic press: 85-100
- Gimenez-Abian MI, Utrilla L, Canovas JL, Gimenez-Martin G, Navarrete MH, De la Torre C** (1998) The positional control of mitosis and cytokinesis in higher-plant cells. *Planta* **204**: 37-43
- Glotzer M** (2001) Animal cell cytokinesis. *Annual Review of Cell and Developmental Biology* **17**: 351-386
- Goddard RH, Wick SM, Silflow CD, Snustad DP** (1994) Microtubule Components of the Plant-Cell Cytoskeleton. *Plant Physiology* **104**: 1-6
- Goldstein LSB** (2001) Molecular motors: from one motor many tails to one motor many tales. *Trends in Cell Biology* **11**: 477-482
- Granger C, Cyr R** (2001) Use of abnormal preprophase bands to decipher division plane determination. *J Cell Sci* **114**: 599-607
- Granger CL, Cyr RJ** (2000) Microtubule reorganization in tobacco BY-2 cells stably expressing GFP-MBD. *Planta* **210**: 502-509
- Green PB** (1980) Organogenesis - a Biophysical View. *Annual Review of Plant Physiology and Plant Molecular Biology* **31**: 51-82
- Hackney DD** (1994) Evidence for Alternating Head Catalysis by Kinesin During Microtubule-Stimulated Atp Hydrolysis. *Proceedings of the National Academy of Sciences of the United States of America* **91**: 6865-6869
- Hall DH, Hedgecock EM** (1991) Kinesin-Related Gene Unc-104 Is Required for Axonal-Transport of Synaptic Vesicles in *C-Elegans*. *Cell* **65**: 837-847
- Hancock WO, Howard J** (1998) Processivity of the motor protein kinesin requires two heads. *Journal of Cell Biology* **140**: 1395-1405
- Hardham AR, Gunning BES** (1978) Structure of Cortical Microtubule Arrays in Plant-Cells. *Journal of Cell Biology* **77**: 14-34
- Hatsumi M, Endow SA** (1992) Mutants of the Microtubule Motor Protein, Nonclaret Disjunctional, Affect Spindle Structure and Chromosome Movement in Meiosis and Mitosis. *Journal of Cell Science* **101**: 547-559
- Heese M, Mayer U, Jurgens G** (1998) Cytokinesis in flowering plants: cellular process and developmental integration. *Current Opinion in Plant Biology* **1**: 486-491
- Henningsen U, Steinberg G, Schliwa M** (1997) Using chimeras to study kinesin velocity and polarity. *Molecular Biology of the Cell* **8**: 2045-2045
- Higuchi H, Endow SA** (2002) Directionality and processivity of molecular motors. *Current Opinion in Cell Biology* **14**: 50-57

- Hill E, Clarke N, Barr FA** (2000) The Rab6-binding kinesin, Rab6-KIFL, is required for cytokinesis. *Embo Journal* **19**: 5711-5719
- Himmelspach R, Williamson RE, Wasteneys GO** (2003) Cellulose microfibril alignment recovers from DCB-induced disruption despite microtubule disorganization. *Plant Journal* **36**: 565-575
- Hoenger A, Thormahlen M, Diaz-Avalos R, Doerhoefer M, Goldie KN, Muller J, Mandelkow E** (2000) A new look at the microtubule binding patterns of dimeric kinesins. *Journal of Molecular Biology* **297**: 1087-1103
- Hogan CJ** (1987) Microtubule Patterns During Meiosis in 2 Higher-Plant Species. *Protoplasma* **138**: 126-136
- Hollenbeck PJ, Swanson JA** (1990) Radial Extension of Macrophage Tubular Lysosomes Supported by Kinesin. *Nature* **346**: 864-866
- Howard J** (1996) The movement of kinesin along microtubules. *Annual Review of Physiology* **58**: 703-729
- Howard J** (1997) Molecular motors: structural adaptations to cellular functions. *Nature* **389**: 561-567
- Howard J, Hudspeth AJ, Vale RD** (1989) Movement of Microtubules by Single Kinesin Molecules. *Nature* **342**: 154-158
- Hua W, Chung J, Gelles J** (2002) Distinguishing inchworm and hand-over-hand processive kinesin movement by neck rotation measurements. *Science* **295**: 844-848
- Hulskamp M, Parekh NS, Grini P, Schneitz K, Zimmermann I, Lolle SJ, Pruitt RE** (1997) The *STUD* gene is required for male-specific cytokinesis after telophase II of meiosis in *Arabidopsis thaliana*. *Developmental Biology* **187**: 114-124
- Hush JM, Wadsworth P, Callahan DA, Hepler PK** (1994) Quantification of Microtubule Dynamics in Living Plant-Cells Using Fluorescence Redistribution after Photobleaching. *Journal of Cell Science* **107**: 775-784
- Hussey PJ, Hawkins TJ** (2001) Plant microtubule-associated proteins: the HEAT is off in temperature-sensitive *mor1*. *Trends in Plant Science* **6**: 389-392
- Hussey PJ, Hawkins TJ, Igarashi H, Kaloriti D, Smertenko A** (2002) The plant cytoskeleton: recent advances in the study of the plant microtubule-associated proteins MAP-65, MAP-190 and the *Xenopus* MAP215-like protein, MOR1. *Plant Molecular Biology* **50**: 915-924
- Itoh R, Fujiwara M, Yoshida S** (2001) Kinesin-related proteins with a mitochondrial targeting signal. *Plant Physiology* **127**: 724-726
- Jiang CJ, Sonobe S** (1993) Identification and Preliminary Characterization of a 65-Kda Higher-Plant Microtubule-Associated Protein. *Journal of Cell Science* **105**: 891-901
- Joshi HC, Cleveland DW** (1989) Differential Utilization of Beta-Tubulin Isoforms in Differentiating Neurites. *Journal of Cell Biology* **109**: 663-673
- Joshi HC, Palevitz BA** (1996) gamma-Tubulin and microtubule organization in plants. *Trends in Cell Biology* **6**: 41-44
- Juang YL, Huang J, Peters JM, McLaughlin ME, Tai CY, Pellman D** (1997) APC-mediated proteolysis of Ase 1 and the morphogenesis of the mitotic spindle. *Science* **275**: 1311-1314
- Kaseda K, Higuchi H, Hirose K** (2003) Alternate fast and slow stepping of a heterodimeric kinesin molecule. *Nature Cell Biology* **5**: 1079-1082
- Kierszenbaum AL** (2002) Sperm axoneme: A tale of tubulin posttranslational diversity. *Molecular Reproduction and Development* **62**: 1-3
- Kikkawa M, Sablin EP, Okada Y, Yajima H, Fletterick RJ, Hirokawa N** (2001) Switch-based mechanism of kinesin motors. *Nature* **411**: 439-445
- Kim AJ, Endow SA** (2000) A kinesin family tree. *Journal of Cell Science* **113**: 3681-+
- Kline-Smith SL, Walczak CE** (2004) Mitotic spindle assembly and chromosome segregation: Refocusing on microtubule dynamics. *Molecular Cell* **15**: 317-327
- Knop M, Schiebel E** (1997) Spc98p and Spc97p of the yeast gamma-tubulin complex mediate binding to the spindle pole body via their interaction with Spc110p. *Embo J* **16**: 6985-6995
- Konishi M, Sugiyama M** (2003) Genetic analysis of adventitious root formation with a novel series of temperature-sensitive mutants of *Arabidopsis thaliana*. *Development* **130**: 5637-5647
- Kopczak SD, Haas NA, Hussey PJ, Silflow CD, Snustad DP** (1992) The Small Genome of *Arabidopsis* Contains at Least 6 Expressed Alpha-Tubulin Genes. *Plant Cell* **4**: 539-547
- Kost B, Mathur J, Chua NH** (1999) Cytoskeleton in plant development. *Curr Opin Plant Biol* **2**: 462-470
- Lambert AM** (1993) Microtubule-organizing centers in higher plants. *Curr Opin Cell Biol* **5**: 116-122
- Lawrence CJ, Dawe RK, Christie KR, Cleveland DW, Dawson SC, Endow SA, Goldstein LSB, Goodson HV, Hirokawa N, Howard J, Malmberg RL, McIntosh JR, Miki H, Mitchison TJ, Okada Y,**

- Reddy ASN, Saxton WM, Schliwa M, Scholey JM, Vale RD, Walczak CE, Wordeman L** (2004) A standardized kinesin nomenclature. *Journal of Cell Biology* **167**: 19-22
- Lawrence CJ, Malmberg RL, Muszynski MG, Dawe RK** (2002) Maximum likelihood methods reveal conservation of function among closely related kinesin families. *Journal of Molecular Evolution* **54**: 42-53
- Lawrence CJ, Morris NR, Meagher RB, Dawe RK** (2001) Dyneins have run their course in plant lineage. *Traffic* **2**: 362-363
- Ledbetter MC** (1981) Citation Classic - a Microtubule in Plant-Cell Fine-Structure. *Current Contents/Agriculture Biology & Environmental Sciences*: 20-20
- Ledbetter MC, Porter KR** (1963) A "microtubule" in plant cell fine structure. *Journal of Cell Biology* **19**: 239-250
- Lee G** (1993) Non-motor microtubule-associated proteins. *Curr Opin Cell Biol* **5**: 88-94
- Lee YR, Giang HM, Liu B** (2001) A novel plant kinesin-related protein specifically associates with the phragmoplast organelles. *Plant Cell* **13**: 2427-2439
- Lee YR, Liu B** (2000) Identification of a phragmoplast-associated kinesin-related protein in higher plants. *Curr Biol* **10**: 797-800
- Lee YR, Liu B** (2004) Cytoskeletal motors in Arabidopsis. Sixty-one kinesins and seventeen myosins. *Plant Physiol* **136**: 3877-3883
- Liu B, Cyr RJ, Palevitz BA** (1996) A kinesin-like protein, KatAp, in the cells of arabidopsis and other plants. *Plant Cell* **8**: 119-132
- Liu B, Lee YRJ** (2001) Kinesin-related proteins in plant cytokinesis. *Journal of Plant Growth Regulation* **20**: 141-150
- Liu B, Marc J, Joshi HC, Palevitz BA** (1993) A Gamma-Tubulin-Related Protein Associated with the Microtubule Arrays of Higher-Plants in a Cell Cycle-Dependent Manner. *Journal of Cell Science* **104**: 1217-1228
- Lloyd C** (1995) Plant morphogenesis. Life on a different plane. *Curr Biol* **5**: 1085-1087
- Lockerbie RO, Edde B, Prochiantz A** (1989) Cyclic Amp-Dependent Protein-Phosphorylation in Isolated Neuronal Growth Cones from Developing Rat Forebrain. *Journal of Neurochemistry* **52**: 786-796
- Lohman TM, Thorn K, Vale RD** (1998) Staying on track: Common features of DNA helicases and microtubule motors. *Cell* **93**: 9-12
- Liu L, Lee YR, Pan R, Maloof JN, Liu B** (2004) An Internal Motor Kinesin Is Associated with the Golgi Apparatus and Plays a Role in Trichome Morphogenesis in Arabidopsis. *Mol Biol Cell*
- Mackey AT, Gilbert SP** (2000) Moving a microtubule may require two heads: A kinetic investigation of monomeric Ncd. *Biochemistry* **39**: 1346-1355
- Macneal RK, Purich DL** (1978) Stoichiometry and Role of Gtp Hydrolysis in Bovine Neurotubule Assembly. *Journal of Biological Chemistry* **253**: 4683-4687
- Maekawa T, Ogihara S, Murofushi H, Nagai R** (1990) Green Algal Microtubule-Associated Protein with a Molecular-Weight of 90 Kda Which Bundles Microtubules. *Protoplasma* **158**: 10-18
- Mandelkow E, Mandelkow EM** (1995) Microtubules and microtubule-associated proteins. *Curr Opin Cell Biol* **7**: 72-81
- Marcus AI, Ambrose JC, Blickley L, Hancock WO, Cyr RJ** (2002) Arabidopsis thaliana protein, ATK1, is a minus-end directed kinesin that exhibits non-processive movement. *Cell Motil Cytoskeleton* **52**: 144-150
- Marcus AI, Li W, Ma H, Cyr RJ** (2003) A kinesin mutant with an atypical bipolar spindle undergoes normal mitosis. *Mol Biol Cell* **14**: 1717-1726
- Mathur J, Chua NH** (2000) Microtubule stabilization leads to growth reorientation in Arabidopsis trichomes. *Plant Cell* **12**: 465-477
- Mathur J, Mathur N, Kernebeck B, Srinivas BP, Hulskamp M** (2003) A novel localization pattern for an EB1-like protein links microtubule dynamics to endomembrane organization. *Current Biology* **13**: 1991-1997
- Mayer U, Jurgens G** (2004) Cytokinesis: lines of division taking shape. *Current Opinion in Plant Biology* **7**: 599-604
- McClinton RS, Chandler JS, Callis J** (2001) cDNA isolation, characterization, and protein intracellular localization of a katanin-like p60 subunit from Arabidopsis thaliana. *Protoplasma* **216**: 181-190
- McEwen BF, Chan GKT, Zubrowski B, Savoian MS, Sauer MT, Yen TJ** (2001) CENP-E is essential for reliable bioriented spindle attachment, but chromosome alignment can be achieved via redundant mechanisms in mammalian cells. *Molecular Biology of the Cell* **12**: 2776-2789

- McNally FJ, Thomas S** (1998) Katanin is responsible for the M-phase microtubule-severing activity in *Xenopus* eggs. *Mol Biol Cell* **9**: 1847-1861
- McNally KP, Bazirgan OA, McNally FJ** (2000) Two domains of p80 katanin regulate microtubule severing and spindle pole targeting by p60 katanin. *J Cell Sci* **113 (Pt 9)**: 1623-1633
- Merdes A, Heald R, Samejima K, Earnshaw WC, Cleveland DW** (2000) Formation of spindle poles by dynein/dynactin-dependent transport of NuMA. *Journal of Cell Biology* **149**: 851-861
- Mews M, Sek FJ, Moore R, Volkmann D, Gunning BES, John PCL** (1997) Mitotic cyclin distribution during maize cell division: implications for the sequence diversity and function of cyclins in plants. *Protoplasma* **200**: 128-145
- Miki H, Setou M, Kaneshiro K, Hirokawa N** (2001) All kinesin superfamily protein, KIF, genes in mouse and human. *Proceedings of the National Academy of Sciences of the United States of America* **98**: 7004-7011
- Mimori-Kiyosue Y, Shiina N, Tsukita S** (2000) The dynamic behavior of the APC-binding protein EB1 on the distal ends of microtubules. *Current Biology* **10**: 865-868
- Mineyuki Y** (1999) The preprophase band of microtubules: Its function as a cytokinetic apparatus in higher plants. *International Review of Cytology - a Survey of Cell Biology, Vol 187* **187**: 1-49
- Mineyuki Y, Gunning BES** (1990) A Role for Preprophase Bands of Microtubules in Maturation of New Cell-Walls, and a General Proposal on the Function of Preprophase Band Sites in Cell-Division in Higher-Plants. *Journal of Cell Science* **97**: 527-537
- Mineyuki Y, Marc J, Palevitz BA** (1991a) Relationship between the Preprophase Band, Nucleus and Spindle in Dividing Allium Cotyledon Cells. *Journal of Plant Physiology* **138**: 640-649
- Mineyuki Y, Murata T, Wada M** (1991b) Experimental Obliteration of the Preprophase Band Alters the Site of Cell-Division, Cell Plate Orientation and Phragmoplast Expansion in *Adiantum* Protonemata. *Journal of Cell Science* **100**: 551-557
- Mineyuki Y, Yamashita M, Nagahama Y** (1991c) P34cdc2 Kinase Homolog in the Preprophase Band. *Protoplasma* **162**: 182-186
- Mitchison T, Kirschner M** (1984) Dynamic instability of microtubule growth. *Nature* **312**: 237-242
- Mizuno K** (1993) Microtubule-Nucleation Sites on Nuclei of Higher-Plant Cells. *Protoplasma* **173**: 77-85
- Moore A, Wordeman L** (2004) The mechanism, function and regulation of depolymerizing kinesins during mitosis. *Trends in Cell Biology* **14**: 537-546
- Moore JD, Endow SA** (1996) Kinesin proteins: A phylum of motors for microtubule-based motility. *Bioessays* **18**: 207-219
- Moore RC, Zhang M, Cassimeris L, Cyr RJ** (1997) In vitro assembled plant microtubules exhibit a high state of dynamic instability. *Cell Motility and the Cytoskeleton* **38**: 278-286
- Moritz M, Agard DA** (2001) gamma-Tubulin complexes and microtubule nucleation. *Current Opinion in Structural Biology* **11**: 174-181
- Mountain V, Compton DA** (2000) Dissecting the role of molecular motors in the mitotic spindle. *Anatomical Record* **261**: 14-24
- Muller S, Smertenko A, Wagner V, Heinrich M, Hussey PJ, Hauser MT** (2004) The plant microtubule-associated protein AtMAP65-3/PLE is essential for cytokinetic phragmoplast function. *Curr Biol* **14**: 412-417
- Murata T, Wada M** (1991) Effects of Centrifugation on Preprophase-Band Formation in *Adiantum* Protonemata. *Planta* **183**: 391-398
- Murata T, Wada M** (1993) Cell-Division in Caffeine-Induced Binucleate Protonemal Cells of *Adiantum* .2. Formation of the Preprophase Band and Cell-Division in Centrifuged and Non-Centrifuged Cells. *Journal of Plant Research* **106**: 313-318
- Murphy SM, Urbani L, Stearns T** (1998) The mammalian gamma-tubulin complex contains homologues of the yeast spindle pole body components spc97p and spc98p. *J Cell Biol* **141**: 663-674
- Nacry P, Mayer U, Jurgens G** (2000) Genetic dissection of cytokinesis. *Plant Molecular Biology* **43**: 719-733
- Nakajima K, Furutani I, Tachimoto H, Matsubara H, Hashimoto T** (2004) SPIRAL1 encodes a plant-specific microtubule-localized protein required for directional control of rapidly expanding *Arabidopsis* cells. *Plant Cell* **16**: 1178-1190
- Nebenfuhr A, Frohlick JA, Staehelin LA** (2000) Redistribution of Golgi stacks and other organelles during mitosis and cytokinesis in plant cells. *Plant Physiol* **124**: 135-151

- Nishihama R, Soyano T, Ishikawa M, Araki S, Tanaka H, Asada T, Irie K, Ito M, Terada M, Banno H, Yamazaki Y, Machida Y** (2002) Expansion of the cell plate in plant cytokinesis requires a kinesin-like protein/MAPKKK complex. *Cell* **109**: 87-99
- Nogales E** (1999) A structural view of microtubule dynamics. *Cellular and Molecular Life Sciences* **56**: 133-142
- O'Connell MJ, Meluh PB, Rose MD, Morris NR** (1993) Suppression of the bimC4 mitotic spindle defect by deletion of klpA, a gene encoding a KAR3-related kinesin-like protein in *Aspergillus nidulans*. *J Cell Biol* **120**: 153-162
- Oppenheimer DG, Pollock MA, Vacik J, Szymanski DB, Ericson B, Feldmann K, Marks MD** (1997) Essential role of a kinesin-like protein in *Arabidopsis* trichome morphogenesis. *Proc Natl Acad Sci U S A* **94**: 6261-6266
- Otegui M, Staehelin LA** (2000) Cytokinesis in flowering plants: more than one way to divide a cell. *Current Opinion in Plant Biology* **3**: 493-502
- Palevitz BA** (1987) Actin in the Preprophase Band of *Allium-Cepa*. *Journal of Cell Biology* **104**: 1515-1519
- Palevitz BA** (1993) Organization of the Mitotic Apparatus During Generative Cell-Division in *Nicotiana-Tabacum*. *Protoplasma* **174**: 25-35
- Palevitz BA, Hepler PK** (1974) Control of Plane of Division During Stomatal Differentiation in *Allium*. 1. Spindle Reorientation. *Chromosoma* **46**: 297-326
- Pan R, Lee YR, Liu B** (2004) Localization of two homologous *Arabidopsis* kinesin-related proteins in the phragmoplast. *Planta* **220**: 156-164
- Panteris E, Apostolakos P, Galatis B** (1995) The Effect of Taxol on *Triticum* Preprophase Root-Cells - Preprophase Microtubule Band Organization Seems to Depend on New Microtubule Assembly. *Protoplasma* **186**: 72-78
- Panteris E, Apostolakos P, Graf R, Galatis B** (2000) Gamma-tubulin colocalizes with microtubule arrays and tubulin paracrystals in dividing vegetative cells of higher plants. *Protoplasma* **210**: 179-187
- Pechatnikova E, Taylor EW** (1999) Kinetics processivity and the direction of motion of Ncd. *Biophysical Journal* **77**: 1003-1016
- Pierre P, Scheel J, Rickard JE, Kreis TE** (1992) Clip-170 Links Endocytic Vesicles to Microtubules. *Cell* **70**: 887-900
- Piperno G, Ledizet M, Chang XJ** (1987) Microtubules Containing Acetylated Alpha-Tubulin in Mammalian-Cells in Culture. *Journal of Cell Biology* **104**: 289-302
- Preuss ML, Delmer DP, Liu B** (2003) The cotton kinesin-like calmodulin-binding protein associates with cortical microtubules in cotton fibers. *Plant Physiology* **132**: 154-160
- Preuss ML, Kovar DR, Lee YRJ, Staiger CJ, Delmer DP, Liu B** (2004) A plant-specific kinesin binds to actin microfilaments and interacts with cortical microtubules in cotton fibers. *Plant Physiology* **136**: 3945-3955
- Reddy AS, Day IS** (2001) Kinesins in the *Arabidopsis* genome: a comparative analysis among eukaryotes. *BMC Genomics* **2**: 2
- Reddy ASN** (2001) Molecular motors and their functions in plants. *International Review of Cytology - a Survey of Cell Biology*, Vol 204 **204**: 97-178
- Reilein AR, Rogers SL, Tuma MC, Gelfand VI** (2001) Regulation of molecular motor proteins. *Int Rev Cytol* **204**: 179-238
- Rice S, Lin AW, Safer D, Hart CL, Naber N, Carragher BO, Cain SM, Pechatnikova E, Wilson-Kubalek EM, Whittaker M, Pate E, Cooke R, Taylor EW, Milligan RA, Vale RD** (1999) A structural change in the kinesin motor protein that drives motility. *Nature* **402**: 778-784
- Rogers GC, Rogers SL, Schwimmer TA, Ems-McClung SC, Walczak CE, Vale RD, Scholey JM, Sharp DJ** (2004) Two mitotic kinesins cooperate to drive sister chromatid separation during anaphase. *Nature* **427**: 364-370
- Rogers SL, Tint IS, Fanapour PC, Gelfand VI** (1997) Regulated bidirectional motility of melanophore pigment granules along microtubules in vitro. *Proceedings of the National Academy of Sciences of the United States of America* **94**: 3720-3725
- Romagnoli S, Cai G, Cresti M** (2003) Kinesin-like proteins and transport of pollen tube organelles. *Cell Biology International* **27**: 255-256
- Rothwell SW, Grasser WA, Murphy DB** (1986) Tubulin Variants Exhibit Different Assembly Properties. *Annals of the New York Academy of Sciences* **466**: 103-110
- Saunders WS, Hoyt MA** (1992) Kinesin-Related Proteins Required for Structural Integrity of the Mitotic Spindle. *Cell* **70**: 451-458

- Savage C, Hamelin M, Culotti JG, Coulson A, Albertson DG, Chalfie M** (1989) Mec-7 Is a Beta-Tubulin Gene Required for the Production of 15-Protofilament Microtubules in *Caenorhabditis-Elegans*. *Genes & Development* **3**: 870-881
- Saxton WM, Stemple DL, Leslie RJ, Salmon ED, Zavortink M, Mcintosh JR** (1984) Tubulin Dynamics in Cultured Mammalian-Cells. *Journal of Cell Biology* **99**: 2175-2186
- Schaar BT, Chan GKT, Maddox P, Salmon ED, Yen TJ** (1997) CENP-E function at kinetochores is essential for chromosome alignment. *Journal of Cell Biology* **139**: 1373-1382
- Schiefelbein J, Galway M, Masucci J, Ford S** (1993) Pollen tube and root-hair tip growth is disrupted in a mutant of *Arabidopsis thaliana*. *Plant Physiol* **103**: 979-985
- Schliwa M, Woehlke G** (2001) Molecular motors - Switching on kinesin. *Nature* **411**: 424-425
- Schmit AC** (2002) Acentrosomal microtubule nucleation in higher plants. *Int Rev Cytol* **220**: 257-289
- Schnapp BJ, Crise B, Sheetz MP, Reese TS, Khan S** (1990) Delayed Start-up of Kinesin-Driven Microtubule Gliding Following Inhibition by Adenosine 5'-[Beta,Gamma-Imido]Triphosphate. *Proceedings of the National Academy of Sciences of the United States of America* **87**: 10053-10057
- Scholey JM, Brust-Mascher I, Mogilner A** (2003) Cell division. *Nature* **422**: 746-752
- Scholey JM, Heuser J, Yang JT, Goldstein LSB** (1989) Identification of Globular Mechanochemical Heads of Kinesin. *Nature* **338**: 355-357
- Schuyler SC, Pellman D** (2001) Microtubule "plus-end-tracking proteins": The end is just the beginning. *Cell* **105**: 421-424
- Sedbrook JC, Ehrhardt DW, Fisher SE, Scheible WR, Somerville CR** (2004) The *Arabidopsis* sku6/spiral1 gene encodes a plus end-localized microtubule-interacting protein involved in directional cell expansion. *Plant Cell* **16**: 1506-1520
- Seltzer V, Pawlowski T, Campagne S, Canaday J, Erhardt M, Evrard JL, Herzog E, Schmit AC** (2003) Multiple microtubule nucleation sites in higher plants. *Cell Biology International* **27**: 267-269
- Sharp DJ, Brown HM, Kwon M, Rogers GC, Holland G, Scholey JM** (2000a) Functional coordination of three mitotic motors in *Drosophila* embryos. *Molecular Biology of the Cell* **11**: 241-253
- Sharp DJ, Rogers GC, Scholey JM** (2000b) Microtubule motors in mitosis. *Nature* **407**: 41-47
- Shaw SL, Kamyar R, Ehrhardt DW** (2003) Sustained microtubule treadmilling in *Arabidopsis* cortical arrays. *Science* **300**: 1715-1718
- Shibaoka H** (1994) Plant Hormone-Induced Changes in the Orientation of Cortical Microtubules - Alterations in the Cross-Linking between Microtubules and the Plasma-Membrane. *Annual Review of Plant Physiology and Plant Molecular Biology* **45**: 527-544
- Shuster CB, Burgess DR** (2002) Targeted new membrane addition in the cleavage furrow is a late, separate event in cytokinesis. *Proceedings of the National Academy of Sciences of the United States of America* **99**: 3633-3638
- Smertenko A, Saleh N, Igarashi H, Mori H, Hauser-Hahn I, Jiang CJ, Sonobe S, Lloyd CW, Hussey PJ** (2000) A new class of microtubule-associated proteins in plants. *Nature Cell Biology* **2**: 750-753
- Smertenko AP, Chang HY, Wagner V, Kaloriti D, Fenyk S, Sonobe S, Lloyd C, Hauser MT, Hussey PJ** (2004) The *Arabidopsis* microtubule-associated protein AtMAP65-1: Molecular analysis of its microtubule bundling activity. *Plant Cell* **16**: 2035-2047
- Smirnova EA, Bajer AS** (1994) Microtubule Converging Centers and Reorganization of the Interphase Cytoskeleton and the Mitotic Spindle in Higher-Plant *Haemanthus*. *Cell Motility and the Cytoskeleton* **27**: 219-233
- Smirnova EA, Bajer AS** (1998) Early stages of spindle formation and independence of chromosome and microtubule cycles in *Haemanthus* endosperm (vol 40, pg 22, 1998). *Cell Motility and the Cytoskeleton* **40**: 315-315
- Smirnova EA, Reddy AS, Bowser J, Bajer AS** (1998) Minus end-directed kinesin-like motor protein, Kcbp, localizes to anaphase spindle poles in *Haemanthus* endosperm. *Cell Motil Cytoskeleton* **41**: 271-280
- Smith LG** (1999) Divide and conquer: cytokinesis in plant cells. *Curr Opin Plant Biol* **2**: 447-453
- Smith LG, Gerttula SM, Han SC, Levy J** (2001) TANGLED1: A microtubule binding protein required for the spatial control of cytokinesis in maize. *Journal of Cell Biology* **152**: 231-236
- Smith LG, Hake S, Sylvester AW** (1996) The tangled-1 mutation alters cell division orientations throughout maize leaf development without altering leaf shape. *Development* **122**: 481-489
- Song H, Golovkin M, Reddy ASN, Endow SA** (1997) In vitro motility of AtKCBP, a calmodulin-binding kinesin protein of *Arabidopsis*. *Proceedings of the National Academy of Sciences of the United States of America* **94**: 322-327

- Staehein LA, Hepler PK** (1996) Cytokinesis in higher plants. *Cell* **84**: 821-824
- Stoppin V, Vantard M, Schmit AC, Lambert AM** (1994) Isolated Plant Nuclei Nucleate Microtubule Assembly: The Nuclear Surface in Higher Plants Has Centrosome-like Activity. *Plant Cell* **6**: 1099-1106
- Stoppin-Mellet V, Gaillard J, Vantard M** (2002) Functional evidence for in vitro microtubule severing by the plant katanin homologue. *Biochem J* **365**: 337-342
- Stoppin-Mellet V, Gaillard J, Vantard M** (2003) Plant katanin, a microtubule severing protein. *Cell Biology International* **27**: 279-279
- Stoppin-Mellet V, Peter C, Lambert AM** (2000) Distribution of gamma-tubulin in higher plant cells: Cytosolic gamma-tubulin is part of high molecular weight complexes. *Plant Biology* **2**: 290-296
- Strompen G, El Kasmi F, Richter S, Lukowitz W, Assaad FF, Jurgens G, Mayer U** (2002) The Arabidopsis HINKEL gene encodes a kinesin-related protein involved in cytokinesis and is expressed in a cell cycle-dependent manner. *Curr Biol* **12**: 153-158
- Sugimoto K, Himmelspach R, Williamson RE, Wasteneys GO** (2003) Mutation or drug-dependent microtubule disruption causes radial swelling without altering parallel cellulose microfibril deposition in Arabidopsis root cells. *Plant Cell* **15**: 1414-1429
- Sylvester AW** (2000) Division decisions and the spatial regulation of cytokinesis. *Curr Opin Plant Biol* **3**: 58-66
- Tanaka H, Ishikawa M, Kitamura S, Takahashi Y, Soyano T, Machida C, Machida Y** (2004) The AtNACK1/HINKEL and STUD/TETRASPORE/AtNACK2 genes, which encode functionally redundant kinesins, are essential for cytokinesis in Arabidopsis. *Genes to Cells* **9**: 1199-1211
- Tanaka Y, Kanai Y, Okada Y, Nonaka S, Takeda S, Harada A, Hirokawa N** (1998) Targeted disruption of a mouse conventional kinesin heavy chain, kif5B, results in perinuclear clustering of mitochondria. *Molecular Biology of the Cell* **9**: 30a-30a
- Tanudji M, Shoemaker J, L'Italien L, Russell L, Chin G, Schebye XM** (2004) Gene silencing of CENP-E by small interfering RNA in HeLa cells leads to missegregation of chromosomes after a mitotic delay. *Molecular Biology of the Cell* **15**: 3771-3781
- Tassin AM, Celati C, Moudjou M, Bornens M** (1998) Characterization of the human homologue of the yeast spc98p and its association with gamma-tubulin. *J Cell Biol* **141**: 689-701
- Thitamadee S, Tuchiara K, Hashimoto T** (2002) Microtubule basis for left-handed helical growth in Arabidopsis. *Nature* **417**: 193-196
- Tirnauer JS, Grego S, Salmon ED, Mitchison TJ** (2002) EB1-microtubule interactions in Xenopus egg extracts: Role of EB1 in microtubule stabilization and mechanisms of targeting to microtubules. *Molecular Biology of the Cell* **13**: 3614-3626
- Torresruiz RA, Jurgens G** (1994) Mutations in the FASS Gene Uncouple Pattern-Formation and Morphogenesis in Arabidopsis Development. *Development* **120**: 2967-2978
- Touitou I, Lhomond G, Pruliere G** (2001) Boursin, a sea urchin bimC kinesin protein, plays a role in anaphase and cytokinesis. *Journal of Cell Science* **114**: 481-491
- Tournebize R, Popov A, Kinoshita K, Ashford AJ, Rybina S, Pozniakovskiy A, Mayer TU, Walczak CE, Karsenti E, Hyman AA** (2000) Control of microtubule dynamics by the antagonistic activities of XMAP215 and XKCM1 in Xenopus egg extracts. *Nature Cell Biology* **2**: 13-19
- Traas J, Bellini C, Nacry P, Kronenberger J, Bouchez D, Caboche M** (1995) Normal Differentiation Patterns in Plants Lacking Microtubular Preprophase Bands. *Nature* **375**: 676-677
- Twell D, Park SK, Hawkins TJ, Schubert R, Schmidt R, Smertenko A, Hussey PJ** (2002) MOR1/GEM1 has an essential role in the plant-specific cytokinetic phragmoplast. *Nature Cell Biology* **4**: 711-714
- Vale RD, Fletterick RJ** (1997) The design plan of kinesin motors. *Annual Review of Cell and Developmental Biology* **13**: 745-777
- Vale RD, Milligan RA** (2000) The way things move: Looking under the hood of molecular motor proteins. *Science* **288**: 88-95
- Vale RD, Reese TS, Sheetz MP** (1985) Identification of a Novel Force-Generating Protein, Kinesin, Involved in Microtubule-Based Motility. *Cell* **42**: 39-50
- Valiron O, Caudron N, Job D** (2001) Microtubule dynamics. *Cell Mol Life Sci* **58**: 2069-2084
- Van Damme D, Bouget FY, Van Poucke K, Inze D, Geelen D** (2004a) Molecular dissection of plant cytokinesis and phragmoplast structure: a survey of GFP-tagged proteins. *Plant J* **40**: 386-398
- Van Damme D, Van Poucke K, Boutant E, Ritzenthaler C, Inze D, Geelen D** (2004b) In Vivo Dynamics and Differential Microtubule-Binding Activities of MAP65 Proteins. *Plant Physiol* **136**: 3956-3967
- Vanlammeren AAM** (1988) Structure and Function of the Microtubular Cytoskeleton During Endosperm Development in Wheat - an Immunofluorescence Study. *Protoplasma* **146**: 18-27

- Vantard M, Levilliers N, Hill AM, Adoutte A, Lambert AM** (1990) Incorporation of Paramecium axonemal tubulin into higher plant cells reveals functional sites of microtubule assembly. *Proc Natl Acad Sci U S A* **87**: 8825-8829
- Vantard M, Schellenbaum P, Fellous A, Lambert AM** (1991) Characterization of Maize Microtubule-Associated Proteins, One of Which Is Immunologically Related to Tau. *Biochemistry* **30**: 9334-9340
- Vasquez RJ, Gard DL, Cassimeris L** (1994) Xmap from *Xenopus* Eggs Promotes Rapid Plus End Assembly of Microtubules and Rapid Microtubule Polymer Turnover. *Journal of Cell Biology* **127**: 985-993
- Vasquez RJ, Gard DL, Cassimeris L** (1999) Phosphorylation by CDK1 regulates XMAP215 function in vitro. *Cell Motility and the Cytoskeleton* **43**: 310-321
- Verma DP** (2001) Cytokinesis and Building of the Cell Plate in Plants. *Annu Rev Plant Physiol Plant Mol Biol* **52**: 751-784
- Vos JW, Dogterom M, Emons AMC** (2004) Microtubules become more dynamic but not shorter during preprophase band formation: A possible "search-and-capture" mechanism for microtubule translocation. *Cell Motility and the Cytoskeleton* **57**: 246-258
- Vos JW, Safadi F, Reddy AS, Hepler PK** (2000) The kinesin-like calmodulin binding protein is differentially involved in cell division. *Plant Cell* **12**: 979-990
- Wainwright S** (1976) *Mechanical Design in Organisms*. London: Edward Arnold Limited
- Walczak CE, Mitchison TJ, Desai A** (1996) XKCM1: A *Xenopus* kinesin-related protein that regulates microtubule dynamics during mitotic spindle assembly. *Cell* **84**: 37-47
- Walker ML, Burgess SA, Sellers JR, Wang F, Hammer JA, Trinick J, Knight PJ** (2000) Two-headed binding of a processive myosin to F-actin. *Nature* **405**: 804+
- Walker RA, O'Brien ET, Pryer NK, Soboeiro MF, Voter WA, Erickson HP, Salmon ED** (1988) Dynamic instability of individual microtubules analyzed by video light microscopy: rate constants and transition frequencies. *J Cell Biol* **107**: 1437-1448
- Wasteney GO** (2002) Microtubule organization in the green kingdom: chaos or self-order? *J Cell Sci* **115**: 1345-1354
- Wasteney GO** (2004) Progress in understanding the role of microtubules in plant cells. *Current Opinion in Plant Biology* **7**: 651-660
- Webb M, Jouannic S, Foreman J, Linstead P, Dolan L** (2002) Cell specification in the Arabidopsis root epidermis requires the activity of ECTOPIC ROOT HAIR 3--a katanin-p60 protein. *Development* **129**: 123-131
- Webb MC, Gunning BES** (1990) Embryo Sac Development in Arabidopsis-Thaliana .1. Megasporogenesis, Including the Microtubular Cytoskeleton. *Sexual Plant Reproduction* **3**: 244-256
- Webb MC, Gunning BES** (1991) The Microtubular Cytoskeleton During Development of the Zygote, Proembryo and Free-Nuclear Endosperm in Arabidopsis-Thaliana (L) Heynh. *Planta* **184**: 187-195
- Webb MC, Gunning BES** (1994) Embryo Sac Development in Arabidopsis-Thaliana .2. The Cytoskeleton During Megagametogenesis. *Sexual Plant Reproduction* **7**: 153-163
- Weingartner M, Binarova P, Drykova D, Schweighofer A, David JP, Heberle-Bors E, Doonan J, Bogre L** (2001) Dynamic recruitment of Cdc2 to specific microtubule structures during mitosis. *Plant Cell* **13**: 1929-1943
- Whittington AT, Vugrek O, Wei KJ, Hasenbein NG, Sugimoto K, Rashbrooke MC, Wasteney GO** (2001) MOR1 is essential for organizing cortical microtubules in plants. *Nature* **411**: 610-613
- Wick S** (2000) Plant microtubules meet their MAPs and mimics. *Nat Cell Biol* **2**: E204-206
- Wick SM** (1991) Spatial aspects of cytokinesis in plant cells. *Curr Opin Cell Biol* **3**: 253-260
- Wick SM, Duniec J** (1983) Immunofluorescence microscopy of tubulin and microtubule arrays in plant cells. I. Preprophase band development and concomitant appearance of nuclear envelope-associated tubulin. *J Cell Biol* **97**: 235-243
- Wicker-Planquart C, Stoppin-Mellet V, Blanchoin L, Vantard M** (2004) Interactions of tobacco microtubule-associated protein MAP65-1b with microtubules. *Plant Journal* **39**: 126-134
- Wilson PG, Simmons R, Shigali S** (2004) Novel nuclear defects in KLP61F-deficient mutants in *Drosophila* are partially suppressed by loss of Ncd function. *J Cell Sci* **117**: 4921-4933
- Wymer CL, Fisher DD, Moore RC, Cyr RJ** (1996) Elucidating the mechanism of cortical microtubule reorientation in plant cells. *Cell Motility and the Cytoskeleton* **35**: 162-173
- Yang CY, Spielman M, Coles JP, Li Y, Ghelani S, Bourdon V, Brown RC, Lemmon BE, Scott RJ, Dickinson HG** (2003) TETRASPORE encodes a kinesin required for male meiotic cytokinesis in Arabidopsis. *Plant J* **34**: 229-240

- Yang JT, Laymon RA, Goldstein LSB** (1989) A 3-Domain Structure of Kinesin Heavy-Chain Revealed by DNA-Sequence and Microtubule Binding Analyses. *Cell* **56**: 879-889
- Yang JT, Saxton WM, Stewart RJ, Raff EC, Goldstein LSB** (1990) Evidence That the Head of Kinesin Is Sufficient for Force Generation and Motility In Vitro. *Science* **249**: 42-47
- Yildiz A, Forkey JN, McKinney SA, Ha T, Goldman YE, Selvin PR** (2003) Myosin V walks hand-over-hand: Single fluorophore imaging with 1.5-nm localization. *Science* **300**: 2061-2065
- Young T, Hyams JS, Lloyd CW** (1994) Increased Cell Cycle-Dependent Staining of Plant-Cells by the Antibody Mpm-2 Correlates with Preprophase Band Formation. *Plant Journal* **5**: 279-284
- Zhang D, Wadsworth P, Hepler PK** (1993) Dynamics of Microfilaments Are Similar, but Distinct from Microtubules During Cytokinesis in Living, Dividing Plant-Cells. *Cell Motility and the Cytoskeleton* **24**: 151-155
- Zhang DH, Wadsworth P, Hepler PK** (1990) Microtubule Dynamics in Living Dividing Plant-Cells - Confocal Imaging of Microinjected Fluorescent Brain Tubulin. *Proceedings of the National Academy of Sciences of the United States of America* **87**: 8820-8824
- Zhong R, Burk DH, Morrison WH, 3rd, Ye ZH** (2002) A kinesin-like protein is essential for oriented deposition of cellulose microfibrils and cell wall strength. *Plant Cell* **14**: 3101-3117

The background of the slide is a large fluorescence microscopy image of Arabidopsis cells. The cell walls are stained with a bright green fluorescent marker, creating a honeycomb-like pattern. Within several of these cells, the internal structures, particularly the nuclei and chromosomes, are also stained with the same green marker, indicating the presence of mitotic kinesins. A smaller, more detailed inset image is located in the upper left quadrant, showing a similar but more magnified view of the cell walls and internal structures.

Chapter 2

Mitotic kinesins in Arabidopsis

Adapted from 'Mitotic kinesins in Arabidopsis' by Vanstraelen M, Inzé D and Geelen D. In preparation.

Chapter page: *Arabidopsis thaliana* leaf epidermal cells, expressing free GFP, imaged using confocal microscopy (GFP filter settings).

Abstract

During cell division, plant cells make unique MT structures such as the PPB and the phragmoplast that contribute to aspects of division orientation and cytokinesis. MAPs play an important role in regulating MT behavior to establish these plant specific MT arrays. We searched for kinesins in the Arabidopsis genome that are cell cycle controlled. In the publicly available Affymetrix microarray data of synchronized Arabidopsis tissue culture cells, 22 kinesin genes were found that show increased expression during mitosis. The presence of putative phosphorylation sites, protein degradation boxes and regulatory promoter elements support a function for these motors in cell division. A comparison between kinesins from plants, animal, yeast and fungi kinesins suggests that functions for kinesins in establishing spindle bipolarity are conserved between eukaryotes. Some homologues of animal kinesins that function in chromosome movement play unrelated roles in plant cells and appear to be involved in processes during interphase. Seven mitotic kinesins belong to the C-terminal subfamily. Because C-terminal kinesins typically show minus-end directed movement, one can assume that some of their functions relate to that of dyneins for which no homologues are found in plants. Also, plants lack centrosomes at spindle poles where MT minus-ends congregate and therefore may require specially adapted kinesins. Finally, nine kinesins that are transcriptionally up-regulated during mitosis may be plant specific. Some of these were shown to function in phragmoplast dynamics during cytokinesis. The analysis of uncharacterized plant specific kinesins with a mitotic expression profile may shed light on the function of motor proteins in PPB formation, a structure that is not very well understood.

Introduction

During cell division, the plant cytoskeleton rearranges into different conformations to segregate the sister chromatids and to align and build the cell plate (Wasteneys, 2002). The organization of MTs into different arrays requires the cooperation of MAPs. Numerous MAPs, both structural as motor MAPs have already been discovered in plants (Gardiner and Marc, 2003). The diversity of these MAPs indicates that the cellular machinery regulating MT organization is complex. In animal mitosis, kinesins play many roles in MT organization and dynamics and chromosome movement. The knowledge of plant kinesins in these processes is limited. In addition, plant cells use specialized MT arrays such as the PPB and the phragmoplast that are absent in other kingdoms. The functioning of these plant specific structures suggest specialized functions for kinesins in plants as well as the presence of plant specific motor proteins.

Results and Discussion

22 kinesins are specifically transcribed during M-phase

The development of synchronization methods for *A. thaliana* suspension cultures facilitated transcript profiling of cell cycle regulation on genome scale (Menges and Murray, 2002). We consulted the publicly available Affymetrix microarray data of synchronized Arabidopsis tissue culture cells (Menges et al., 2003) and identified 22 kinesin genes that were up-regulated during mitosis (Fig. 2.1, Table 2.1). More recently, Menges et al. (2005) used the expression profiles of A- and B-type cyclins to identify genes involved in early mitosis. 10 out of the 22 selected mitotic kinesins showed peaks at the G2/M boundary (Table 2.1).

The expression of mitotic cyclins during cell cycle depends on the presence of cis-acting elements in the promoters, called the MSA (mitosis specific activation) elements. These are necessary and sufficient for periodic promoter activation at the G2/M boundary (Ito et al., 1998; Araki et al., 2004). Two MSA motifs are present in the promoter of the plant specific kinesin NACK1. Tobacco NACK1 transcript is almost undetectable before mitosis. It accumulates during M-phase and peaks when the mitotic index (MI) is highest. Mutant NACK1 promoters, in which both MSA motifs were destroyed, showed that the MSA elements in the promoter drove G2/M specific transcription (Ito et al., 2001). This illustrates that MSA elements also determine transcriptional expression of kinesin genes. Consistent with the NACK1 transcription level, the NACK1 protein accumulated during M-phase and peaked one time point later than the MI. In tobacco and Arabidopsis, NACK1 functions in the lateral expansion of the phragmoplast MTs (Nishihama et al., 2002).

We analyzed the promoters of the 22 mitotically up-regulated kinesins in Arabidopsis and found that MSA motifs were strongly represented. In total, 48 MSA motifs were identified and 19 of the 22 mitotic kinesin promoters contained at least one MSA element (Table 2.1).

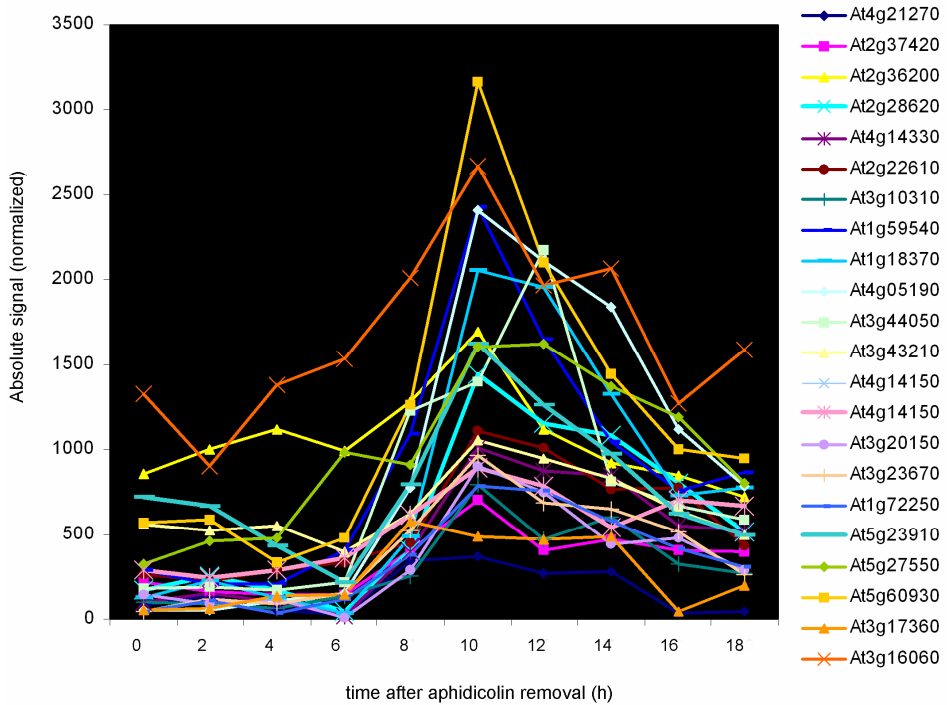


Figure 2.1 Transcript levels of 22 mitotic up-regulated kinesins through the cell cycle.

Arabidopsis cell suspension cultures were chemically synchronized in the presence of DNA polymerase inhibitor aphidicolin. Transcript levels of all 61 Arabidopsis kinesins were quantified before and after release from the S-phase block with Affymetrix microarray chips, as described by Menges et al. (2003). Profiles are only shown for those that were found up-regulated during mitosis.

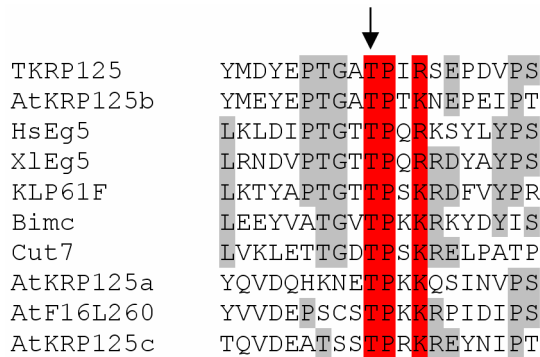


Figure 2.2 Alignment of the bimC box in BimC/Kinesin-5 members. Alignment of bimC boxes from tobacco (TKRP125), Arabidopsis (AtKRP125a-c), human (HsEg5), Xenopus (XlEg5), Drosophila (KLP61F) and yeast (Cut7 and bimC). The consensus site for CDK (S/TPxK/R) is highlighted in red and the phosphorylated threonine is indicated by an arrow. Other amino acids that are identical are highlighted in grey.

Cell cycle regulation by protein phosphorylation

Cell cycle progression is controlled by reversible phosphorylation by protein kinases and phosphatases, and in particular the serine-threonine kinase activity of cyclin dependent kinase (CDK) complexes are of key importance (Morgan, 1997). In yeast and animal cells, CDK regulates MT organization and dynamics by phosphorylation of proteins that function in MT arrangement and transport activities (Cassimeris, 1999; Andersen, 2000). Kinesins are one of the targets for CDK phosphorylation. Members of the BimC/Kinesin-5 subfamily contain a phosphorylation site around a conserved sequence motif, called the BimC box. Phosphorylation of the human BimC kinesin Eg5 regulates binding to the mitotic spindle, which ensures the formation of a bipolar spindle (Blangy et al., 1995; Sawin and Mitchison, 1995). The cytoskeleton in plants is also under control of CDK kinases (Vantard et al., 2000). Plant A-type CDKs, such as CDKA;1 associate with MTs in dividing cells, including the PPB and the phragmoplast (Stals et al., 1997; Weingartner et al., 2001). Microinjection of CDK1 in *Tradescantia* cells causes rapid disassembly of the PPB MTs (Hush et al., 1996) and treatment of metaphase cells with inhibitors of CDKs results in abnormal spindles (Binarova et al., 1998a). The tobacco kinesin TKRP125 belongs to the BimC/Kinesin-5 subfamily and consistent with this, it contains a CDK phosphorylation site in the BimC box (Asada et al., 1997). TKRP125 localizes to the PPB, spindle and phragmoplast. It is possible that association of TKRP125 with these mitotic structures is under control of CDK phosphorylation.

We looked for the occurrence of CDKA;1 phosphorylation sites in the set of 22 kinesins up-regulated during mitosis. In addition to cell cycle controlled accumulation during M-phase, 13 out of 22 kinesins contained at least one CDKA;1 phosphorylation site (Table 2.1). Amongst these were the three *Arabidopsis* homologues of the tobacco TKRP125. Alignment of the BimC boxes from tobacco TKRP125, the three *Arabidopsis* homologues and those in animal and yeast shows that the BimC boxes of tobacco TKRP125 and *Arabidopsis* AtKRP125b are closest related to those of yeast and animal (Fig. 2.2).

Other animal kinesins that are phosphorylated by CDKA;1 belong to the Chromokinesin/Kinesin-4, CENP-E/Kinesin-7 and MKLP1/Kinesin-6 subfamilies (Reilein et al., 2001). According to the nomenclature of Lawrence et al. (2004), there are no *Arabidopsis* kinesins that belong to the MKLP/Kinesin-6 subfamily. Chromokinesins and CENP-E family members are present in *Arabidopsis* and according to our analysis, each subfamily contains one mitotic kinesin. These did not contain a CDKA;1 phosphorylation site, suggesting that in contrast to their animal counterparts, they are not regulated by CDK phosphorylation.

Cell cycle control of kinesin protein level

Several key cell cycle regulators are rapidly degraded during anaphase to allow exit from mitosis. These carry a destruction box (D-box) in their protein sequence that is essential for its degradation at the onset of anaphase by the 26S proteasome complex (Glotzer et al., 1991). Among the many

functions of the proteasome is the regulation of MT arrays during mitosis. The yeast MAP Ase1 localizes to the anaphase spindle midzone and is required for the elongation of the spindle during anaphase B. Mutations in the D-box of Ase1 delayed spindle disassembly, indicating that the proteasome mediates spindle disintegration by degradation of MAPs (Juang et al., 1997). A conserved D-box is also present in members of the plant specific subfamily of MAP65 proteins. AtMAP65-1 and the tobacco homologue NtMAP65-1 localize to the PPB, spindle and phragmoplast MTs during mitosis (Smertenko et al., 2000; Smertenko et al., 2004; Van Damme et al., 2004a and b). AtMAP65-4 only localizes to the spindle MTs, predominantly at the spindle poles and disappears at the end of anaphase (Van Damme et al., 2004b). The presence of a D-box in these MAPs, suggests that in plants proteolytic degradation of MAPs also controls the organization of MTs in the spindle and in plant specific MT arrays like the PPB and phragmoplast (Hussey et al., 2002; Van Damme et al., 2004b). We found at least one conserved D-box in all the 22 mitotic kinesins, suggesting that plant kinesins are substrates of the proteasome complex (Table 2.1). Whether their protein products are subjected to proteolytic degradation *in vivo* awaits further experimental confirmation.

During mitosis, APC substrates are degraded to allow sister chromatid separation during anaphase. For instance chromokinesins generate polar ejection forces during animal mitosis thereby contributing to chromosome alignment (Levesque and Compton, 2001; Kapoor and Compton, 2002). Degradation of chromokinesins, like Xkid at anaphase down regulates antipolar forces, allowing the separated chromatids to be transported to the opposite spindle poles (Funabiki and Murray, 2000; Scholey et al., 2003). *Xenopus* Xkid contains 5 putative D-box sequences; however it is degraded by the proteasome in a D-box independent pathway (Castro et al., 2003). To date, it is not known whether the single mitotically up-regulated chromokinesin of *Arabidopsis* functions in chromosome movements during metaphase. We found 4 D-boxes in the protein sequence of this kinesin. Experimental data will determine whether this chromokinesin is degraded by the proteasome in D-box dependent or independent pathway to allow sister chromatid separation.

For several plant kinesins, protein levels have been investigated throughout cell cycle in synchronized BY-2 cells (Mitsui et al., 1996; Asada et al., 1997; Bowser and Reddy, 1997; Nishihama et al., 2002). The tobacco kinesins ATK2, ATK3, TKRP125, KCBP and NACK1 protein levels increased during M-phase, reached the highest level at the MI peak, and decreased afterwards. TKRP125 and NACK1 function in phragmoplast dynamics (Asada et al., 1997; Nishihama et al., 2002). *Arabidopsis* homologues of these kinesins are transcriptionally up-regulated during mitosis (Table 2.1) and their protein sequences contain respectively, 4-5 and 3 D-boxes. The *Arabidopsis* counterparts of ATK2, ATK3 and KCBP were not recognized as mitotic kinesins based on transcript levels during cell division. They all contain one or more D-boxes, pointing to a possible control of protein level during M-phase by proteolytic degradation. KCBP localizes to all mitotic arrays during cell division and a function in spindle pole formation has been proposed based on antibody microinjection experiments (Bowser and Reddy, 1997; Vos et al., 2000). The intracellular localization and involvement of the ATK2 and ATK3 kinesins in cell division still remains to be

determined. Thus, absence of kinesins from the list of mitotically up-regulated kinesins does not exclude a function in cell division. For instance, KCA1 and KCA2 are not transcriptionally up-regulated during mitosis. Yet, the proteins interact with the cell cycle kinase CDKA₁, suggesting control of these proteins during cell division (Vanstraelen et al., 2004).

M-phase specific kinesins related to animal kinesins

The Arabidopsis genome counts 21 C-terminal/Kinesin-14 members of which 7 are transcriptionally up-regulated during mitosis. *In vitro* experiments for three members of the Arabidopsis C-terminal subfamily, including ATK1 and ATK5, shows that they move towards the minus-end of MTs (Song et al., 1997; Marcus et al., 2002; Ambrose et al., 2005), suggesting that C-terminal kinesins in plants also display minus-end directed motility. In animal cells, minus-end directed kinesins, like Ncd function in several aspects of the formation of the bipolar spindle. Ncd localizes to the spindle poles and cooperates with dynein to bundle MTs into spindle poles which are attached to the centrosome (Hatsumi and Endow, 1992; Merdes et al., 2000). The Arabidopsis kinesins ATK1 and ATK5 are related to animal Ncd (Reddy and Day, 2001) and are mitosis specific (Table 2.1). Both localize to the spindle MTs (Chen et al., 2002; Marcus et al., 2003; Ambrose et al., 2005). Knock-out mutants form spindles with abnormally broad poles, similar to Ncd defective spindles, suggesting that ATK1 and ATK5 focus the minus-ends of spindle MTs into spindle poles.

In animal cells, kinesins of the C-terminal/Kinesin-14 subfamily antagonize the forces of BimC/Kinesin-5 members to establish the bipolar mirror-like structure of the spindle (Sharp et al., 2000b). BimC-like kinesins, like *Drosophila* KLP61F are plus-end directed bipolar homotetramers that cross-link and slide antiparallel MTs of spindle midzone, thereby generating poleward forces. Failure of BimC-like kinesins to associate with the spindle, results in the formation of monopolar spindles (Blangy et al., 1995; Wilson et al., 2004). This phenotype can be partially rescued by mutations in the C-terminal kinesin Ncd, suggesting that a balance of plus- and minus-end directed forces establishes the bipolar spindle (Wilson et al., 2004). These results were obtained for C-terminal and BimC-like kinesins from animal, yeast and fungi (Saunders and Hoyt, 1992; O'Connell et al., 1993; Wilson et al., 2004), suggesting that functions for kinesins in establishing spindle bipolarity are conserved among eukaryotes. Three out of the four BimC-like kinesins of Arabidopsis are transcriptionally up-regulated during M-phase. These are homologues of the tobacco TKRP125, which localizes to MTs of the PPB, spindle and phragmoplast (Asada et al., 1997). In addition, poleward translocation of phragmoplast MTs was inhibited upon microinjection of an antibody against TKRP125, suggesting that plant BimC kinesins slide antiparallel MTs polewards, similar to animal BimC kinesins. Mutations in the C-terminal kinesin ATK1 not only cause spindle poles to broaden, but also result in reduced bipolarity of the spindle, suggesting that ATK1 functions in both establishing bipolarity and spindle pole formation (Chen et al., 2002). It is possible that ATK1 and AtKRP125 function antagonistically in the spindle midzone to establish a bipolar spindle during metaphase in plant cells. By anaphase, Ncd appears to have no effect on spindle pole movements,

suggesting that its activity is down-regulated at this time, to allow BimC-like kinesins to drive spindle elongation during anaphase B (Sharp et al., 2000a). This might explain why spindle abnormalities in ATK1 mutants were rectified by anaphase in somatic cells and is consistent with the presence of a D-box in the protein sequence of ATK1 (Marcus et al., 2003).

In plant cells, spindles are formed in absence of centrosomes and consistent with this spindle poles in plants are broader than in animal cells (Wasteneys, 2002). Centrosomes are also absent from *Drosophila* oocytes (Merdes and Cleveland, 1997; Kwon and Scholey, 2004; Manandhar et al., 2005). Here, acentrosomal spindle assembly is accomplished in two steps; spontaneous nucleation of MTs around condensed chromatin followed by sorting of randomly oriented MTs into a bipolar spindle (Manandhar et al., 2005). The latter involves the antagonizing action of BimC and C-terminal kinesins to establish spindle bipolarity and the cooperation between C-terminal kinesin and dynein to bundle MT minus-ends into spindle poles. In this way, spindle organization in plants might resemble acentrosomal spindle formation in *Drosophila* oocytes. γ -tubulin and Spc98p have been localized to plant kinetochores (Binarova et al., 1998b) indicating that spindle MTs arise by de novo assembly at kinetochore MTOCs. AtKRP125 and ATK1 could be involved in establishing spindle bipolarity while ATK5 and ATK1 focus minus-ends of spindle MTs into poles (Marcus et al., 2003; Ambrose et al., 2005). Dynein on the other hand is not present in plant cells (Lawrence et al., 2001), which seem to have employed unique kinesins to focus spindle poles. The minus-end directed motor KCBP is special in that its MT binding and motor activity is inhibited upon binding Ca^{++} /calmodulin (Narasimhulu et al., 1997; Song et al., 1997; Deavours et al., 1998). This motor localizes to the spindle poles in *Haemanthus* endosperm and is proposed to converge MT minus-ends into spindle poles by sliding and bundling MTs during nuclear envelope breakdown and anaphase (Smirnova et al., 1998; Vos et al., 2000).

After nuclear envelope breakdown in animal cells, pairs of sister chromatids associate with the spindle and oscillate until they are bi-oriented (attached to both spindle poles) and aligned at the metaphase plate (Murray and Mitchison, 1994). Chromosome alignment requires the cooperative action of kinesins from different subfamilies, generating poleward or antipoleward forces. Members of the Chromokinesin/Kinesin-4, CENP-E/Kinesin-7, Kip3/Kinesin-8 and MCAK/Kinesin-13 subfamily contribute to chromosome alignment (Schaar et al., 1997; Antonio et al., 2000; Yucel et al., 2000; West et al., 2002; Kline-Smith et al., 2004). Chromosome oscillation till metaphase alignment has also been observed in plants and members of the kinesin subfamilies that function in chromosome alignment are present in *Arabidopsis* (Yu et al., 1997; Reddy and Day, 2001). We looked for mitotic kinesins in subfamilies that are implicated in chromosome movements in animal cells. *Arabidopsis* contains three chromokinesins of which one is up-regulated during mitosis (Table 2.1). Chromokinesins push chromosome arms towards the spindle equator and generate a force gradient that diminishes with increasing distance from the spindle pole (Levesque and Compton, 2001; Kapoor and Compton, 2002). For instance, immunodepletion of Xkid in frog egg extracts results in chromosome misalignment during metaphase (Castro et al., 2003). Other chromokinesins, like Xklp1 and KLP-18 orient the MT plus-ends towards the chromosomes and the minus-ends away,

thereby contributing to bipolar spindle assembly in *Drosophila* oocytes (Vernos et al., 1995; Segbert et al., 2003). The single mitotic chromokinesin in *Arabidopsis* might fulfill a related function in plants. AtFRA1 is an *Arabidopsis* chromokinesin that is not up-regulated during cell division. Consistent with this, AtFRA1 is not implicated in cell division but functions in orientating cellulose microfibrils in fiber walls (Zhong et al., 2002).

MCAK/Kinesin-13 family members (also called Kin-I in animals) depolymerize MTs and contribute to multiple aspects of chromosome movement. They localize to the centromeres, centrosomes and spindle midzone during mitosis. Depletion or disruption of MCAK activity has shown that they function in spindle maintenance, chromosome alignment and segregation and in controlling the proper attachment of MTs to sister chromatids (Moore and Wordeman, 2004). Mammals have three Kin-I kinesins: Kif2A, Kif2B and MCAK and *Drosophila melanogaster* has four: Klp10A, Klp59C, Klp59D and Klp67A. Kif2A and Klp10A depolymerize MTs from the centrosome, whereas MCAK and Klp59C depolymerize MTs from the centromere and Klp67A functions in spindle assembly. *Arabidopsis* contains two members of the MCAK/Kinesin-13 subfamily, AtKinesin-13A and AtKinesin-13B (Lawrence et al., 2004). Only Kinesin-13B is transcriptionally up-regulated during mitosis. This suggests that in contrast to animal cells, functions for MT depolymerizing kinesins in plant mitosis are limited. The similarity of Kinesin13-A and Kinesin13-B to family members from other kingdoms is restricted to the catalytic core. They lack a Lys-rich neck motif that is commonly found in animal Kinesin-13s, implying that they function different from their animal counterparts (Lee and Liu, 2004). Indeed, Kinesin-13A is not up-regulated during mitosis. It localizes to Golgi stacks and contributes to their distribution in *Arabidopsis* trichomes (Lu et al., 2004).

Members of the Kinesin-7/CENP-E subfamily function in chromosome alignment and segregation. They control the interaction of the MT plus-ends of the spindle with the kinetochores of the chromosomes both during metaphase congression and anaphase segregation (Schaar et al., 1997; McEwen et al., 2001; Tanudji et al., 2004). Two members of this subfamily are represented in *Arabidopsis* of which one is up-regulated during mitosis (Table 2.1).

The survey of mitotic kinesins conserved in plants indicates that kinesin subfamilies involved in chromosome movement are present except for the Kip3/Kinesin-8 subfamily (Lawrence et al., 2004). Although these kinesins are represented by several copies in *Arabidopsis*, only a subset is mitotically regulated. However, transcript levels do not always reflect protein accumulation and functions for these kinesin members related to chromosome movement may be controlled at the protein level. *Arabidopsis* has 21 C-terminal/Kinesin-14 members of which 7 are up-regulated during mitosis (Table 2.1). This high number might compensate for functions carried out by dyneins in other organisms. In addition, C-terminal motors like Ncd function in chromosome segregation (Endow et al., 1990; Ali et al., 2000). Possibly, the contribution of C-terminal motors in chromosome movements has expanded in plants.

M-phase specific kinesins unique to plants

At first sight, cytokinesis in plant cells differs substantially from animal cells. In animal cells, cytokinesis is accomplished by an actin-myosin ring that forms around the cell equator and constricts inwards at telophase. As a consequence, interpolar MTs from the anaphase spindle bundle into a central spindle which is further compressed into a compact midbody at the end of cytokinesis (Glotzer, 2001). In contrast, plants construct a phragmoplast consisting of anti-parallel MTs. They guide Golgi-derived vesicles to the midline, and fusion of these vesicles forms a cell plate which will divide the daughter cells as the phragmoplast expands to the parent wall (Verma, 2001). Thus, animal cells appear to emphasize the use of a contractile ring, while plant cells appear more partial to membrane addition (Glotzer, 2001). However, the central spindle in animal cells seems to play a similar role as the phragmoplast in plant cells (Bowerman and Severson, 1999). During furrow ingression, membrane vesicles accumulate at the leading edge of the cleavage furrows and MT depolymerization blocks addition of new membrane during cytokinesis (Bluemink and Delaat, 1973; Danilchik et al., 1998). In addition, brefeldin A, an inhibitor of the vesicle traffic machinery, blocks cell plate formation in plants and inhibits the terminal phase of cytokinesis in *C. elegans* (Yasuhara et al., 1995; Yasuhara and Shibaoka, 2000; Skop et al., 2001). These findings emphasize an overlap to some extent in the roles that MT based motor proteins play in animal and plant cytokinesis. Several members of the BimC subfamily, localize to the midbody during cleavage furrow ingression in animal cells and to the phragmoplast in plant cells, suggesting that in addition to spindle formation, they perform a role in cytokinesis as well (Asada et al., 1997; Whitehead and Rattner, 1998; Giet et al., 1999; Uzbekov et al., 1999). In particular, sea urchin Borsin is required to complete cytokinesis, which was shown by expression of rigor-type mutant of Borsin in sea urchin embryos (Touitou et al., 2001). In BY-2 cells, TKRP125 localizes to the phragmoplast MTs and injection of an antibody directed against TKRP125 inhibited MT translocation in the phragmoplast (Asada et al., 1997). The Arabidopsis homologues of TKRP125 were up-regulated in mitosis and might also function in the establishment of the bipolar phragmoplast. MKLP1, CHO1, PavKLP and Zen4 are animal members from different organisms that belong to the MKLP1 subfamily (Glotzer, 2001). They localize to a narrow zone of the central spindle and are essential to cytokinesis by their role in central spindle assembly. Human Rab6-KIFL is related to MKLP1. It accumulates at the central spindle and becomes highly concentrated in the midbody. Although this kinesin is involved in membrane traffic through the Golgi apparatus during interphase, it is also required for completion of cytokinesis (Echard et al., 1998; Hill et al., 2000; Fontijn et al., 2001). It is possible that Rab6-KIFL functions in the delivery of vesicles from the Golgi apparatus to the site of membrane fusion.

Members of the MKLP1/Kinesin-6 subfamily are absent from Arabidopsis, suggesting that plants and animals mainly employ different kinesins to exert their divergent modes of cytokinesis. Arabidopsis counts 29 kinesins that do not belong to any of the established kinesin subfamilies and are unique to Arabidopsis (Lawrence et al., 2004). Nine of these (Table 2.1; numbers 14 – 22) are up-

regulated during mitosis, suggesting that these might be implicated in plant specific MT related processes linked with the PPB and the phragmoplast. Indeed all plant specific kinesins that are known to function in phragmoplast dynamics are mitotically up-regulated (Table 2.1).

AtPAKRP1 and the related AtPAKRP1L are associated with the MTs of the cylinder- and ring-like phragmoplast (Lee and Liu, 2000; Pan et al., 2004). It was proposed that they maintain the bipolar structure of the phragmoplast once BimC motors have established bipolarity (Lee and Liu, 2000). Single mutants do not reveal any phenotype suggesting that they can compensate for their loss of function (Pan et al., 2004). AtPAKRP2 is not related to any other kinesin. It localizes to the phragmoplast in a punctuate manner and accumulates at the cell plate. Membrane association and disruption of the localization after BFA treatment, suggest that AtPAKRP2 delivers Golgi-derived vesicles to the phragmoplast midline (Lee et al., 2001). NACK1 and NACK2 play a role in phragmoplast dynamics. NACK1/HIK is essential to somatic cytokinesis and functions in the reorganization of MTs during the lateral expansion of the cell plate (Nishihama et al., 2002; Strompen et al., 2002). NACK2/TES/STUD is the closest homologue of NACK1 and takes part in the assembly of the radial MT array in male meiotic cytokinesis (Hulskamp et al., 1997; Yang et al., 2003). Both NACK1 and NACK2 interact with NPK1 which is a MAPKKK, required for phragmoplast expansion (Nishihama et al., 2002).

Till now, roles for kinesin motors in the formation and dynamics of the PPB are lacking. This circular band of MTs is formed at the start of mitosis and at the same time MTs elsewhere in the cortex largely disappear (Mineyuki, 1999). It can be hypothesized that MTs are translocated by motor proteins from elsewhere in the cortex to congregate at the PPB site (Wymer et al., 1996; Asada et al., 1997). Recent studies however did not observe MT sliding during PPB formation and the authors concluded that molecular motors are not involved (Vos et al., 2004). Instead, the PPB is formed by an increase in dynamic instability of cortical MTs, which are preferentially bundled and stabilized at the PPB site (Dhonukshe and Gadella, 2003; Vos et al., 2004). MT stabilizing, bundling and dynamics are typical functions for structural MAPs. However, kinesins also play a role in MT dynamics and bundling (Goldstein and Philp, 1999; Hunter and Wordeman, 2000; Moore and Wordeman, 2004). Several plant kinesins have been localized to the PPB, among which tobacco TKRP125 (Liu et al., 1996; Asada et al., 1997; Bowser and Reddy, 1997; Barroso et al., 2000). At the PPB, kinesins could bundle the parallel MTs by a MT sliding mechanism. Four mitotically up-regulated plant specific kinesins that do not belong to the classic kinesin subfamilies remain uncharacterized to date. These might reveal functions for kinesins in PPB formation.

Arabidopsis kinesins that do not belong to any of the established kinesin subfamilies are assigned to different Arabidopsis subgroups and those that remain ungrouped are called orphan kinesins (Lawrence et al., 2004). Two Arabidopsis specific kinesin groups, At2 and group 1 do not have representatives that are mitotically up-regulated. These motor proteins may have functions more related to plant specific processes taking place during interphase.

General conclusions

We report that 22 out of 61 Arabidopsis kinesins are up-regulated during mitosis. Most of the kinesins that function in cell division in Arabidopsis or in other plants with homologues in Arabidopsis are represented in our dataset. MSA elements, CDKA;1 phosphorylation sites and D-boxes were strongly represented in the mitosis specific kinesins, supporting a role for these kinesins during cell division.

A comparison between plant-like and animal-like functions of kinesins during cell division suggests that functions for kinesins in bipolar spindle assembly are conserved among eukaryotes. For instance, the cooperation between C-terminal/Kinesin-14 and BimC/Kinesin-5 is documented in animal cells, yeast and fungi and data in the plant field also point in that direction.

However, many aspects of cell division addressed in the animal field remain unresolved in plants. Till now, no plant kinesins have been identified that function in chromosomal movements during mitosis, while numerous kinesins from different subfamilies contribute to these motions in animal cells (Kline-Smith and Walczak, 2004; Moore and Wordeman, 2004). In addition, non-mitotic plant members of these subfamilies fulfill unrelated functions when compared to their animal counterparts and function during interphase (Zhong et al., 2002; Lu et al., 2004). Finally, several aspects of cell division are unique to plants. MT arrays, like the PPB and phragmoplast play an important role in cell plate formation and alignment. A whole range of plant specific kinesins are present in Arabidopsis. Several of these function in phragmoplast and cell plate formation and were up-regulated during mitosis. Four other are not yet characterized and might shed light on the functions of motor proteins in PPBs.

Table 2.1 Arabidopsis kinesins that are transcriptionally up-regulated during mitosis.

| Kinesin subfamily | Nr | MIPs code | MSA elements | CDK sites | Destruction boxes |
|-----------------------------|-----------|------------------------|--|---|--|
| Chromokinesin/ Kinesin-4 | 1 | At5g60930 | cgtAACGgtct | | RLKELLDN RETLSGAN RNADGKEN RGAMLLQN |
| BimC/Kinesin-5 | 2 | At2g37420 | tacAACGgtac | TPKK | RTADTLLN RSAQEISN REEKQALN RTPFLEVN |
| | | AtKRP125a | cccAACGgtta | | |
| | 3 | At2g36200 AtKRP125b | gcgAACGgacg ttaAACGgcga | TPTK | REVAVSQN RTAETFLN RLHKANAN RFVLLLHN |
| CENPE/ Kinesin-7 | 4 | At2g28620 | cacAACGgtcg | TPRK | RDFRVDSN RTAETLLN RQLELLNN RFDPFLYN RPPLTAIN |
| | | AtKRP125c | catAACGgttc gctAACGgcgt cgtAACGgctc atcAACGgaga | | |
| | | 5 | At1g59540 | tcaAACGgctt taaAACGgtaa tcaAACGgcac | |
| MCAK/ Kinesin-13 | 6 | At3g16060 | tttAACGgatc | | RPTNQRKN RSRVLAEN RGADTTDN RLEGAEIN RPDMKKS |
| C-terminal/ Kinesin-14 | 7 | At4g21270 ATK1 | | | RQAFSAVN |
| | 8 | At2g47500 | tgaAACGgaaa ccaAACGgtag agaAACGgtag | | RESTSSQN RSVLDGYN RSPQSRNN |
| | | | 9 | At2g22610 | gttAACGgtaa cttAACGgtcg |
| | 10 | At3g10310 | tgtAACGgttt gtcAACGgctt | TPPR TPVK TPFR | RNGMILCN RDLMELGN RSVMDGYN RTIGKLIN RSPLGVAN |
| | | | 11 | At4g05190 ATK5 | |
| | 12 | At1g72250 | tcaAACGgcac atcAACGgtcg cgcAACGgaaa | TPQK | RECEEALN RVRLSIGN |
| | | | 13 | At5g27550 | |

| Kinesin subfamily | Nr | MIPs code | MSA elements | CDK sites | Destruction boxes |
|-------------------|----|------------------------|--|------------------------------|--|
| At1 | 14 | At1g18370 AtNACK1 | caaAACGgtca tctAACGgcta | TPER TPQK TPAR | RSYMASLN RNTLYFAN RAKEVTNN |
| At1 | 15 | At3g43210 AtNACK2 | cacAACGgtca ttgAACGgtca gagAACGgaa tgtAACGgaaa | TPPK | RMNRMKYKN RKEMFELN |
| / | 16 | At3g44050 | atgAACGgctg | | RSQSFEFN RAKLIKNN RGMGGVDN RLQKLVND RAKDVHTN |
| | 17 | At3g17360 | attAACGgcct | SPSR TPTR | RSRFARLN RAKLIQNN RVKVKNNM RILVAEMN RKQVITPN |
| / | 18 | At4g14150 AtPAKRP1 | cgtAACGggtc tccAACGgagg tttAACGgctc | | RTGATSVN RSLSQLGN RMKNDGNN RSLPHEDN RTQEEVEN RQYLRDEN |
| / | 19 | At3g20150 | tataACGgtcg | SPCR | RDALSGYN RGLDIIDN RLPSANEN RDLLKKN |
| / | 20 | At3g23670 AtPAKRP1L | tcaAACGgtcg tctAACGgata atcAACGgaga attAACGgctc | SPAK SPSK | RTGATSVN RSLSQLGN RVKDDKGN RWTEAESN |
| Orphan | 21 | At4g14330 AtPAKRP2 | ctaAACGgcta cacAACGgtta | TPNK SPDK | RVVESIAN |
| | 22 | At5g23910 | ataAACGgaaa cacAACGgcaa agaAACGgtac agaAACGgaa taaAACGgtgc cttAACGgtc | TPRK TPEK SPWK SPFK | RKLFGEAN RLQELSNN |

Methods

Sequence analysis

CDK phosphorylation sites and D-box sequences were identified with PATTINPROT, available at the ExPASy server (<http://www.expasy.org/tools/>). The patterns [ST]-P-x-[KR] and R-x(2)-L-x(4)-N were used respectively to search for these sites. MatInspector (version 2.2) was used to search for MSA motifs within the promoter region 1000 bp upstream of the ATG start codon of the selected genes (BIOBASE, Biological Databases, <http://www.gene-regulation.com/>) (Quandt et al., 1995).

Acknowledgements

We thank Stephane Rombauts for bioinformatic support for MSA box analysis of kinesin promoter sequences.

References

- Ali MY, Siddiqui ZK, Malik AB, Siddiqui SS** (2000) A novel C-terminal kinesin subfamily may be involved in chromosomal movement in *Caenorhabditis elegans*. *Febs Letters* **470**: 70-76
- Ambrose JC, Li W, Marcus A, Ma H, Cyr R** (2005) A Minus-End Directed Kinesin with +TIP Activity Is Involved in Spindle Morphogenesis. *Mol Biol Cell*
- Andersen SS** (2000) Spindle assembly and the art of regulating microtubule dynamics by MAPs and Stathmin/Op18. *Trends Cell Biol* **10**: 261-267
- Antonio C, Ferby I, Wilhelm H, Jones M, Karsenti E, Nebreda AR, Vernos I** (2000) Xkid, a chromokinesin required for chromosome alignment on the metaphase plate. *Cell* **102**: 425-435
- Araki S, Ito M, Soyano T, Nishihama R, Machida Y** (2004) Mitotic cyclins stimulate the activity of c-Myb-like factors for transactivation of G2/M phase-specific genes in tobacco. *J Biol Chem* **279**: 32979-32988
- Asada T, Kuriyama R, Shibaoka H** (1997) TKRP125, a kinesin-related protein involved in the centrosome-independent organization of the cytokinetic apparatus in tobacco BY-2 cells. *Journal of Cell Science* **110**: 179-189
- Barroso C, Chan J, Allan V, Doonan J, Hussey P, Lloyd C** (2000) Two kinesin-related proteins associated with the cold-stable cytoskeleton of carrot cells: characterization of a novel kinesin, DcKRP120-2. *Plant Journal* **24**: 859-868
- Binarova P, Dolezel J, Draber P, Heberle-Bors E, Strnad M, Bogre L** (1998) Treatment of *Vicia faba* root tip cells with specific inhibitors to cyclin-dependent kinases leads to abnormal spindle formation. *Plant Journal* **16**: 697-707
- Binarova P, Hause B, Dolezel J, Draber P** (1998) Association of gamma-tubulin with kinetochore/centromeric region of plant chromosomes. *Plant Journal* **14**: 751-757
- Blangy A, Lane HA, dHerin P, Harper M, Kress M, Nigg EA** (1995) Phosphorylation by p34(cdc2) regulates spindle association of human Eg5, a kinesin-related motor essential for bipolar spindle formation in vivo. *Cell* **83**: 1159-1169
- Bluemink JG, Delaat SW** (1973) New Membrane Formation During Cytokinesis in Normal and Cytochalasin B-Treated Eggs of *Xenopus-Laevis* .1. Electron-Microscope Observations. *Journal of Cell Biology* **59**: 89-108
- Bowerman B, Severson AF** (1999) Cell division: Plant-like properties of animal cell cytokinesis. *Current Biology* **9**: R658-R660
- Bowser J, Reddy AS** (1997) Localization of a kinesin-like calmodulin-binding protein in dividing cells of *Arabidopsis* and tobacco. *Plant J* **12**: 1429-1437
- Cassimeris L** (1999) Accessory protein regulation of microtubule dynamics throughout the cell cycle. *Curr Opin Cell Biol* **11**: 134-141
- Castro A, Vigneron S, Bernis C, Labbe JC, Lorca T** (2003) Xkid is degraded in a D-box, KEN-box, and A-box-independent pathway. *Mol Cell Biol* **23**: 4126-4138
- Chen C, Marcus A, Li W, Hu Y, Calzada JP, Grossniklaus U, Cyr RJ, Ma H** (2002) The *Arabidopsis* ATK1 gene is required for spindle morphogenesis in male meiosis. *Development* **129**: 2401-2409
- Danilchik MV, Funk WC, Brown EE, Larkin K** (1998) Requirement for microtubules in new membrane formation during cytokinesis of *Xenopus* embryos. *Developmental Biology* **194**: 47-60
- Deavours BE, Reddy ASN, Walker RA** (1998) Ca²⁺/calmodulin regulation of the *Arabidopsis* kinesin-like calmodulin-binding protein. *Cell Motility and the Cytoskeleton* **40**: 408-416
- Dhonukshe P, Gadella TWJ** (2003) Alteration of microtubule dynamic instability during preprophase band formation revealed by yellow fluorescent protein-CLIP170 microtubule plus-end labeling. *Plant Cell* **15**: 597-611
- Echard A, Jollivet F, Martinez O, Lacapere JJ, Rousselet A, Janoueix-Lerosey I, Goud B** (1998) Interaction of a Golgi-associated kinesin-like protein with Rab6. *Science* **279**: 580-585
- Endow SA, Henikoff S, Solerniedziela L** (1990) Mediation of Meiotic and Early Mitotic Chromosome Segregation in *Drosophila* by a Protein Related to Kinesin. *Nature* **345**: 81-83
- Fontijn RD, Goud B, Echard A, Jollivet F, van Marle J, Pannekoek H, Horrevoets AJG** (2001) The human kinesin-like protein RB6K is under tight cell cycle control and is essential for cytokinesis. *Molecular and Cellular Biology* **21**: 2944-2955
- Funabiki H, Murray AW** (2000) The *Xenopus* chromokinesin Xkid is essential for metaphase chromosome alignment and must be degraded to allow anaphase chromosome movement. *Cell* **102**: 411-424

- Gardiner J, Marc J** (2003) Putative microtubule-associated proteins from the Arabidopsis genome. *Protoplasma* **222**: 61-74
- Giet R, Uzbekov R, Cubizolles F, Le Guellec K, Prigent C** (1999) The *Xenopus laevis* aurora-related protein kinase pEg2 associates with and phosphorylates the kinesin-related protein XI Eg5. *Journal of Biological Chemistry* **274**: 15005-15013
- Glotzer M** (2001) Animal cell cytokinesis. *Annual Review of Cell and Developmental Biology* **17**: 351-386
- Glotzer M, Murray AW, Kirschner MW** (1991) Cyclin is degraded by the ubiquitin pathway. *Nature* **349**: 132-138
- Goldstein LS, Philp AV** (1999) The road less traveled: emerging principles of kinesin motor utilization. *Annu Rev Cell Dev Biol* **15**: 141-183
- Hatsumi M, Endow SA** (1992) Mutants of the Microtubule Motor Protein, Nonclaret Disjunctional, Affect Spindle Structure and Chromosome Movement in Meiosis and Mitosis. *Journal of Cell Science* **101**: 547-559
- Hill E, Clarke N, Barr FA** (2000) The Rab6-binding kinesin, Rab6-KIFL, is required for cytokinesis. *Embo Journal* **19**: 5711-5719
- Hulskamp M, Parekh NS, Grini P, Schneitz K, Zimmermann I, Lolle SJ, Pruitt RE** (1997) The *STUD* gene is required for male-specific cytokinesis after telophase II of meiosis in *Arabidopsis thaliana*. *Developmental Biology* **187**: 114-124
- Hunter AW, Wordeman L** (2000) How motor proteins influence microtubule polymerization dynamics. *J Cell Sci* **113 Pt 24**: 4379-4389
- Hush J, Wu LP, John PCL, Hepler LH, Hepler PK** (1996) Plant mitosis promoting factor disassembles the microtubule preprophase band and accelerates prophase progression in *Tradescantia*. *Cell Biology International* **20**: 275-287
- Hussey PJ, Hawkins TJ, Igarashi H, Kaloriti D, Smertenko A** (2002) The plant cytoskeleton: recent advances in the study of the plant microtubule-associated proteins MAP-65, MAP-190 and the *Xenopus* MAP215-like protein, MOR1. *Plant Molecular Biology* **50**: 915-924
- Ito M, Araki S, Matsunaga S, Itoh T, Nishihama R, Machida Y, Doonan JH, Watanabe A** (2001) G2/M-phase-specific transcription during the plant cell cycle is mediated by c-Myb-like transcription factors. *Plant Cell* **13**: 1891-1905
- Ito M, Iwase M, Kodama H, Lavisse P, Komamine A, Nishihama R, Machida Y, Watanabe A** (1998) A novel cis-acting element in promoters of plant B-type cyclin genes activates M phase-specific transcription. *Plant Cell* **10**: 331-341
- Juang YL, Huang J, Peters JM, McLaughlin ME, Tai CY, Pellman D** (1997) APC-mediated proteolysis of Ase1 and the morphogenesis of the mitotic spindle. *Science* **275**: 1311-1314
- Kapoor TM, Compton DA** (2002) Searching for the middle ground: mechanisms of chromosome alignment during mitosis. *J Cell Biol* **157**: 551-556
- Kline-Smith SL, Khodjakov A, Hergert P, Walczak CE** (2004) Depletion of centromeric MCAK leads to chromosome congression and segregation defects due to improper kinetochore attachments. *Mol Biol Cell* **15**: 1146-1159
- Kline-Smith SL, Walczak CE** (2004) Mitotic spindle assembly and chromosome segregation: Refocusing on microtubule dynamics. *Molecular Cell* **15**: 317-327
- Kwon M, Scholey JM** (2004) Spindle mechanics and dynamics during mitosis in *Drosophila*. *Trends in Cell Biology* **14**: 194-205
- Lawrence CJ, Dawe RK, Christie KR, Cleveland DW, Dawson SC, Endow SA, Goldstein LSB, Goodson HV, Hirokawa N, Howard J, Malmberg RL, McIntosh JR, Miki H, Mitchison TJ, Okada Y, Reddy ASN, Saxton WM, Schliwa M, Scholey JM, Vale RD, Walczak CE, Wordeman L** (2004) A standardized kinesin nomenclature. *Journal of Cell Biology* **167**: 19-22
- Lawrence CJ, Morris NR, Meagher RB, Dawe RK** (2001) Dyneins have run their course in plant lineage. *Traffic* **2**: 362-363
- Lee YR, Giang HM, Liu B** (2001) A novel plant kinesin-related protein specifically associates with the phragmoplast organelles. *Plant Cell* **13**: 2427-2439
- Lee YR, Liu B** (2000) Identification of a phragmoplast-associated kinesin-related protein in higher plants. *Curr Biol* **10**: 797-800
- Lee YR, Liu B** (2004) Cytoskeletal motors in Arabidopsis. Sixty-one kinesins and seventeen myosins. *Plant Physiol* **136**: 3877-3883
- Levesque AA, Compton DA** (2001) The chromokinesin Kid is necessary for chromosome arm orientation and oscillation, but not congression, on mitotic spindles. *J Cell Biol* **154**: 1135-1146

- Liu B, Cyr RJ, Palevitz BA** (1996) A kinesin-like protein, KatAp, in the cells of arabidopsis and other plants. *Plant Cell* **8**: 119-132
- Lu L, Lee YR, Pan R, Maloof JN, Liu B** (2004) An Internal Motor Kinesin Is Associated with the Golgi Apparatus and Plays a Role in Trichome Morphogenesis in Arabidopsis. *Mol Biol Cell*
- Manandhar G, Schatten H, Sutovsky P** (2005) Centrosome reduction during gametogenesis and its significance. *Biology of Reproduction* **72**: 2-13
- Marcus AI, Ambrose JC, Blickley L, Hancock WO, Cyr RJ** (2002) Arabidopsis thaliana protein, ATK1, is a minus-end directed kinesin that exhibits non-processive movement. *Cell Motil Cytoskeleton* **52**: 144-150
- Marcus AI, Li W, Ma H, Cyr RJ** (2003) A kinesin mutant with an atypical bipolar spindle undergoes normal mitosis. *Mol Biol Cell* **14**: 1717-1726
- McEwen BF, Chan GKT, Zubrowski B, Savoian MS, Sauer MT, Yen TJ** (2001) CENP-E is essential for reliable bioriented spindle attachment, but chromosome alignment can be achieved via redundant mechanisms in mammalian cells. *Molecular Biology of the Cell* **12**: 2776-2789
- Menges M, de Jager SM, Gruitsem W, Murray JA** (2005) Global analysis of the core cell cycle regulators of Arabidopsis identifies novel genes, reveals multiple and highly specific profiles of expression and provides a coherent model for plant cell cycle control. *Plant J* **41**: 546-566
- Menges M, Hennig L, Gruitsem W, Murray JA** (2003) Genome-wide gene expression in an Arabidopsis cell suspension. *Plant Mol Biol* **53**: 423-442
- Menges M, Murray JA** (2002) Synchronous Arabidopsis suspension cultures for analysis of cell-cycle gene activity. *Plant J* **30**: 203-212
- Merdes A, Cleveland DW** (1997) Pathways of spindle pole formation: Different mechanisms; Conserved components. *Journal of Cell Biology* **138**: 953-956
- Merdes A, Heald R, Samejima K, Earnshaw WC, Cleveland DW** (2000) Formation of spindle poles by dynein/dynactin-dependent transport of NuMA. *Journal of Cell Biology* **149**: 851-861
- Mineyuki Y** (1999) The preprophase band of microtubules: Its function as a cytokinetic apparatus in higher plants. *International Review of Cytology - a Survey of Cell Biology, Vol 187* **187**: 1-49
- Mitsui H, Hasezawa S, Nagata T, Takahashi H** (1996) Cell cycle-dependent accumulation of a kinesin-like protein, KatB/C in synchronized tobacco BY-2 cells. *Plant Mol Biol* **30**: 177-181
- Moore A, Wordeman L** (2004) The mechanism, function and regulation of depolymerizing kinesins during mitosis. *Trends in Cell Biology* **14**: 537-546
- Morgan DO** (1997) Cyclin-dependent kinases: engines, clocks, and microprocessors. *Annu Rev Cell Dev Biol* **13**: 261-291
- Murray AW, Mitchison TJ** (1994) Mitosis. Kinetochores pass the IQ test. *Curr Biol* **4**: 38-41
- Narasimhulu SB, Kao YL, Reddy ASN** (1997) Interaction of Arabidopsis kinesin-like calmodulin binding protein with tubulin subunits: modulation by Ca²⁺-calmodulin. *Plant Journal* **12**: 1139-1149
- Nishihama R, Soyano T, Ishikawa M, Araki S, Tanaka H, Asada T, Irie K, Ito M, Terada M, Banno H, Yamazaki Y, Machida Y** (2002) Expansion of the cell plate in plant cytokinesis requires a kinesin-like protein/MAPKKK complex. *Cell* **109**: 87-99
- O'Connell MJ, Meluh PB, Rose MD, Morris NR** (1993) Suppression of the bimC4 mitotic spindle defect by deletion of klpA, a gene encoding a KAR3-related kinesin-like protein in *Aspergillus nidulans*. *J Cell Biol* **120**: 153-162
- Pan R, Lee YR, Liu B** (2004) Localization of two homologous Arabidopsis kinesin-related proteins in the phragmoplast. *Planta* **220**: 156-164
- Quandt K, Frech K, Karas H, Wingender E, Werner T** (1995) MatInd and MatInspector: New fast and versatile tools for detection of consensus matches in nucleotide sequence data. *Nucleic Acids Research* **23**: 4878-4884
- Reddy AS, Day IS** (2001) Kinesins in the Arabidopsis genome: a comparative analysis among eukaryotes. *BMC Genomics* **2**: 2
- Reilein AR, Rogers SL, Tuma MC, Gelfand VI** (2001) Regulation of molecular motor proteins. *Int Rev Cytol* **204**: 179-238
- Saunders WS, Hoyt MA** (1992) Kinesin-Related Proteins Required for Structural Integrity of the Mitotic Spindle. *Cell* **70**: 451-458
- Sawin KE, Mitchison TJ** (1995) Mutations in the kinesin-like protein Eg5 disrupting localization to the mitotic spindle. *Proc Natl Acad Sci U S A* **92**: 4289-4293

- Schaar BT, Chan GKT, Maddox P, Salmon ED, Yen TJ** (1997) CENP-E function at kinetochores is essential for chromosome alignment. *Journal of Cell Biology* **139**: 1373-1382
- Scholey JM, Brust-Mascher I, Mogilner A** (2003) Cell division. *Nature* **422**: 746-752
- Segbert C, Barkus R, Powers J, Strome S, Saxton WM, Bossinger O** (2003) KLP-18, a Klp2 kinesin, is required for assembly of acentrosomal meiotic spindles in *Caenorhabditis elegans*. *Mol Biol Cell* **14**: 4458-4469
- Sharp DJ, Brown HM, Kwon M, Rogers GC, Holland G, Scholey JM** (2000a) Functional coordination of three mitotic motors in *Drosophila* embryos. *Molecular Biology of the Cell* **11**: 241-253
- Sharp DJ, Rogers GC, Scholey JM** (2000b) Microtubule motors in mitosis. *Nature* **407**: 41-47
- Skop AR, Bergmann D, Mohler WA, White JG** (2001) Completion of cytokinesis in *C. elegans* requires a brefeldin A-sensitive membrane accumulation at the cleavage furrow apex. *Current Biology* **11**: 735-746
- Smertenko A, Saleh N, Igarashi H, Mori H, Hauser-Hahn I, Jiang CJ, Sonobe S, Lloyd CW, Hussey PJ** (2000) A new class of microtubule-associated proteins in plants. *Nature Cell Biology* **2**: 750-753
- Smertenko AP, Chang HY, Wagner V, Kaloriti D, Fenyk S, Sonobe S, Lloyd C, Hauser MT, Hussey PJ** (2004) The Arabidopsis microtubule-associated protein AtMAP65-1: Molecular analysis of its microtubule bundling activity. *Plant Cell* **16**: 2035-2047
- Smirnova EA, Reddy AS, Bowser J, Bajer AS** (1998) Minus end-directed kinesin-like motor protein, Kcbp, localizes to anaphase spindle poles in *Haemanthus endosperm*. *Cell Motil Cytoskeleton* **41**: 271-280
- Song H, Golovkin M, Reddy ASN, Endow SA** (1997) In vitro motility of AtKCBP, a calmodulin-binding kinesin protein of Arabidopsis. *Proceedings of the National Academy of Sciences of the United States of America* **94**: 322-327
- Stals H, Bauwens S, Traas J, Van Montagu M, Engler G, Inze D** (1997) Plant CDC2 is not only targeted to the pre-prophase band, but also co-localizes with the spindle, phragmoplast, and chromosomes. *FEBS Lett* **418**: 229-234
- Strompen G, El Kasmi F, Richter S, Lukowitz W, Assaad FF, Jurgens G, Mayer U** (2002) The Arabidopsis HINKEL gene encodes a kinesin-related protein involved in cytokinesis and is expressed in a cell cycle-dependent manner. *Curr Biol* **12**: 153-158
- Tanudji M, Shoemaker J, L'Italien WA, Russell L, Chin G, Schebye XM** (2004) Gene silencing of CENP-E by small interfering RNA in HeLa cells leads to missegregation of chromosomes after a mitotic delay. *Molecular Biology of the Cell* **15**: 3771-3781
- Touitou I, Lhomond G, Pruliere G** (2001) Boursin, a sea urchin bimC kinesin protein, plays a role in anaphase and cytokinesis. *Journal of Cell Science* **114**: 481-491
- Uzbekov R, Prigent C, Arlot-Bonnemains Y** (1999) Cell cycle analysis and synchronization of the *Xenopus laevis* XL2 cell line: Study of the kinesin related protein XIEg5. *Microscopy Research and Technique* **45**: 31-42
- Van Damme D, Bouget FY, Van Poucke K, Inze D, Geelen D** (2004) Molecular dissection of plant cytokinesis and phragmoplast structure: a survey of GFP-tagged proteins. *Plant J* **40**: 386-398
- Van Damme D, Van Poucke K, Boutant E, Ritzenthaler C, Inze D, Geelen D** (2004) In Vivo Dynamics and Differential Microtubule-Binding Activities of MAP65 Proteins. *Plant Physiol* **136**: 3956-3967
- Vanstraelen M, Torres Acosta JA, De Veylder L, Inze D, Geelen D** (2004) A plant-specific subclass of C-terminal kinesins contains a conserved a-type cyclin-dependent kinase site implicated in folding and dimerization. *Plant Physiol* **135**: 1417-1429
- Vantard M, Cowling R, Delichere C** (2000) Cell cycle regulation of the microtubular cytoskeleton. *Plant Molecular Biology* **43**: 691-703
- Verma DP** (2001) Cytokinesis and Building of the Cell Plate in Plants. *Annu Rev Plant Physiol Plant Mol Biol* **52**: 751-784
- Vernos I, Raats J, Hirano T, Heasman J, Karsenti E, Wylie C** (1995) Xklp1, a chromosomal *Xenopus* kinesin-like protein essential for spindle organization and chromosome positioning. *Cell* **81**: 117-127
- Vos JW, Dogterom M, Emons AMC** (2004) Microtubules become more dynamic but not shorter during preprophase band formation: A possible "search-and-capture" mechanism for microtubule translocation. *Cell Motility and the Cytoskeleton* **57**: 246-258
- Vos JW, Safadi F, Reddy AS, Hepler PK** (2000) The kinesin-like calmodulin binding protein is differentially involved in cell division. *Plant Cell* **12**: 979-990
- Wasteneys GO** (2002) Microtubule organization in the green kingdom: chaos or self-order? *J Cell Sci* **115**: 1345-1354

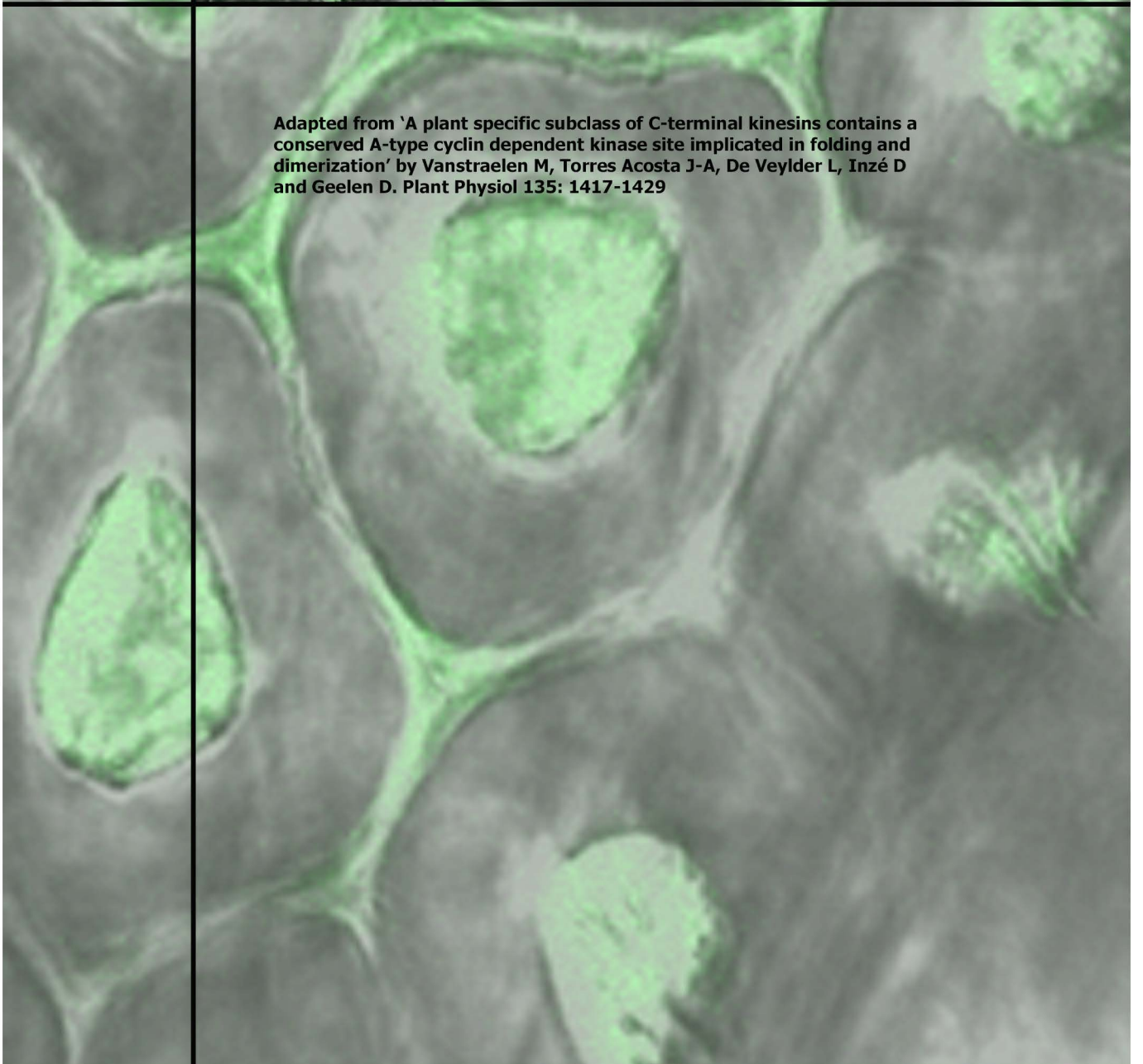
- Weingartner M, Binarova P, Drykova D, Schweighofer A, David JP, Heberle-Bors E, Doonan J, Bogre L** (2001) Dynamic recruitment of Cdc2 to specific microtubule structures during mitosis. *Plant Cell* **13**: 1929-1943
- West RR, Malmstrom T, McIntosh JR** (2002) Kinesins klp5(+) and klp6(+) are required for normal chromosome movement in mitosis. *J Cell Sci* **115**: 931-940
- Whitehead CM, Rattner JB** (1998) Expanding the role of HsEg5 within the mitotic and post-mitotic phases of the cell cycle. *Journal of Cell Science* **111**: 2551-2561
- Wilson PG, Simmons R, Shigali S** (2004) Novel nuclear defects in KLP61F-deficient mutants in *Drosophila* are partially suppressed by loss of Ncd function. *J Cell Sci* **117**: 4921-4933
- Wymer CL, Fisher DD, Moore RC, Cyr RJ** (1996) Elucidating the mechanism of cortical microtubule reorientation in plant cells. *Cell Motility and the Cytoskeleton* **35**: 162-173
- Yang CY, Spielman M, Coles JP, Li Y, Ghelani S, Bourdon V, Brown RC, Lemmon BE, Scott RJ, Dickinson HG** (2003) TETRASPORE encodes a kinesin required for male meiotic cytokinesis in *Arabidopsis*. *Plant J* **34**: 229-240
- Yasuhara H, Shibaoka H** (2000) Inhibition of cell-plate formation by brefeldin A inhibited the depolymerization of microtubules in the central region of the phragmoplast. *Plant Cell Physiol* **41**: 300-310
- Yasuhara H, Sonobe S, Shibaoka H** (1995) Effects of brefeldin A on the formation of the cell plate in tobacco BY-2 cells. *Eur J Cell Biol* **66**: 274-281
- Yu HG, Hiatt EN, Chan A, Sweeney M, Dawe RK** (1997) Neocentromere-mediated chromosome movement in maize. *J Cell Biol* **139**: 831-840
- Yucel JK, Marszalek JD, McIntosh JR, Goldstein LS, Cleveland DW, Philp AV** (2000) CENP-meta, an essential kinetochore kinesin required for the maintenance of metaphase chromosome alignment in *Drosophila*. *J Cell Biol* **150**: 1-11
- Zhong R, Burk DH, Morrison WH, 3rd, Ye ZH** (2002) A kinesin-like protein is essential for oriented deposition of cellulose microfibrils and cell wall strength. *Plant Cell* **14**: 3101-3117



Chapter 3

A plant specific subclass of C-terminal kinesins contains a conserved A- type cyclin dependent kinase site implicated in folding and dimerization

Adapted from 'A plant specific subclass of C-terminal kinesins contains a conserved A-type cyclin dependent kinase site implicated in folding and dimerization' by Vanstraelen M, Torres Acosta J-A, De Veylder L, Inzé D and Geelen D. *Plant Physiol* 135: 1417-1429



Chapter page: *Arabidopsis thaliana* seed coat, imaged using confocal microscopy (transmission light and GFP filter settings).

Abstract

Cyclin-dependent kinases (CDKs) control cell cycle progression through timely coordinated phosphorylation events. Two kinesin-like proteins that interact with CDKA;1 were identified and designated KCA1 and KCA2. They are 81% identical and have a similar three-partite domain organization. The N-terminal domain contains an ATP and MT-binding site typical for kinesin motors. A green fluorescent protein (GFP) fusion of the N-terminal domain of KCA1 decorated MTs in Bright Yellow-2 (BY-2) cells, demonstrating MT-binding activity. During cytokinesis the full-length GFP-fusion protein accumulated at the midline of young and mature expanding phragmoplasts. Two-hybrid analysis and co-immunoprecipitation experiments showed that coiled coil structures of the central stalk were responsible for homo- and heterodimerization of KCA1 and KCA2. By Western blot analysis, high molecular weight KCA molecules were detected in extracts from BY-2 cells overproducing the full-length GFP fusion. Treatment of these cultures with the phosphatase inhibitor vanadate caused an accumulation of these KCA molecules. In addition to dimerization, interactions within the C-terminally located tail domain were revealed, indicating that the tail could fold onto itself. The tail domains of KCA1 and KCA2 contained two adjacent putative CDKA;1 phosphorylation sites one of which is conserved in KCA homologs from other plant species. Site-directed mutagenesis of the conserved phosphorylation sites in KCA1 resulted in a reduced binding with CDKA;1 and abolished intramolecular tail interactions. The data show that phosphorylation of the CDKA;1 site provokes a conformational change in the structure of KCA with implications in folding and dimerization.

Introduction

Although cell division is elementary to growth, the process itself only claims a small part of the complete plant cell cycle period. During that short time, the MT cytoskeleton undergoes major transitions and consecutively a PPB, spindle, and phragmoplast are formed (Vantard et al., 2000; Hasezawa and Kumagai, 2002). These MT arrays are the basis for scaffolds along which chromosomes are aligned and separated into daughter nuclei and cell wall material is transported to the site where the new cell plate emerges. The exact order of event demands for a perfect orchestration of the action of many proteins. Phosphorylation is an important regulatory mechanism in the control of MT organization during the mitotic processes.

Plant A-type CDKs, such as CDKA;1 in *Arabidopsis thaliana*, are the principal regulators of the orderly progression of the cell cycle. CDKA;1 is associated with MTs in dividing and interphase cells (Stals et al., 1997; Hemsley et al., 2001; Weingartner et al., 2001) and is involved in the organization of the cytoskeleton during cell division. Short association of the CDKA;1-cyclin B complex to the PPB causes desintegration of this structure before nuclear envelope breakdown (Hush et al., 1996). Treatment of metaphase cells with inhibitors of CDKs results in abnormal spindles with chromosomes not aligned at the metaphase plate (Binarová et al., 1998). Therefore, CDK plays a major role in the regulation of some of the steps that lead to MT rearrangements in dividing cells.

In yeast and animal cells, CDK regulates MT organization and function by controlling the activity or distribution of multiple proteins that are involved in MT arrangement and transport activities. CDK phosphorylates MT-associated proteins, which are important for MT dynamics and stability (Cassimeris, 1999; Andersen, 2000). MT-based motors, such as kinesins, are one of the targets phosphorylated by CDK (Liao et al., 1994; Blangy et al., 1995). Kinesins belong to a large class of conserved genes that fall into nine subfamilies. In general, the different classes are involved in separate cellular processes related to cytoskeleton organization and intracellular transport (Moore and Endow, 1996). In dividing cells, they are implicated in the organization and stabilization of the spindle and phragmoplast structures, chromosome movement, and vesicular transport to the site of division (Reddy, 2001). The majority of kinesins consist of a motor domain with a catalytic core that binds MTs and hydrolyzes ATP to generate force and a tail domain that interacts with the cargo (Vale and Fletterick, 1997). The conformational organization and the quaternary structure of kinesins vary, depending on the subfamily, and reflect the wide range of functions with which they are associated and the complex regulatory mechanisms to which they are subjected as well. Although some kinesins operate as monomers, many form homo- or heterodimers, heterotrimers, or bipolar homotetramers (Reilein et al., 2001). Oligomerization usually takes place by means of the interactions of a series of coiled coils that are located in the stalk domain. In addition to oligomerization, kinesins also have complex folding properties that provide the driving force to bind cargo or to control the activity of the motor domain.

Several kinesins carry one or more putative CDK consensus serine/threonine phosphorylation sites. For example, the BimC/Kinesin-5 kinesin subfamily contains a phosphorylation site around a conserved sequence motif, called the bimC box. Phosphorylation of the embedded threonine in the human BimC

kinesin Eg5 is a prerequisite for Eg5 to localize to the mitotic spindle and to ensure the formation of a bipolar organization of the spindle (Blangy et al., 1995; Sawin and Mitchinson, 1995). The BimC kinesins contain a second MT-binding site outside the motor domain that mediates the cross-linking of antiparallel MTs at the spindle mid-zone to provide sliding forces (Kashina et al., 1997). BimC-type representatives have been found in plant species, including Arabidopsis, carrot, and tobacco (Asada et al., 1997; Barroso et al., 2000; Lawrence et al., 2002). In these instances, phosphorylation or a potential interaction with CDK kinase has not been investigated and remains therefore elusive. Nevertheless, a function analogous to the BimC kinesins has been shown in tobacco. The kinesin TKRP125 is targeted to the mid-zone of the spindle and the phragmoplast where it provides the mechanic force for sliding of antiparallely arranged MTs (Asada et al., 1997). Phosphorylation may also be implicated in localization and functioning of KCBP, a minus-end directed kinesin required for correct trichome branching (Oppenheimer et al., 1997). Besides the presence of a putative CDK consensus phosphorylation site, KCBP interacts with a plant-specific protein kinase KIPK, suggesting that KCBP is phosphorylated by KIPK (Day et al., 2000).

We report the isolation and characterization of two Arabidopsis kinesin-like proteins that interact with CDKA;1, designated KCA1 and KCA2 (acronym for kinesin CDKA;1-associated). KCA1 and KCA2 are unusual kinesins in that they are unique to plants and possess an N-terminal motor domain that is most similar to that of the C-terminal subfamily of kinesins. We show that KCA1 and KCA2 dimerize through a coiled-coil region in the center and fold intramolecularly through interactions within the tail domain. These conformational properties are regulated by a phosphorylation dependent control mechanism that involves a putative CDKA consensus phosphorylation site.

Results

Cloning of KCA1 and KCA2

We screened a cDNA λ phage library with a partial kinesin fragment TH65 that had been isolated previously in a two-hybrid screen with *CDKA;1* (De Veylder et al., 1997). Partial cDNAs were isolated that were elongated to a putative full-length cDNA of 3816 bp by RACE-PCR, and designated *KCA1* (Arabidopsis gene At5g10470). Recently, the same TH65 fragment has been isolated in two other two-hybrid screens with the geminivirus AL1 protein and the Arabidopsis katanin p60 subunit as baits (Kong and Hanley-Bowdoin, 2002; Bouquin et al., 2003). A second, homologous cDNA was isolated from the library, corresponding to a gene designated *KCA2*, also on chromosome 5 (gene At5g65460). The comparison of the cDNA sequences with genomic DNA revealed a conservation of their gene structures, consisting of 23 exons that encoded putative proteins with 81% identity and 89% similarity. The deduced protein sequences carried an N-terminally located motor domain with the signature sequence SKLSLVDLGSE and an ATP-binding motif or P-loop, which are the most common features of kinesin motor domains. The motor domain was preceded by a short stretch of approximately 140 amino acids that contained a coiled coil and a neck sequence carrying a conserved GN motif that is confined to

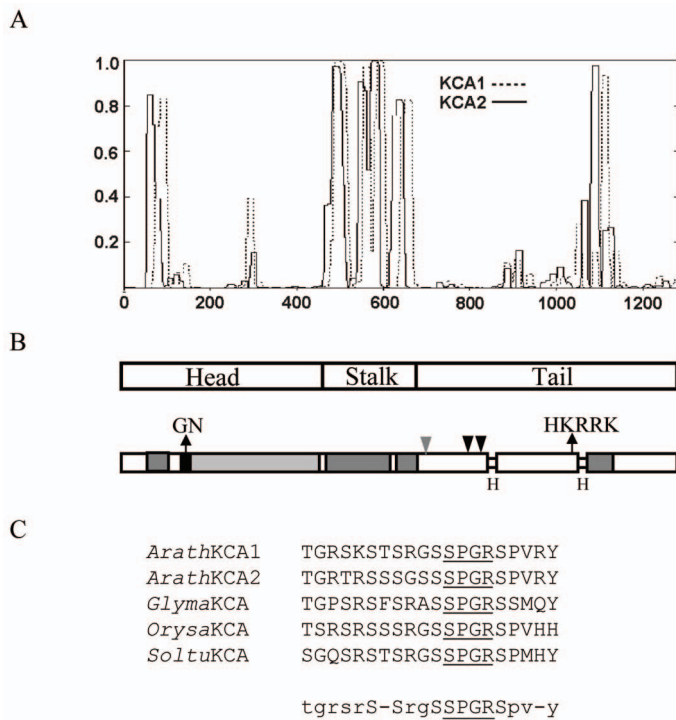


Figure 3.1 Secondary structure and domain organization of the Arabidopsis KCAs. A, Coiled coil domains of KCA1 (dotted line) and KCA2 (dashed line) predicted by the algorithm of Lupas et al. (2001). The abscissa represents the amino acid residue number and the ordinate the probability of coiled coil formation. B, Composition of KCA1 and KCA2; the N-terminal head contains the motor domain (light grey box), preceded by a neck region (black box) with the residues -GN-. Coiled coil domains (dark grey boxes) were found in the centrally located stalk domain. Additional coiled coils were present in the head and tail domain. The C-terminal tail carries a NLS sequence -HKRRK- and two hinge regions (H). KCA1 and KCA2 share two adjacent consensus CDK phosphorylation sites (S/T-P-x-K/R) in the tail domain (black arrowheads). An additional phosphorylation site is present in the tail of KCA1 (grey arrowhead). C, Alignment of the conserved CDK phosphorylation sites -SPGR- (underlined) in KCA-related kinesins in *Glycine max* (*Glyma*KCA, accession AW200832), *Oryza sativa* (*Orysa*KCA, accession AQ794870), and *Solanum tuberosum* (*Soltu*KCA, accession BF053293).

minus-end directed kinesins (Fig. 3.1B). The KCA proteins consisted of two additional domains, a coiled coil region at the center, designated stalk domain, and a C-terminal tail domain containing a single coiled coil, a nuclear localization signal (NLS), and two glycine-rich regions of low complexity commonly present in kinesins (Fig. 3.1, A and B). The structural organization of the KCA kinesins was more closely related to the tripartite structure of plus-end directed kinesins that have a N-terminally located motor domain. Because of sequence similarity with the group of C-terminal kinesins, KCA were tentatively classified within that group (Kim and Endow, 2000). Database sequence comparison of the tail domain to other kinesins and proteins indicated that although KCA1 and KCA2 were conserved in higher plant

species, they did not share significant homology with any other currently described protein domain. A recent phylogenetic analysis of kinesin motor domains separates KCA1 and KCA2 in a distinct subclass with the minus-end kinesin KCBP from *Arabidopsis* as the closest relative (Dagenbach and Endow, 2004).

Because KCA1 is potentially phosphorylated by CDKA;1, the presence of consensus CDK phosphorylation sites (S/T-P-X-K/R) was searched for. The tail contained putative A-type CDK phosphorylation sites at positions 698, 849, and 853 in KCA1 and at positions 827 and 831 in KCA2 (Fig. 3.1B). A single SPGR site in the N-terminal part of the tail domain was fully conserved in KCA-like sequences of other species (Fig. 3.1C).

Transcriptional expression patterns of KCA1 and KCA2

The presence of *KCA* mRNA transcripts was analyzed in different plant organs and developmental stages by RT-PCR with gene specific primers. DNA fragments of the expected size corresponding to *KCA1* or *KCA2* transcripts were visualized after hybridization (Fig. 3.2A). *KCA1* and *KCA2* mRNA were detected in young seedlings and in log-phase cell suspension cultures. *KCA1* transcripts were more abundant and required a shorter film exposure to be visualized. Expression of *KCA1* and *KCA2* transcripts was found in all the organs tested (roots, leaves, stems, and flowers) and was more elevated in roots and flowers. Steady state expression levels were observed for the *ACT2* gene, which served as a loading control.

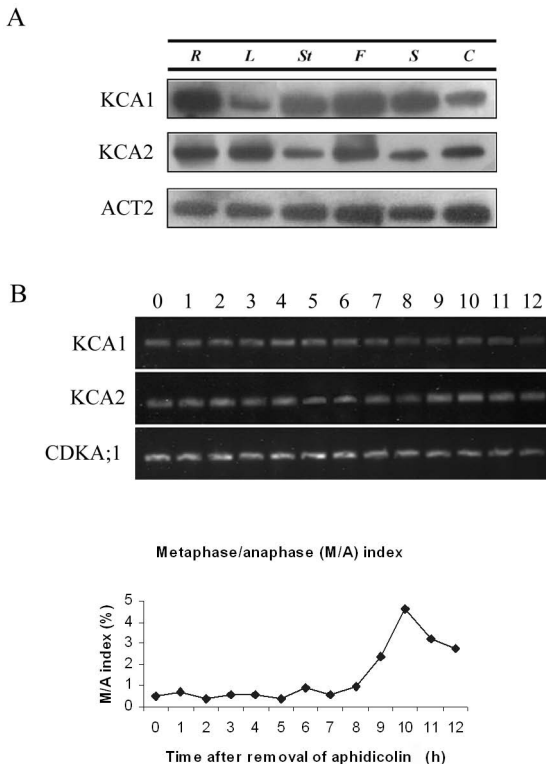


Figure 3.2 Expression analysis of KCAs in different organs and in synchronized Arabidopsis cells.

A, Semi-quantitative RT-PCR analysis of the transcript levels of *KCA1* and *KCA2* mRNA in 3-week-old Arabidopsis organs, 1-week-old seedlings, and 3-day-old cell suspension. RNA was extracted from roots (R), leaves (L), stems (St), flowers (F), seedlings (S), and cell suspensions (C). The Arabidopsis gene actin 2 (*ACT2*) was used as loading control. **B**, *KCA* mRNA levels during cell cycle. Aphidicolin-treated Arabidopsis MM2d cells were released from the G1/S block and RNA samples analyzed by semi-quantitative RT-PCR (top panel) at the indicated successive time points. The metaphase/anaphase index is shown in the lower panel.

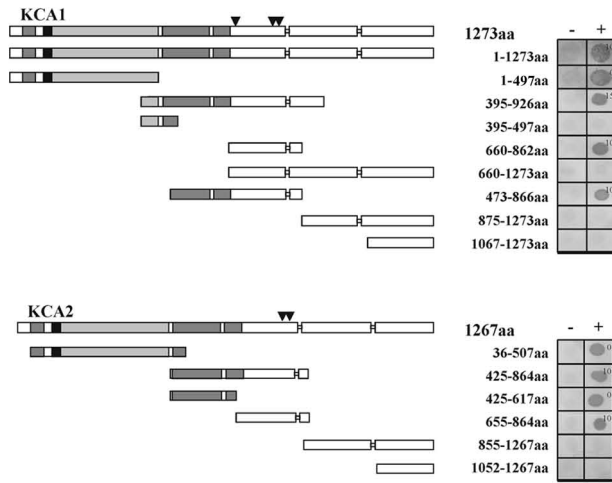
To determine the transcriptional activity of KCA1 and KCA2 during the course of the cell cycle, an Arabidopsis cell suspension culture was synchronized at G1/S by applying aphidicolin (Menges and Murray, 2002). Samples were prepared from 1-hour intervals after drug release and RNA subjected to semi-quantitative RT-PCR analysis. The transcriptional levels of KCA1 and KCA2 were constant throughout the cell cycle (Fig. 3.2B). This is consistent with the ubiquitous expression pattern revealed by immunoblot and immunolocalization by Kong and Hanley-Bowdoin (2002).

Interaction of KCA with CDKA;1

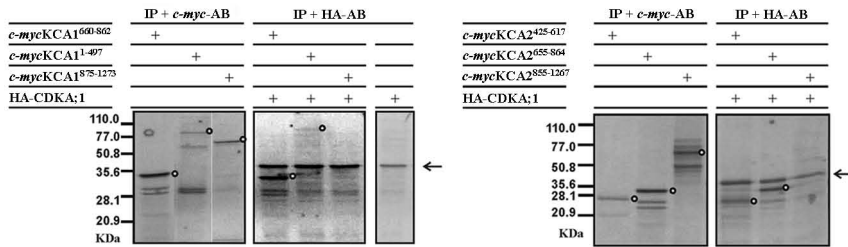
The CDKA;1-binding sites of KCA1 and KCA2 were determined by two-hybrid analysis whereby positive interactions were defined by the ability to grow on medium without histidine. The different KCA1 and KCA2 fragments used for the analysis are presented in Figure 3.3A. The CDKA;1-binding sites were mapped to the head domain (KCA1¹⁻⁴⁹⁷ and KCA2³⁶⁻⁵⁰⁷), the centrally located stalk region (KCA1³⁹⁵⁻⁹²⁶, KCA1⁴⁷³⁻⁸⁶⁶, KCA2⁴²⁵⁻⁶¹⁷, and KCA2⁴²⁵⁻⁸⁶⁴), and the N-terminal part of the tail domain (KCA1⁶⁶⁰⁻⁸⁶² and KCA2⁶⁵⁵⁻⁸⁶⁴). In addition, the full-length KCA1 protein showed CDKA;1-binding affinity (Fig. 3.3A). The interaction strength of the individual peptide fragments and full length was estimated by including the HIS3 competitive inhibitor 3-AT in the growth medium. The strongest interactions were observed with KCA fragments that included the conserved CDK phosphorylation site SPGR, with the exception of the complete tail domain (KCA1⁶⁶⁰⁻¹²⁷³) that did not interact with CDKA;1. These data indicate that the three separate KCA domains contribute to the interaction with CDKA;1 and that the C-terminal part of the tail has an inhibitory effect on the binding with CDKA;1.

Figure 3.3 Identification of CDKA;1-binding sites in KCA1 and KCA2. A, The various KCA fragments fused with the GAL4 DNA-binding domain (pGBT9), are shown at the left. The *CDKA;1* gene was cloned in frame with the GAL4 transcription activation domain (pGAD424). Co-transformants (+) were spotted from an equal cell suspension culture on selective medium (-Leu, -Trp, and -His). As a negative control, the pGBT9-KCA fragments were co-transformed with the empty pGAD424 vector (-) and spotted on the same medium. Different concentrations of 3-AT were tested. The associated numbers correspond to the maximum dose of 3-AT (in mM) that allowed growth. B, Co-immunoprecipitation of ³⁵S-methionine-labeled HA-tagged CDKA;1 with different ³⁵S-methionine-labeled c-Myc tagged versions of KCA1 (KCA1¹⁻⁴⁹⁷, KCA1⁶⁶⁰⁻⁸⁶² and KCA1⁸⁷⁵⁻¹²⁷³; left) and KCA2 (KCA2⁴²⁵⁻⁶¹⁷, KCA2⁶⁵⁵⁻⁸⁶⁴ and KCA2⁸⁵⁵⁻¹²⁶⁷; right). C-Myc-KCA fragments (circles) were immunoprecipitated with anti-c-Myc antibody (left column of each panel) or with an anti-HA antibody after mixing with the HA-CDKA;1 (middle column of each panel). As positive control, HA-CDKA;1 (arrow) was incubated with the anti-HA antibody (right column of left panel). Molecular markers indicate protein size in kDa at the left of each panel. C, Western blotting of p10^{CKSIAt} affinity purifications of WT BY-2 cells (WT) and transgenic lines carrying GFP-KCA1⁶⁶⁰⁻¹²⁷³ (tail), GFP-KCA1¹⁻⁴⁹⁷ (motor), and non-induced (-) and induced GFP-KCA1¹⁻¹²⁷³ (KCA1). 30 µg of protein from crude extract (CE) and p10^{CKSIAt} supernatant (SN) was loaded on gel. The p10^{CKSIAt} pellet (P) corresponds to purified protein from 300 µg of crude extract. In the lower panel, CDKA is detected after stripping and probing the membrane with an anti-PSTAIR antibody (1/2500). The right panel shows a Western blot of 30 µg GFP-KCA1¹⁻¹²⁷³ protein extracts from control cells (Co) and cells

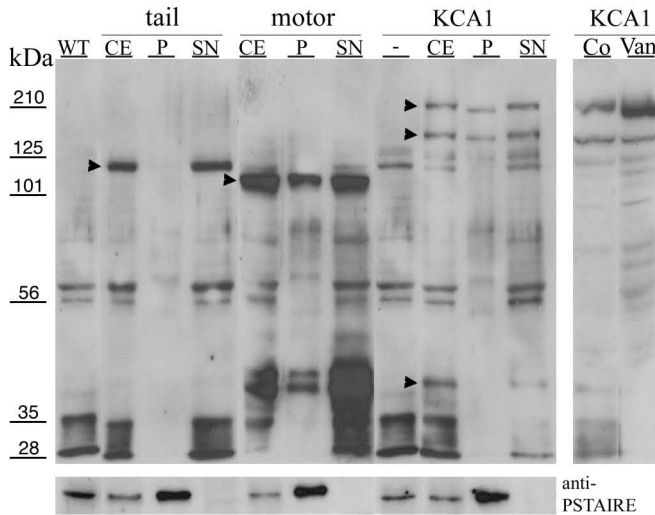
A



B



C



The KCA-CDKA;1 interaction was also analyzed by co-immunoprecipitation experiments using a coupled transcription-translation system in which the KCA1 and KCA2 fragments were tagged with *c*-Myc and CDKA;1 with HA (Fig. 3.3B). In the control experiment, the *c*-Myc-tagged peptides precipitated with a *c*-Myc monoclonal antibody, confirming the correct synthesis of the KCA peptide fragments. Next, the *c*-Myc- and HA-tagged translation products were mixed and pulled down with monoclonal anti-HA antibodies. The KCA1 peptide fragments containing either the N-terminal tail (KCA1⁶⁶⁰⁻⁸⁶²) or the head (KCA1¹⁻⁴⁹⁷) co-sedimented with HA-CDKA;1, whereas the fragment containing the C-terminal tail domain (KCA1⁸⁷⁵⁻¹²⁷³) did not (Fig. 3.3B, left panel). Similar results were obtained with peptide fragments of KCA2. The stalk (KCA2⁴²⁵⁻⁶¹⁷) and the N-terminal part of the tail (KCA2⁶⁵⁵⁻⁸⁶⁴) were pulled down together with HA-CDKA;1, whereas the C-terminal tail (KCA2⁸⁵⁵⁻¹²⁶⁷) was not (Fig. 3.3B, right panel). The results confirmed the interactions between KCA and CDKA;1 interactions that had been revealed by the two-hybrid analysis. None of the KCA fragments were able to bind with the anti-HA antibody in the absence of HA-CDKA;1 (data not shown).

To investigate the association of KCA1 with CDKA;1 *in vivo*, CDK-protein complexes were purified from BY-2 transgenic cell cultures that produced GFP-tagged versions of the full-length and fragments containing the motor (KCA1¹⁻⁴⁹⁷) or the tail domain (KCA1⁶⁶⁰⁻¹²⁷³) (Fig. 3.3C). Extracts of the transgenic cultures and control wild type (WT) BY-2 cells were mixed with p10^{CKS1At} CDKA;1 affinity beads. Crude extract, pellet, and supernatant were analyzed by Western blot and developed with polyclonal GFP antibody. As shown in Figure 3.3C, GFP-fusion products corresponding to the predicted molecular weight were detected in the separated crude BY-2 extracts. Compared to the non-induced protein extract (-) three kinesin-related protein products were present in the preparations from dexamethasone induced cells producing the full-length kinesin GFP-fusion protein. The 160-kD band corresponded to the intact GFP-KCA protein, whereas the smallest 40-kD protein resulted from degradation or prematurely arrested translation. The high molecular weight band at approximately 250 kD may represent a GFP-KCA1 dimer. The presence of kinesin dimers in denaturing polyacrylamide gels has been reported before (Fontijn *et al.*, 2001). Pull-down assays with p10^{CKS1At} beads indicated a strong interaction of CDKA;1 with KCA1, confirming the interaction between the full-length construct and CDKA;1 in two-hybrid experiments (Fig. 3.3, A and C). The head also interacted with CDKA;1, whereas the tail GFP-fusion did not co-sediment and remained in the soluble fraction. In light of the two-hybrid interaction data and the co-immunoprecipitation experiments, KCA1 seems to be arranged into multiple folding configurations with differential CDKA;1-binding capacities. Together, three CDKA;1-binding sites were revealed by these experiments, one in the motor domain, one in the stalk, and one in the N-terminal half of the tail.

Localization of KCA1 in BY-2 cells

An important property of kinesin molecules is their ability to attach to MTs either for transport or control of MT organization (Walczak, 2003). To investigate the *in vivo* protein localization, we fused KCA1 and KCA1 subdomains to the C-terminal end of GFP and transformed tobacco BY-2 suspension cells. The

GFP-KCA1 fusion product (KCA1¹⁻¹²⁷³) resided in the cytoplasmic space excluded from the vacuoles and the nucleus (Fig. 3.4A). Scanning of the cell periphery and center by confocal optical sectioning did not reveal specific labeling of the cortical or endosomal MTs, indicating that the full-length GFP-fusion protein did not bind the interphase MT structures. In contrast, the N-terminal half of KCA1 containing the motor domain (KCA1¹⁻⁴⁹⁷) associated with MTs (Fig. 3.4B). Cortical and endocyttoplasmic MTs were brightly fluorescent in freshly transformed calli. These observations demonstrated that the motor domain as a separate entity exhibited MT-binding activity. Some kinesins, such as the calmodulin-binding kinesin KCBP, carry a nucleotide-independent MT-binding site outside of their motor domain to facilitate MT sliding (Narasimhulu and Reddy, 1998; Kao et al., 2000). Therefore, we analyzed the KCA1 tail domain (KCA1⁶⁶⁰⁻¹²⁷³) and expressed it as a GFP fusion protein in BY-2 cells. Fluorescence was observed in the cytoplasm and in the nucleus without association with MT structures (Fig. 3.4C). Surprisingly, both the motor and the tail GFP-fusion proteins were present in the nucleus, although the motor accumulated at much higher concentrations than the tail (Fig. 3.4C). Putative nuclear localization signals were identified in the tail domain, but not in the motor (Fig. 3.1). CDKA;1 also concentrates in the nucleus without a classic NLS-targeting signal and associates tightly with interphase chromatin (Weingartner et al., 2001). In addition, it binds MTs similarly to what we observed with the GFP-fused KCA1 motor domain (Geelen and Inzé, 2001). Because CDKA;1 interaction with chromatin is resistant to mild nonionic detergent extraction, we performed a similar extraction procedure on BY-2 cells that produced the GFP-motor or the GFP-tail domains. Figure 3.4 (D-I) shows that GFP-CDKA;1 and GFP-motor were retained in the nucleus, whereas free GFP (data not shown) or the GFP-tail was readily and completely removed upon the detergent washes. Therefore, the motor protein must be tightly bound to the nuclear matrix, presumably as part of a protein complex that possibly also contains the CDKA;1 protein.

The full-length GFP-KCA1 fusion protein was followed during cell division (Fig. 3.4J). Throughout mitosis, the fusion protein remained in the cortical cytoplasm and the cytoplasmic strands, and it invaded the unrestricted space of the spindle in metaphase and anaphase cells (Fig. 3.4J). Fluorescence was diffuse and did not reveal fibrous structures, indicating that the fusion protein did not attach to MTs (Fig. 3.4J). Once the daughter chromosomes were separated, GFP-KCA1 fluorescence accumulated at the midline of the emerging phragmoplast where Golgi-derived vesicles accumulate to form the cell plate (Fig. 3.4J). In a second stage of cell plate development, concomitant with expansion of the phragmoplast, fluorescence was most bright at the leading edges (Fig. 3.4J). Reduced fluorescence was observed at the centre of the centrifugally expanding phragmoplast, where the cell plate starts to mature and MTs are depolymerized.

In contrast to the findings of Kong and Hanley-Bowdoin (2002), GFP-KCA1 did not concentrate in the nucleus nor did it associate with condensed chromosomes in metaphase cells. As the N-terminal domain in front of the motor domain may be implicated in nuclear targeting or chromosome binding, we analyzed the subcellular localization of a C-terminal fusion of KCA1 in BY-2 cells. KCA1-GFP was excluded from the nucleus and vacuoles (Fig 3.4K). In the cytoplasm, it was associated with a reticulated network resembling the endoplasmic reticulum (ER) (Fig. 3.4K). During division (Fig. 3.4L),

KCA1-GFP was distributed to the polar sides of the spindle and the midline of the phragmoplast reminiscent to the subcellular localization of an ER-targeted marker in BY-2 cells (Saint-Jore et al., 2002).

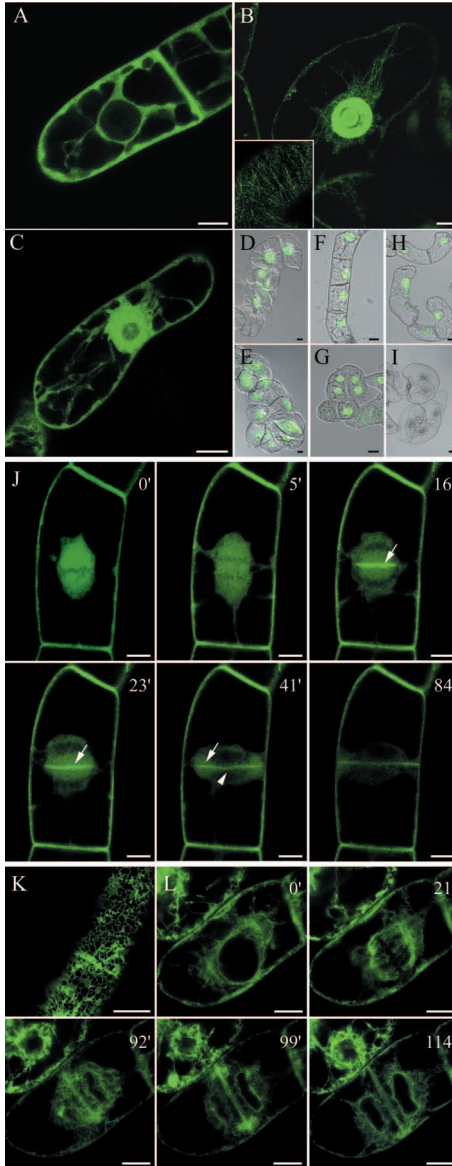


Figure 3.4 Intracellular localization of GFP-fused KCA derivatives in BY-2 cells.

A, Localization of GFP-KCA1¹⁻¹²⁷³ (full length) in the cytoplasm and exclusion from the nucleus. **B**, Labeling of the cytoplasmic and cortical MTs (inset) by the motor domain (GFP-KCA1¹⁻⁴⁹⁷). The motor domain is abundantly present in the nucleus. **C**, Presence of the tail domain (GFP-KCA1⁶⁶⁰⁻¹²⁷³) throughout nucleus and cytoplasm. **D-I**, Detergent extraction of BY-2 cells carrying GFP-CDKA;1 (**D**, **E**), GFP-KCA1¹⁻⁴⁹⁷ (**F**, **G**), and GFP-KCA1⁶⁶⁰⁻¹²⁷³ (**H**, **I**). Images were taken before (**D**, **F**, and **H**), and after (**E**, **G**, and **I**), extraction with Triton X-100 (0.1%). GFP-CDKA;1 and GFP-KCA1¹⁻⁴⁹⁷ were removed from the cytoplasm, but remained attached to the nuclear matrix. In contrast, GFP-KCA1⁶⁶⁰⁻¹²⁷³ was removed both from the nucleus and the cytoplasm. **J**, Time series of N-terminally tagged GFP-KCA1¹⁻¹²⁷³ fluorescence throughout cell division. At metaphase (0') and anaphase (5'), GFP-KCA1 is present in the cytoplasm of the cell cortex and spindle region. During cytokinesis (16'- 41'), GFP-KCA1 labels the midline (arrow) and the forming cell plate (arrowhead). Cell plate labeling decreases when the cell plate has reached the mother cell wall (84'). **K**, Association of C-terminally tagged KCA1¹⁻¹²⁷³-GFP to a reticulate network at the cell periphery. **L**, Time series of KCA1-GFP subcellular localization throughout the cell cycle. Interphase (0'), metaphase (21'), early cytokinesis (92'), late cytokinesis (99') and completed cell plate (114'). Bar = 10 μm.

KCA1 and KCA2 display complex oligomerization

Several observations suggested that the KCA kinesins adopt different folding configurations with distinct properties in terms of interaction with CDKA;1 and in relation to their subcellular localization. Firstly, the N-terminal part of the tail domain could bind CDKA;1 only when the C-terminal part was not included. The inhibitory activity of the C-terminal part of the tail was not evident when the full-length proteins were tested, indicating that these had taken on an alternative configuration immune to control by the tail domain. Secondly, the full-length KCA1 GFP-fusion product was excluded from the nucleus while the head and tail as separate GFP fusion fragments entered the nucleus. Thirdly, MTs were not associated with GFP fused to full-length proteins, but with the GFP-head fusion product. Therefore, we examined the intra- and intermolecular interactions of KCA1 and KCA2 peptides by two-hybrid and immunoprecipitation assays.

Full-length KCA and peptide fragments containing the complete or part of the central coiled-coil region resulted in yeast growth (combinations pGBT-KCA1³⁹⁵⁻⁹²⁶ with pGAD-KCA1¹⁴⁷³⁻⁸⁶⁶ and pGBT-KCA2⁴²⁵⁻⁶¹⁷ with pGAD-KCA2⁴²⁵⁻⁸⁶⁴), indicating that both KCA1 and KCA2 could form homodimers (Fig. 3.5A). Evidence for heterodimerization through the central coiled coil region followed from yeast growth when the stalk domains of both kinesins were tested against each other (combinations of both pGBT-KCA2⁴²⁵⁻⁶¹⁷ and pGBT-KCA2⁴²⁵⁻⁸⁶⁴ with pGAD-KCA1⁴⁷³⁻⁸⁶⁶).

Two-hybrid interactions were also observed between the N-terminal and the C-terminal halves of the tail of KCA1 (combination pBGT-KCA1⁶⁶⁰⁻⁸⁶² with pGAD-KCA1⁸⁷⁵⁻¹²⁷³) and KCA2 (combination pGBT-KCA2⁴²⁵⁻⁸⁶⁴ with pGAD-KCA2⁸⁵⁵⁻¹²⁶⁷), pointing out that the tail domains had a tendency to fold onto themselves. A similar type of interaction also occurred between the N- and C-terminal tail domains of KCA1 and KCA2 (combinations pGBT-KCA1⁶⁶⁰⁻⁸⁶² with pGAD-KCA2⁸⁵⁵⁻¹²⁶⁷ and pBGT-KCA1⁸⁷⁵⁻¹²⁷³ with pGAD-KCA2⁴²⁵⁻⁸⁶⁴). The folding of the KCA tails probably occurred via bending of two predicted hinge regions that were present in the tail domain (Fig. 3.1B). The tail fragment upstream of the first hinge region was essential for the interaction (Fig. 3.5), whereas that downstream of the second hinge did not interact in two-hybrid tests, indicating that the tail fragment between the two hinges was responsible for the interactions observed (combination pGBT-KCA1¹⁰⁶⁷⁻¹²⁷³ and pGAD-KCA1⁴⁷³⁻⁸⁶⁶, and pGBT-KCA2¹⁰⁵²⁻¹²⁶⁷ with pGAD-KCA2⁴²⁵⁻⁸⁶⁴, and the reciprocal combinations). The tail interactions of KCA1 and KCA2 were confirmed by co-immunoprecipitation assays (Fig. 3.5B). Protein fragments containing the N-terminal part of the tail of KCA1 or KCA2 pulled down a KCA1 fragment containing sequences downstream of the first hinge region (Fig. 3.5B).

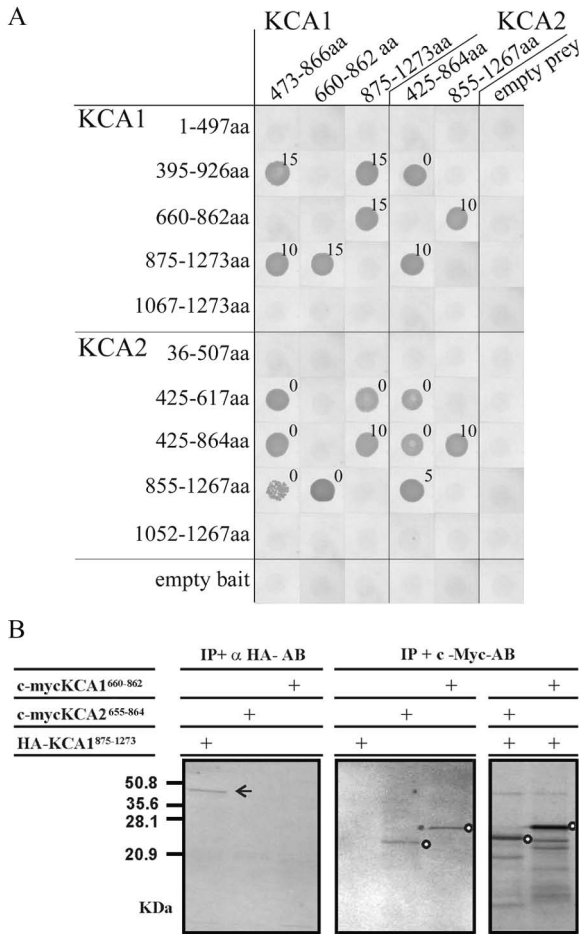


Figure 3.5 Oligomerization of the various KCA1 and KCA2 fragments. A, Yeast two-hybrid analysis of KCA1 and KCA2 fragments. The KCA fragments used are described in Figure 3. The KCA derivatives in the pGBT9 vector are indicated on the left, those in the pGAD242 at the top. Positive protein-protein interactions were identified by colony growth on selective medium. As control, the pGBT9-KCA and pGAD242-KCA constructs were co-transformed with the pGAD242 and pGBT9 empty vectors (referred to as empty bait and prey), respectively. The number above each dot represents the maximum dose of 3-AT (in mM) that still allowed growth. B, Co-immunoprecipitation assay confirming the yeast two-hybrid interactions. In vitro-translated ³⁵S-methionine-labeled HA-KCA1⁸⁷⁵⁻¹²⁷³, c-Myc-KCA1⁶⁶⁰⁻⁸⁶², and c-Myc-KCA2⁶⁵⁵⁻⁸⁶⁴ were immunoprecipitated with anti-HA (left) or anti-c-Myc antibodies (middle and right). ³⁵S-Methionine-labeled c-Myc-KCA1⁶⁶⁰⁻⁸⁶² and c-Myc-KCA2⁴²⁵⁻⁸⁶⁴ were co-immunoprecipitated in the presence of ³⁵S-methionine-labeled HA-CDKA;1 with an anti-c-Myc antibody (right panel). Circles indicate the c-Myc-KCA1⁶⁶⁰⁻⁸⁶² and c-Myc-KCA2⁴²⁵⁻⁶¹⁷ fragments and the arrow indicates the HA-KCA1⁸⁷⁵⁻¹²⁷³ band. Molecular markers (kDa) are shown on the left.

Site-directed mutagenesis of the conserved CDKA;1 phosphorylation site affects tail folding

We showed that KCA1 and KCA2 formed homo- or heterodimers and that both proteins can occur in a folded conformation. In addition, both proteins bind to CDKA;1 and contain CDKA;1 phosphorylation sites in the tail domain. Hence, we investigated whether CDKA;1 phosphorylation was implicated in KCA dimerization and folding.

Western blot of BY-2 cells transformed with GFP fused to the full-length KCA1 protein (Fig. 3.3C) revealed two high molecular weight bands, one of which probably represents a dimeric form of GFP-KCA1. To test the role of phosphorylation in dimer formation, a phosphatase inhibitor was applied to the cells. BY-2 cells transformed with GFP-KCA1 were treated with vanadate (10 mM) (Brown et al., 1999) and equal amounts of proteins of control non-treated and treated cells were loaded on a polyacrylamide gel and blotted (Fig. 3.3C). The concentration of the 250-kD band increased, at the expense of the 160-kD band (Fig. 3.3C). These results show that phosphatase inhibition favored the formation of KCA dimers.

To investigate whether CDKA;1 phosphorylation could have implications for CDKA;1 binding and KCA folding, we introduced mutations in the putative phosphorylation sites at positions 698-701 [TPNK] and 841-848 [SPGR/SPVR] in the pGBT-KCA1⁶⁶⁰⁻⁸⁶² sequence that contains the N-terminal tail of KCA1. Threonine (T⁶⁹⁸) and serine (S⁸⁴¹ and S⁸⁴⁵) were replaced by either an alanine (A) as a nonphosphorylatable residue or by a glutamate (E) that mimics the phosphorylated residue (Table 3.1). We assessed the effects these changes had on the ability to interact with either CDKA;1 or with the KCA tail by means of two-hybrid analysis. Replacement of T⁶⁹⁸ by either an A or E had no consequences on

Table I. Mutational analysis in the stalk region of the KCA1

| Point mutations | CDKA;1 | KCA1 ⁸⁷⁵⁻¹²⁷³ | KCA2 ⁸⁵⁵⁻¹²⁶⁷ | Empty vector |
|---|--------|--------------------------|--------------------------|--------------|
| T ⁶⁹⁸ S ⁸⁴¹ S ⁸⁴⁵ | ++ | +++ | ++ | - |
| T ⁶⁹⁸ → A ⁶⁹⁸ | ++ | +++ | ++ | - |
| T ⁶⁹⁸ → E ⁶⁹⁸ | ++ | +++ | ++ | - |
| S ⁸⁴¹ → A ⁸⁴¹ | ++ | +++ | ++ | - |
| S ⁸⁴¹ → E ⁸⁴¹ | - | + | + | - |
| S ⁸⁴¹ S ⁸⁴⁵ → A ⁸⁴¹ A ⁸⁴⁵ | + | +++ | ++ | - |
| S ⁸⁴¹ S ⁸⁴⁵ → E ⁸⁴¹ E ⁸⁴⁵ | - | - | - | - |

Point mutations were introduced at the CDKA;1 phosphorylation sites 698-701 (TPNK), 841-844 (SPGR), and 845-848 (SPVR) into the KCA1⁶⁶⁰⁻⁸⁶² fragment in the pGBT9 backbone. The nucleotide changes resulted in nonphosphorylatable or phosphorylation mimicry CDKA;1 sites. The resulting amino acid residue substitutions in the pGTB9-KCA1⁶⁶⁰⁻⁸⁶² are shown on the left. The mutated pGTB9-KCA1⁶⁶⁰⁻⁸⁶² vectors were tested in two-hybrid assays against the CDKA;1, KCA1⁸⁷⁵⁻¹²⁷³, and KCA2⁸⁵⁵⁻¹²⁶⁷ in the pGAD424 vector and against the empty pGAD424 vector to check for self-activation (last column). As control, the non-mutated pGTB9-KCA1⁶⁶⁰⁻⁸⁶² was used (first row). (+) and (-) refer to positive and negative interactions, respectively. The increments in "+" correspond to the different 3-AT concentrations (0, 5, 10, and 15 mM) that allowed growth on the selective medium.

the interaction with CDKA;1. On the contrary, substitution of the consensus sequences further downstream, S⁸⁴¹ or S^{841/845} (S⁸⁴¹ and S⁸⁴⁵ double substitution) with E residues, disallowed the yeast strain to grow on selective medium. Replacement of these residues by an A had little or no effect. These results indicated that CDKA;1 binding was sensitive to the phosphorylation status of residues S⁸⁴¹ and S⁸⁴⁵.

The same mutagenized KCA1⁶⁶⁰⁻⁸⁶² fragments were tested against the C-terminal tail fragments KCA1⁸⁷⁵⁻¹²⁷³ and KCA2⁸⁵⁵⁻¹²⁶⁷ in the pGAD vector. Alteration of T⁶⁹⁸ in either A or E had no effect on the tail interactions. However, substitution of S⁸⁴¹ into an E residue strongly reduced the interaction with the C-terminal tail regions of both KCA1 and KCA2, while replacement of both S⁸⁴¹ and S⁸⁴⁵ completely abolished the interaction (Table I). Changing these residues by an A did not alter the growth of yeast. The results suggest that phosphorylation at the consensus sequences 841-844 and 845-848 in KCA1 influences the protein conformation that has important consequences concerning their activity.

Discussion

CDKA governs control over the progression of the cell division processes through the interaction with several partners and selective phosphorylation of target proteins. Despite considerable efforts, only few potential targets phosphorylated by CDKA complexes have been identified in plants so far (Reindl et al., 1997; Nakagami et al., 1999; Boniotti and Gutierrez, 2001). The kinesin KCA1 is a novel candidate target that is phosphorylated in a cell cycle kinase-dependent manner in insect cells (Kong and Hanley-Bowdoin, 2002). We report on the interaction of KCA1, and a highly homologous protein KCA2, with CDKA;1 and the role of a conserved CDKA phosphorylation site in dimerization and folding.

KCA1 and KCA2 share high sequence identity and have a conserved structural organization that is reminiscent to classic kinesin molecules. The N-terminal region contains an ATP-loop and an MT-binding site and is most similar to the motor domain of the C-terminal subfamily of kinesins (Kim and Endow, 2000). This class of kinesins typically has a conserved neck sequence that precedes the core motor domain, which is sufficient and necessary to direct these molecules toward the minus-end of MTs (Vale and Fletterick, 1997). The same motif has been found in that of KCA1 and KCA2, suggesting that these kinesins confer minus-end directed motility.

The calmodulin-binding protein KCBP is a minus-end kinesin that belongs to the C-terminal clad, which is nearest to that containing KCA1 and KCA2 (Dagenbach and Endow, 2004). The KCA kinesins are peculiar because they consist of N-terminal motor proteins that are all of plant origin. We searched the publicly available databases for KCA-like sequences and found representatives from plant species only. Therefore, the KCA kinesins seem to have evolved to a separate class of kinesins unique to plants. To prove that KCA kinesins are able to bind MTs, we have demonstrated that the GFP-tagged KCA1 head was associated with cortical and endocytic MTs in BY-2 cells. The association with MTs occurs when the motor domain is fused to GFP independently from the tail domain and is not observed with a fusion containing the full-length protein. Thus, MT-binding activity is strictly regulated through an activity residing in the C-terminally located tail domain.

Binding of MTs with KCBP is controlled by calcium through the interaction with calcium calmodulin (Narasimhulu et al., 1997), which binds next to the motor domain near the C-terminal end, thereby preventing the MT binding of KCBP and disallowing stimulation of motor ATPase activity (Deavours et al., 1988). The KCA1 and KCA2 sequences do not contain a predicted calmodulin-binding site, suggesting that MT binding is controlled by another molecule. Alternatively, MT binding and motor activity could also be controlled directly by an interaction between the tail and motor domains, a phenomenon referred to as tail inhibition (Coy et al., 1999). However, two-hybrid experiments with different peptide fragments did not uncover the existence of such a type of interaction in KCA. At this point, we do not know what controls the MT-binding activity. It has been well established that phosphorylation regulates motor activity in a number of cases (Reilein et al., 2001). The stimulation of the human kinesin Eg5, for example, is accomplished by phosphorylation of a serine in the motor domain. Upon phosphorylation of this particular residue by the cell cycle kinase p34^{cdc2}, association with the spindle MTs is stimulated and the bipolar organization of the spindle ascertained (Blangy et al., 1995). In the case of other motor proteins, such as dynein and kinesin II, phosphorylation events control MT-binding and motor activity indirectly by modulating the interacting proteins dynactin and kinesin light chain, respectively (Lindesmith et al., 1997; Reese and Haimo, 2000). The Arabidopsis KCBP interacts with a protein kinase KIPK, suggesting that in addition to control by calcium KCBP targeting is regulated by KIPK-mediated phosphorylation (Day et al., 2000). To test whether phosphorylation is important for the targeting of KCA, we applied drugs that inhibit phosphorylation to BY-2-producing GFP-tagged KCA full-length protein or fragments. No effect on the localization was observed suggesting that modulation of the phosphorylation status of KCA was not crucial for the interaction with MTs (data not shown). Because the MT-binding property of the GFP-KCA head was lost upon continuous propagation of the transgenic BY-2 cell lines, we decided to analyze the properties of the tail domain in more detail.

KCBP carries an MT-binding site in the N-terminally located tail domain that is independent from calmodulin (Narasimhulu and Reddy, 1998). A computer-assisted analysis of the KCA1 and KCA2 tails did not reveal a known MT-binding signature. Instead, we found a NLS motif and hinge regions that are important for the flexibility and, hence, the folding properties of the tail (Kirchner et al., 1999). The GFP-tagged KCA1 tail leads to an accumulation of fluorescence in the nucleus in agreement with the presence of an NLS. However, GFP-tagged full-length KCA1 was totally excluded from the nucleus. Neither the N- nor C-terminally tagged KCA1 entered the nucleus, indicating that the NLS was not activated in these protein fusions. Kong and Hanley-Bowdoin (2002) demonstrated by means of immunolocalization experiments, in which an antiserum was used that did not discriminate KCA1 and KCA2, that abundant KCA epitopes are concentrated in the nuclei of *N. benthamiana* leaves and root cells. In addition, they showed accumulation of label at the chromosomes in chemically fixed mitotic cells. We interpret the absence of the full-length GFP-KCA1 protein in BY-2 nuclei and from condensed chromosomes as an inability of these fusion molecules to undergo the necessary refolding and/or interactions that are needed for nuclear import and chromosome binding.

As certain folding configurations may no longer have been possible because of the presence of the GFP-moiety, a different subcellular localization of KCA was revealed. C-terminally tagged KCA1-GFP appeared to associate with the ER. It concentrated at the polar sides of the metaphase spindle where ER and Golgi derived organelles are known to congregate (Nebenführ et al., 2000; Saint-Jore et al., 2002). KCA antiserum also decorated the spindle poles in *N. benthamiana* immunolocalizations reported by Kong and Hanley-Bowdoin (2002). During cytokinesis, N-terminally tagged GFP-KCA1 labeled the phragmoplast midline and fluorescence intensity was strongest at the edges of the expanding phragmoplast. This localization pattern is reminiscent to that of Golgi-derived vesicles accumulating at the phragmoplast midline through an MT-dependent transport mechanism, involving the action of one or more kinesins (Smith, 2002). At this point however, it is uncertain whether KCA1 contributes to the transport of Golgi vesicles. Targeting of vesicular compartments to the midline would require a plus-end directed kinesin because of the antiparallel organization of the phragmoplast MTs. The AtPAKRP2 kinesin is in that respect a more likely candidate for Golgi-vesicle transport to the growing cell plate (Lee et al., 2001). The ER, to which the KCA1-GFP was targeted, also accumulates at the phragmoplast midline and may have functions that are unrelated to deposition of cell plate forming vesicles (Nebenführ et al., 2000; Saint-Jore et al., 2002). To resolve a possible function in cytokinesis it will be necessary to investigate cell lines or plants in which KCA is inactivated.

The KCA proteins have been shown to interact with CDKA;1 in two-hybrid assays (De Veylder et al., 1997; Kong and Hanley-Bowdoin, 2002; own results). Because kinesin motor activity is often tightly coupled to regulatory phosphorylation and because the tail domains of KCA1 and KCA2 carry putative CDKA;1 phosphorylation sites, we analyzed the KCA domains responsible for CDKA;1 binding. Two-hybrid experiments and immunoprecipitation assays indicated that the motor domain, the central region, and the tail domain interacted independently with CKDA;1. For two proteins to interact, they have to co-localize at a given point in time. Several studies have shown that CDKA;1 is predominantly nuclear (Stals et al., 1997; Weingartner et al., 2001). We found that the N-terminal motor (head) and the tail fragments were both targeted to the nucleus. GFP-CDKA;1 and the GFP-tagged KCA1 head fragment were attached to the nuclear content in a Triton X-100-resistant manner. This observation points toward a possibility that both proteins are in a complex in interphase nuclei. Further support came from pull-down experiments that show a strong interaction between the KCA1 head and CDKA;1. CDKA;1 has also been shown to interact with interphase and mitotic MTs presumably because of dynamic association with cellular targets attached to the MT cytoskeleton (Stals et al., 1997; Hemsley et al., 2000; Weingartner et al., 2001; Joubès et al., 2003). Throughout mitosis, GFP-tagged KCA1 remained in the cytoplasm and did not appear to associate with the PPB, spindle, or phragmoplast MTs. Because immunolocalization data and the GFP-fusion analysis did not indicate a prevailing association of KCA with MTs, other proteins than KCA must be responsible for targeting CDKA;1 to the MTs (Kong and Hanley-Bowdoin, 2002).

The coiled coils in the stalk region have been implicated in kinesin oligomerization that is necessary for proper control of motility and cargo binding (Vale and Fletterick, 1997). The conventional kinesin I from neurons is a typical example that forms homodimers for progressive movement along the MT with at

least one motor domain in contact with the MT at all times (Bloom et al., 1988). KCA1 and KCA2 carry three coiled coils in the stalk domain. Two-hybrid and immunoprecipitation experiments suggested that the stalk contributes to homo- and/or heterodimerization of KCA1 and KCA2. Indeed, a doublet protein band with molecular weights corresponding to theoretically predicted weights of homomeric and dimeric fusion protein appeared in Western blots from BY-2 extracts that produced GFP-KCA1. In the presence of the broad phosphatase inhibitor vanadate, cell extracts contained more dimers, indicating that phosphorylation events play a role in the control over the ratio of dimers and homomers. The fluorescence pattern was unaltered in the vanadate-treated cells, indicating that dimerization was not sufficient to target KCA to MTs. Because CDKA;1 may phosphorylate the KCA tail to trigger a conformational shift, which, in turn, drives the dimerization of KCA1, it is possible that in the presence of the phosphatase inhibitor less dimer is cycled back to the monomeric form. Alternatively, CDKA;1 may bind to the stalk domain and compete with stalk-stalk interactions under conditions that are affected by vanadate.

The KCA tail domain carries a CDKA;1 phosphorylation site that is conserved in all KCA-like kinesins found in the publicly available databases. Therefore, this site is the best candidate for a general role in the functioning of the KCA kinesins. Two-hybrid and immunoprecipitation experiments revealed that the N-terminal part of the tail domain interacted with CDKA;1 as well as intramolecularly between the N-terminal part of the tail and a downstream region flanked by the two hinges. These interactions are probably mutually exclusive because the tail, when tested in its entirety, did not bind CDKA;1. The folding of the tail fragment would have prevented an interaction with CDKA;1.

How could CDKA;1 affect the conformational changes and functioning of KCA? The phosphorylation, dimerization, and the internal tail interactions are probably interdependent and may be implicated in phosphorylation controlled activation and/or binding of cargo. Point mutations in the putative CDKA phosphorylation sites of the KCA1 tail abolished the intramolecular tail interaction. Thus, KCA molecules not phosphorylated at the serine residues in the tail would have a compact folding conformation. This conformational stage might keep the KCA inactive until modulated by the cell cycle-controlled CDKA;1 kinase. The opening up of the tail would prepare the single KCA molecules to bind the cargo they need to transport. Alternatively to the stimulation of cargo binding upon phosphorylation, it is also possible that the "opened up" kinesin tail no longer prevents the homo- or heterodimerization that is driven by the stalk domain.

Materials and methods

Isolation and cDNA characterization of KCA1 and KCA2

A cDNA λ phage library of *Arabidopsis thaliana* (L.) Heynh. ecotype Columbia 0 was used to screen for the full-length clone matching fragment TH65 that had been isolated previously in a two-hybrid experiment with CDKA;1 as bait (De Veylder et al., 1997). Two new cDNA fragments were isolated and sequenced that corresponded to the C-terminal region of the *KCA1* gene, including a poly(A) tail region

of 226 bp. The *KCA2* gene was found by sequence homology with *KCA1*. The complete 5' terminus of *KCA1* and the full length of *KCA2* were isolated by RACE-PCR according to the manufacturer's instructions (Clontech, Palo Alto, CA) with the primers 5' -ATGGCCGATCAGAGAAGTAAAACC-3' and 5'-GCCACAACCTCTTGTTCAGATTCTG-3' for *KCA1* and 5' ATGGCGGAGCAGAAGAGTACCAA 3' and 5' GGATTTACTCTCGGGTTGTCTCAGAG 3' for *KCA2*. The reported nucleotide sequences have been submitted to the GenBank/EMBL Data Bank under accession numbers AX449336 and AX449307.

Sequence analysis

The Arabidopsis KCA proteins and KCA homologs were aligned by the CLUSTAL method (PILEUP) from the GCG Wisconsin package version 10.1 program (Accelrys, San Diego, CA) without penalizing gaps. A set of analysis tools was applied for a compressive sequence interpretation. As BLAST browsers, the programs AtBlast (<http://www.arabidopsis.org/blast/>) (Huala et al., 2001) and WU-BLAST2 (<http://dove.embl-heidelberg.de/Blast2/>) (Altschul et al., 1990) were used to search databases for homologous sequences in Arabidopsis and other organisms. The Arabidopsis sequence map and gene redundancy were studied with different tools from the Munich Institute for Protein Sequences (Martiensried, Germany) (<http://mips.gsf.de/proj/thal/db/index.html>). Protein domains were analyzed with SMART (<http://smart.embl-heidelberg.de/>) (Schultz et al., 2000), general motifs were predicted and CDKA;1 phosphorylation sites were identified with ScanProsite (<http://hits.isb-sib.ch/cgi-bin/PFSCAN>) (Sternberg, 1991), and coiled coils were estimated with the algorithm of Lupas et al. (1991) by using the program COILS, (http://www.ch.embnet.org/software/COILS_form.html).

Reverse transcription (RT)-PCR

RNA was prepared from 200 mg of 3-day-old Arabidopsis cell suspensions, 3-week-old plants (roots, rosette leaves, stems, and flowers), and 1-week-old seedlings. Total RNA was isolated with the RNeasy Plant Mini Kit (Qiagen, Hilden, Germany) and used as template for semi-quantitative RT-PCR with Superscript RT II reverse transcriptase (Invitrogen, Carlsbad, CA) and oligo d(T)₁₈. From the 50 µl PCR reaction, 10 µl was separated on a 1% tris-acetate ethylenediaminetetraacetic acid agarose gel and transferred onto Hybond N⁺ membranes (Amersham Bioscience, Little Chalfont, UK). The membranes were hybridized at 65°C with fluorescein-labeled probes (Gene Images random prime module; Amersham Biosciences) and detected with the CDP Star detection module (Amersham Biosciences). For RT-PCR, the following primers were used: 5' GTGCCGTTTTATCCTCGTTGACATCC 3' and 5' CGTATCAAGATATCGAACAGGGG 3' for the *KCA1* gene (position 1185-2556 bp); 5' CCGATGATCGTCAACATTTGTCCAAGTGC 3' and 5' ACGGATTCTTGAACTACAGATACC 3' for the *KCA2* gene (position 1275-2592 bp); and 5' CTAAGCTCTCAAGATCAAAGGCTTA 3' and 5' TTAACATTGCAAAGAGTTCAAGGT 3' for *Arath*; *ACT2* (U41998).

For cell cycle dependent expression analysis, a suspension culture of the Arabidopsis cell line MM2d (Menges and Murray, 2002) was grown in 1 x Murashige and Skoog medium, supplemented with 3% sucrose, 0.5 mg/mg/l naphthalene acetic acid, 0.05 mg l⁻¹ kinetin (pH 5.7). MM2d cells were maintained weekly by subculturing of 5 ml stationary culture in 45 ml of fresh medium in 250 ml Erlenmeyer flasks and grown at 27°C in the dark on a shaker (130 rpm). The cells were synchronized at the G1/S boundary by treating them with 4 µg/ml aphidicolin for 14 h. To obtain cell populations at different stages of the cell cycle, cells were washed twice and then released into complete medium. They were incubated under cultivation conditions as above, and samples were taken hourly after release of the drug. The metaphase/anaphase index was determined according to Menges and Murray (2002). RNA was prepared following the method described by Leyman et al. (2000) and used as a template for the SuperScript™ First-Strand Synthesis System for RT-PCR (Invitrogen). RT-PCR primers for quantification of the mRNA level were as follows; 5' CCGGAGACCTCATTAGAA 3' and 5' ACTCCAGTTCACCTAACCAAGGTC 3' for KCA1; 5' TCGACTGAAACCGATGTGTC 3' and 5' CTAGAGTATCGAGCCCGTGTG 3' for KCA2; 5'GGTGAAGGAAGTACGGTGTGG 3' and 5' GCTCCAGGGCGGCTCTTGCG 3' for CDKA;1. For semi-quantitative RT-PCR analysis, 27 cycles were run for KCA1 and KCA2 and 24 cycles were run for CDKA;1.

Two-hybrid experiments

The CDKA;1 interaction site was mapped by constructing deletion fragments of the *KCA* genes. The DNA fragments were created by PCR with the *Pfu* polymerase (Stratagene, La Jolla, CA) and subcloned in the pGBT9 vector. The *CDKA;1* was inserted into the pGAD424 vector (Clontech). A series of deletion fragments of *KCA1* and *KCA2* cDNA were amplified with primers containing *EcoRI* and *BamHI* enzyme restriction sites. The amplified DNA fragments were inserted into the *EcoRI* and *BamHI* sites of the pGBT9 and pGAD424 vectors. The original pGADTH65 clone (residues 473-866) was also included as a positive control for CDKA;1 binding. Yeast strain HF7c reporter strain (*MATa ura3-52 his3-200 ade2-101 lys2-801 trp1-901 leu2-3112 gal4-542 gal80-538 LYS2::GAL1_{UAS}-GAL1_{TATA}-HIS3, URA3::GAL4_{17-mers(x3)}-CYC-1_{TATA}-LacZ* (Clontech) was co-transformed with pGADKCAx (x is deletion fragment) and pGADCDKA;1 or the empty vector as described previously (De Veylder et al., 2001). After incubation on medium without leucine and tryptophan, colonies were plated on histidine-lacking medium. The strength of the protein-protein interactions were measured by the ability to grow on histidine-free medium supplemented with 0, 5, 10, or 15 mM of 3-amino-1,2,4-triazole (3-AT; Sigma-Aldrich, St. Louis, MO).

In vitro transcription-translation and immunoprecipitation

The same *KCA* deletion fragments generated by PCR for the two-hybrid assays were used to generate the pBSK-*c*-Myc and pBSK-HA vectors (Stratagene). The Arabidopsis *CDKA;1* was recloned from the

pGADCDKA;1 vector in the pBSK-HA vector with *EcoRI* and *BamHI* restriction sites. Plasmids were sequenced to verify in-frame cloning with the *c-Myc*-tag and hemagglutinin (HA) tag.

In vitro transcription and translation experiments were performed separately for each construct with the TNT®T7-coupled wheat germ extract kit (Promega, Madison, WI) primed with the appropriate template for 90 min at 30°C. For immunoprecipitation assays, 10 µl of the *c-Myc*-KCA total *in vitro* translated extract (50 µl) was mixed with 5 µl of the HA-CDKA;1 total *in vitro* translated extract, diluted at 1:5 in Nonidet P40 buffer (50 mM Tris-HCl, pH 7.4, 150 mM NaCl, 1% Nonidet P40, 1 mM phenylmethylsulfonyl fluoride, 10 µg/ml leupeptin/aprotinin/pepstatin), and incubated for 2 h at 4°C with anti-HA antibodies (9E10; BabCo-Covance, Berkeley, CA). Protein-A-Sepharose beads (40 µl 25% [v/v]) were added and incubated for 1 h at 4°C. The beads were washed four times with 1 ml Nonidet P40 buffer. Immune complexes were eluted with 10 µl of 2× sodium dodecyl sulfate sample buffer, analyzed by a 13% sodium dodecyl sulfate-polyacrylamide gel electrophoresis, and autoradiographed. The same procedure was followed using the *c-Myc*-KCAs and HA-KCAs constructs to test for dimerization.

Construction of GFP-fusion proteins

The *KCA1* full-length open reading frame and fragments were cloned behind the open reading frame of enhanced GFP by using the GATEWAY® system (Invitrogen). GATEWAY-compatible vectors were designed by inserting the EGFP-coding region and the GATEWAY rfa cassette into the pBin19 backbone. The expression of the fusion was under the control of the cauliflower mosaic virus 35S promoter and 35S polyadenylation signal. For the construction of the inducible vector, a similar strategy was followed. The EGFP-rfa cassette was cloned into the pTA7002 vector allowing dexamethasone (Sigma-Aldrich)-inducible expression of the fusion protein (Aoyama and Chua, 1997).

The *KCA1* full-length and fragments were amplified with GATEWAY *attB*-flanked primers with the *Pfx* polymerase (Invitrogen). Via BP and subsequent LR reactions, the fragments were introduced into the destination vectors described above. The borders of the inserted fragments were sequenced prior to further analysis.

Growth, transformation, and fluorescence microscopy

Growth of BY-2 cells was according to Nagata et al. (1992). The transformation was performed with *Agrobacterium tumefaciens* strain LBA4404.pBBR1MCS-5.virGN54D (van der Fits et al., 2000). For co-cultivation, 4 ml of a 3-day-old culture (10 times diluted) was mixed with *Agrobacterium* cultures. After 3 days at 28°C, the cells were plated on BY-2 medium containing 500 µg/ml carbenicillin, 200 µg/ml vancomycin, and 100 µg/ml kanamycin for the constitutive vector or 30 µg/ml hygromycin for the inducible vector.

BY-2 cultures were transformed with pBin19GFP carrying the *KCA1* motor (*KCA1*₁₋₄₉₇), and the *KCA1* tail (*KCA1*⁶⁶⁰⁻¹²⁷³), leading to constitutive expression of fusion protein. For subcellular localization

of the full-length KCA1 protein, the dexamethasone inducible vector pTA7002GFP carrying the KCA1¹⁻¹²⁷³ fragment was used. Calli producing GFP fusion proteins were identified by fluorescence microscopy. BY-2 cells transformed with the inducible expression vector were induced overnight on BY-2 agar containing 10 μ M dexamethasone. Callus material was transferred on a slide with a coverslip, and observed with an epifluorescence microscope (Axioplan 2; Zeiss, Jena, Germany) equipped with a fluorescein isothiocyanate filter set. GFP-positive calli were transferred to liquid BY-2 medium with selection and grown as cell suspensions.

Confocal images were taken with a scanning confocal microscope (LSM 510; Zeiss) with argon laser illumination at 488 nm and a fluorescein isothiocyanate filter set. For transmission light images, differential interference contrast optics was used. Images were taken with 25% laser power to reduce photobleaching.

Detergent extraction of cells

Cells were incubated in liquid BY-2 medium containing 0.1% Triton X-100 (Sigma-Aldrich) for 15 min with gentle agitation. Cells were washed twice in BY-2 medium, transferred to a slide, and covered with a coverslip. The detergent-extracted cells were observed directly with the confocal microscope.

Protein gel blot analysis

Three day old liquid cultures of BY-2 transgenic lines, also used for GFP-localization experiments, and wild type BY-2 cells, were ground in liquid nitrogen with a mortar and pestle and homogenized in ice-cold P10 buffer (25 mM Tris-HCl, pH 7.6, 15 mM ethyleneglycol-bis(β -aminoethyl)tetra-acetate, 1 mM dithiothreitol, 15 mM MgCl₂, 85 mM NaCl, 15 mM pNO₂PhePO₄, 60 mM glycerol phosphate, 0.1% NP40, 1 mM NaF, 0.1 mM Na₃VO₄, and 100 μ l protease inhibitor cocktail; Sigma-Aldrich). The homogenate was centrifuged at 10,000 *g* for 10 min in an Eppendorf centrifuge 5417 at 4°C to remove cell debris. The supernatant was then centrifuged at 14,000 *g* for 10 min. A sample was taken and kept on ice as crude extract. Then, 50 μ l of 50% (v/v) p10^{CKS1At} Sepharose beads was added to 300 μ g of proteins and incubated at 4°C for 1 h on a rotating wheel. The beads were collected by centrifugation; the supernatant was removed and kept on ice. Beads were washed three times with bead buffer (50 mM Tris-HCl pH 7.5, 5 mM NaF, 250 mM NaCl, 5 mM EGTA, 5 mM EDTA, 10 μ g/ml leupeptin, 10 μ g/ml aprotinin, 0.1 mM benzamidine, and 0.1 mM Na₃VO₄). Loading buffer (Laemmli, 1970) was added and the samples were heated for 10 min at 95°C. After centrifugation at 14,000 *g* for 4 min, 30 μ g crude extract protein, 30 μ g p10^{CKS1At} supernatant, and p10^{CKS1At} pellet purified from 300 μ g initial crude extract was separated on a 12% gel. The amount protein loaded was verified in a separate gel by coomassie staining. Gels were blotted onto nitrocellulose membranes (Hybond-C super; Amersham Biosciences) in 190 mM glycine and 25 mM Tris with a liquid mini-blotting system (Bio-Rad, Hercules, CA) for 1 h. The protein on the blotted membrane was verified by Ponceau red staining. Membranes were blocked overnight at 4°C in Tris buffered saline with 0.1% Tween-20 (TBST) and 5% skimmed milk

(BD Difco; Becton Dickinson, Franklin Lakes, NJ). For immunodetection, an anti-GFP rabbit serum (Chemicon, Temecula, CA) was applied in the blocking buffer at a dilution of 1:1000 and anti-rabbit Ig horseradish peroxidase from donkey (Amersham Biosciences) was used as a second antibody at a dilution of 1:10000. Membranes were stripped at 60 °C for 30 min. in buffer containing 100mM β -mercapto-ethanol, 2% SDS, and 62,5 mM Tris-HCl pH 6.7. They were washed twice with TBST for 10 min., blocked in TBST containing 3% skimmed milk for 2 h. at room temperature. CDKA protein was detected using a 1/2500 dilution of cdc2 PSTAIRE antibody (Santa Cruz Biotechnology, Santa Cruz, California) and a 1/10000 dilution of secondary anti-rabbit Ig horseradish peroxidase from donkey in TBST with 3% skim milk. Proteins were detected by the chemiluminescence procedure (Bio-Rad).

For drug analysis, 10 mM Na_3VO_4 was added to a 2-day-old BY-2 culture, transformed with the inducible GFP-KCA1 construct. As control, a non-treated culture was cultured simultaneously. After 24 h of growth at 28°C, crude protein extracts were prepared in the P10 homogenization buffer. Thirty μg of proteins was loaded on a 12% gel and processed as described above.

Site-directed mutagenesis

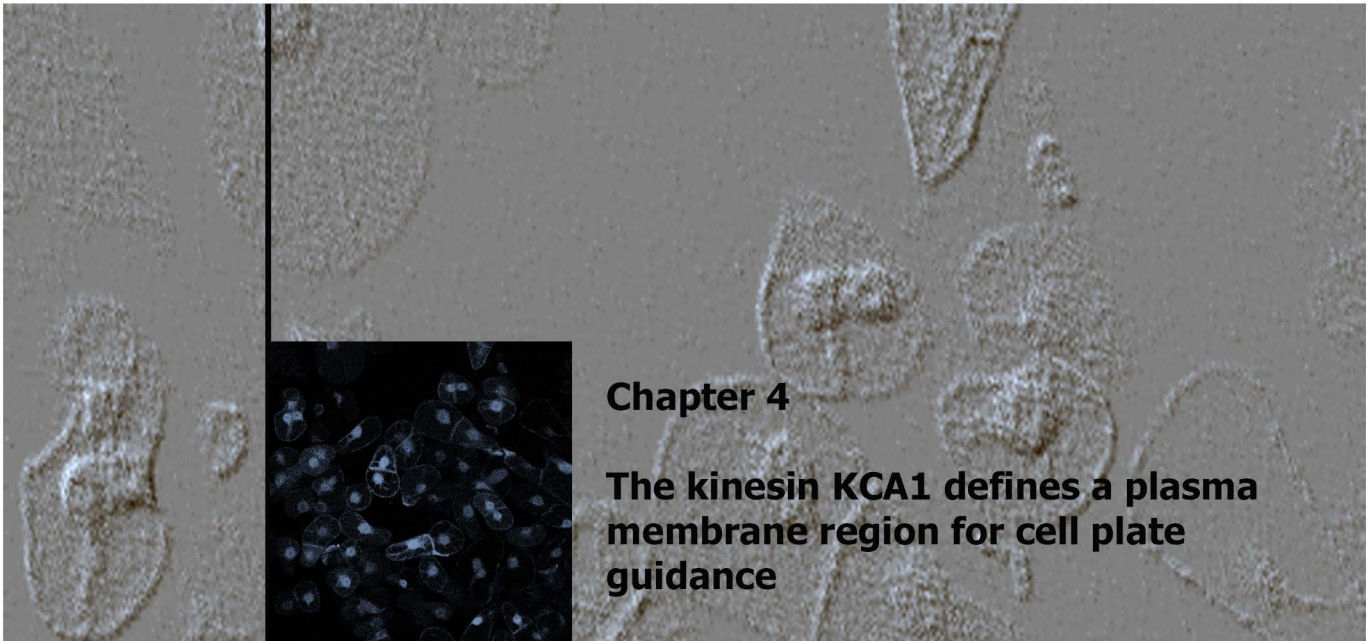
Point mutations were introduced by PCR site-directed mutagenesis in the pGTB-KCA1⁶⁶⁰⁻⁸⁵² plasmid with the Advantage® polymerase mix (Clontech). The linear PCR product was circularized by ligation. The nucleotide changes were verified by sequencing the KCA1 inserts in two directions.

References

- Altschul SF, Gish W, Miller W, Myers EW, Lipman DJ** (1990) Basic local alignment search tool. *J Mol Biol* **215**: 403-410
- Andersen SSL** (2000) Spindle assembly and the art of regulating microtubule dynamics by MAPs and Stathmin/Op18. *Trends Cell Biol* **10**: 261-267
- Aoyama T, Chua N-H** (1997) A glucocorticoid-mediated transcriptional induction system in transgenic plants. *Plant J* **11**: 605-612
- Asada T, Kuriyama R, Shibaoka H** (1997) TKRP125, a kinesin-related protein involved in the centrosome-independent organization of the cytokinetic apparatus in tobacco BY-2 cells. *J Cell Sci* **110**: 179-189
- Barroso C, Chan J, Allan V, Doonan J, Hussey P, Lloyd C** (2000) Two kinesin-related proteins associated with the cold-stable cytoskeleton of carrot cells: characterization of a novel kinesin, DcKRP120-2. *Plant J* **24**: 859-868
- Binarová P, Dole_el J, Draber P, Heberle-Bors E, Strnad M, Bögre L** (1998) Treatment of *Vicia faba* root tip cells with specific inhibitors to cyclin-dependent kinases leads to abnormal spindle formation. *Plant J* **16**: 697-707
- Blangy A, Lane HA, d'Hérin P, Harper M, Kress M, Nigg EA** (1995) Phosphorylation by p34^{cdc2} regulates spindle association of human Eg5, a kinesin-related motor essential for bipolar spindle formation in vivo. *Cell* **83**: 1159-1169
- Bloom GS, Wagner MC, Pfister KK, Brady ST** (1988) Native structure and physical properties of bovine brain kinesin and identification of the ATP-binding subunit polypeptide. *Biochemistry* **27**: 3409-3416
- Boniotti MB, Gutierrez C** (2001) A cell-cycle-regulated kinase activity phosphorylates plant retinoblastoma protein and contains, in *Arabidopsis*, a CDKA/cyclin D complex. *Plant J* **28**: 341-350
- Bouquin T, Mattsson O, Næsted H, Foster R, Mundy J** (2003) The *Arabidopsis* *lue1* mutant defines a katanin p60 ortholog involved in hormonal control of microtubule orientation during cell growth. *J Cell Sci* **116**: 791-801
- Brown NR, Noble MEM, Lawrie AM, Morris MC, Tunnah P, Divita G, Johnson LN, Endicott JA** (1999) Effects of phosphorylation of threonine 160 on cyclin-dependent kinase 2 structure and activity. *J Biol Chem* **274**: 8746-8756
- Cassimeris L** (1999) Accessory protein regulation of microtubule dynamics throughout the cell cycle. *Curr Opin Cell Biol* **11**: 134-141
- Coy DL, Hancock WO, Wagenbach M, Howard J** (1999) Kinesin's tail domain is an inhibitory regulator of the motor domain. *Nat Cell Biol* **1**: 288-292
- Dagenbach EM, Endow SA** (2004) A new kinesin tree. *J Cell Sci* **117**: 3-7
- Day IS, Miller C, Golovkin M, Reddy ASN** (2000) Interaction of a kinesin-like calmodulin-binding protein with a protein kinase. *J Biol Chem* **275**: 13737-13745
- De Veylder L, Beeckman T, Beeemster GTS, Krols L, Terras F, Landrieu I, Van Der Schueren E, Maes S, Naudts M, Inzé D** (2001) Functional analysis of cyclin-dependent kinase inhibitors of *Arabidopsis*. *Plant Cell* **13**: 1653-1667
- De Veylder L, Segers G, Glab N, Van Montagu M, Inzé D** (1997) Identification of proteins interacting with the *Arabidopsis* Cdc2aAt protein. *J Exp Bot* **48**: 2113-2114
- Deavours BE, Reddy ASN, Walker RA** (1988) Ca²⁺/calmodulin regulation of the *Arabidopsis* kinesin-like calmodulin-binding protein. *Cell Motil Cytoskel* **40**: 408-416
- Fontijn RD, Goud B, Echard A, Jollivet F, van Marle J, Pannekoek H, Horrevoets AJG** (2001) The human kinesin-like protein RB6K is under tight cell cycle control and is essential for cytokinesis. *Mol Cell Biol* **21**: 2944-2955
- Geelen DNV, Inzé DG** (2001) A bright future for the Bright Yellow-2 cell culture. *Plant Physiol* **127**: 1375-1379
- Hasezawa S, Kumagai F** (2002) Dynamic changes and the role of the cytoskeleton during the cell cycle in higher plant cells. *Int Rev Cytol* **214**: 161-191
- Hemsley R, McCutcheon S, Doonan J, Lloyd C** (2001) P34^{cdc2} kinase is associated with cortical microtubules from higher plant protoplasts. *FEBS Lett* **508**: 157-161
- Huala E, Dickerman AW, Garcia-Hernandez M, Weems D, Reiser L, LaFond F, Hanley D, Kiphart D, Zhuang M, Huang W et al.** (2001) The *Arabidopsis* Information Resource (TAIR): a comprehensive database and web-based information retrieval, analysis, and visualization system for a model plant. *Nucleic Acids Res* **29**: 102-105
- Hush J, Wu L, John PCL, Hepler LH, Hepler PK** (1996) Plant mitosis promoting factor disassembles the microtubule preprophase band and accelerates prophase progression in *Tradescantia*. *Cell Biol Int* **20**: 275-287

- Joubès J, Inzé D, Geelen D** (2003) Improvements of the molecular toolbox for cell cycle studies in BY-2 cells. *In* T Nagata, S Hasezawa, D Inzé, eds, Tobacco BY-2 Cells, Biotechnology in Agriculture and Forestry Series, Vol 53. Springer, Berlin, pp 7-23.
- Kao Y-L, Deavours BE, Phelps KK, Walker RA, Reddy ASN** (2000) Bundling of microtubules by motor and tail domains of a kinesin-like calmodulin-binding protein from *Arabidopsis*: regulation by Ca^{2+} /calmodulin. *Biochem Biophys Res Commun* **267**: 201-207
- Kashina AS, Rogers GC, Scholey JM** (1997) The *bimC* family of kinesins: essential bipolar mitotic motors driving centrosomes separation. *Biochim Biophys Acta* **1357**: 257-271
- Kim AJ, Endow SA** (2000) A kinesin family tree. *J Cell Sci* **113**: 3681-3682
- Kirchner J, Seiler S, Fuchs S, Schliwa M** (1999) Functional anatomy of the kinesin molecule *in vivo*. *EMBO J* **18**: 4404-4413
- Kong L-J, Hanley-Bowdoin L** (2002) A geminivirus replication protein interacts with a protein kinase and a motor protein that display different expression patterns during plant development and infection. *Plant Cell* **14**: 1817-1832
- Laemmli UK** (1970) Cleavage of structural proteins during the assembly of the head of bacteriophage T4. *Nature (London)* **227**: 680-685
- Lawrence CJ, Malmberg RL, Muszynski MG, Dawe RK** (2002) Maximum likelihood methods reveal conservation of function among closely related kinesin families. *J Mol Evol* **54**: 42-53
- Lee Y-RJ, Giang HM, Liu B** (2001) A novel plant kinesin-related protein specifically associates with the phragmoplast organelles. *Plant Cell* **13**: 2427-2439
- Leyman B, Geelen D, Blatt MR** (2000) Localization and control of expression in Nt-Syr1, a tobacco snare protein. *Plant J* **24**: 369-381
- Liao H, Li G, Yen TJ** (1994) Mitotic regulation of microtubule cross-linking activity of CENP-E kinetochore protein. *Science* **265**: 394-398
- Lindesmith L, McIlvain JM Jr, Argon Y, Sheetz MP** (1997) Phosphotransferases associated with the regulation of kinesin motor activity. *J Biol Chem* **272**: 22929-22933
- Lupas A, Van Dyke M, Stock J** (1991) Predicting coiled coils from protein sequences. *Science* **252**: 1162-1164
- Menges M, Murray JAH** (2002) Synchronous *Arabidopsis* suspension cultures for analysis of cell-cycle gene activity. *Plant J* **20**: 203-212
- Moore JD, Endow SA** (1996) Kinesin proteins: a phylum of motors for microtubule-based motility. *BioEssays* **18**: 207-219
- Nagata T, Nemoto Y, Hasezawa S** (1992) Tobacco BY-2 cell line as the "HeLa" cell in the cell biology of higher plants. *Int Rev Cytol* **132**: 1-30
- Nakagami H, Sekine M, Murakami H, Shinmyo A** (1999) Tobacco retinoblastoma-related protein phosphorylated by a distinct cyclin-dependent kinase complex with Cdc2/cyclin D *in vitro*. *Plant J* **18**: 243-252
- Narasimhulu SB, Reddy ASN** (1998) Characterization of microtubule binding domains in the Arabidopsis kinesin-like calmodulin binding protein. *Plant Cell*, **10**: 957-965
- Narasimhulu SB, Kao Y-L, Reddy ASN** (1997) Interaction of *Arabidopsis* kinesin-like calmodulin-binding protein with tubulin subunits: modulation by Ca^{2+} -calmodulin. *Plant J* **12**: 1139-1149
- Nebenführ A, Frohlich JA, Staehelin LA** (2000) Redistribution of Golgi stacks and other organelles during mitosis and cytokinesis in plant cells. *Plant Physiol* **124**: 135-151
- Oppenheimer DG, Pollock MA, Vacik J, Szymanski DB, Ericson B, Feldmann K, Marks MD** (1997) Essential role of a kinesin-like protein in *Arabidopsis* trichome morphogenesis. *Proc Natl Acad Sci USA* **94**: 6261-6266
- Reddy ASN** (2001) Molecular motors and their functions in plants. *Int Rev Cytol* **204**: 97-178
- Reese EL, Haimo LT** (2000) Dynein, dynactin, and kinesin II's interaction with microtubules is regulated during bidirectional organelle transport. *J Cell Biol* **151**: 155-165
- Reilein AR, Rogers SL, Tuma MC, Gelfand VI** (2001) Regulation of molecular motor proteins. *Int Rev Cytol* **204**: 179-238
- Reindl A, Schöffl F, Schell J, Konz C, Bakó L** (1997) Phosphorylation by a cyclin-dependent kinase modulates DNA binding of the Arabidopsis heat-shock transcription factor HSF1 *in vitro*. *Plant Physiol* **115**: 93-100
- Saint-Jore CM, Evins J, Batoko H, Brandizzi F, Moore I, Hawes C** (2002) Redistribution of membrane proteins between the Golgi apparatus and endoplasmic reticulum in plants is reversible and not dependent on cytoskeletal networks. *Plant J* **29**: 661-678
- Sawin KE, Mitchison TJ** (1995) Mutations in the kinesin-like protein Eg5 disrupting localization to the mitotic spindle. *Proc Natl Acad Sci USA* **92**: 4289-4293

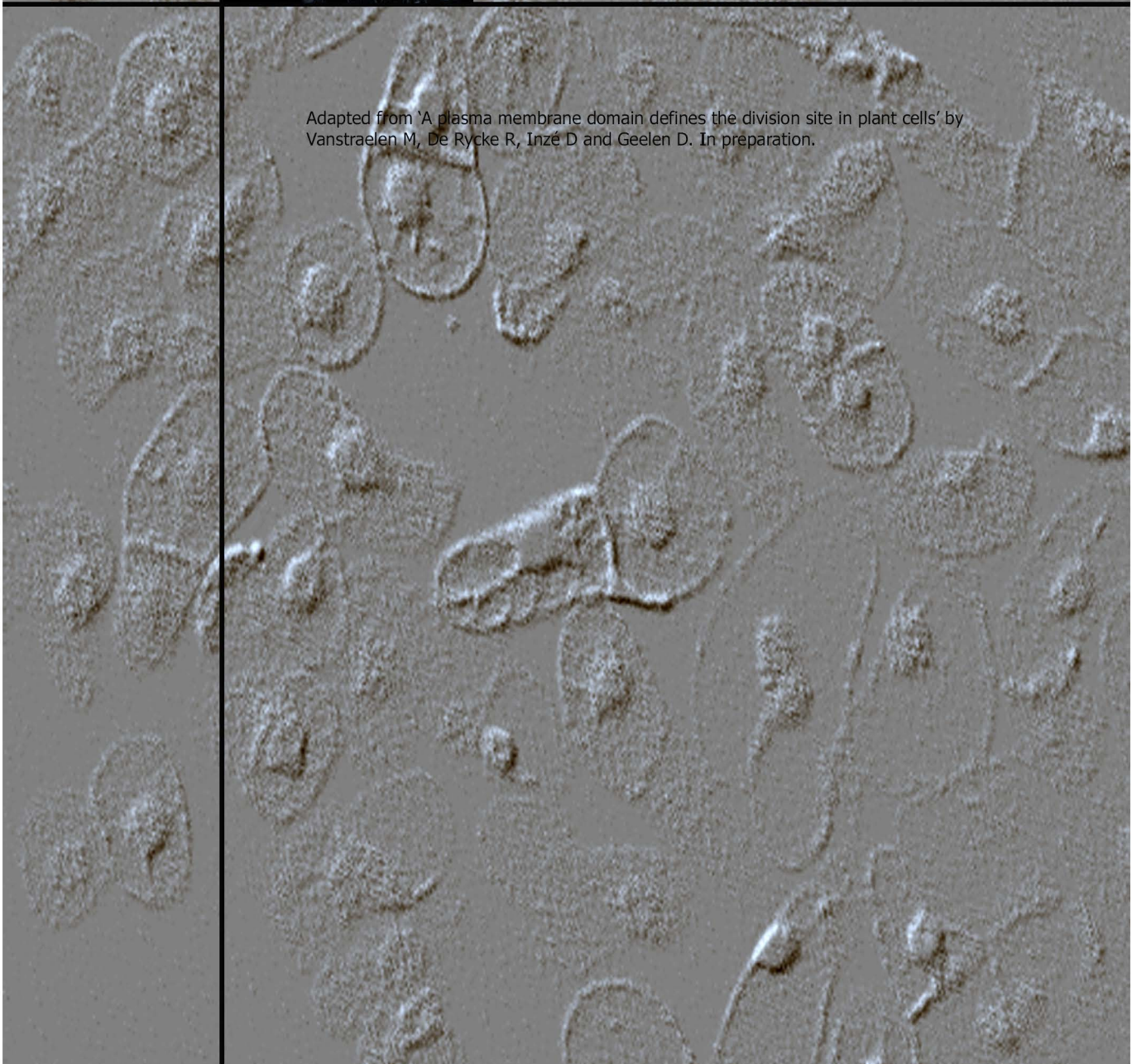
- Schultz J, Copley RR, Doerks T, Ponting CP, Bork P** (2000) SMART: a web-based tool for the study of genetically mobile domains. *Nucleic Acids Res* **28**: 231-234
- Smith LG** (2002) Plant cytokinesis: motoring to the finish. *Curr Biol* **12**: R206-R209
- Stals H, Bauwens S, Traas J, Van Montagu M, Engler G, Inzé D** (1997) Plant CDC2 is not only targeted to the pre-prophase band, but also co-localizes with the spindle, phragmoplast, and chromosomes. *FEBS Lett* **418**: 229-234
- Sternberg MJ** (1991) PROMOT: a FORTRAN program to scan protein sequences against a library of known motifs. *Comput Appl Biosci* **7**: 257-260
- Vale RD, Fletterick RJ** (1997) The design plan of kinesin motors. *Annu Rev Cell Dev Biol* **13**: 745-777
- van der Fits L, Deakin EA, Hoge JHC, Memelink J** (2000) The ternary transformation system: constitutive *virG* on a compatible plasmid dramatically increases *Agrobacterium*-mediated plant transformation. *Plant Mol Biol* **43**: 495-502
- Vantard M, Cowling R, Delichère C** (2000) Cell cycle regulation of the microtubular cytoskeleton. *Plant Mol Biol* **43**: 691-703
- Walczak CE** (2003) The Kin I kinesins are microtubule end-stimulated ATPases. *Mol Cell* **11**: 286-288
- Weingartner M, Binarova P, Drykova D, Schweighofer A, David J-P, Heberle-Bors E, Doonan J, Bögre L** (2001) Dynamic recruitment of *cdc2* to specific microtubule structures during mitosis. *Plant Cell* **13**: 1929-1943



Chapter 4

The kinesin KCA1 defines a plasma membrane region for cell plate guidance

Adapted from 'A plasma membrane domain defines the division site in plant cells' by Vanstraelen M, De Rycke R, Inzé D and Geelen D. In preparation.



Chapter page: Tobacco BY-2 cells expressing GFP fused to the KCA1-del-Nstalk fragment, imaged using confocal microscopy (GFP filter settings).

Abstract

Surrounded by a rigid cell wall plant cells are stationary and require a strict regulation of the division plane to control the direction of growth and the spatial organization of their organs. The mechanisms that underlie division plane establishment are poorly understood. The kinesin KCA1 was previously shown to associate with the developing cell plate at the phragmoplast midline in BY-2 cells. Here, we report that KCA1 is also targeted to the plasma membrane. Cell plate and plasma membrane accumulation was independent of the MT binding motor domain. Brefeldin A prevented association to these compartments, indicating that a Golgi derived vesicle traffic route was required. Different peptide domains in the KCA1 stalk/tail domain were responsible for cell plate and plasma membrane targeting, suggesting that two separate targeting mechanisms control the localization of the KCA1 protein. At the onset of mitosis, GFP-KCA1 accumulated at the plasma membrane. Simultaneously, a region depleted in GFP-KCA1 fluorescence appeared at the plasma membrane corresponding to the site of the preprophase band. We designated this plasma membrane domain the KCA1 depleted zone or KDZ. Throughout mitosis, the KDZ revealed the division site and served as guide for phragmoplast and cell plate expansion. Upon plasmolysis, strong connections were revealed between the cell wall and plasma membrane at the KDZ. In conclusion, the data show that KCA1 reveals a subdomain of the plasma membrane that defines the division site in plant cells.

Introduction

In plants, the presence of a cell wall shared with neighboring cells permanently defines spatial relationships between cells and puts considerable constraints on the type of shaping that can be achieved during cell expansion. Thus for morphogenesis to proceed normally, it is necessary for plants to regulate the positioning of the new wall that partitions the parent cell at cytokinesis.

Control of cell plate alignment involves two steps, the establishment of the site at the cortex where the cell plate will insert in the mother cell wall, called the division site, and guidance of the phragmoplast to the division site during cytokinesis. The establishment of the division site occurs long before cytokinesis and involves the formation of the PPB. This ring of transverse MTs and actin filaments encircles the cell at the cortex. The PPB appears first as a broad band, which then narrows to a thinner ring. Simultaneously the prophase spindle is formed around the nucleus, prepared to catch the chromosomes once the nuclear membrane dissolves. When this occurs, the PPB disappears leaving the cell cortex devoid of cortical MTs for the rest of cell division (Wick, 1991).

After PPB breakdown a hallmark is left behind to guide the phragmoplast to the plasma membrane at the division site. How the division site is marked remains elusive. Cyclin-dependent kinases (CDKs) have been localized to PPB (Colasanti et al., 1993; Stals et al., 1997; Weingartner et al., 2001). One hypothesis is that marker proteins are phosphorylated by CDKs (Cleary, 1995). Moreover, injection of CDKs accelerates the disassembly of the PPB, also suggesting that cell cycle progression is involved in marking the site (Hush et al., 1996). At the cytological level, the division site is marked by cell wall thickenings. Thus the function of the PPB in division site establishment could be to direct the local deposition of membranes and molecules in the plasma membrane and/or cell wall that serve as landmarks for the guidance of the phragmoplast during cytokinesis (Smith, 1999). The importance of the PPB in division plane establishment is supported by *ton/fass* mutants lacking a PPB, that fail to correctly align new cell plates (Torresruiz and Jurgens, 1994; Traas et al., 1995).

When the PPB disappears, actin filaments at the division site also disassemble but are retained elsewhere in the cell cortex. The region of its depletion at the division site is called the actin depleted zone (ADZ) (Staelin and Hepler, 1996). Persistent cortical actin in mitotic cells define two cytoplasmic domains separated by the ADZ, which will be portioned during cytokinesis (Cleary et al., 1992; Cleary, 1995; Pickett-Heaps et al., 1999). Apart from actin, there are no other proteins known that differentially label the division site throughout cell division.

During cytokinesis, Golgi derived vesicles containing cell wall components, are transported along the phragmoplast MTs to the midline where fusion of these vesicles initiates the formation of a new cell plate. To complete cytokinesis, the phragmoplast expands centrifugally until it reaches the mother cell wall at the division site (Verma, 2001). The guiding mechanisms that direct the phragmoplast to the division site remain largely unknown. Actin-myosin complexes are believed to be involved in this process. Through its absence at the division site, actin can balance pulling forces

from either side of the ADZ to guide the cell plate towards the division site (Wick, 1991). A number of kinesins have been localized to the phragmoplast. Till now, their functions seem to be more related to the organization and dynamics of the phragmoplast structure and the transport of Golgi derived vesicles to the midline (Bednarek and Falbel, 2002).

The kinesin KCA1 was previously found at the phragmoplast midline (Vanstraelen et al., 2004). Here, we show that KCA1 also labels the plasma membrane. Both cell plate and plasma membrane association were motor independent but required controlled vesicle trafficking. KCA1 accumulated at the plasma membrane in a cell cycle controlled manner, except at the division site where it remained absent from preprophase till the end of cytokinesis. During cytokinesis, the cell plate was guided to the KCA1 depleted zone at the plasma membrane. Differential localization of KCA1 at the division site was invariable linked to the presence of the PPB MTs and occurred independent of the presence of actin filaments at the cell cortex. Moreover, strong connections are maintained between the plasma membrane and the cell wall at the division site upon plasmolysis. The data show for the first time that the plasma membrane is differentially marked by a kinesin motor protein that marks the division site in plant cells.

Results

KCA1 is localized to the midline of the cylindrical and ring-like phragmoplast

Previously, we reported the localization of KCA1 in BY-2 cells and showed that GFP-KCA1 accumulated at the midline of the expanding phragmoplast (Vanstraelen et al., 2004). To study the behavior of the GFP-KCA1 in relation to MT organization, we used a monomeric red fluorescent protein tagged tubulin (TUA2-RFP) that labels all MT arrays throughout cell division (Van Damme et al., 2004). Stably transformed BY-2 cells expressing the GFP-KCA1 construct were transformed with the TUA2-RFP construct and green and red fluorescence was followed in time using the confocal microscope.

During prophase, TUA2-RFP labeled the PPB, a ring of MTs seen as two wide marks on either side of the nucleus in confocal optical sections (Fig. 4.1, 0'). As the PPB narrowed to a thinner band, the prophase spindle assembled around the still intact nucleus at the centre of the cell (Fig. 4.1, 60'). Subsequently, the nucleus dissolved and MTs invaded the space previously occupied by the nucleus, forming the spindle. During meta- and anaphase, TUA2-RFP labeled the spindle MTs (Fig. 4.1, 100'-125'). In contrast, GFP-KCA1 did not associate to MTs of the PPB or spindle. It remained present in the cortical and endoplasmic cytoplasm during prophase (Fig. 4.1). The GFP signal invaded the spindle area after nucleus breakdown but was not associated to MTs. At the start of cytokinesis, TUA2-RFP labeled the MTs of the cylindrical phragmoplast, except at the midline where the cell plate was formed (Fig. 4.1, 135'-140'). As cell plate formation proceeded, the TUA2-RFP labeled phragmoplast reorganized into a ring-like structure and expanded further towards the mother cell wall (Fig. 4.1, 144'-154'). GFP-KCA1 was not associated with the phragmoplast MTs. It highlighted

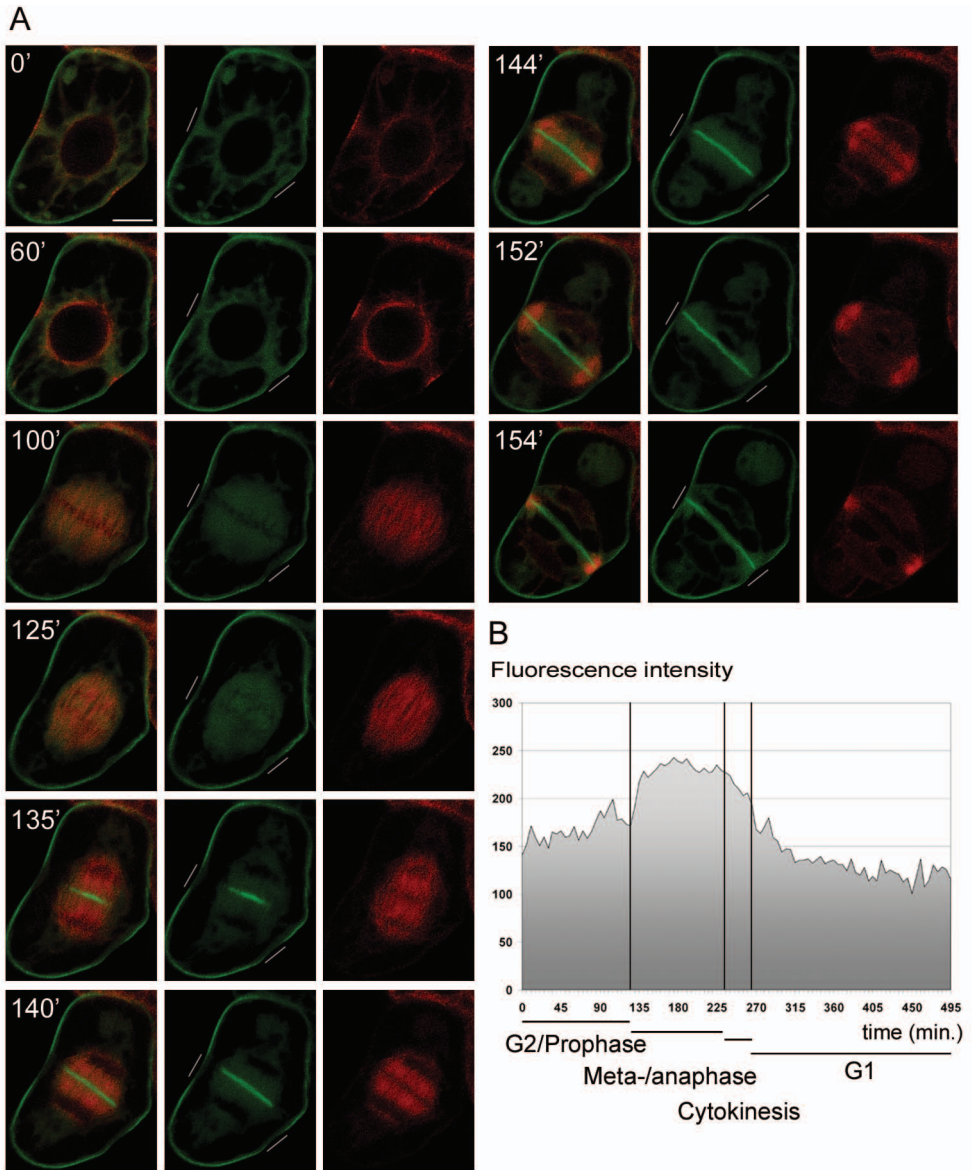


Figure 4.1 The localization of GFP-KCA1 relative to MTs during cell division. A, Time-lapse photography recording of a BY-2 cell expressing GFP-KCA1 and TUA2-RFP. Subsequent images show different stages throughout mitosis: early preprophase (0'), late preprophase (60'), metaphase (100'), anaphase (125') and cytokinesis with cylindrical (135'-140') and ring-like (144'-154') phragmoplast. The left column shows the merged fluorescence, the middle GFP-KCA1 in green and the right TUA2-RFP in red. Time points are indicated in the top left corner in minutes. Bar = 10 μ m. B, Accumulation of GFP-KCA1 at the plasma membrane during mitosis. The absolute fluorescent intensity (y-axis) indicated as arbitrary units in the Y-axis, from a 5 μ m long plasma membrane stretch was plotted as a function time (x-axis). The corresponding mitotic phase is indicated below.

the midline of the cylindrical phragmoplast and the signal expanded simultaneously with phragmoplast growth. GFP-KCA1 remained present at the cell plate where MTs had depolymerized suggesting that KCA1 was not associated with the MT plus-ends of the phragmoplast (Fig. 4.1, 152'). However, GFP signal was highest at the leading edges of the cell plate, where phragmoplast MTs guide the delivery of Golgi derived vesicles to the cell plate (Fig. 4.1, 154'). Areas of highest GFP-KCA1 fluorescence coincided with peaks of TUA2-RFP fluorescence, suggesting that KCA1 arrives at the cell plate via MTs (data not shown). Absence of yellow color in the overlays indicates that KCA1 is not concentrated at the MTs of mitotic arrays. The labeling of KCA1 at the cell cortex is discussed later.

The KCA1 tail domain confers targeting to the cell plate

Comparison of the predicted structure of the KCA1 kinesin revealed a tripartite domain organization typical for kinesins, consisting of a head, stalk and tail domain (Fig. 4.2A). To identify the region responsible for midline localization, we constructed deletion fragments of the KCA1 open reading frame.

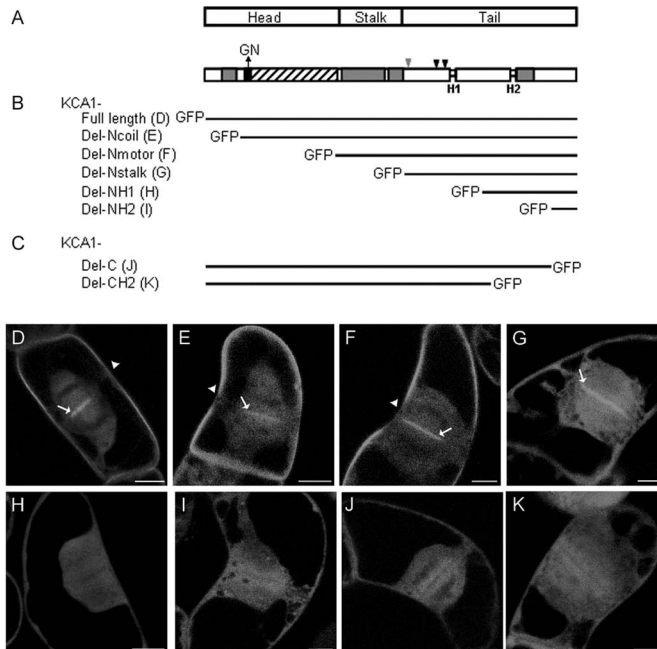


Figure 4.2 Identification of the KCA1 domain responsible for subcellular targeting. A, Secondary structure and domain organization of KCA1. Neck with conserved GN motif for minus-end directed motility; black box, motor domain; dashed box, coiled coils; grey boxes, conserved CDKA₁ phosphorylation sites; black arrowheads and hinge regions, H1 and H2. B, nested KCA1 deletion fragments from the N-terminus. GFP was fused N-terminally to the full length and deletion fragments. C, Schematic diagram of the nested KCA1 deletion fragments from the C-terminus. GFP was fused C-terminally to these fragments. D-K, GFP-localizations of the KCA1 fragments. BY-2 cells, stably expressing respectively GFP-KCA1 (D), GFP-KCA1-del-Ncoil (E), GFP-KCA1-del-Nmotor (F), GFP-KCA1-del-Nstalk (G), GFP-KCA1-del-NH1 (H) GFP-KCA1-del-NH2 (I), KCA1-del-C-GFP (J) and KCA1-del-CH2-GFP (K) were imaged at cytokinesis. The accumulation of GFP signal at the cell plate (arrow) and the presence of the KDZ (arrowhead) are indicated. Bar = 10 μ m.

Figure 4.2B shows the nested deletions from the N-terminal end of KCA1 that were fused to the C-terminus of GFP. The fusions were stably transformed in BY-2 cells and their localization patterns were observed throughout cell division (Fig. 4.2, D-I). Deletion of the N-terminal motor up to the beginning of the tail domain did not abolish accumulation of GFP signal at the phragmoplast midline (Fig. 4.2, D-G). However, the midline was not labeled when the N-terminal part of the tail domain was removed (Fig. 4.2H). The results indicated that the tail domain of KCA1 was sufficient for midline localization, and that the N-terminal part of the tail domain contains sequences that are essential for targeting to the midline. Surprisingly, neither the motor domain nor the stalk domain was necessary for midline localization. The importance of the KCA1 tail was further tested by a series of C-terminal deletion fragments fused to the N-terminus of GFP (Fig. 4.2C). The removal of a small part of the C-terminus up to the second hinge abolished accumulation at the cell plate (Fig. 4.2, J and K). Thus the N- and the C-terminal part of the tail domain are essential for cell plate targeting.

KCA1 localizes to a membrane compartment in the cell plate

As motor activity was not required for KCA1 to concentrate at the phragmoplast midline and since there were no indications for the MT binding activity in the stalk or tail domain, we tested whether KCA1 travels via the vesicle trafficking machinery similar to the cytokinesis specific SNARE protein KNOLLE (Lukowitz et al., 1996). Brefeldin A (BFA) was applied to GFP-KCA1 expressing cells to inhibit the vesicle trafficking pathway and prevent the coating of vesicles at the Golgi apparatus. As a consequence, Golgi derived vesicles no longer accumulate at the phragmoplast midline during cytokinesis and no cell plate is formed (Yasuhara et al., 1995; Yasuhara and Shibaoka, 2000).

GFP-KCA1 expressing cells were treated in prophase and monitored throughout cytokinesis (Fig. 4.3A). Cytokinesis started around 81 min after adding BFA and a phragmoplast was formed as indicated by the diffuse green fluorescence in the centre of the cell between the two negatively stained daughter nuclei. The corresponding differential interference contrast (dic) image shows that no cell plate is formed (compare with first dic image of Fig. 4.3B) and consistent with this, GFP-KCA1 signal was absent from the phragmoplast midline. Despite the absence of a forming cell plate, the phragmoplast reorganized in a ring-like structure (Fig. 4.3A, 124') and expanded till it reached the mother cell wall (Fig. 4.3A, 155'). Thus, KCA1 travels via the vesicle traffic pathway towards the phragmoplast midline, but phragmoplast expansion did not require the formation of a cell plate. Taxol is an inhibitor of MT depolymerization and therefore promotes the stability of MTs. In cytokinetic cells, taxol treatments cause an increase in the accumulation of vesicles at the midline while simultaneously inhibiting the centrifugal growth of the phragmoplast (Yasuhara et al., 1993). Applying this drug to young phragmoplasts froze the outward growth of the phragmoplast within 10 minutes (Fig. 4.3B).

GFP-KCA1 associated fluorescence accumulated at the phragmoplast midline without any centrifugal expansion of the signal, indicating that delivery of GFP-KCA1 containing vesicles was maintained.

The results support a MT dependent transport of KCA1 to the cell plate presumably via Golgi-derived vesicles.

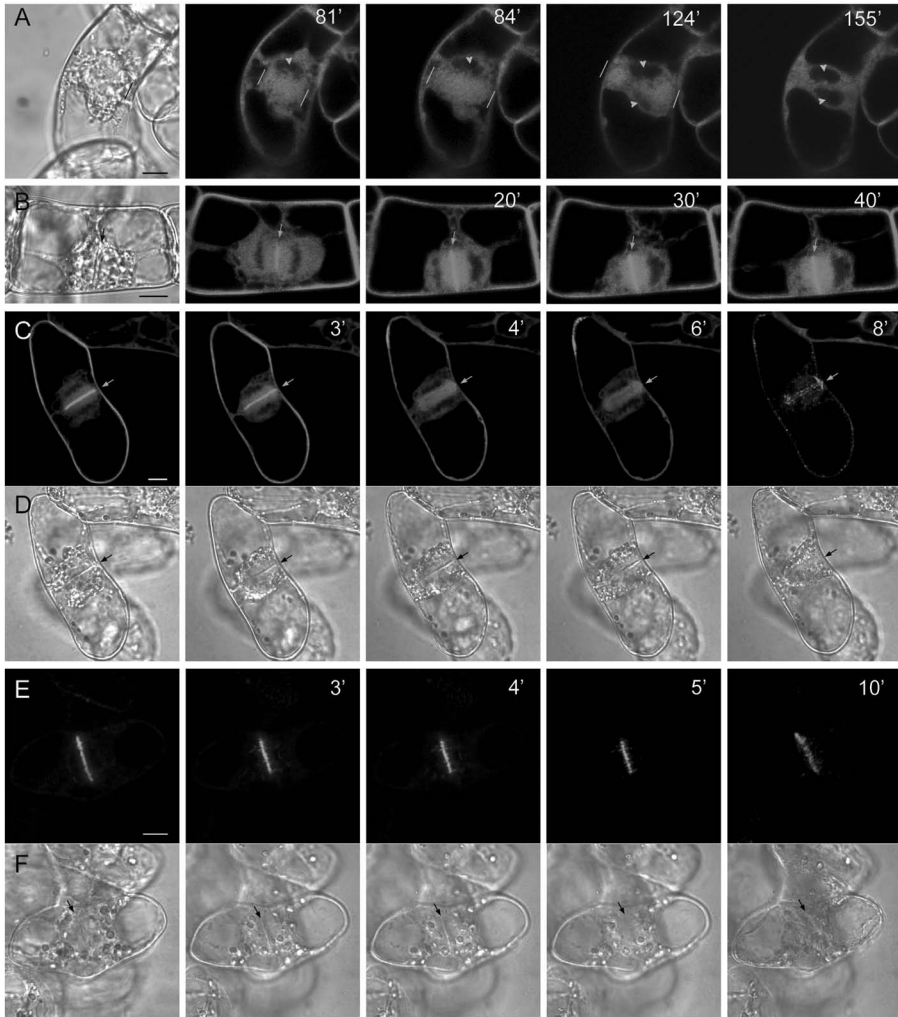


Figure 4.3 GFP-KCA1 is associated with membranes of the cell plate. A, BFA was added to a final concentration of 20 $\mu\text{g}/\text{mL}$ to a GFP-KCA1 prophase cell. Images were made afterwards during cytokinesis of the cylindrical (81'–84') and ring-like (124') phragmoplast till the end of cytokinesis (155'). The image to the left is a differential interference contrast (dic) image corresponding to 81' after BFA was added. Bars indicate the position of the phragmoplast leading edges and arrowheads designate the nucleus. B, Taxol treatment of a GFP-KCA1 expressing cell showing accumulation of GFP fluorescence at the phragmoplast midline. The dic image corresponds to time point 20'. Taxol (20 μM) was added to the sample after the first fluorescent image taken. Arrows indicate the cell plate. C – F show the fluorescent (C and E) and corresponding dic (D and F) images of detergent treated GFP-KCA1 and MAP65-3-GFP cells. First image of each row is taken before adding 0,1% Triton-x-100. GFP-KCA1 is extracted from the cell plate 4' after adding the detergent, whereas MAP65-3-GFP remains associated with the MT plus-ends of the phragmoplast. Black (D and F) and white (C and E) arrows indicate the cell plate. Time points after adding BFA, Taxol or Triton-X-100 are indicated at the top right corner. Bar = 10 μm .

To investigate the association of KCA1 with membranes, we treated GFP-KCA1 cells with the detergent Triton X-100 (Fig. 4.3, C and D). After four minutes of detergent extraction, GFP-KCA1 disappeared from the phragmoplast midline while the cell plate was still present. Eight minutes later, the cell plate itself was completely dissolved and GFP-KCA1 appeared in a punctate pattern around the former cell plate position and at the cell cortex, close to the perforated plasma membrane. To test the specificity of the extraction method, BY-2 cells expressing AtMAP65-3-GFP were also treated with detergent (Fig. 4.3, E and F). AtMAP65-3 is a MT-associated protein that accumulates at the midline of the phragmoplast (Hussey et al., 2002). Fused to GFP, it specifically accumulates during cytokinesis and labels the center of the phragmoplast where MTs overlap (Van Damme et al., 2004a). Application of Triton X-100 to cytokinetic cells did not remove MAP65-3-GFP from the midline (Fig. 4.3, E and F). However, the phragmoplast did not enlarge in these cells, suggesting that interference with membrane structure was detrimental to cell plate formation and expansion. The results show that GFP-KCA1 is bound to membranes of the cell plate and prove that MTs do not anchor GFP-KCA1 at phragmoplast midline.

To provide further evidence that KCA1 was associated to a membrane compartment of the cell plate, we localized the endogenous KCA protein using an antibody raised against the KCA2 stalk domain (anti-KCA2;stalk), which recognizes both KCA1 and 2 on a western blot (data not shown). Root tips of Arabidopsis seedlings were processed for cryofixation and gold labeling was performed on the sections with the anti-KCA2;stalk serum and pre-immune serum as control. Panels of Figure 4.4 are derived from a dividing cell with an expanding cell plate at the centre of the cell.

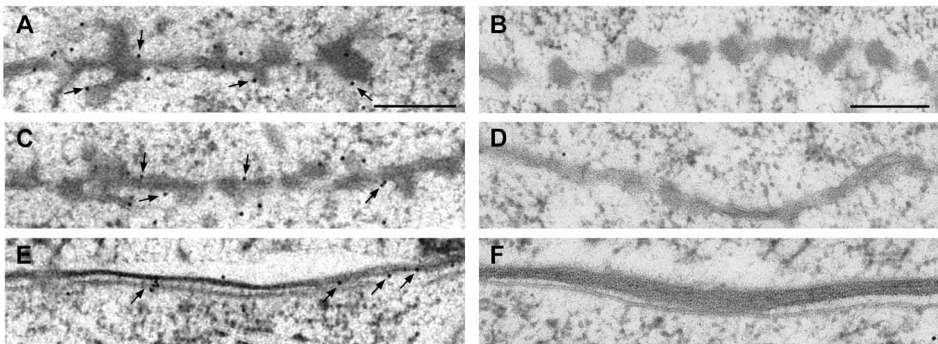


Figure 4.4 Endogenous KCA1 is localized to the developing cell plate and the plasma membrane. Immunogold labeling of 5 days old Arabidopsis root tips with anti-KCA2;stalk antiserum (A, C and E) and pre immune serum (B, D and F) viewed by the transmission electron microscope. Images A, C and E and images B, D and F are each derived from a single dividing cell with a ring-like phragmoplast. Gold particles (indicated by arrows) are present both at the cell plate region of the ring-like phragmoplast (A) and at the centre of the cell plate where phragmoplast MTs have depolymerized (C). MTs were not conserved in these preparations. Gold label was also observed at the plasma membrane (E). Label was absent from the cell plate (B and D) and the plasma membrane (F) in cells incubated with the pre-immune serum. Bar = 200 nm.

The pre-immune serum did not reveal any label at the cell plate (Fig. 4.4, B and D). On the contrary, KCA associated Gold label was present both at the centre of the cell plate and at the leading edges (Fig. 4.4, A and C), in agreement with the localization of GFP-KCA1 in expanding cell plates (Fig. 4.1, 152'). The large majority of the Gold label occurred at the periphery of the dense cell plate material, suggesting it was bound to the cytoplasmic side of the cell plate membrane. The Golgi was only scarcely labeled, indicating that KCA1 is not resident to this compartment. Together the data confidently show that the KCA1 kinesin is a membrane-associated protein traveling on vesicles to the cell plate.

KCA1 is associated with the plasma membrane

In addition to cell plate labeling, we observed bright GFP-KCA1 fluorescence at the cell cortex (Fig. 4.1, Fig. 4.2D and Fig. 4.3C). Upon detergent treatment, cortical labeling was lost, whereas fluorescence in the cytoplasm remained (Fig. 4.3C, 4'). Therefore we analyzed the association of GFP-KCA1 with the plasma membrane.

To visualize the plasma membrane, GFP-KCA1 BY-2 cells were stained with FM4-64 that exhibits long-wavelength red fluorescence. FM4-64 belongs to a group of styryl FM dyes that have previously been used to demonstrate endocytosis in animals (Betz et al., 1996), yeast (Vida and Emr, 1995) and plant cells (Emans et al., 2002). The green fluorescent analog FM1-43 showed a gradual distribution in BY-2 cells, first staining the plasma membrane, later after 30 min it accumulated in cytoplasmic vesicles and subsequently after 120 minutes it labeled the vacuolar membrane (Emans et al., 2002). FM4-64 showed a similar behavior in BY-2 cells expressing GFP-KCA1 (data not shown). During the first 20-30 min, red fluorescence was exclusively present at the plasma membrane (Fig. 4.5A). The yellow/orange color in Figure 4.5 indicates colocalization of GFP-KCA1 and FM4-64 at the plasma membrane. To assess the level of co-localization, green and red fluorescence intensity was measured in FM4-64 stained cells expressing untagged GFP, GFP-KCA1, or AtFH6-GFP, a fusion protein that is targeted to the plasma membrane (Favery et al., 2004; Van Damme et al., 2004). Figure 4.5 shows the fluorescence levels along a line that sections the plasma membrane at both sides of the observed cell. At the position where the plasma membrane is crossed, green and red signal intensified and partially overlapped. In cells that expressed GFP-KCA1 and AtFH6-GFP, the fluorescence peaks of GFP and FM4-64 perfectly coincided (Fig. 4.5, A and C). This was not the case for cells producing free GFP molecules, in which fluorescence was also abundant at the cell periphery, but the green and red fluorescence peaks were clearly separated (Fig. 4.5B). These results indicated that GFP-KCA1 was closely associated with the plasma membrane in BY-2 cells. The presence of endogenous KCA1 protein at the plasma membrane was also investigated by immunolocalisation. In EM sections of dividing Arabidopsis root cells, anti-KCA2;stalk serum was concentrated at the plasma membrane (Fig. 4.4E). Pre-immune serum did not label the plasma membrane (Fig. 4.4F). Thus, KCA kinesin is bound to the plasma membrane.

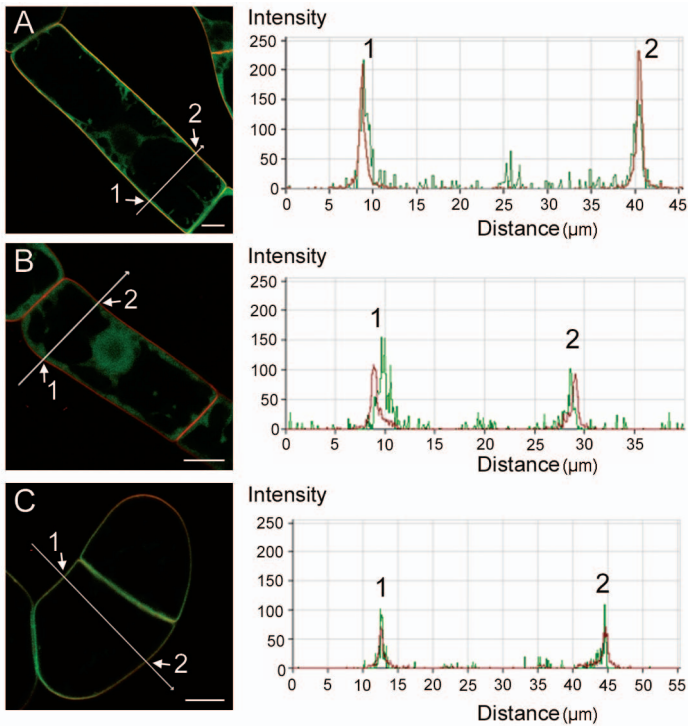


Figure 4.5 KCA1 is associated with the plasma membrane. A-C, FM4-64 staining (red) of cells expressing GFP-KCA1 (A), free GFP (B) and AtFH6-GFP (C) in green. Orange-yellow signal in A and C indicates colocalization of FM4-64 with GFP-KCA1 and AtFH6-GFP respectively. The corresponding fluorescence intensity graph is shown at the right. Intensity was measured along the white intersecting line shown in the fluorescence image. Numbers in the fluorescent images correspond to the fluorescent peaks in the intensity graph. Bar = 10 μ m.

GFP-KCA1 displays a mitosis specific differential localization at the plasma membrane

We noticed that GFP-KCA1 fluorescence at the plasma membrane was most prominent in cells that were dividing (Fig. 4.1A). Therefore, the localization of KCA1 at the plasma membrane was followed throughout the cell cycle. The plot in Figure 4.1B shows the fluorescence intensity at the plasma membrane of a GFP-KCA1 transformed cell from G2 until the next G1 phase. During prophase, GFP-fluorescence gradually increased and reached a maximum at metaphase that was maintained until cytokinesis. Once the cell plate reached the mother cell wall, plasma membrane fluorescence quickly decreased to the levels from before mitosis. During the period of strong fluorescence at the plasma membrane, GFP-KCA1 was not homogenously distributed along the plasma membrane, but showed a zone at the equatorial plane where it was depleted (Fig. 4.1 and Fig. 4.6, A and D). This zone of about 7 μ m wide (n=35) occurred at a position opposite to the leading edges of the

developing cell plate. To analyze the distribution of GFP-KCA1 at the plasma membrane it was compared to that of FM4-64 and AtFH6-GFP. In contrast to GFP-KCA1, FM4-64 (Fig. 4.6, B and E) nor AtFH6-GFP (Fig. 4.6, C and F) revealed a depleted zone and evenly labeled the plasma membrane. Green and red fluorescence were quantified at the plasma membrane in a cross section through the equatorial plane (point 1 in Fig. 4.6, G and H) and elsewhere (point 2 in Fig. 4.6, G and H) in a GFP-KCA1 cell stained with FM4-64. GFP-KCA1 fluorescence peak was absent from the region near the equatorial plane and therefore this region was called the KCA1 depleted zone or KDZ. The yellow/orange color in Figure 4.6G indicates co-localization of GFP-KCA1 and FM4-64 at the plasma membrane in cells that are dividing, except at a location opposing the cell plate edges. Thus, GFP-KCA1 is differentially targeted to the plasma membrane throughout the cell cycle, revealing a divergent subdomain in the plasma membrane during mitosis.

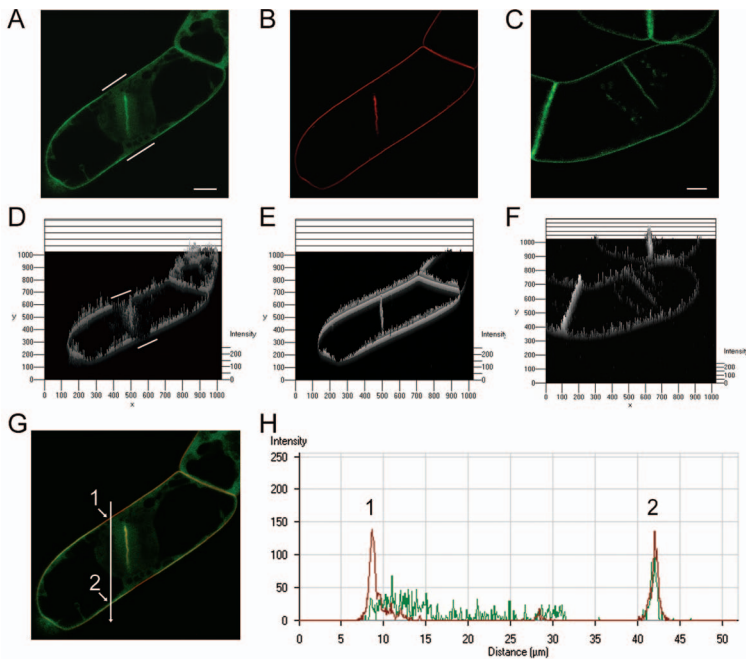


Figure 4.6 GFP-KCA1 is excluded from a cortical zone at the equator during division. A-B, fluorescent images of a cytokinetic GFP-KCA1 cell (A) stained with FM4-64 (B) and a cytokinetic cell expressing AtFH6-GFP (C). GFP-KCA1 was absent from the plasma membrane at either side opposing the cell plate (A, bars). The image in D displays the fluorescence intensity measured within the image and shows that the fluorescence intensity is minimal in the KDZ. Label along the plasma membrane was constant for FM4-64 (B) and AtFH6-GFP (C). Consistent with this, fluorescence intensity as visualized within the image (E and F) remained high along the plasma membrane. The overlay of (A) and (B) is shown in (G) and the fluorescence measured along the intersecting line drawn in (G) is shown in (H). Colocalisation was observed at the plasma membrane (2) but not at regions opposing the cell plate (1). Bar = 10μm.

KDZ co-localizes with the PPB and marks the position to which the cell plate is guided

Next the dynamic behavior of the expanding cell plate in relation to the KDZ was analyzed. It appeared that the phragmoplast was guided towards the region where GFP-KCA1 fluorescence was reduced and that cell plates fused with the mother cell wall exactly at the center of the KDZ (Fig. 4.1). In several occasions, we observed that at first the axis of the growing cell plate did not align with the position of the KDZ. However, in each case the position of the cell plate was readjusted to fit with the KDZ so that the plate eventually fused with the mother cell wall indicated by the KDZ. An example of such an event is shown in Figure 4.1. At time point 135' in mitosis, the cell plate matched with the KDZ at one side of the cell but not at the other. Subsequently, the plate moved slightly so that both the leading edges pointed toward the KDZ. Thus, the KDZ appeared to mark a zone to which the cell plate was guided.

In plant cells, a ring of MTs also known as the PPB determines the division site. The PPB disappears at nucleus disintegration but its former position predicts where the cell plate will insert the mother wall during cytokinesis (Wick, 1991). These features of the PPB prompted us to ask two questions; does the KDZ match with the former position of the PPB and is KDZ formation coincident with PPB formation? Figure 4.1 shows that the KDZ appeared after the PPB was formed and then started to narrow down (compare time points 0' and 60' in Fig. 4.1). Moreover, the position of the KDZ exactly corresponded to the position of the PPB. However, after the PPB had disappeared, the KDZ remained at the plasma membrane till the end of cell division. In conclusion, the KDZ matches with the position of the PPB and thus marks the division site from preprophase till the end of cell division.

The formation of the KDZ depends on MT organization

During preprophase, the PPB establishes the division site by steering the localized deposition of factors necessary for cell plate guidance and insertion (Mineyuki and Gunning, 1990). As the nucleus disintegrates, the PPB disappears leaving the cell cortex devoid of MTs throughout the rest of cell division (Staehelin and Hepler, 1996). The time series in Figure 4.1 showed that the KDZ was formed during preprophase and unlike the PPB, the KDZ lingered till cell plate insertion. These data suggested that the PPB MTs are involved in the construction of the KDZ, but that MTs are not engaged in its preservation. To check this hypothesis we added MT depolymerizing drugs to dividing GFP-KCA1/TUA2-RFP cells. Disappearance of TUA2/RFP red fluorescence was indicative for the depolymerization of the MTs. Amiprophos-methyl (APM) added to a cell in early cytokinesis, cleared phragmoplast MTs within 16 minutes (Fig. 4.7A). The KDZ was unaffected by the addition of AMP and even after 60' of treatment only a small reduction in GFP-KCA1 concentration at the cell plate and the plasma membrane was noticed. MTs were therefore not needed to keep GFP-KCA1 at the cell plate or to maintain the KDZ at the plasma membrane.

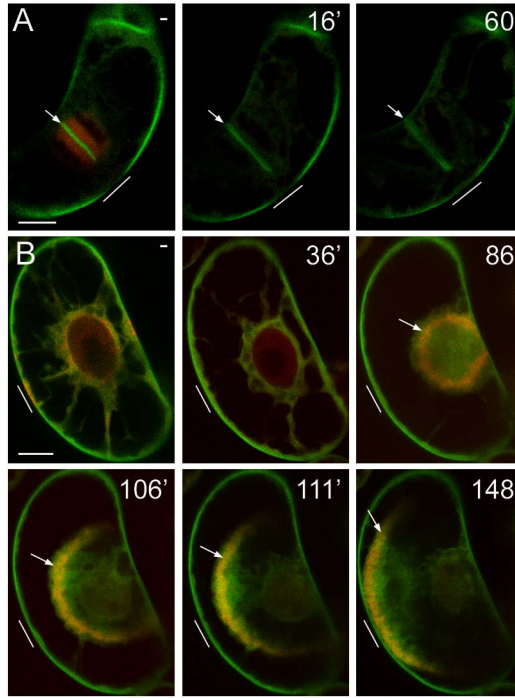


Figure 4.7 The KDZ formation is invariably linked to cell plate positioning.

A, The MT depolymerizing drug, APM was added to a GFP-KCA1/TUA2-RFP expressing cell in cytokinesis (-). GFP-KCA1 cell plate label (arrow) and the KDZ (bar) remained present 16' and 60' after adding APM. Time points after adding APM are indicated in the upper right corner. B, Propyzamide treatment of GFP-KCA1/TUA2-RFP cells in preprophase. Propyzamide was added to cells in early preprophase when the KDZ was not yet formed (B, -). The drug was washed out after TUA2-RFP labeled MTs were depolymerized and cells were followed throughout cell division (B, 36'-148'). Bars indicate the former position of the PPB. Time points in the upper right corner indicate the time after washing out the drug solution. The PPB was not reconstructed in B, 36' and consequently the KDZ was not established. During cytokinesis, the division plane had changed by 90° (B, 86'-148'). The ring-like phragmoplast (arrow) (B, 86'-148') expanded and the cell plate was not inserted at the previous PPB site (B, 148'). Bar = 10 μ m.

To investigate the contribution of PPB MTs in the construction of the KDZ, cells showing a broad PPB that had not yet developed a KDZ, were treated with MT depolymerizing drugs and allowed to continue throughout mitosis by washing the drug out. The washing steps were started as soon as all MTs labeled with TUA2-RFP had disappeared. Cells did not cycle further when APM was used (data not shown). Instead, MT depolymerization and inhibition of mitosis by propyzamide were reversible (Nagata et al., 1994). Propyzamide was added to a cell with a broad PPB and no KDZ and MT depolymerization was monitored in time. After one hour, TUA2-RFP associated label at the site previously taken by the broad PPB had disappeared and the drug was washed out. Subsequent imaging showed that in most cases the PPB was reconstructed, narrowed and accordantly the KDZ

appeared. These cells cycled further throughout cell division with division planes correctly aligned at the KDZ (data not shown). However, in several recordings, a 90° tilting of the division plane had occurred during drug treatment. Figure 4.7B shows such an event. The first image (Fig. 4.7B, -) is taken before adding propyzamide. The PPB marks the plasma membrane at either site of the cell, but a KDZ is not yet formed. Propyzamide was added to the cell at this stage and was washed out after PPB MTs had completely depolymerized. Subsequently, the cell was followed throughout mitosis. Remarkably, the PPB was not reconstructed at the original site and confirming our hypothesis, the KDZ did not emerge at the plasma membrane (Fig. 4.7B, 36'). Later, during cytokinesis (Fig. 4.7B, 86'-148') the cell plate was not formed in the original division plane as determined by the PPB in Fig. 4.7B, -. In contrast, both the phragmoplast and the cell plate were expanding in a 90° angle with the original division plane. This is evident in the confocal section by the fact that the ring-like phragmoplast is actually visible as a ring and not as two discrete parts (compare with Fig. 4.1, 152'). Accordingly, the cell plate was not recognizable as a fluorescent line that expanded towards opposing sites of the parent wall, but as a GFP labeled plane within the phragmoplast ring that expanded in circumference as the ring-like phragmoplast broadened (Fig. 4.7, 86'-148'). This suggests that in absence of the KDZ, the cell plate is not guided to the position originally marked by the PPB. It is of course possible that a new PPB and a subsequent KDZ was reconstructed in 90° to the original PPB. Even so, it would still indicate that cell plates are invariably guided to the KDZ.

In conclusion, the data show that PPB MTs differentially mark the plasma membrane, thereby creating the KDZ. After PPB disintegration, the cell cortex lacks MTs and the KDZ exists independent of cortical MTs. In absence of a KDZ, cell plates are not guided to a region initially marked by the PPB.

The central coiled coil is involved in KDZ formation

To investigate the peptide domains of KCA1 responsible for the differential localization at the plasma membrane, we reexamined the GFP-KCA1 deletion fragments and looked for the presence of a KDZ (Fig. 4.2). Deleting the N-terminal sequence and motor domain did not effect KDZ formation indicating that motor activity was not required (Fig. 4.2, E and F). Deletion of the central stalk caused a loss of differential fluorescence at the plasma membrane (Fig. 4.2G). The latter result was also obtained with the nested deletions from the C-terminal end (Fig. 4.2, J and K).

To analyse the accumulation of the deletion fragments at the plasma membrane, GFP-KCA1;del-Nmot, GFP-KCA1;del-Nstalk, KCA1;delC-GFP and KCA1;delCH2-GFP expressing cells were stained with FM4-64 (Fig. 4.8). During interphase, neither of the GFP fusions colocalized with FM4-64 (data not shown). However during mitosis, GFP-KCA1;del-Nmotor colocalized with the FM dye at the plasma membrane, whereas the other GFP-fusions did not. Thus the KCA1 stalk domain is required for plasma membrane association during cell division and consequently the marking of a depleted zone at the division site. The coiled coils in the stalk domain have been shown to be implicated in

dimerization of KCA1 (Vanstraelen et al., 2004), suggesting that dimerization is a prerequisite for plasma membrane association. In addition, the small C-terminal sequence is necessary for the association of KCA1 with both the plasma membrane and the cell plate, and thus probably contains sequences essential for membrane association.

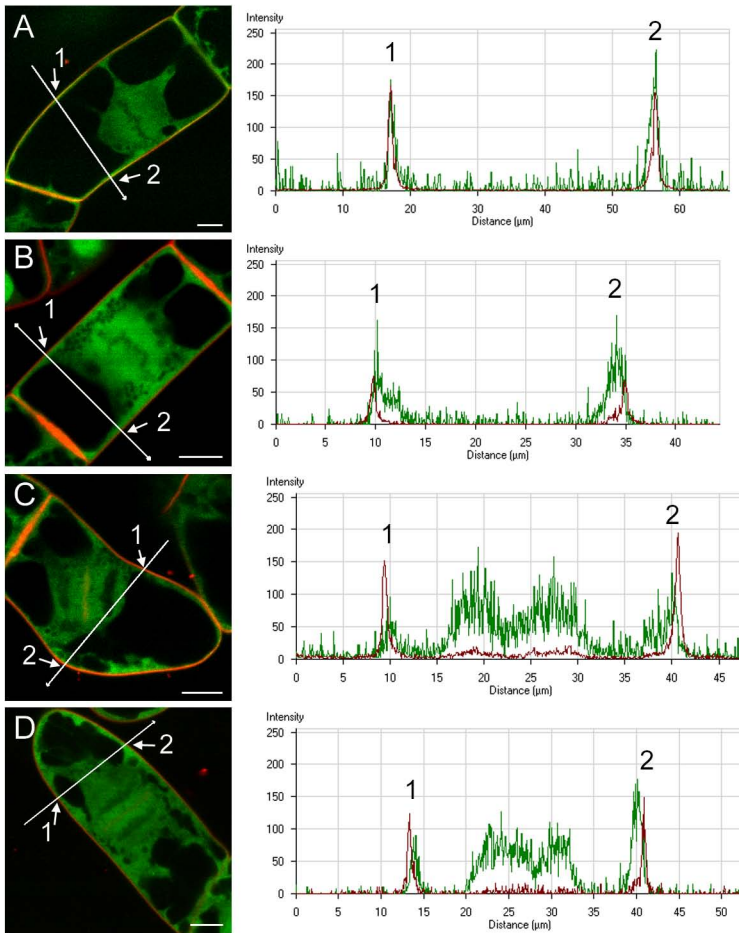


Figure 4.8 The KCA1 dimerization domain is required for targeting to the plasma membrane. Fluorescent images and corresponding fluorescent intensity graphs of dividing cells expressing GFP fused to KCA1-del-Nmotor (A), del-Nstalk (B), del-C (C) and del-CH2 (D). Intensity was measured along the white intersecting line shown in the fluorescence image. Numbers in the fluorescent images correspond to the fluorescent peaks in the intensity graph. Bar = 10 μm.

The KDZ colocalizes with the position of the actin depleted zone, but does not depend on actin

As mentioned above, the cell cortex becomes devoid of MTs as the PPB disappears. Actin filaments at the division site also disassemble but are retained elsewhere in the cell cortex (Staehelein and Hepler, 1996). This region is called the actin depleted zone (ADZ) and marks the division site from PPB break down till cell plate insertion. This behavior resembles that of GFP-KCA1 and thus we investigated whether the KDZ and ADZ coincided and whether the persistence of the KDZ throughout mitosis was supported by the differential localization of actin filaments at the cell cortex. To this end, the actin binding domain 2 of fimbrin was fused N-terminally to RFP (ABD2-RFP) and stably transformed in GFP-KCA1 cells. Figure 4.9 shows a metaphase cell expressing GFP-KCA1 (Fig. 4.9A) and ABD2-RFP (Fig. 4.9B). ABD2-RFP was associated with the fine meshwork of actin filaments at the cell cortex except at the sides facing the metaphase plate, the ADZ. Compressed 3 dimensional imaging showed that the ADZ actually forms a band encircling the cell at the cortex (Fig 4.9B, inset). The merged image shows that the KDZ colocalizes with the ADZ (Fig. 4.9C).

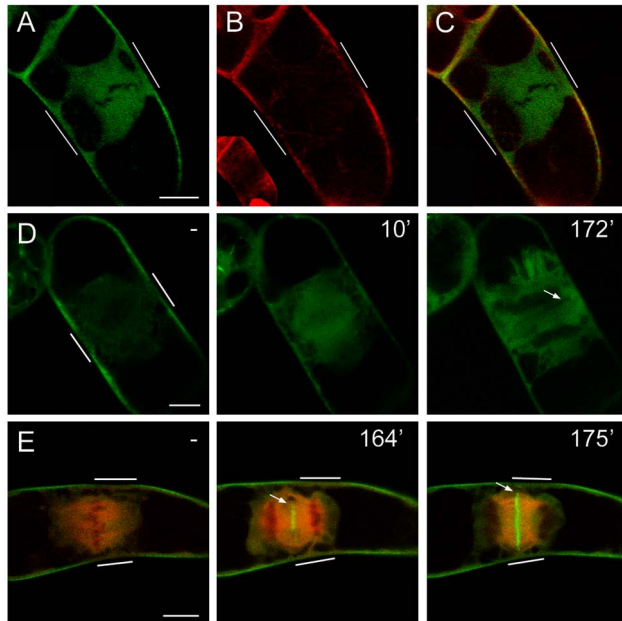


Figure 4.9 The KDZ coincides with the actin depleted zone, but is not dependent on actin distribution. A-C, Mitotic cell expressing GFP-KCA1 (A) and ABD2-RFP (B) with overlay in (C). Inset in (B) shows collapsed Z-stack revealing the fine actin network at the cell cortex, that is absent from the equatorial zone. Bars indicate the position of KDZ and ADZ. D-E, Treatment of metaphase cells, expressing ABD2-GFP (D, -) or GFP-KCA1/TUA2-RFP (E, -) with LatB. Bars indicate the position of the ADZ in (D) and the KDZ in (E). Time points after drug addition are indicated in the top right corner in minutes. D, Mitotic actin filaments and the ADZ disappear 10' after adding LatB, but a cell plate (arrow) is still formed (D, 172'). E, The KDZ remains intact after LatB treatment and a GFP-KCA1 labeled cell plate (arrow) is formed (164') that expands towards the KDZ (bar) (175'). Bar = 10 μ m.

Next, the dependence of the KDZ on actin filaments was studied. In a control experiment, GFP-ABD2 expressing cells revealing an ADZ were treated with Latrunculin B (Lat B), an actin depolymerizing agent (Fig. 4.9D). Within 10 min of treatment, the network of actin filaments at the cortex had depolymerized and the ADZ had disappeared.

LatB was then added to GFP-KCA1/TUA2-RFP cells in metaphase and the cells were followed till the end of cytokinesis (Fig. 4.9E). Breakdown of the actin filament network did not seem to affect the accumulation of GFP-KCA1 at the plasma membrane or the cell plate and the KDZ was still intact. Moreover, KCA1 labeled cell plates were still guided to the KDZ and finally fused with the mother cell wall at these sites (Fig. 4.9E, 175'). The process took 3h26 from metaphase till the end of cytokinesis, which is much longer than in non-treated cells (65 minutes; Fig. 4.1). In some occasions, aberrations in cell plate expansion were observed, with cell plates that arrived at the mother cell wall at the KDZ continuing to expand into an S shaped form or a 90° tilting of the plane of cell division (data not shown). Lat B was also added to cells in interphase, before a KDZ or ADZ was present (data not shown). The cells however managed to form a KDZ and passed through cell division with the cell plate aligned with the position of the KDZs. Also here, cell division as measured from the formation of the PPB till completion of cell plate formation took much longer than in untreated cells. The data show that distribution of GFP-KCA1 and actin filaments at the cell cortex are similar during mitosis, however, actin filaments are not required to form the KDZ.

The KDZ is physically attached to the cell wall

When cells are plasmolysed, the plasma membrane detaches from the cell wall and the cell shrinks within the cell wall cage. Adding 0.3M sucrose induces a mild plasmolysis, allowing the plasma membrane to detach slightly from the cell wall (Cleary, 2001). BY-2 cells expressing GFP-KCA1, AtFH6-GFP and free GFP were plasmolysed and stained with FM4-64 (Fig. 4.10, A-C). GFP-KCA1 and AtFH6-GFP localized to the plasma membrane and no staining was observed at the cell wall. The results confirm that KCA1 and AtFH6 are exclusively localized to the plasma membrane and not to the cell wall.

When cells were treated with 0.6% NaCl, cells are more severely plasmolysed. The plasma membrane shrinks further away from the cell wall and the connections between the plasma membrane and cell wall, known as Hechtian strands, become evident (Zhu et al., 1993). Plasma membrane proteins appear in these Hechtian strands. Both GFP-KCA1 and GFP-AtFH6 colocalized with FM4-64 in the plasma membrane-cell wall connections, whereas free GFP did not (Fig. 4.10, D-F). The results confirm that KCA1 is associated to the plasma membrane and reveal the presence of KCA1 in plasma membrane-cell wall connections.

During mitosis, localized wall thickenings have been observed at the PPB site, suggesting that the PPB modifies the plasma membrane and/or cell wall in preparation for cell plate guidance and insertion (Galatis et al., 1982). In addition, plasmolysis revealed adhesion of the plasma membrane to the cell wall at the PPB (Cleary, 2001). As the position of the KDZ corresponds to the PPB site,

dividing GFP-KCA1 cells were plasmolysed to investigate whether these plasma membrane-cell wall connections persisted at the KDZ after PPB breakdown.

Dividing cells revealing a KDZ were selected and stained with FM4-64. Then BY-2 medium containing 0.6 % NaCl was added and cells were imaged further. The cell in Figure 4.10G is in anaphase and the FM4-64 associated red fluorescence at the plasma membrane indicates the position of the KDZ. Upon plasmolysis, Hechtian strands, labeled with FM4-64 and GFP-KCA1 were formed. By this time, the cell entered cytokinesis and a GFP-KCA1/FM4-64 fluorescent cell plate was constructed (Fig. 4.10H). More intriguingly, the plasma membrane remained connected to the cell wall at the regions of the cortex previously marked by the KDZ. The data suggest that PPB mediated modifications at the plasma membrane include the firm attachment of the plasma membrane to the cell wall. These adhesion points are maintained throughout mitosis, possibly ensuring that the cell plate is inserted at correct sites both at the plasma membrane and cell wall.

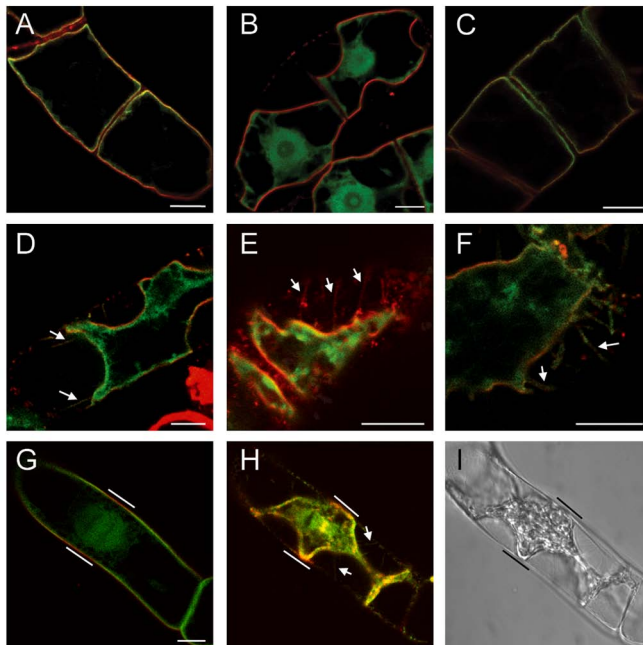


Figure 4.10 Plasmolysis reveals GFP-KCA1 in plasma membrane-cell wall connections and the position of the division site.

A-F, Plasmolysis of FM4-64 stained cells shows co-localization of GFP-KCA1 and AtFH6-GFP at the plasma membrane after mild salt treatment (A and C) and at the Hechtian strands (arrows) after stringent salt treatment (D and F). Co-localization was not observed in free GFP expressing cells at these positions (B and E, respectively). G-I, Plasmolysis of the GFP-KCA1 dividing cell, stained with FM4-64 (G) reveals persistent plasma membrane-cell wall attachment at the division site (H). Bars indicate the position of the division site before (G) and after (H and I) treatment. The corresponding DIC image of (H) is shown in (I). Bar = 10 μ m.

Discussion

Because plant cells are surrounded by a rigid cell wall, plant morphology is controlled by the strict regulation of cell plate alignment. This process involves two steps, first the establishment of the site where the cell plate will insert into the mother cell wall, called the division site and secondly guidance of the cell plate to the division site during cytokinesis. Aside from actin and the so-called Golgi belt (Nebenfuhr et al., 2000), other markers for the division site after PPB breakdown remain elusive (Smith, 1999). Previously we showed that KCA1 localizes to the phragmoplast midline. Here, we report that KCA1 accumulates at the plasma membrane in a cell cycle controlled manner revealing the division site at the plasma membrane from preprophase till the end of cytokinesis. Cell plates were invariably inserted at the KCA1 marked region of the plasma membrane. Moreover, strong connections are maintained between the plasma membrane and the cell wall after plasmolysis at the division site. The data show for the first time that the plasma membrane is differentially marked at the division site, where strong adhesion with the cell wall probably assures a correct insertion of the cell plate within a given tissue context.

KCA1 labeled the phragmoplast midline during cytokinesis and expansion of GFP-KCA1 signal followed the leading edges of the phragmoplast MTs. Several plant kinesins have been shown to localize at the phragmoplast midline during cytokinesis. All follow the dynamic expansion of phragmoplast MTs and disappear from the centre of the cell plate where MTs have depolymerized. AtPAKRP1, AtPAKRP1L and NACK1 are specifically associated with MTs at the phragmoplast midzone and they are believed to be involved in the dynamic organization of the phragmoplast MTs (Lee and Liu, 2000; Lee et al., 2001; Nishihama et al., 2002; Pan et al., 2004). Another phragmoplast-associated kinesin, AtPAKRP2, is associated with Golgi derived vesicles at the midline (Lee et al., 2001). AtPAKRP2 is a plus-end directed kinesin and its relocalisation along with phragmoplast MTs supports the hypothesis that this kinesin transports the vesicles containing cell wall material, to the equator. Unlike these motor proteins, KCA1 remains associated with the cell plate where MTs have depolymerized, suggesting that KCA1 is involved in later steps of cell plate formation. KCA1 is likely a minus-end directed kinesin. If KCA1 is mobile, it moves away from the midline, supporting the possibility that KCA function takes care of the recycling of excess membrane away from the cell plate (Otegui and Staehelin, 2000).

In plants and animals, motor proteins drive the transport of a wide variety of organelles and vesicular cargoes including endoplasmic reticulum (ER), Golgi, endosomes, lysosomes, mitochondria and transport vesicles (Goldstein and Yang, 2000; Lee and Liu, 2004). However, this is the first report on the localization of a kinesin at the plasma membrane. Immunogold labeling with an antibody directed against the stalk domain of KCA localized endogenous KCA to the cell plate and plasma membrane, confirming the GFP analysis. GFP-KCA1 accumulation at the plasma membrane or cell plate does not involve the MT binding motor domain as GFP fused to the stalk-tail domain of KCA1 managed to localize at these positions during cell division. The tail domain as a separate GFP fusion only labeled the phragmoplast midline. This indicates that targeting of KCA1 to the plasma

membrane differs from that to the cell plate. In contrast to secretable GFP, which is transported via the default secretion pathway towards both the cell plate and plasma membrane for secretion (Batoko et al., 2000), two separate targeting mechanisms control the localization of the KCA1 protein. The stalk domain of KCA1 contains several coiled coil domains. This central region of KCA1 was shown to be involved in dimerization of KCA1 in homo- or heterodimers with its closest homologue KCA2 (Vanstraelen et al., 2004). The data suggest that monomeric KCA1 molecules accumulate at the phragmoplast midline whereas only dimeric KCA1 arrives at the plasma membrane. On the other hand, other modifications than dimerization can drive KCA1 to the plasma membrane. In this case, dimerized KCA1 is transported to the phragmoplast midline during cytokinesis. An extra transport signal sequence in the stalk domain or molecular interaction of another protein with the KCA1 stalk domain drives KCA1 to the plasma membrane.

Accumulation of KCA1 to the cell plate and plasma membrane was not dependent on MTs, but was membrane associated. Treatment of cells with a mild detergent or BFA abolished KCA1 signal at the plasma membrane and midline. Wortmannin also removed KCA1 from the plasma membrane (data not shown). Although both drugs affect endocytosis, BFA stimulates endocytosis whereas wortmannin inhibits this process (Clague et al., 1995; Emans et al., 2002). Thus a well-controlled and dynamic membrane trafficking system supports KCA1 localization at the plasma membrane.

Upon deletion of a small C-terminal part of the KCA1 tail domain, cell plate and plasma membrane localization was lost, suggesting that this part of KCA1 contains sequences essential for membrane association. Targeting domains for the protein sorting machinery are often located at the N-terminal end of a protein but may be present in the C-terminus (Raikhel and Chrispeels, 2000). However, signal peptides were absent from the C terminus or elsewhere in the protein. In addition, there are no transmembrane regions, suggesting that KCA1 is a soluble protein. This is supported by the absence of KCA1 in microsomal fractions (data not shown) and argues that KCA1 binds via other proteins to the membranes of the cell plate and the plasma membrane. Accumulation of GFP-KCA1 at the cell plate upon taxol treatment can then be interpreted as an accumulation of target membrane at the midline. On the other hand, it is possible that KCA1 arrives at the cell plate at the surface of Golgi derived vesicles along the phragmoplast MTs. The latter is most likely the case for AtPAKRP2, which is present in membrane fractions of protein extractions and in addition contains a signal peptide for Golgi targeting (Lee et al., 2001).

KCA1 displays a dynamic association to the plasma membrane with a gradual accumulation of GFP-KCA1 at the beginning of mitosis. Cell division dependent accumulation of GFP signal was more prominent with the stalk-tail fragment of KCA1 that only associated to the plasma membrane during cell division. KCA1 contains two adjacent conserved CDKA;1 phosphorylation sites in the N-terminal part of the tail domain and interaction of KCA1 with CDKA;1 has been repeatedly reported (De Veylder et al., 1997; Vanstraelen et al., 2004). CDKA;1 phosphorylation prevented tail folding and favored the dimeric form of KCA1 over the monomeric form. It is known for several kinesins that MT and cargo binding are controlled by phosphorylation (Reilein et al., 2001) and in case of conventional kinesin, it involves the unfolding of the tail domain (Cross and Scholey, 1999).

Phosphorylation of KCA1 during cell division could therefore lead to an accumulation of unfolded KCA1, allowing protein dimerization and accumulation of KCA1 at the plasma membrane.

During cell division, GFP-KCA1 revealed a differential localization at the plasma membrane. At the level of the cell equator, a region depleted of KCA1 fluorescence, called the KDZ, persisted till the end of cytokinesis. This differential behavior at the plasma membrane was specific to KCA1 as neither the FM dye or the formin AtFH6 revealed a similar pattern. The KDZ was formed during preprophase and became more obvious during PPB narrowing. It colocalized with the PPB and ADZ and is thus the first protein shown to reveal the division site at the level of the plasma membrane throughout cell division. The KDZ also supports the idea that the plasma membrane is modified at the division site to serve as a landmark for guidance of phragmoplasts during cytokinesis (Smith, 1999; Cleary, 2001). Indeed, expanding cell plates invariably fused with the plasma membrane exactly at the KDZ. The PPB would then direct the local deposition of membrane bound molecules at the plasma membrane (Mineyuki and Gunning, 1990) and this matches with the formation of the KDZ during PPB maturation. The appearance of the KDZ was invariably linked to the presence of the PPB and when both were absent, cell plates were misguided, suggesting a function for the KDZ in cell plate guidance.

When plant cells are plasmolysed, membrane strands connect the cell wall to the disconnected plasma membrane at certain points. GFP-KCA1 colocalized with the FM4-64 dye in these strands, consolidating the plasma membrane association of KCA1 and suggesting that KCA1 could act as a sensor or linker molecule between the cytoskeleton and plasma membrane/cell wall continuum. Remarkably, during cell division the plasma membrane remained attached to the cell wall at exactly the KDZ/division site when cells were plasmolysed. The result corresponds to observations made in epidermal peels of *Tradescantia* cells with sustained plasma membrane-cell wall attachments at the PPB site (Cleary, 2001). Here, it was claimed that cytoskeleton-transmembrane complexes are involved in the preservation of the division plane. It seems however more likely that the function of the cytoskeleton is limited to the establishment of the division site and not in its conservation. Depolymerization of MTs or actin filaments during cytokinesis did not obliterate the KDZ. In contrast, the formation of the KDZ was independent of actin filaments, but consistently linked to the presence of PPB MTs. Thus, the PPB MTs seem to establish the division site before metaphase and then disappear. This is consistent with observations made in wheat root tips, where initial formation of the actin filament band in the PPB was sensitive to drugs that depolymerized MTs, whereas later the conservation of this actin band was independent of MTs (McCurdy and Gunning, 1990). Whether the plasma membrane-cell wall connections mark the division site before the PPB does, is not known. Anyway, its persistence at the division site after PPB breakdown indicates its involvement in the maintenance of this site. In a developmental context, these connections might assure that developing cell plates arrive at the right place of the rigid cell wall within a given tissue context.

Does the absence of KCA1 at the division site indicate a function of KCA1 in phragmoplast guidance or does it reflect the absence of scaffolding protein at the plasma membrane? Two hybrid experiments revealed an interaction of the tail domain of KCA1 with a tropomyosin and a myosin-

like protein (Torres Acosta, De Veylder and Inzé, unpublished data). KCA1 could act as a linker protein between the plasma membrane and myosin-actin complexes. The absence of KCA1 at the division site then results in a depletion of myosin-actin complexes in the division site, thereby allowing actin pulling forces at the phragmoplast edges from either site of the division site (Wick, 1991; Smith, 1999; Sylvester, 2000). On the other hand, an interaction of KCA1 with the katanin P60 subunit AtKSS has been reported (Bouquin et al., 2003). In animal cells, katanins act as heterodimers of a catalytic P60 subunit and a regulatory P80 subunit and sever MTs from centrosomes (Hartman et al., 1998; McNally et al., 2000). Several mutants in the AtKSS gene have been analysed (Bichet et al., 2001; Burk et al., 2001; Webb et al., 2002; Bouquin et al., 2003). Their most common features are defects in cell elongation accompanied by failure to align the cortical MTs in a transverse array as cells leave the mitotic zone. In vitro MT-severing activity of AtKSS has been reported (Stoppin-Mellet et al., 2002). The interaction between KCA1 and AtKSS, can be interpreted as KCA1 acting as a sensor protein between the plasma membrane and the microtubular cytoskeleton, driving AtKSS towards MTs that do not co-align with transverse microfibers for MT severing. In this way, the KCA1-AtKSS complex contributes to the transverse alignment of cortical MTs leading to cell elongation. In the katanin mutants, reorganization of MTs during mitosis occurred normally, however, misaligned cell plates were observed in some tissues (Bichet et al., 2001; Burk et al., 2001; Webb et al., 2002). During cell division, KCA1 is phosphorylated by CDKA₁, resulting in an accumulation of unfolded KCA1, allowing dimerization. This results in an accumulation of KCA1 at plasma membrane during cell division and an increased MT severing activity at the cell cortex. As a result, cortical MTs along the entire plasma membrane are severed except at the site of the PPB, from where KCA1 is excluded. It would thus be interesting to cross katanin and KCA mutants and investigate whether the katanin phenotype is reinforced.

Materials and methods

Construction of GFP fusion proteins

The expression of the inducible KCA1 full-length open reading frame, pTANGKCA1 was done as previously described (Vanstraelen et al., 2004). For constitutive expression, the KCA1 full length was cloned into the GATEWAY vector pK7WGF2 leading to 35S driven expression of the insert (Karimi et al., 2002). Nested deletion fragments from the N-terminus were cloned by PCR. The gene specific sequences used as forward primers were: KCA1-FWD CAATGGCCGATCAGAGAAGTAAAA; KCA1-del-NcoI GGATATCTCCACTTATCAAT; KCA1-del-Nmotor TTGGCAATCGAGATACAATC; KCA1-del-Nstalk CAATGGCTGTTTCGACCCAG; KCA1-del-NH1 TTCTGTCCGAGTATGCAAAA; KCA1-del-NH2 TAAAATGTGGAGGCAACAAC. The reverse primer was: KCA1-REV TTAATCCAGTTCACATAACAA. For nested deletion fragments from the C-terminus, the KCA1-FWD was the forward primer. The gene

specific sequences for the reverse primers were: KCA1-del-C TTATGATGAATGGGGCTGAA and KCA1-del-CH2 GAAGCTGCCCCGAGAGCATCT.

35S promoter-driven GFP fusion constructs were generated in the destination vector pK7WGF2 for N-terminal fusions via GATEWAY LR reactions (Karimi et al., 2002). For the construction of the actin marker, a fimbrin sequence was used to subclone an actin binding domain, using primers: ABD2-FWD CCTCTTGAAAGAGCTGAATTGGTT and ABD2-REV TTCGATGGATGCTTCTCTGAGA. PCR products were cloned in the pDONR211 vector and transferred via LR reactions to the pK7FWG2 and pK7RWG2 vector. AtFH6-GFP, TUA2-RFP and MAP65-3-RFP were described previously (Van Damme et al., 2004a; Van Damme et al., 2004b).

Growth, transformation, and fluorescence microscopy

Culturing of BY-2 cells was according to Nagata et al. (1992) and stable BY-2 transformation was carried out as described (Geelen and Inze, 2001). Transgenic calli were screened for the production of GFP fusions using fluorescence microscopy. For GFP/RFP colocalization, BY-2 cells stably transformed with the inducible pTANGKCA1 construct were transformed with the RFP constructs pK7RWG2-ABD2 and pK7RWG2-TUA2. BY-2 cells transformed with the inducible pTANGKCA1 vector were induced overnight on BY-2 agar containing 10 μ M dexamethasone.

Confocal images were taken with a scanning confocal microscope 100M with software package LSM 510 version 3.2 (Zeiss) equipped with a 63x water corrected objective (numerical aperture of 1.2). GFP fluorescence was imaged with argon laser illumination at 488 nm and 500-530 nm band emission filter. Dual GFP and RFP fluorescence was imaged in a multichannel setting with 488 nm and 543 nm light for GFP and RFP excitation, respectively. Emission fluorescence was captured in the line-scanning mode, altering GFP fluorescence via a 500-530 nm band pass emission filter and RFP via a 560 nm cut-off filter. Fluorescence intensity measurements along cross-sections or within images were obtained using the LSM software under respectively the profile or 2.5D option tool. For transmission light images, differential interference contrast optics was used. Images were taken with 25% laser power to minimize photobleaching.

Sample preparation

For life cell recordings, samples were applied to a chambered cover glass (Lab-Tek, Naperville, IL, USA) coated with 5 mg/mL poly-L-lysine (Sigma-Aldrich) and immobilized in a thin layer of 100-200 μ L of BY-2 medium containing vitamins and 0.8% of low melting point agar (Invitrogen). For time experiments without drug treatments, 1mL of BY-2 medium containing vitamins was added to the sample after polymerization of the agar and the chambered cover glass was sealed with parafilm to prevent dehydration of the sample.

For detergent extraction, selected cells were imaged before adding Triton X-100 (Sigma-Aldrich). Then 100 μL of BY-2 medium containing vitamins and 0.1% Triton X-100 was added on top of the agar and cells were followed immediately after adding the detergent in a time sequence.

For drug experiments, selected cells were imaged before addition of amiprofos-methyl (10 μM final concentration; Duchefa, Haarlem, The Netherlands), propyzamide (6 μM final concentration; Chem Service, West Chester, USA), Latrunculin D (24 μM , Calbiochem, Darmstadt, Germany), Taxol (20 μM , Sigma-Aldrich) or Brefeldin A (20 $\mu\text{g}/\text{mL}$, Molecular Probes, Leiden, The Netherlands). Drugs were added in a volume of 1000 μL of BY-2 medium with added vitamins and the drug at a concentration adjusted to a final volume of 1100-1200 μL . Stock solutions of APM (10mM), propyzamide (600 μM) were dissolved in dimethylsulfoxide, Taxol (10mg/mL) and LatB (24mM) in ethanol and BFA (50mg/mL) in methanol respectively. As control, 1000x and 100x dilutions of the solvent in BY-2 medium were used. The behavior of KCA1 at the cell plate and plasma membrane was monitored in time series taken directly after drug application.

FM4-64 labeling

FM4-64 (Molecular Probes, Leiden, The Netherlands) was kept as a 33mM stock in sterile nanopure water. To label the plasma membrane of GFP expressing BY-2 cells, FM4-64 dye was freshly diluted 100 x from the stock solution in BY-2 medium containing vitamins. Cells were added to this solution and imaged directly under the confocal microscope using the same settings as for dual GFP/RFP visualization. Fluorescence intensity along an intersecting line was measured using the LSM software under the profile option.

Plasmolysis experiments

For mild plasmolysis 0.3M sucrose solutions and for stringent plasmolysis 4% NaCl solutions were made in BY-2 medium containing vitamins. Cells were added to the solution and used directly for imaging.

To study the behavior of dividing cells upon plasmolysis, samples were prepared in chambered cover glasses with low melting point agar as described above. Selected cells were imaged before starting plasmolysis. Then, 100 μL of BY-2 medium containing vitamins and FM4-64 dye was added and cells were imaged again. Finally, 1000 μL of BY-2 medium containing vitamins and 0.3M sucrose was added to the sample and the cells were followed further.

EM analysis

Rabbit polyclonal antibodies were raised against the KCA stalk domain (425-864aa). The specificity of the antiserum was tested on western blot against GST tagged KCA1 and KCA2 from induced and non-induced bacterial pellets.

For EM analysis, root tips of 4-day-old *Arabidopsis* seedlings Columbia ecotype were excised, immersed in dextrane (20%) and frozen immediately in a high pressure freezer (EM Pact, Leica Microsystems, Vienna, Austria). Freeze substitution was carried out in a Leica EM AFS. Over a period of 4 days, root tips were substituted in dry acetone+ 0.1% OsOs₄. Samples were infiltrated at 4°C stepwise in spurr and embedded in molds. The polymerisation was performed at 70°C for 16 h. Ultra thin sections of gold interference color were cut using an ultramicrotome (ultracut E / Reichert-Jung) and collected on formvar-coated copper slot grids.

All steps of immunolabeling were performed in a humid chamber at RT. Samples were blocked in blocking solution (5 % BSA, 1% FSG in PBS) for 15 min followed by a wash step for 5 min (1% BSA in PBS). Incubation in a dilution (1% BSA in PBS) of primary antibodies for 60 min (anti-KCA;stalk, 1:100; pre-immune, 1:100) was followed by washing four times 5 min (0.1 % BSA in PBS). The grids were then incubated with PAG_{10nm} (Cell Biology, Utrecht, University) and washed twice 5 min each (0.1 % BSA in PBS, PBS and ddH₂O). Sections were post stained in a LKB ultra stainer for 30 min in uranylacetate at 40° C and 5 min in lead stain at 20° C. Control experiments consisted of treating sections with PAG_{10nm} alone. Grids were viewed by using a JEOL 1010 TEM operating system at 80 kV.

References

- Batoko H, Zheng HQ, Hawes C, Moore I** (2000) A Rab1 GTPase is required for transport between the endoplasmic reticulum and Golgi apparatus and for normal Golgi movement in plants. *Plant Cell* **12**: 2201-2217
- Bednarek SY, Falbel TG** (2002) Membrane trafficking during plant cytokinesis. *Traffic* **3**: 621-629
- Betz WJ, Mao F, Smith CB** (1996) Imaging exocytosis and endocytosis. *Curr Opin Neurobiol* **6**: 365-371
- Bichet A, Desnos T, Turner S, Grandjean O, Hofte H** (2001) BOTERO1 is required for normal orientation of cortical microtubules and anisotropic cell expansion in Arabidopsis. *Plant J* **25**: 137-148
- Bouquin T, Mattsson O, Naested H, Foster R, Mundy J** (2003) The Arabidopsis lue1 mutant defines a katanin p60 ortholog involved in hormonal control of microtubule orientation during cell growth. *J Cell Sci* **116**: 791-801
- Burk DH, Liu B, Zhong R, Morrison WH, Ye ZH** (2001) A katanin-like protein regulates normal cell wall biosynthesis and cell elongation. *Plant Cell* **13**: 807-827
- Clague MJ, Thorpe C, Jones AT** (1995) Phosphatidylinositol 3-kinase regulation of fluid phase endocytosis. *FEBS Lett* **367**: 272-274
- Cleary AL** (1995) F-Actin Redistributions at the Division Site in Living Tradescantia Stomatal Complexes as Revealed by Microinjection of Rhodamine-Phalloidin. *Protoplasma* **185**: 152-165
- Cleary AL** (2001) Plasma membrane-cell wall connections: roles in mitosis and cytokinesis revealed by plasmolysis of Tradescantia virginiana leaf epidermal cells. *Protoplasma* **215**: 21-34
- Cleary AL, Gunning BES, Wasteneys GO, Hepler PK** (1992) Microtubule and F-Actin Dynamics at the Division Site in Living Tradescantia Stamen Hair-Cells. *Journal of Cell Science* **103**: 977-988
- Colasanti J, Cho SO, Wick S, Sundaesan V** (1993) Localization of the Functional P34(Cdc2) Homolog of Maize in Root-Tip and Stomatal Complex Cells - Association with Predicted Division Sites. *Plant Cell* **5**: 1101-1111
- Cross R, Scholey J** (1999) Kinesin: the tail unfolds. *Nat Cell Biol* **1**: E119-121
- De Veylder L, Segers G, Glab N, Van Montagu M, Inzé D** (1997) Identification of proteins interacting with the Arabidopsis Cdc2aAt protein. *J Exp Bot* **48**: 2113-2114
- Emans N, Zimmermann S, Fischer R** (2002) Uptake of a fluorescent marker in plant cells is sensitive to brefeldin A and wortmannin. *Plant Cell* **14**: 71-86
- Favery B, Chelysheva LA, Lebris M, Jammes F, Marmagne A, De Almeida-Engler J, Lecomte P, Vauy C, Arkowitz RA, Abad P** (2004) Arabidopsis formin AtFH6 is a plasma membrane-associated protein upregulated in giant cells induced by parasitic nematodes. *Plant Cell* **16**: 2529-2540
- Galatis B, Apostolakis P, Katsaros C, Loukari H** (1982) Pre-Prophase Microtubule Band and Local Wall Thickening in Guard-Cell Mother Cells of Some Leguminosae. *Annals of Botany* **50**: 779-791
- Geelen DN, Inze DG** (2001) A bright future for the bright yellow-2 cell culture. *Plant Physiol* **127**: 1375-1379
- Goldstein LS, Yang Z** (2000) Microtubule-based transport systems in neurons: the roles of kinesins and dyneins. *Annu Rev Neurosci* **23**: 39-71
- Hartman JJ, Mahr J, McNally K, Okawa K, Iwamatsu A, Thomas S, Cheesman S, Heuser J, Vale RD, McNally FJ** (1998) Katanin, a microtubule-severing protein, is a novel AAA ATPase that targets to the centrosome using a WD40-containing subunit. *Cell* **93**: 277-287
- Hush J, Wu LP, John PCL, Hepler LH, Hepler PK** (1996) Plant mitosis promoting factor disassembles the microtubule preprophase band and accelerates prophase progression in Tradescantia. *Cell Biology International* **20**: 275-287
- Hussey PJ, Hawkins TJ, Igarashi H, Kaloriti D, Smertenko A** (2002) The plant cytoskeleton: recent advances in the study of the plant microtubule-associated proteins MAP-65, MAP-190 and the Xenopus MAP215-like protein, MOR1. *Plant Molecular Biology* **50**: 915-924
- Karimi M, Inze D, Depicker A** (2002) GATEWAY vectors for Agrobacterium-mediated plant transformation. *Trends Plant Sci* **7**: 193-195
- Lee YR, Giang HM, Liu B** (2001) A novel plant kinesin-related protein specifically associates with the phragmoplast organelles. *Plant Cell* **13**: 2427-2439
- Lee YR, Liu B** (2000) Identification of a phragmoplast-associated kinesin-related protein in higher plants. *Curr Biol* **10**: 797-800
- Lee YR, Liu B** (2004) Cytoskeletal motors in Arabidopsis. Sixty-one kinesins and seventeen myosins. *Plant Physiol* **136**: 3877-3883

- Lukowitz W, Mayer U, Jurgens G** (1996) Cytokinesis in the Arabidopsis embryo involves the syntaxin-related KNOLLE gene product. *Cell* **84**: 61-71
- Mccurdy DW, Gunning BES** (1990) Reorganization of Cortical Actin Microfilaments and Microtubules at Preprophase and Mitosis in Wheat Root-Tip Cells - a Double Label Immunofluorescence Study. *Cell Motility and the Cytoskeleton* **15**: 76-87
- McNally KP, Bazirgan OA, McNally FJ** (2000) Two domains of p80 katanin regulate microtubule severing and spindle pole targeting by p60 katanin. *J Cell Sci* **113 (Pt 9)**: 1623-1633
- Mineyuki Y, Gunning BES** (1990) A Role for Preprophase Bands of Microtubules in Maturation of New Cell-Walls, and a General Proposal on the Function of Preprophase Band Sites in Cell-Division in Higher-Plants. *Journal of Cell Science* **97**: 527-537
- Nagata T, Kumagai F, Hasezawa S** (1994) The Origin and Organization of Cortical Microtubules During the Transition between M-Phase and G(1)-Phase of the Cell-Cycle as Observed in Highly Synchronized Cells of Tobacco by-2. *Planta* **193**: 567-572
- Nagata T, Nemoto Y, Hasezawa S** (1992) Tobacco by-2 Cell-Line as the Hela-Cell in the Cell Biology of Higher-Plants. *International Review of Cytology-a Survey of Cell Biology* **132**: 1-30
- Nebenfuhr A, Frohlick JA, Staehelin LA** (2000) Redistribution of Golgi stacks and other organelles during mitosis and cytokinesis in plant cells. *Plant Physiol* **124**: 135-151
- Nishihama R, Soyano T, Ishikawa M, Araki S, Tanaka H, Asada T, Irie K, Ito M, Terada M, Banno H, Yamazaki Y, Machida Y** (2002) Expansion of the cell plate in plant cytokinesis requires a kinesin-like protein/MAPKKK complex. *Cell* **109**: 87-99
- Otegui M, Staehelin LA** (2000) Cytokinesis in flowering plants: more than one way to divide a cell. *Current Opinion in Plant Biology* **3**: 493-502
- Pan R, Lee YR, Liu B** (2004) Localization of two homologous Arabidopsis kinesin-related proteins in the phragmoplast. *Planta* **220**: 156-164
- Pickett-Heaps JD, Gunning BES, Brown RC, Lemmon BE, Cleary AL** (1999) The cytoplasmic concept in dividing plant cells: Cytoplasmic domains and the evolution of spatially organized cell division. *American Journal of Botany* **86**: 153-172
- Raikhel N, Chrispeels MJ** (2000) Protein Sorting and Vesicle Traffic. In *Biochemistry and Molecular Biology of Plants*, B.B. Buchanan, W. Gruissem, and R.L. Jones (Eds.). Rockville, American Society of Plant Physiologists: 202-258
- Reilein AR, Rogers SL, Tuma MC, Gelfand VI** (2001) Regulation of molecular motor proteins. *Int Rev Cytol* **204**: 179-238
- Smith LG** (1999) Divide and conquer: cytokinesis in plant cells. *Curr Opin Plant Biol* **2**: 447-453
- Staehelin LA, Hepler PK** (1996) Cytokinesis in higher plants. *Cell* **84**: 821-824
- Stals H, Bauwens S, Traas J, VanMontagu M, Engler G, Inze D** (1997) Plant CDC2 is not only targeted to the pre-prophase band, but also co-localizes with the spindle, phragmoplast, and chromosomes. *Febs Letters* **418**: 229-234
- Stoppin-Mellet V, Gaillard J, Vantard M** (2002) Functional evidence for in vitro microtubule severing by the plant katanin homologue. *Biochem J* **365**: 337-342
- Sylvester AW** (2000) Division decisions and the spatial regulation of cytokinesis. *Curr Opin Plant Biol* **3**: 58-66
- Torresruiz RA, Jurgens G** (1994) Mutations in the FASS Gene Uncouple Pattern-Formation and Morphogenesis in Arabidopsis Development. *Development* **120**: 2967-2978
- Traas J, Bellini C, Nacry P, Kronenberger J, Bouchez D, Caboche M** (1995) Normal Differentiation Patterns in Plants Lacking Microtubular Preprophase Bands. *Nature* **375**: 676-677
- Van Damme D, Bouget FY, Van Poucke K, Inze D, Geelen D** (2004a) Molecular dissection of plant cytokinesis and phragmoplast structure: a survey of GFP-tagged proteins. *Plant J* **40**: 386-398
- Van Damme D, Van Poucke K, Boutant E, Ritzenthaler C, Inze D, Geelen D** (2004b) In Vivo Dynamics and Differential Microtubule-Binding Activities of MAP65 Proteins. *Plant Physiol* **136**: 3956-3967
- Vanstraelen M, Torres Acosta JA, De Veylder L, Inze D, Geelen D** (2004) A plant-specific subclass of C-terminal kinesins contains a conserved a-type cyclin-dependent kinase site implicated in folding and dimerization. *Plant Physiol* **135**: 1417-1429
- Verma DP** (2001) Cytokinesis and Building of the Cell Plate in Plants. *Annu Rev Plant Physiol Plant Mol Biol* **52**: 751-784
- Vida TA, Emr SD** (1995) A new vital stain for visualizing vacuolar membrane dynamics and endocytosis in yeast. *J Cell Biol* **128**: 779-792

- Webb M, Jouannic S, Foreman J, Linstead P, Dolan L** (2002) Cell specification in the Arabidopsis root epidermis requires the activity of ECTOPIC ROOT HAIR 3--a katanin-p60 protein. *Development* **129**: 123-131
- Weingartner M, Binarova P, Drykova D, Schweighofer A, David JP, Heberle-Bors E, Doonan J, Bogre L** (2001) Dynamic recruitment of Cdc2 to specific microtubule structures during mitosis. *Plant Cell* **13**: 1929-1943
- Wick SM** (1991) Spatial aspects of cytokinesis in plant cells. *Curr Opin Cell Biol* **3**: 253-260
- Yasuhara H, Shibaoka H** (2000) Inhibition of cell-plate formation by brefeldin A inhibited the depolymerization of microtubules in the central region of the phragmoplast. *Plant Cell Physiol* **41**: 300-310
- Yasuhara H, Sonobe S, Shibaoka H** (1993) Effects of Taxol on the Development of the Cell Plate and of the Phragmoplast in Tobacco by-2 Cells. *Plant and Cell Physiology* **34**: 21-29
- Yasuhara H, Sonobe S, Shibaoka H** (1995) Effects of brefeldin A on the formation of the cell plate in tobacco BY-2 cells. *Eur J Cell Biol* **66**: 274-281
- Zhu JK, Shi J, Singh U, Wyatt SE, Bressan RA, Hasegawa PM, Carpita NC** (1993) Enrichment of Vitronectin-Like and Fibronectin-Like Proteins in NaCl-Adapted Plant-Cells and Evidence for Their Involvement in Plasma-Membrane Cell-Wall Adhesion. *Plant Journal* **3**: 637-646



Chapter 5

Arabidopsis trehalose-6-P synthase AtTPS1 forms a high molecular weight protein complex, together with cell cycle proteins CDKA;1 and the kinesin KCA1

Adapted from 'Arabidopsis trehalose-6-P synthase AtTPS1 forms a high molecular weight protein complex, together with cell cycle proteins CDKA;1 and the kinesin KCA1' by Geelen Danny, Royackers Katrien, Vanstraelen Marleen*, De Bus Martien, Inzé Dirk, Van Dijck Patrick, Thevelein Johan M. and Leyman Barbara. In preparation.

(*) contributed to the presented work starts from the interaction of AtTPS1 with KCA1 and CDKA;1

Chapter page: *Arabidopsis thaliana* root hairs, imaged using confocal microscopy (transmission light).

Abstract

The trehalose-6-phosphate synthase AtTPS1 is involved in regulating sugar metabolism and partitioning in connection with plant morphogenesis and development in an as yet unknown fashion. AtTPS1 expressed in yeast supports the synthesis of trehalose as well as an essential regulatory function in glucose consumption. The gene is essential for embryo development in *Arabidopsis* and its overproduction leads to sugar insensitivity as well as increased drought tolerance. Here we report on the physical interactions of the AtTPS1 protein with cell cycle related proteins. AtTPS1 formed a protein complex in yeast and *Arabidopsis* and was part of a 600-800 kDa particle in FPLC separated extracts. The *Arabidopsis* AtTPS1 co-migrated with the cell cycle kinase CDKA;1 and tubulin. In two hybrid experiments, AtTPS1 interacted with CDKA;1 and the CDKA;1 interacting protein KCA1. KCA1 is a kinesin motor protein implicated in CDKA;1 dependent phosphoregulation of cell division. The AtTPS1 domain responsible for the interaction with KCA1 and CDKA;1 was mapped to an N-terminal extension of the AtTPS1 protein that controls the trehalose synthase enzymatic activity. AtTPS1 co-precipitated with CDKA;1 affinity beads indicating that it is part of a protein complex that contains KCA1 and tubulin. The data presented here provide the first physical link between control of cell division and sugar metabolism.

Introduction

Trehalose is a disaccharide (alpha, alpha 1,1-diglucose) with unusual stress-protective properties that is accumulated to high levels in many bacteria, fungi and in some desert resurrection plants. *In vitro* it protects membranes and proteins against denaturation under different stress conditions, in particular during dehydration. Accumulation of trehalose apparently helps to survive the cells against harsh conditions (Paiva and Panek, 1996). Trehalose is synthesized via the intermediate trehalose-6-phosphate (T6P). In a first step UDP-glucose and glucose-6-phosphate are converted to T6P, a reaction catalyzed by TPS (T6P synthase) (Cabib and Leloir, 1958). In a second step, T6P is dephosphorylated by TPP (T6P phosphatase). In *Saccharomyces cerevisiae*, both reactions are catalyzed by a large oligomeric enzyme, consisting of Tps1 (TPS), Tps2 (TPP) and a third, regulatory protein redundantly encoded by *TPS3* and *TSL1*, in an unknown stoichiometric ratio (Reinders et al., 1997; Bell et al., 1998). All components have a part with sequence similarity to Tps1 and these parts might be involved in the build-up of the oligomeric complex. In *S. cerevisiae* trehalose metabolism, and in particular the level of T6P, also exerts an essential control on the influx of glucose into glycolysis through restriction of hexokinase activity (Blazquez et al., 1993; Neves et al., 1995). Therefore, deletion of the *TPS1* gene not only causes undetectable levels of trehalose but also inability to grow on fast fermented sugars like glucose. How the T6P synthase/phosphatase complex is able to control the level of free T6P is unclear although additional Tps1, not present in the complex, might be involved (Bell et al., 1998).

The disaccharide trehalose is barely detectable in higher plants like *Arabidopsis* (Vogel et al., 2001). Hence, trehalose levels are clearly not sufficiently high for a function as stress protectant. However in the *Arabidopsis* genome, 11 TPS-related genes have been identified that fall into two classes (Leyman et al., 2001). The genes AtTPS1 to 4 of the first class show high similarity with the T6P synthase Tps1 of yeast, while the genes of the second class AtTPS 5 to 11 exhibit higher similarity to the T6P phosphatase Tps2 of yeast and also contain the typical phosphatase domains. So far, only AtTPS1 has been characterized in more detail. AtTPS1 can be functionally interchanged to some extent with Tps1 in yeast (Blazquez et al., 1998; Van Dijck et al., 2002). Expression of *AtTPS1* in a *Sctps1Δ* strain restores growth on glucose and increases the level of trehalose, albeit to a minor extent. This indicates that AtTPS1 can complement not only for the catalytic function but also the regulatory function of Tps1. However complementation and activity of AtTPS1 is weak. Truncation of the plant specific N-terminal extension of AtTPS1 increases its TPS activity, resulting in higher accumulation of trehalose upon expression in yeast and improved growth on glucose. Proper homeostasis of the glycolytic intermediates was not restored indicating that AtTPS1 was unable to substitute fully for the yeast enzyme in the regulation of hexokinase (Van Dijck et al., 2002).

Because of the absence of substantial trehalose accumulation in *Arabidopsis*, its TPS genes and trehalose metabolism are more likely to play a regulatory role. However, it has not been possible to relate this role in a straightforward way to the regulatory role of yeast TPS in restricting the influx

of glucose into glycolysis. For instance, T6P does not inhibit Arabidopsis hexokinase activity *in vitro* (Eastmond et al., 2002). Nevertheless, modification of T6P levels causes dramatic effects on carbohydrate metabolism and partitioning as well as on morphogenesis and development in Arabidopsis (Goddijn and van Dun, 1999; Paul et al., 2001; Schlupepmann et al., 2003). Interestingly, *AtTPS1* is an essential gene, and knocking the gene out results in an embryo lethal phenotype (Eastmond et al., 2002). Embryo development is blocked early in the phase of cell expansion and storage reserve accumulation. This phenotype can be partially suppressed by reducing external sugar levels, indicating a hypersensitivity to sugar. In vegetative stage, *AtTPS1* is essential for normal growth in particular for the development of the flowers (van Dijken et al., 2004). Consistently, overexpression of *AtTPS1* in Arabidopsis reduces sensitivity to external sugar (Avonce et al., 2004; Avonce et al., 2005). This sugar insensitivity may be due to the altered expression level of the glucose sensor hexokinase HXK1 and of the ABI4 transcription factor, which is also involved in sugar signaling. In addition, those transgenic plants also displayed insensitivity to the abscisic acid (ABA) hormone and a higher tolerance for drought in comparison to wild type plants.

These results point towards a central function of *AtTPS1* in the regulation of sugar and ABA signaling. However the mode of action as well as any components interacting with *AtTPS1*, are still unknown. Therefore, we have investigated the possible molecular environment of *AtTPS1 in vivo*. We have identified an oligomeric protein complex in extracts from Arabidopsis flowers and stem, with a composition clearly different from the yeast trehalose synthase complex. Interestingly, the presence of *AtTPS1* in a complex with the cell cycle proteins kinesin KCA1 and CDKA;1 helps us to understand how *AtTPS1* connects plant sugar metabolism to the control of cell growth, morphogenesis and development.

Results

Complementation of *tps1Δ* yeast strains by *AtTPS1* derivatives

The Arabidopsis *AtTPS1* protein has an unusual N-terminal extension that largely prevents trehalose-6-phosphate synthase activity (Van Dijk et al., 2002). To identify proteins interacting with *AtTPS1*, the *AtTPS1* gene and the allele encoding its N-terminal truncated form $\Delta NAtTPS1$ were fused to the HA-tag in the pSAL6 vector. The activity of the chimeric constructs was tested in the trehalose deficient *tps1Δ* strain, which is unable to grow on glucose as sole carbon source (Breitenbach-Schmitt et al., 1984; Van Aelst et al., 1993). The *AtTPS1* derivatives were placed under the control of the *CUPI* promoter driving copper inducible gene expression. Expression of the HA-tagged proteins *AtTPS1HA* and $\Delta NAtTPS1HA$ was tested by immuno-blot analysis of yeast crude protein extracts using the anti-HA antibody (Fig. 5.1C). The empty pSAL6 vector failed to complement the growth and trehalose synthesis defects of *tps1Δ*. A low level of $\Delta NAtTPS1$ or $\Delta NAtTPS1HA$ expression restored the growth on glucose slightly (Fig. 5.1A). Increasing the

expression with Cu^{2+} was sufficient to fully complement growth. Without the Cu^{2+} inducer, full length *AtTPS1* or *AtTPS1HA* completely failed to complement the *tps1Δ* growth defect. When Cu^{2+} was added, the transgenic yeast still grew poorly on glucose (Fig. 5.1A) (Van Dijck et al., 2002). In addition, the transformants also produced different levels of trehalose. The full length *AtTPS1* and *AtTPS1HA* constructs complemented the trehalose synthesis defect of *tps1Δ* partially whereas the N-terminal truncated $\Delta\text{NA}t\text{TPS1}$ or $\Delta\text{NA}t\text{TPS1HA}$ showed almost complete complementation (Fig. 5.1B) (Van Dijck et al., 2002). The addition of a HA tag had no apparent effect on the capacity to complement the *tps1Δ* growth and trehalose synthesis defects.

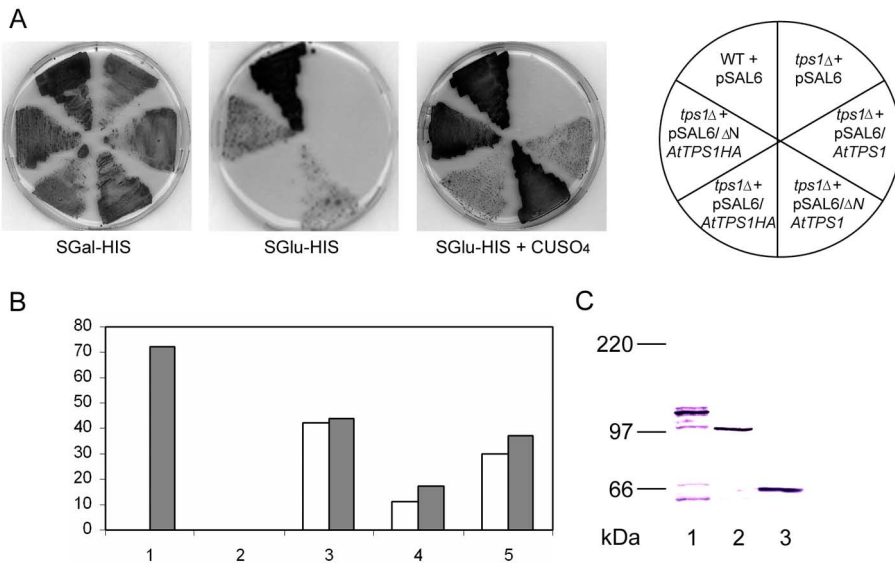


Figure 5.1 A, Functional complementation of yeast *tps1Δ* strain for growth on glucose-containing medium by *AtTPS1*, *AtTPS1HA*, $\Delta\text{NA}t\text{TPS1}$ and $\Delta\text{NA}t\text{TPS1HA}$. Media contained 2% glucose (SGlu) or 2% galactose (SGal) lacking Uracil (-URA) or Histidine (-HIS) supplemented with 100 μM CUSO₄ as indicated. B, Trehalose levels in yeast strains grown in 2% galactose (SGal) with CUSO₄. Grey bars represent non-tagged and white bars represent HA-tagged TPS1 alleles. 1. wild type; 2. *tps1Δ*; 3. *tps1Δ* (YCplac33/*ScTPS1*); 4. *tps1Δ* (pSAL6/*AtTPS1*); 5. *tps1Δ* (pSAL6/ $\Delta\text{NA}t\text{TPS1}$). C, Western blot analysis of *tps1Δ* yeast protein extracts using the anti-HA antibody. The *tps1Δ* strains were transformed with 1. pSAL6/*AtTPS1HA* (*AtTPS1* \pm 106 kDa); 2. pSAL6/ $\Delta\text{NA}t\text{TPS1HA}$; 3. YCplac33/*ScTPS1HA*.

AtTPS1 forms a protein complex in yeast of 600-800 kDa different from the endogenous TPS complex.

AtTPS1 is, at least in part, functionally interchangeable with *ScTPS1* in *S. cerevisiae*, raising the question whether AtTPS1 forms a protein complex similar to ScTPS1 (Bell et al., 1998). FPLC gel exclusion chromatography was used to fractionate native crude yeast protein extract. The molecular mass of the yeast trehalose synthase complex was estimated to be 600-800 kDa (Bell et al., 1998). Calibration of the FPLC column indicated a molecular weight (MW) of 600-800 kDa for proteins eluting in the fractions 11 to 13. Protein extract of the *tps1Δ* strains expressing *AtTPS1HA* and Δ *NAtTPS1HA* were fractionated by FPLC and equal volumes of each fraction were separated by SDS-PAGE for immuno-blot analysis. Both plant proteins were mainly detected in fractions 11 to 15, indicating the presence of a protein complex with a high MW similar in size to the wild type ScTps1 containing complex (Fig. 5.2A) (Bell et al., 1998). AtTPS1HA and Δ NAtTPS1HA were also present to a small extent in fractions 16 to 18, containing proteins with a lower MW, corresponding to that of the monomeric proteins (Fig. 5.2A). The immuno-blot results with the full length AtTPS1HA displayed a second band with a lower MW. This band is apparently due to protein degradation during experimental treatment, as this band is absent when the yeast cells were immediately boiled in protein sample buffer before for further analysis (data not shown).

The endogenous ScTps1 complex contains the TPP ScTps2, that dephosphorylates the intermediate T6P, and it contains the regulatory proteins encoded by *ScTPS3* and *ScTSL1* (Bell et al., 1998). We checked for the presence of these proteins in the AtTPS1HA and Δ NAtTPS1HA protein complex. For this purpose, the AtTPS1HA and Δ NAtTPS1HA proteins were expressed in the M5 *fil1 tps1Δ hxk2Δ* strain. This was necessary to allow proper detection on western blot of the other yeast TPS proteins as these were more abundantly produced in this background (Versele et al., 2004). Analysis of the FPLC protein fractions using different specific antisera revealed that the yeast TPS proteins ScTsl1, ScTps3 and ScTps2 were present in a protein complex in fractions 11 to 15 (Fig. 5.2B). In the same fractions, AtTPS1HA and Δ NAtTPS1HA were eluted. To determine whether the co-elution was due to the presence of AtTPS1HA and Δ NAtTPS1HA in the same complex as the other yeast proteins, similar experiments were performed with different *ScTPS* deletion strains. Removal of one of the contributing partners would be expected to lead to a shift to smaller MW fractions or absence of the complex all together in the case the proteins reside in the same complex. We analyzed the FPLC profile of the *tps1Δ tps2Δ* double mutant strain transformed with the pSAL6 constructs containing the plant TPS1 ORFs. In both strains, the protein complex with AtTPS1HA or Δ NAtTPS1HA was not affected by the deletion of the *ScTPS2* gene (Fig. 5.2C). In a second approach, the *AtTPS1HA* and Δ *NAtTPS1HA* alleles were expressed in the quadruple deletion strain *tps1Δ tps2Δ tps3Δ tsl1Δ* that lacks all endogenous TPS protein. For this experiment, the plant genes were cloned in the YEplac195/*KanMX* vector containing the dominant *KanMX* marker because no auxotrophic marker could be used. FPLC fractionation of the protein extracts followed by immuno-blot analysis of the fractions revealed no shift in the size of the AtTPS1HA and Δ NAtTPS1HA containing high MW

protein complexes (Fig. 5.2D). The formation of AtTPS1HA and Δ NAAtTPS1HA protein complexes therefore did not require any endogenous TPS protein.

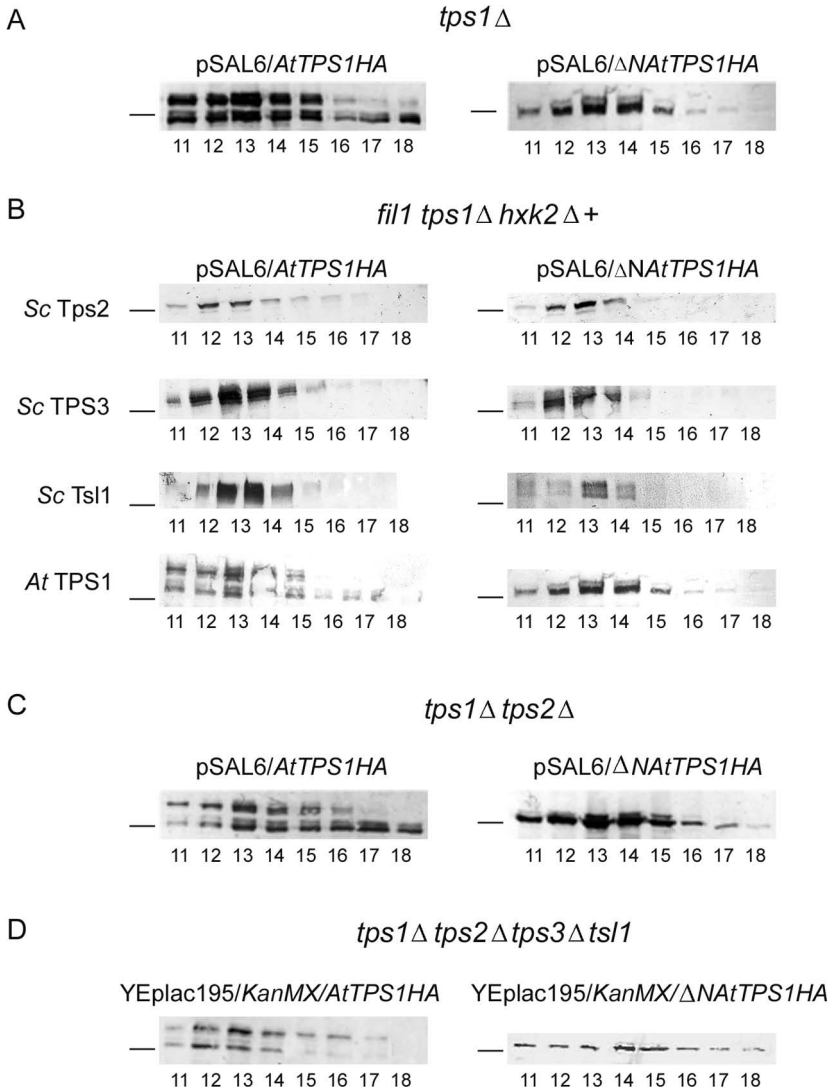


Figure 5.2 Western blot analysis of FPLC elution fractions 11 to 18. A, Proteins were extracted from *W303-1A tps1*Δ strains containing the pSAL6/*AtTPS1HA* or pSAL6/ Δ NA*AtTPS1HA* constructs. B, Protein extracts were obtained from the *M5fil1tps1*Δ*hxx2*Δ strain containing pSAL4/*AtTPS1HA* or pSAL4/ Δ NA*AtTPS1HA* constructs. Specific polyclonal antibodies were used against the *Saccharomyces cerevisiae* Tsl1, Tps3 and Tps2 proteins and against AtTPS1. C, Proteins were extracted from *W303-1A tps1*Δ *tps2*Δ strains containing the pSAL6/*AtTPS1HA* or pSAL6/ Δ NA*AtTPS1HA* constructs. D, Proteins were extracted from the quadruple yeast deletion strain *W303-1A tps1*Δ *tps2*Δ *tps3*Δ *tsl1*Δ containing either pYEplac/*KanMX/AtTPS1* or YEplac/*KanMX/* Δ NA*AtTPS1*. In A, B, and C, an anti-HA antibody was used. Bars represent the 97 kDa marker protein. The triangle points towards the expected AtTPS1HA protein.

AtTPS1 is expressed in inflorescence tissue predominantly as part of a protein complex

The presence of AtTPS1 protein in extracts of Arabidopsis plant tissue was analyzed via immunodetection using AtTPS1 specific polyclonal antibody. In total extract from Arabidopsis seedlings a single protein band was detected on western blot with a MW of approximately 100 kDa, corresponding to the predicted MW of AtTPS1 (Fig. 5.3A). Arabidopsis transgenic lines carrying an antisense *AtTPS1* construct showed reduced levels of the 100 kDa protein band. Arabidopsis plants with a *35S::AtTPS1* construct overproduced the AtTPS1 protein. The distribution of AtTPS1 was analyzed with protein extracts of different organs from wild type Arabidopsis. Considerable amounts of AtTPS1 were detected in inflorescence tissue including flowers, stems and cauline leaves. Little or no AtTPS1 protein was observed in rosette leaves and roots (Fig. 5.3A). Hence, FPLC separation experiments to analyze the occurrence of AtTPS1 protein complexes were performed with extracts

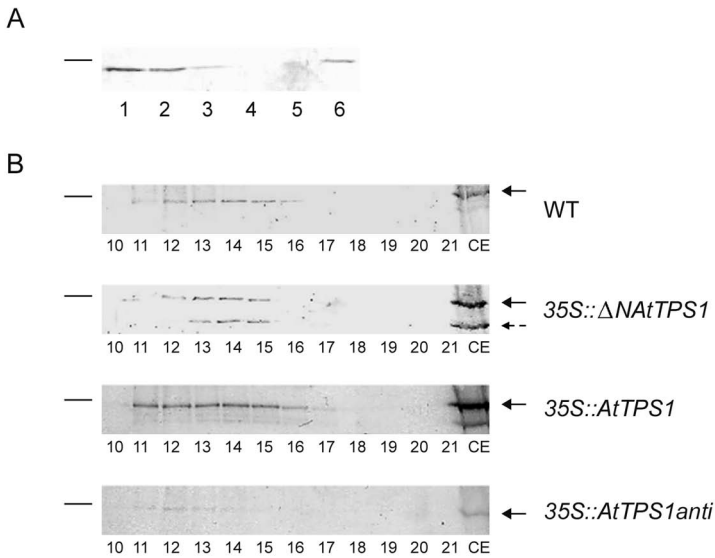


Figure 5.3 Western blot analysis using the specific anti-AtTPS1 antibody. A, Protein extracts from different Arabidopsis organs: 1.flowers, 2. stems, 3. cauline leaves, 4. rosette leaves, 5. roots, 6. crude extract. B, Extracts from stem plus flower and cauline leaves fractionated by FPLC. Wild type plants (WT), AtTPS1 antisense plants (*35S::AtTPS1anti*), AtTPS1 overexpressing plants (*35S::AtTPS1*), and ΔN AtTPS1 overexpressing plants (*35S:: ΔN AtTPS1*). CE = crude extracts. Arrows and dotted arrow indicate wild type and truncated AtTPS1 protein respectively. Bars represent the 114 kDa marker protein.

of inflorescence tissue. The AtTPS1 protein was found in the FPLC fractions 11 to 16 corresponding to components with a MW ranging from 600-800 kDa in fractions 11-13 to 300 kDa in fraction 16 (Fig. 5.3B). AtTPS1 overproducing lines contained higher amounts of AtTPS1 protein that showed a

FPLC separation profile similar to that of wild type extracts. As expected, less AtTPS1 protein complex was found in extracts from antisense plants (Avonce et al., 2004). To analyze a possible role of the N-terminal end of AtTPS1 in the formation of the protein complex, protein extracts from Arabidopsis carrying a *35S::ΔNAtTPS1* construct were subjected to FPLC chromatography. Both the wild type and truncated AtTPS1 protein were detected in the extracts (Fig. 5.3B). The N-terminally deleted AtTPS1 protein was present in the high MW fractions 13 to 15, indicating slightly smaller protein complexes than with the wild type protein. Thus, the N-terminal end of AtTPS1 may contribute to the formation of a 600-800 kDa complex, but it is not an essential part.

Purification of AtTPS1 complex by affinity chromatography

AtTPS1 antibody was immobilized to an agarose support matrix to trap AtTPS1 protein together with associated proteins from a plant cell extract. Figure 5.4A shows Silver stain visualization of the different phases obtained after affinity purification of AtTPS1 from wild type inflorescence tissue.

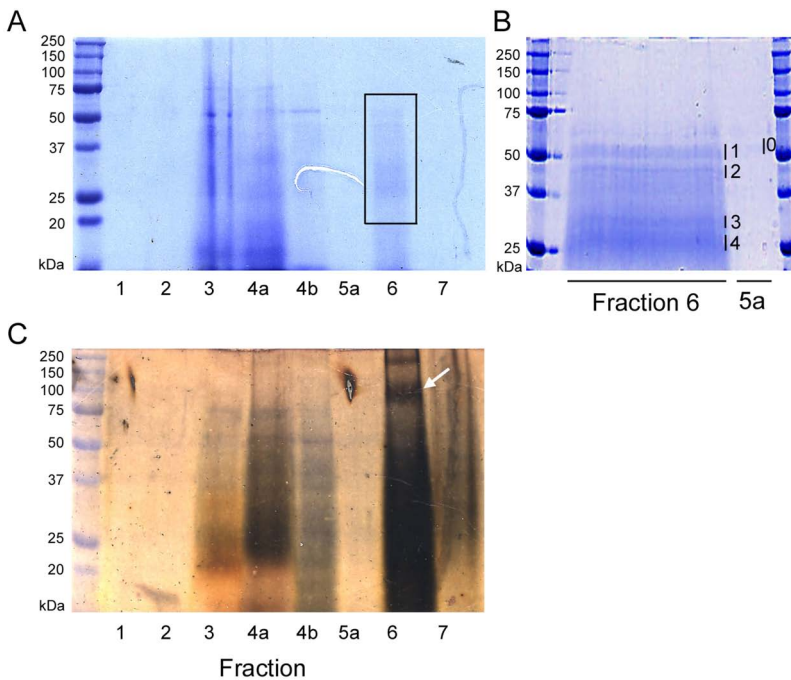


Figure 5.4 SDS page analysis of fractions collected after Affi-Gel® Hz immuno-affinity chromatography. Proteins were stained using a Brilliant Blue G colloidal staining (A and B) or using silver staining solution (C). Lanes represent elution of Sample buffer (1), crude protein extract (2), 0.5 M NaCl wash buffer (3 and 4), 0.2 M NaCl wash buffer (5), NaSCN-urea-guanidine HCL elution buffer (6) and regeneration buffer (7). B, 5 different samples (0 as a negative control and 1-4), have been cut out of the gel and purified for further identification. White arrow represents a protein size of AtTPS1.

Crude extracts were applied to the affinity column and subsequently unbound material was removed with 0.5 M and 0.2 M NaCl washing buffers (Fig. 5.4, lane 1-5). The bound fraction was eluted from the column with NaSCN-urea-guanidine HCl buffer (Fig. 5.4, lane 6). A protein band was detected in the eluate with a MW corresponding to that of the AtTPS1 protein (Fig. 5.4C). A large amount of smaller and higher molecular weight proteins appeared also to be present in the eluted fraction. In order to isolate and identify these proteins, an SDS-PAGE gel was run with a wide slot to increase the amount of protein loaded and improve their separation (Fig. 5.4B). Four prominent bands were detected upon coomassie staining that corresponded to proteins with a MW of approximately 28, 33, 45 and 55 kDa. The gel slices referred to as fractions 1 to 4 in Figure 5.4B were subjected to MALDI-TOF mass spectrometry. As a reference, similar fractions were taken from the separated NaCl wash steps. Fraction 1 contained ribulosebiphosphate carboxylase, a highly abundant protein that was also identified in the corresponding fraction in NaCl eluted extract. The analysis of fraction 2 identified tubulin that was not found in the corresponding fraction in NaCl eluate, suggesting that this protein was specifically retained in the AtTPS1 affinity column. Fractions 3 and 4 did not give predictive sequence data. We concluded that tubulin might be an interaction partner of AtTPS1 but that the affinity purification was not powerful enough to allow identification of other interaction partners.

AtTPS1 interacts with KCA1

As an alternative approach to identify AtTPS1 interacting proteins, we performed a two hybrid screen using an Arabidopsis cDNA library of mature leaves fused to the GAL4 activating domain in pGAD424 as prey. Truncation of AtTPS1 at its N-terminal end, leads to a prominent increase in its regulatory and catalytic activity upon expression in yeast (Van Dijck et al., 2002). Hence, we concluded that the 88 amino acid domain of AtTPS1, plays a crucial role in the regulation of AtTPS1 activity. The full length AtTPS1, the truncated Δ NAtTPS1, and the 264 bp 5' oligomer encoding the inhibitory N-terminal domain of AtTPS1 were fused to the DNA binding domain of the GAL4 transcription factor in the pGBT9 vector. The yeast AH109 strain, containing these bait constructs, was transformed with the library and the transformants were grown on medium without leucine, tryptophane and histidine to select for clones with interacting proteins. Full-length AtTPS1 and Δ NAtTPS1 baits did not result in any yeast colony growing on the auxotrophic medium. However, the regulatory domain of AtTPS1(1-264) yielded yeast colonies that contained a prey plasmid containing a sequence corresponding to a cDNA fragment previously referred to as TH65 (De Veylder et al., 1997). The TH65 fragment is derived from the Arabidopsis gene KCA1 with a predicted amino acid sequence that reveals three major domains: a head containing the kinesin motor domain (N-terminal), a coiled coil stalk domain (central), and a C-terminal tail domain (Fig. 5.5A) (Vanstraelen et al., 2004). The TH65 fragment encodes the peptide from amino acid 473 to 866 containing the stalk domain and the N-terminal part of the tail domain. To define the region of KCA1 that interacts with AtTPS1, various deletion fragments were tested in two hybrid assays.

Figure 5.5A shows the different KCA1 fragments that were used for the analysis: the full length protein KCA1(1-1273), the head KCA1(1-463), TH65 KCA1(473-866), the N-terminal part of the tail (660-862), and the tail KCA1(875-1273). Full length AtTPS1 and the catalytic domain separately did not interact with any of the KCA1 fragments in agreement with the absence of yeast colonies in the library screen (Fig. 5.5B). The regulatory domain AtTPS1(1-264) exclusively interacted with the stalk KCA1⁴⁷³⁻⁸⁶⁶, resulting in yeast colony formation on selective medium containing up to 5 mM 3-AT. No growth was detected of transformants containing either plasmid separately, indicating the absence of auto-activation. When bait and prey fusion constructs were reciprocally exchanged, the interaction was lost, suggesting that the binding of AtTPS1(1-264) with KCA1⁴⁷³⁻⁸⁶⁶ is probably weak. The two-hybrid interaction pointed to KCA1 as a potential candidate to form a complex with AtTPS1.

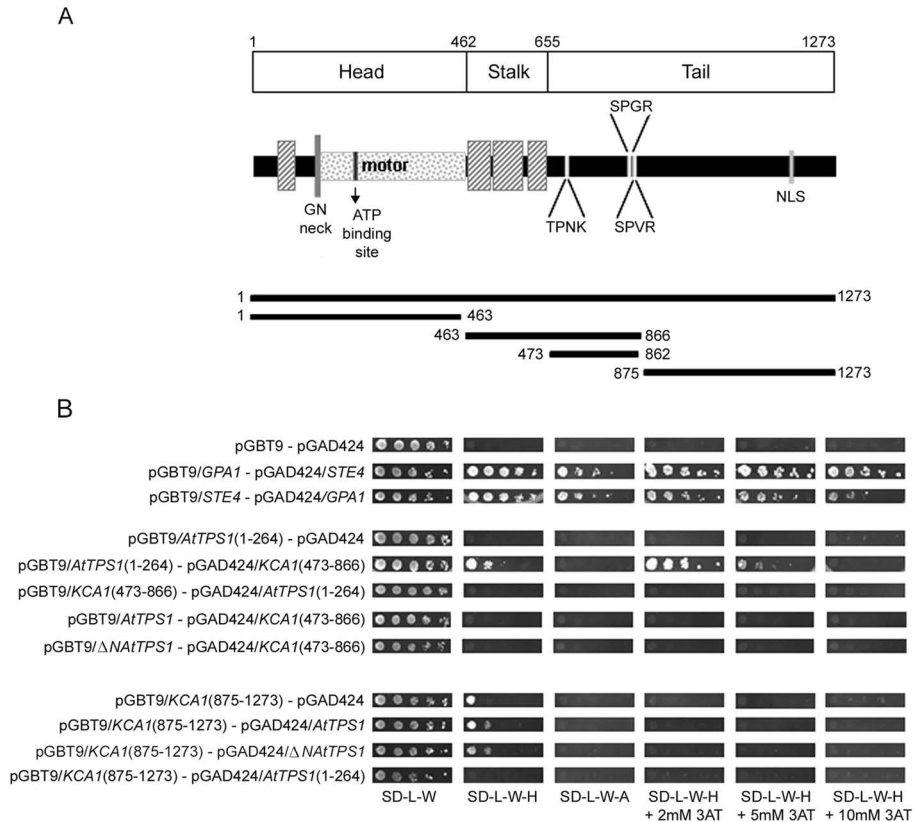


Figure 5.5. A, Scheme of KCA1, and map of two-hybrid constructs. The head consist of a coiled coil domain (dashed box) and a motor domain (dotted box) with ATP binding site and preceded by a G¹⁴¹N¹⁴² neck. The stalk domain contains three different coiled coil regions (dashed boxes). The tail domain carries three different CDK phosphorylation sites (small white boxes) as well as a nuclear localization site (NLS) B, Two hybrid analysis of AtTPS1(1-264), the full length AtTPS1, and Δ NAAtTPS1 with parts of KCA1 ranging from 473 to 866 and 857 to 1273 amino acids. *GPA1* and *STE5* were used as a positive control.

AtTPS1 interacts with the cyclin dependent kinase CDKA;1

Previously it has been suggested that KCA1 is a target for phosphorylation by the cyclin dependent kinase CKDA;1 (De Veylder et al., 1997; Kong and Hanley-Bowdoin, 2002). KCA1 and CDKA;1 interact in two-hybrid and immunoprecipitation experiments, and mutagenesis of a putative phosphorylation site at serine 841 and serine 845 abolishes this interaction (Vanstraelen et al., 2004). To analyze a possible interaction between AtTPS1 and CDKA;1, we performed a two-hybrid test. The N-terminal domain of AtTPS1 (1-264) showed an interaction with CDKA;1 whereas the full length protein and the Δ NAAtTPS1 domain did not (Fig. 5.6A). Since the interaction appeared very weak, an alternative method was chosen to evaluate the findings. CDKA;1 binds to p10^{CKSAT} affinity beads and co-purifies with GFP-tagged KCA1 protein (Vanstraelen et al., 2004). We therefore used p10^{CKSAT} beads to pellet CDKA;1 from Arabidopsis wild type protein extract and tested whether AtTPS1 was co-precipitated. The binding of CDKA;1 to p10^{CKSAT} affinity beads was verified with a

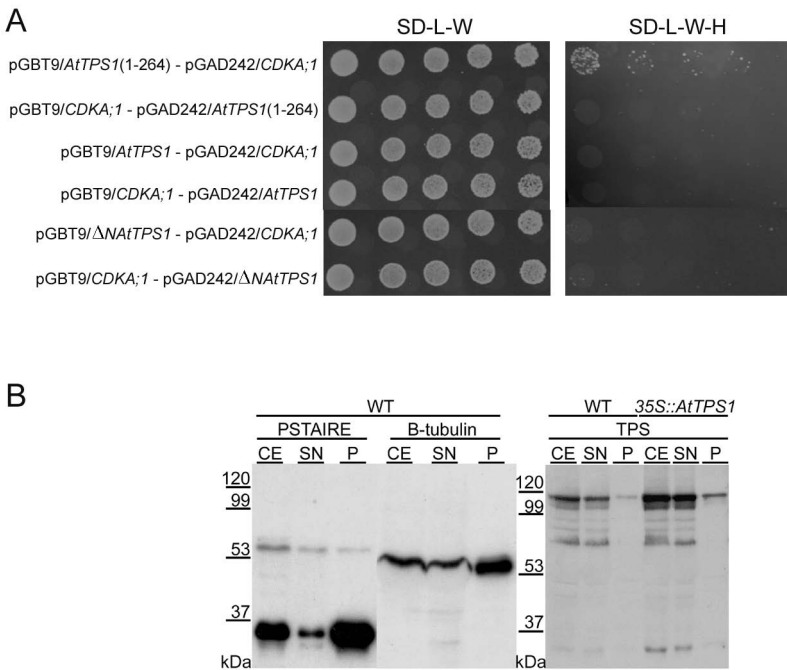


Figure 5.6 A, Two hybrid analysis of AtTPS1, with CDKA;1. Yeast growth on control medium is shown to the left and growth on selective medium is shown in the right panel. B, Western blot detection of CDKA;1, β -tubulin, and AtTPS1 in wild type (WT) and *35S::AtTPS1* protein extracts. Crude extracts (CE) were compared with supernatant (SN) and pellet (P) after pull down experiments using p10^{CKSAT} affinity beads. Antibodies used were (PSTAIRES), β -tubulin and AtTPS1 antiserum.

PSTAIRES specific antibody. AtTPS1 antiserum detected a single protein band associated with the p10^{CKSA^t} bead pellet (Fig. 5.6B). A similar experiment was done with extracts from Arabidopsis plants overproducing AtTPS1 protein. Here a slightly higher amount of AtTPS1 was precipitated (Fig. 5.6B). Next, we tested whether tubulin co-purifies with the p10^{CKSA^t} affinity beads. β -tubulin was found in the pellet indicating that it indeed interacts with the CKS binding complex. The AtTPS1 protein that precipitated with the p10^{CKSA^t} beads represented only a fraction of the total amount detected in the untreated extract. It did not increase upon addition of more p10^{CKSA^t} affinity beads. This indicates that AtTPS1 binds indirectly to the p10^{CKSA^t} affinity beads, perhaps via CDKA;1 and/or KCA1.

The AtTPS1 protein complex from inflorescence tissue contains CDKA;1 and tubulin

Two hybrid and affinity chromatography experiments pointed toward the possibility that CDKA;1 and tubulin were part of a protein complex containing the AtTPS1 protein. We therefore analyzed the presence of CDKA;1 and tubulin in FPLC separated extracts from Arabidopsis inflorescence tissue. CDKA;1 was detected in high as well as low MW fractions (Fig. 5.7). The concentration of CDKA;1 peaked in fractions 16 to 20 that corresponds to components with a MW below 300 kDa. However, CDKA;1 also occurred in fractions 11 to 16 that contain AtTPS1. β -tubulin was also present in fractions 11 to 16 and showed the highest concentration in fractions 13 to 17 (Fig. 5.7). The presence of AtTPS1, CDKA;1 and β -tubulin was also analyzed in FPLC separations of extracts isolated from a KCA1 T-DNA insertion mutant (Vanstraelen et al., unpublished data). Because there was no change in the distribution of these proteins in the KCA1 mutant extracts (results not shown), the KCA1 kinesin may not be an essential component of the complex or alternatively it was replaced by the kinesin homolog KCA2. The occurrence of CDKA;1 and β -tubulin in the high MW fractions suggest that these proteins might contribute to a complex with AtTPS1, albeit that they also associate with other proteins into smaller units.

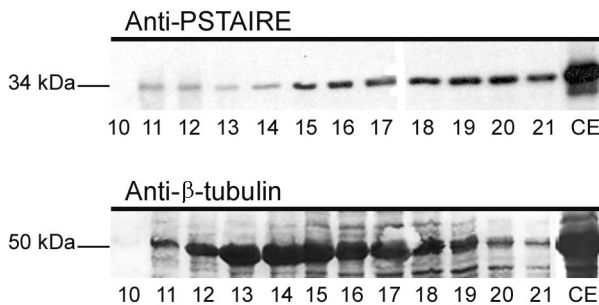


Figure 5.7 Western blot analysis of CDKA;1 and tubulin in Arabidopsis FPLC fractions. Proteins were extracted from the aerial parts of wild type Arabidopsis and analyzed by Western blot. CDKA;1 was detected with PSTAIRES antibody (upper panel), and tubulin using anti- β -tubulin antibody (lower panel). CE = crude extracts.

Localization of GFP-tagged AtTPS1

To analyze the localization of AtTPS1 *in vivo* in Arabidopsis cells, the full length protein and the regulatory N-terminal domain were N-terminally fused to the green fluorescent protein. Tobacco leaves were transiently transfected with the GFP fusion constructs driven by the 35S promoter. Full-length fusion protein was present in the cytoplasm and excluded from the nucleus, whereas the N-terminal domain was present also in the nucleus (data not shown). Similar localization patterns were observed in stably transformed BY-2 tobacco suspension cultures (data not shown). To determine the localization of AtTPS1 and KCA1 in dividing cells, BY-2 cultures were co-transformed with GFP-KCA1 and RFP- AtTPS1 constructs. The BY-2 cultures were also transformed to produce free GFP and GFP fused to a MT-binding domain of the mouse MAP4 protein, GFP-MBD for comparison (Van Damme et al., 2004). Localization patterns were determined at different phases of the cell cycle (Fig. 5.8). Free GFP filled all accessible space except for the vacuolar compartments, while GFP-MBD was predominantly associated with the MTs of the PPB (G2-phase), the spindle

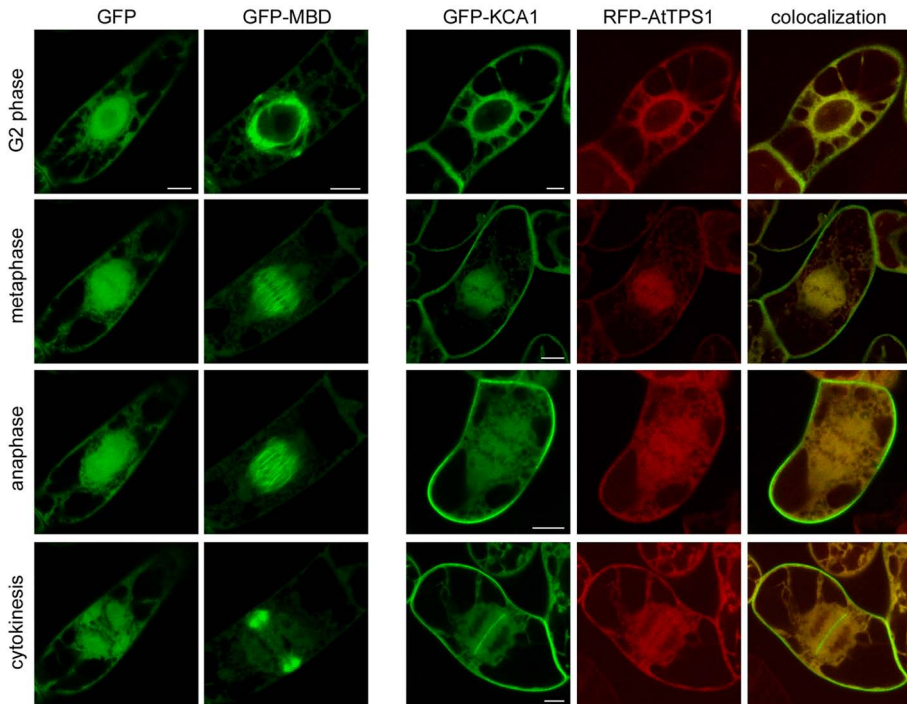


Figure 5.8 Subcellular localization of AtTPS1 and KCA1 in interphase and dividing BY-2 cells. Confocal sections are shown of stably transformed BY-2 cells producing free GFP, GFP-MBD or GFP-KCA1 together with RFP-AtTPS1. Free GFP accumulates in the cytoplasm and the nucleus whereas GFP-MBD binds to MTs. GFP-KCA1 fluorescence is shown in green and RFP-AtTPS1 is shown in red. The column at the right shows the merged images. GFP-KCA1 and RFP-AtTPS1 are co-localized in the cytoplasm, the spindle and the phragmoplast area (yellow signal). During mitosis, RFP-AtTPS1 does not concentrate at the plasma membrane or at the cell plate. Bar = 20 μ m.

(metaphase and anaphase) and the phragmoplast (telophase). GFP-KCA1 and RFP-AtTPS1 were excluded from the nucleus and colocalized in the cytoplasm. During mitosis they accumulated in the area of the spindle and the phragmoplast. In addition, GFP-KCA1 was targeted to the cell plate and the plasma membrane as expected (Vanstraelen et al., 2004). RFP-AtTPS1 however, was not targeted to the cell plate or plasma membrane and remained distributed in the cytoplasm (Fig. 5.8). To determine the localization of the endogenous AtTPS1 protein, antiserum was used in immunostainings on electron microscopic sections of Arabidopsis seedlings. Gold particles were detected mainly in the cytoplasm and not at the membranes of the developing cell plate or plasma membrane (data not shown).

Discussion

We have uncovered a physical interaction between AtTPS1, a protein implicated in the control of sugar metabolism, and two cell division proteins, kinesin KCA1 and the cyclin dependent kinase CDKA;1. These proteins are present in the cytoplasm, presumably in loose association with the MT cytoskeleton. The AtTPS1 protein is most abundant in inflorescence tissue and may regulate cell division in relation to carbon source availability and flower development in Arabidopsis.

Trehalose is widely accepted as a protective molecule in stress response and more recently it has been implicated in processes related to carbon storage. Because trehalose is not produced in detectable amounts in all plant species, its general role in plants has been questioned. The discovery of a family of 11 trehalose synthase like genes in Arabidopsis (Leyman et al., 2001) and the identification of an Arabidopsis embryo lethal mutant carrying an insertion in the AtTPS1 gene (Eastmond et al., 2002), has invigorated the importance of the trehalose molecule in plant growth and development. In AtTPS1 knock-out mutants, embryo development is impaired at the late hart/torpedo stage during which storage reserves accumulate. More recently, it was demonstrated by temporally complementing the insertion mutation that the AtTPS1 gene also has an important function outside the seed-filling stage and is required for normal root growth and for development of inflorescence tissue (van Dijken et al., 2004).

AtTPS1 was previous shown to functionally replace the T6P-synthase Tps1 gene from *Saccharomyces cerevisiae* (Blazquez et al., 1998; Van Dijck et al., 2002). The Tps1 protein is present in extracts both as a free monomeric protein with a MW of 56 kDa and as part of a protein complex of approximately 630-800 kDa. This complex is called the trehalose biosynthesis complex and also includes the T6P-phosphatase Tps2 (102 kDa), Tps3 (115 kDa) and Tsl1 (123 kDa) (Bell et al., 1998). Upon deletion of both *TPS3* or *TSL1* the complex disintegrated partially and a complex with lower MW could be detected. Deleting *TPS2* caused the trehalose complex to destabilize completely (Bell et al., 1998). Apart from the trehalose synthase complex, trehalose biosynthesis proteins have been shown to interact with some other proteins. For example, Tps1 binds Rim15, a protein kinase in the glucose signaling pathway (Pedruzzi et al., 2003). In addition there is evidence

from large-scale two-hybrid screens for Tps2 binding with YAR066w, SBH2 and YDL100C (Ho et al., 2002). However these interactions need to be affirmed by additional experiments.

We initially analyzed Arabidopsis AtTPS1 protein complex formation in a yeast background. Although AtTPS1 was present in a complex similar in size to the endogenous ScTPS1 complex, none of the other yeast Tps components seemed to be involved. Moreover, the hexokinase and hexokinase-like genes AthXK1, AthXK2, AthKL1, AthKL2, AthKL3 were negative in two hybrid tests using AtTPS1 as bait, indicating that AtTPS1 is not strongly associating with sugar metabolizing enzymes (data not shown). Therefore, the identity of the AtTPS1 complex isolated from the AtTPS1 producing yeast is unsolved. In its natural background, AtTPS1 was also incorporated in a protein complex. Increasing the expression of AtTPS1 led to higher amounts of purified protein complex whereas reducing the production of AtTPS1 in antisense transformants led to lower amounts of the complex. These results are expected if AtTPS1 is the rate-limiting factor corroborating the formation of a complex consisting of predominantly the AtTPS1 protein. Note that the antisense line used here shows reduced expression of AtTPS1 as the disruption of the AtTPS1 gene is lethal (Eastmond et al., 2002). AtTPS1 protein complex formation did not require the N-terminal domain as Δ NAtTPS1 co-migrated with the high MW fractions. Strong Δ NAtTPS1 expression did not stimulate an increase in the production of AtTPS1 complex. Therefore, the higher amounts of complex detected in *35S::AtTPS1* lines was the consequence of higher incorporation of the overproduced AtTPS1 protein rather than a stimulation of complex formation.

In order to identify AtTPS1 interacting proteins, two-hybrid and chromatography experiments were performed. Affinity purified proteins retained on an AtTPS1 column, migrated as four major protein bands. One of these contained β -tubulin. The two-hybrid screen resulted in the identification of the tubulin binding kinesin KCA1. This protein is a plant specific kinesin motor protein with the capacity to bind MTs and was previously shown to bind CDKA;1 (De Veylder et al., 1997; Vanstraelen et al., 2004). Additional immunological experiments showed that CDKA;1 interacts with AtTPS1. β -Tubulin was pulled down together with AtTPS1, and CDKA;1 by p10 affinity beads. This AtTPS1 complex including β -tubulin and CDKA;1 was detected in high MW fractions from Arabidopsis inflorescence tissue. The AtTPS1 complex was also found in Arabidopsis mutants that carry a T-DNA insertion in KCA1 (data not shown). The purified AtTPS1 complex may not require KCA1 or it could incorporate the highly similar KCA2 protein. The strong similarity between KCA1 and KCA2 and the high KCA2 expression levels found in inflorescence tissue (Zimmermann et al., 2004) supports this possibility. Taken together, the data indicate that AtTPS1 is part of a protein complex containing β -tubulin, CDKA;1 and KCA1 or KCA2.

The AtTPS1 protein was most abundant in the flowers and stems, less concentrated in cauline leaves, and undetected in mature rosette leaves and roots. These findings are in agreement with earlier RNA expression results (Blazquez et al., 1998) and the *AtTPS1* promoter activity, that is highest in sink organs and in particular flower buds and ripening siliques (Blazquez et al., 1998; van Dijken et al., 2004). Interestingly, even though trehalose itself is present in minute quantities in Arabidopsis, peak levels of the disaccharide have been detected in flowers (Vogel et al., 2001).

KCA1 RNA and protein are also present in aerial parts of Arabidopsis although high transcript levels have been detected in the roots (Kong and Hanley-Bowdoin, 2002; Vanstraelen et al., 2004). In contrast, KCA2 is more abundant in inflorescence tissue and much lower in roots. Thus AtTPS1 and KCA1/KCA2 likely coexist in the same tissue, a prerequisite to form a complex.

RFP tagged AtTPS1 and GFP tagged KCA1 co-localized in the cytoplasm and were excluded from the nucleus. Despite the presence of a MT-binding domain in KCA1, GFP-tagged protein and RFP-AtTPS1 did not bind to MTs but appeared to be more loosely associated with the spindle and the phragmoplast area. The subcellular pattern of KCA1 depends on its C-terminal end, as removal of the tail domain permits specific binding to microtubules (Vanstraelen et al., 2004). The tail domain contains a putative serine/threonine phosphorylation site and may be modified by CDKA;1. CDKA;1 itself is associated with mitotic MTs depending on experimental conditions (Stals et al., 1997; Weingartner et al., 2001). A subpopulation of AtTPS1, KCA1 and CDKA;1 may therefore be temporarily bound to MTs. At the onset of cytokinesis when a new cell plate is formed, KCA1 but not AtTPS1 concentrated at the midline. Here, proteins implicated in vesicular targeting and fusion concentrate (Van Damme et al., 2004a). Immunolocalization of the endogenous AtTPS1 protein confirmed the localization in the cytoplasm and the absence from the cell plate. It therefore appears that KCA1 has a role in cytokinesis and cell plate formation that does not require the interaction with AtTPS1. The interaction of AtTPS1 and KCA1 in two-hybrid analysis could only be observed when parts of both proteins were tested, not when full-length proteins were used. Likewise, the interaction with CDKA;1 could only be established with the N-terminus of AtTPS1 (1-264). The KCA1 protein, and perhaps AtTPS1 as well, occur in different folding configurations that display different subcellular localization patterns (Vanstraelen et al., 2004). The full length AtTPS1 and KCA1 fused to the Gal4 domain may not fold correctly to allow for proper protein interaction. The *in vivo* interaction between AtTPS1, KCA1 and CDKA;1 is therefore conditional.

The finding that AtTPS1 binds to a core regulator of the cell cycle was unexpected. Overexpression of AtTPS1 in Arabidopsis renders the plants insensitive to externally applied sugars (Avonce et al., 2004). Thus, AtTPS1 is implicated in some aspects of sugar signaling (Avonce et al., 2005). The glucose insensitivity could be the consequence of deviating glucose into the trehalose synthesis pathway, or more likely, AtTPS1 is a negative regulator of sugar signaling, and when overproduced, it impedes the sugar sensing mechanism. This mechanism has not been elucidated yet, but likely involves T6P as changes in T6P levels in Arabidopsis plants influences carbohydrate utilization and has dramatic effects on growth and leaf morphology (Schluepmann et al., 2003). The interaction of AtTPS1 with cell cycle proteins CDKA;1 and kinesin KCA1 may provide a link between sugar availability and control over cell division. Because AtTPS1 is essential for embryo maturation, the transition to the flowering stage, and contributes to root growth (Eastmond et al., 2002; van Dijken et al., 2004), it seems to control high energy demanding processes that require sufficient storage reserve in order to be successfully completed. In the absence of required sugar levels, commitment to rounds of cell division is to be prevented. A recent study now shows that in Arabidopsis AtTPS1 null mutants, storage reserve gene expression is not dramatically altered (Gomez et al., 2005). The

principal function of AtTPS1 in development may therefore not be related to the acquisition of carbon sources per se but rather the communication of its availability to the cell cycle machinery. Our findings may provide the necessary connection by which information on available carbohydrate energy is conveyed to the cell cycle regulatory machinery.

Material and Methods

Plant growth conditions

Arabidopsis ecotype Col-0 was grown in a 12h day and night regime at 22/19°C. The overexpressing and antisense plants *35S::AtTPS1* and *35S::AtTPS1anti* have been described previously (Avonce et al., 2004). The truncated *35S::ΔNAtTPS1* was ligated from pSAL6/*ΔNAtTPS1* into the pBN35S. Bright Yellow 2 (BY-2) cells were transformed and grown in conditions as described previously (Vanstraelen et al., 2004).

Constructs, strains and two-hybrid libraries

The pSAL4 and pSAL6 are shuttle vectors between *E. coli* (Amp^R) and *S. cerevisiae*. The pSAL4 vector contains the *URA3* and pSAL6 the *HIS3* auxotrophic marker (Van Dijck et al., 2002). The construction of pSAL6/*AtTPS1* and pSAL6/*ΔNAtTPS1* has been reported previously (Van Dijck et al., 2002). For the construction of the HA-tagged *AtTPS1HA* and *ΔNAtTPS1HA* alleles, the C-terminal part of *AtTPS1* was PCR amplified using the pSAL6/*AtTPS1* construct as template with forward primer ^{5'}CCAAGGAAGCCGCTCTGTGGAAG^{3'} and reverse primer: ^{5'}CTGCATGCTCATGCGTAGTCAGGCACATCATACGGATAAGGTGAGGAAGTGGTGC^{3'}. The PCR fragment together with pSAL6/*AtTPS1* and pSAL6/*ΔNAtTPS1* were digested with the *Clal/SphI* restriction enzymes and ligated to become respectively pSAL6/*AtTPS1HA* and pSAL6/*ΔNAtTPS1HA*. The pSAL4/*AtTPS1HA* and pSAL4/*ΔNAtTPS1HA* were constructed using the pSAL6/*AtTPS1HA* and pSAL6/*ΔNAtTPS1HA*. These plasmids were digested with *BrsGI* and *SpeI* and the *AtTPS1HA* and *ΔNAtTPS1HA* alleles were ligated into the same endonuclease sequence sites in the pSAL4 vector. To obtain YEplac195/*KanMX/AtTPS1HA* and YEplac195/*KanMX/ΔNAtTPS1HA*, the C-terminal part of the *AtTPS1HA* was PCR amplified from the pSAL6/*AtTPS1HA* plasmid with forward primer ^{5'}GGATCAAAATCCTCATCATCC^{3'} and reverse primer ^{5'}CCGGAATTCGCTATTACGCCAGCG^{3'}. The PCR fragment was digested with *BamHI* and *EcoRI* and ligated to the 3084bp *BamHI* fragment of pSAL6/*AtTPS1HA* or the 2820bp *BamHI* fragment of pSAL6/*ΔNAtTPS1HA* and further ligated into the *BamHI* and *EcoRI* digested YEplac195/*KanMX* plasmid (Tanghe et al., 2002).

The bacterial *E. coli* DH5α was used for subcloning and assembly of constructs. The yeast strains used were: wild type W303-1A (*Mata leu 2-3,112 ura3-1 trp1-1 his3-11,15 ade2-1 can1-100 GAL SUC2*) (Thomas and Rothstein, 1989); *tps1Δ*, YSH290 (W303-1A, *tps1Δ::TRP1*) (Hohmann et al., 1993); *tps1Δ tps2Δ* YSH652 (W303-1A, *tps1Δ::TRP1, tps2Δ::LEU2*) (Neves et al., 1995) and *tps1Δ*

tps2Δ tps3Δ tsl1Δ YSH662 (W303-1A, *tps1Δ::TRP1*, *tps2Δ::LEU2 tps3Δ::URA3 tsl1Δ::HIS3*) (Hohmann, MCB laboratory stock) and in a different background: M5 *fil1 tps1Δ hxx2Δ* (*Mata leu2-3,112 ura3-52 trp1-92 fil1 hxx2Δ::LEU2 tps1Δ::TRP1*) (Van Dijck et al., 2000).

The two-hybrid plasmids pGBT9 and pGAD242 were obtained from Clontech. Constructs were made starting with a *NcoI* digestion of pSAL6/*AtTPS1* and pSAL6/*ΔNAtTPS1*, followed by Klenow DNA polymerase activity and by another digestion with *BamHI*. The obtained *AtTPS1* and *ΔNAtTPS1* fragments were ligated into the *SmaI/BamHI* cut pGBT9 and pGAD242 to result in the pGBT9/*AtTPS1*, pGBT9/*ΔNAtTPS1*, pGAD242/*AtTPS1* and pGAD242/*ΔNAtTPS1*. The 264bp fragment at the 5' end of *AtTPS1* was amplified with the following primers: forward primer 5'^{TATAGAATTCATGCCTGGAAATAAGTAC}3' and reverse primer 5'^{TATAGGATCCTTACCTAACTTCTGCCTC}3'. The PCR fragment together with the pGBT9 and pGAD242 vector were digested with *EcoRI* and *BamHI* and ligated resulting in pGBT9/*AtTPS1*(1-264) and pGAD242/*AtTPS1*(1-264). The pGBT9 and pGAD242 constructs containing full length and fragments of KCA1, KCA2 and CDKA;1 have been described before (Vanstraelen et al., 2004). The cDNA library obtained from Clontech was made of 3 week old vegetative Arabidopsis plants and cDNA fragments were fused to the *GAL4* activation domain in the pGAD424 vector. The strain used in the two hybrid experiment was the *AH109* strain (*Mata trp1-901 leu2-3,112 ura3-52 his3-200 gal4Δ gal80Δ LYS::GAL1_{UAS}-GAL1_{TATA}-HIS, GAL2_{UAS}-GAL2_{TATA}-ADE URA::MEL1_{UAS}-MEL1_{TATA}-lacZ MEL1*) (Clontech). The pGBT9 and pGAD242 constructs were cotransformed into the *AH109* strain, selected on medium without Leu and Trp. Single colonies were grown in liquid medium –Leu and –Trp overnight at 30°C and 7 μl drops of a dilution series (OD₆₀₀ 1, 0.2, 0.1, 0.05, 0.025) were spotted on selective medium –Leu, -Trp, -His or –Leu, -Trp, -Ade. as indicated. Medium –Leu, -Trp, -His was supplemented with 0, 2.5, 5 or 10 mM 3AT (Sigma-Aldrich, St. Louis). Plates were grown at 30°C.

GFP-fusion constructs were generated by PCR using primers extended with Gateway® adaptors attB1 and attB2 and recombination into the vector pK7GWF2 and pHGWR2 (Karimi et al., 2002; Karimi et al., 2005).

Fast Performance Liquid Chromatography (FPLC fractionation)

Flowers, stems and cauline leaves of plants were cut and grinded thoroughly into a chilled mortar in homogenization buffer (50 mM Tris pH 8.2, 2 mM EDTA, 5 mM DTT and 20% glycerol) to obtain the plant extracts. Fresh plant extracts and yeast protein extracts (Bell et al., 1998) were filtered through a 0.20 μm filter and concentrated using a vivaspin concentrator column (10 kDa MWCO) by centrifugation for 30 min at 3500 rpm. The superdex 200 HR 10/30 Sepharose-6 FPLC column was washed with 40 ml Phosphate buffer at pH 7.0 (10.7 g/l Na₂HPO₄·2H₂O, 5.5 g/l NaH₂PO₄·H₂O, 7.5 g/l KCl, and 246 mg MgSO₄·7H₂O) for yeast and 40 ml homogenization buffer for plant extracts. 1 ml of the concentrated protein extract was applied onto the column and fractions of 750 μl were

collected. FPLC-fractions were further used in immuno-blot analysis. The column was washed with 40 ml 20% EtOH.

Immuno-blot analysis

Antibodies were either commercially available: Anti-HA High affinity rat IgG (used in a concentration of 1:10000 (v/v); Roche), anti- β TUB mouse IgG (concentration: 1:1000; ab7792, Abcam Ltd, Cambridge), or previously generated against yeast proteins: Anti-Tps2 and anti-Tps3 and anti-Tsl1 rabbit serum, all used in a 1:500 dilution (Bell et al., 1998). Anti-*AtTPS1* was generated in rabbit against an epitope in the C-terminal region of *AtTPS1*. Workable concentration for western blot analysis was determined at a dilution of 1:500.

Proteins were separated by denaturing SDS-PAGE (Laemmli, 1970) and blotted on a nitrocellulose filter (HybondC extra, Amersham) with a liquid miniblotting system (Bio-Rad, Hercules, CA). Filters were blocked in TBST (Tris buffered saline with 0.05% Tween-20) supplemented with 2% BSA (anti-HA and anti- β TUB) or 5% skimmed milk (anti-Tps2, anti-Tps3, anti-Tsl1) for 2h. Primary antibody was added to the same buffer and incubated overnight at 4°C. After washing with TBST (3 x 10 min), the membranes were incubated in fresh buffer with an appropriate alkaline phosphatase linked secondary antibody: goat anti-rat IgG, goat anti-mouse IgG (Sigma, Aldrich) or goat anti-rabbit IgG (Bio-Rad) used in a concentration of 1:1000. For detection, membranes were washed (3 x TBST 10 min) and incubated with 50 mg/ml BCIP and 75 mg/ml NBT in developing buffer (100 mM Tris pH 9.5, 50 mM MgCl₂, 100 mM NaCl) in the dark until bands were visualized. Filters were rinsed with water and air-dried. The CDKA;1 protein was detected using a 1:2500 dilution of cdc2 PSTAIRE antibody (Santa Cruz Biotechnology, Santa Cruz, CA) and a 1:10000 dilution of secondary anti rabbit Ig horseradish peroxidase from donkey in TBST with 3% skimmed milk. Proteins were detected using a chemiluminescence procedure (Bio-Rad).

Affinity chromatography

Anti-*AtTPS1* antibody was coupled to an agarose support matrix Affi-Gel® Hz Immunoaffinity kit (Biorad) using manufacturers instructions. All following manipulations were performed at room temperature. To wash the column prior to each experiment, 3 bed volumes of elution buffer (2 M NaSCN, 3 M urea, 2.5 M guanidine HCl) were put on the column. The column was regenerated with 5 volumes of homogenization buffer (see FPLC fractionation) without DTT and the filtered protein extract was applied to the immobilized IgG column. The column was washed twice with 2 volumes of 0.5 M NaCl, followed by 2 volumes of 0.2 M NaCl in homogenization buffer minus DTT. Retained proteins were eluted in 2 bed volumes of elution buffer. The column was regenerated with 2 volumes homogenization buffer and stored at 4 °C adding 0.02% NaN₃. Collected fractions were dialyzed with Spectra/Por® Membrane, MWCO 6-8 kDa in homogenization buffer without DTT.

Proteins were TCA precipitated and dissolved in 300 μ l homogenization buffer and analyzed by immuno-blot.

Pull down p10^{CKSAT} beads

Arabidopsis plants were homogenized with mortar and pestle. Homogenate was centrifuged at 10,000g for 10 min to remove cell debris. The supernatant was centrifuged at 14,000g for 10 min. A sample was kept on ice and used as crude extract. Then, incubation of 300 μ g of proteins with 50% (v/v) p10^{CKSAT} Sepharose beads and pull down was performed as described before (Vanstraelen et al., 2004). Samples were analyzed via immuno-blot.

Microscopy

Transgenic BY-2 cells from liquid cultures were transferred to the bottom of a coverglass chamber (Lab-Tek, Naperville, IL, USA) and imaged using a Zeiss 100M confocal microscope equipped with LSM510 software (version 3.2). Images were recorded and analyzed as described previously (Van Damme et al., 2004a; Van Damme et al., 2004b). For the analysis of transiently transfected tobacco epidermal cells, leaf blades were injected with dilutions of an Agrobacterium culture (O.D.₆₀₀ = 0.5) and 3 days later mounted on a microslide in water.

References

- Avonce N, Leyman B, Mascorro-Gallardo JO, Van Dijck P, Thevelein JM, Iturriaga G** (2004) The Arabidopsis trehalose-6P-synthase *AtTPS1* gene is a regulator of glucose, stress and stress signaling. *Plant Physiol* **In press**
- Avonce N, Leyman B, Thevelein J, Iturriaga G** (2005) Trehalose metabolism and glucose sensing in plants. *Biochem Soc Trans* **33**: 276-279
- Bell W, Sun W, Hohmann S, Wera S, Reinders A, De Virgilio C, Wiemken A, Thevelein JM** (1998) Composition and functional analysis of the *Saccharomyces cerevisiae* trehalose synthase complex. *J Biol Chem* **273**: 33311-33319
- Blazquez MA, Lagunas R, Gancedo C, Gancedo JM** (1993) Trehalose-6-phosphate, a new regulator of yeast glycolysis that inhibits hexokinases. *FEBS Lett* **329**: 51-54
- Blazquez MA, Santos E, Flores CL, Martinez-Zapater JM, Salinas J, Gancedo C** (1998) Isolation and molecular characterization of the Arabidopsis *TPS1* gene, encoding trehalose-6-phosphate synthase. *Plant J* **13**: 685-689
- Breitenbach-Schmitt I, Schmitt HD, Heinisch J, Zimmermann FK** (1984) Genetic and physiological evidence for the existence of a second glycolytic pathway in yeast parallel to the phosphofructokinase-aldolase reaction sequence. *Mol. Gen. Genet.* **195**: 536-540
- Cabib E, Leloir LF** (1958) The biosynthesis of trehalose phosphate. *J Biol Chem* **231**: 259-275
- De Veylder L, Segers G, Glab N, Casteels P, Van Montagu M, Inze D** (1997) The Arabidopsis *Cks1At* protein binds the cyclin-dependent kinases *Cdc2aAt* and *Cdc2bAt*. *FEBS Lett* **412**: 446-452
- Eastmond PJ, van Dijken AJH, Spielman M, Kerr A, Tissier AF, Dickinson HG, Jones JDG, Smeekens SC, Graham IA** (2002) Trehalose-6-phosphate synthase 1, which catalyses the first step in trehalose synthesis, is essential for Arabidopsis embryo maturation. *Plant Journal* **29**: 225-235
- Goddijn OJ, van Dun K** (1999) Trehalose metabolism in plants. *Trends Plant Sci* **4**: 315-319
- Gomez LD, Baud S, Graham IA** (2005) The role of trehalose-6-phosphate synthase in Arabidopsis embryo development. *Biochem Soc Trans* **33**: 280-282
- Ho Y, Gruhler A, Heilbut A, Bader GD, Moore L, Adams SL, Millar A, Taylor P, Bennett K, Boutilier K, Yang LY, Wolting C, Donaldson I, Schandorff S, Shewnarane J, Vo M, Taggart J, Goudreault M, Muskat B, Alfaro C, Dewar D, Lin Z, Michalickova K, Willems AR, Sassi H, Nielsen PA, Rasmussen KJ, Andersen JR, Johansen LE, Hansen LH, Jespersen H, Podtelejnikov A, Nielsen E, Crawford J, Poulsen V, Sorensen BD, Matthiesen J, Hendrickson RC, Gleeson F, Pawson T, Moran MF, Durocher D, Mann M, Hogue CWV, Figeys D, Tyers M** (2002) Systematic identification of protein complexes in *Saccharomyces cerevisiae* by mass spectrometry. *Nature* **415**: 180-183
- Hohmann S, Neves MJ, de Koning W, Alijo R, Ramos J, Thevelein JM** (1993) The growth and signalling defects of the *ggs1 (fdp1/byp1)* deletion mutant on glucose are suppressed by a deletion of the gene encoding hexokinase PII. *Curr Genet* **23**: 281-289
- Karimi M, De Meyer B, Hilson P** (2005) Modular cloning in plants. *Trends Plant Sci* **in press**
- Karimi M, Inze D, Depicker A** (2002) GATEWAY vectors for Agrobacterium-mediated plant transformation. *Trends Plant Sci* **7**: 193-195
- Kong LJ, Hanley-Bowdoin L** (2002) A geminivirus replication protein interacts with a protein kinase and a motor protein that display different expression patterns during plant development and infection. *Plant Cell* **14**: 1817-1832
- Laemmli UK** (1970) Cleavage of structural proteins during the assembly of the head of bacteriophage T4. *Nature* **227**: 680-685
- Leyman B, Van Dijck P, Thevelein JM** (2001) An unexpected plethora of trehalose biosynthesis genes in Arabidopsis thaliana. *Trends Plant Sci* **6**: 510-513
- Neves MJ, Hohmann S, Bell W, Dumortier F, Luyten K, Ramos J, Cobbaert P, de Koning W, Kaneva Z, Thevelein JM** (1995) Control of glucose influx into glycolysis and pleiotropic effects studied in different isogenic sets of *Saccharomyces cerevisiae* mutants in trehalose biosynthesis. *Curr Genet* **27**: 110-122
- Paiva CL, Panek AD** (1996) Biotechnological applications of the disaccharide trehalose. *Biotechnol Annu Rev* **2**: 293-314
- Paul M, Pellny T, Goddijn O** (2001) Enhancing photosynthesis with sugar signals. *Trends Plant Sci* **6**: 197-200

- Pedruzzi I, Dubouloz F, Cameroni E, Wanke V, Roosen J, Winderickx J, De Virgilio C** (2003) TOR and PKA signaling pathways converge on the protein kinase Rim15 to control entry into G0. *Mol Cell* **12**: 1607-1613
- Reinders A, Burckert N, Hohmann S, Thevelein JM, Boller T, Wiemken A, De Virgilio C** (1997) Structural analysis of the subunits of the trehalose-6-phosphate synthase/phosphatase complex in *Saccharomyces cerevisiae* and their function during heat shock. *Mol Microbiol* **24**: 687-695
- Schluepmann H, Pellny T, van Dijken A, Smeekens S, Paul M** (2003) Trehalose 6-phosphate is indispensable for carbohydrate utilization and growth in *Arabidopsis thaliana*. *Proc Natl Acad Sci U S A* **100**: 6849-6854
- Stals H, Bauwens S, Traas J, VanMontagu M, Engler G, Inze D** (1997) Plant CDC2 is not only targeted to the pre-prophase band, but also co-localizes with the spindle, phragmoplast, and chromosomes. *Febs Letters* **418**: 229-234
- Tanghe A, Van Dijck P, Dumortier F, Teunissen A, Hohmann S, Thevelein JM** (2002) Aquaporin expression correlates with freeze tolerance in baker's yeast, and overexpression improves freeze tolerance in industrial strains. *Appl Environ Microbiol* **68**: 5981-5989
- Thomas BJ, Rothstein R** (1989) Elevated recombination rates in transcriptionally active DNA. *Cell* **56**: 619-630
- Van Aelst L, Hohmann S, Bulaya B, de Koning W, Sierkstra L, Neves MJ, Luyten K, Alijo R, Ramos J, Coccetti P** (1993) Molecular cloning of a gene involved in glucose sensing in the yeast *Saccharomyces cerevisiae*. *Mol Microbiol* **8**: 927-943
- Van Damme D, Bouget FY, Van Poucke K, Inze D, Geelen D** (2004a) Molecular dissection of plant cytokinesis and phragmoplast structure: a survey of GFP-tagged proteins. *Plant J* **40**: 386-398
- Van Damme D, Van Poucke K, Boutant E, Ritzenthaler C, Inze D, Geelen D** (2004b) In Vivo Dynamics and Differential Microtubule-Binding Activities of MAP65 Proteins. *Plant Physiol* **136**: 3956-3967
- Van Dijck P, Ma P, Versele M, Gorwa MF, Colombo S, Lemaire K, Bossi D, Loiez A, Thevelein JM** (2000) A baker's yeast mutant (*fil1*) with a specific, partially inactivating mutation in adenylate cyclase maintains a high stress resistance during active fermentation and growth. *J Mol Microbiol Biotechnol* **2**: 521-530
- Van Dijck P, Mascorro-Gallardo JO, De Bus M, Royackers K, Iturriaga G, Thevelein JM** (2002) Truncation of *Arabidopsis thaliana* and *Selaginella lepidophylla* trehalose-6-phosphate synthase unlocks high catalytic activity and supports high trehalose levels on expression in yeast. *Biochem J* **366**: 63-71
- van Dijken AJ, Schluepmann H, Smeekens SC** (2004) *Arabidopsis* trehalose-6-phosphate synthase 1 is essential for normal vegetative growth and transition to flowering. *Plant Physiol* **135**: 969-977
- Vanstraelen M, Torres Acosta JA, De Veylder L, Inze D, Geelen D** (2004) A plant-specific subclass of C-terminal kinesins contains a conserved a-type cyclin-dependent kinase site implicated in folding and dimerization. *Plant Physiol* **135**: 1417-1429
- Versele M, Thevelein JM, Van Dijck P** (2004) The high general stress resistance of the *Saccharomyces cerevisiae* *fil1* adenylate cyclase mutant (*Cyr1Lys1682*) is only partially dependent on trehalose, Hsp104 and overexpression of Msn2/4-regulated genes. *Yeast* **21**: 75-86
- Vogel G, Fiehn O, Jean-Richard-dit-Bressel L, Boller T, Wiemken A, Aeschbacher RA, Wingler A** (2001) Trehalose metabolism in *Arabidopsis*: occurrence of trehalose and molecular cloning and characterization of trehalose-6-phosphate synthase homologues. *J Exp Bot* **52**: 1817-1826
- Weingartner M, Binarova P, Drykova D, Schweighofer A, David JP, Heberle-Bors E, Doonan J, Bogre L** (2001) Dynamic recruitment of Cdc2 to specific microtubule structures during mitosis. *Plant Cell* **13**: 1929-1943
- Zimmermann P, Hirsch-Hoffmann M, Hennig L, Gruissem W** (2004) GENEVESTIGATOR. *Arabidopsis* microarray database and analysis toolbox. *Plant Physiology* **136**: 2621-2632

The background of the slide is a large, dark-field fluorescence microscopy image of plant cells. The cell walls are stained with a red fluorescent marker, creating a network of bright red lines against a black background. The cells are elongated and arranged in a somewhat regular pattern. In the upper-left quadrant, there is a smaller, rectangular inset image that shows a similar but more magnified view of the cell wall structure, highlighting the individual cell boundaries more clearly.

Chapter 6

Functional analysis of KCA1 and KCA2 in plant growth and development

Chapter page: Confocal microscopy image of the root tip of an *Arabidopsis thaliana* seedling, stained with FM4-64. The cell in the center of the picture is dividing and the forming cell plate has not yet reached the mother cell wall.

Abstract

KCA1 interacts with AtTPS1 and the katanin p60 subunit AtKSS, which are implicated in the development and morphology of Arabidopsis plants. To study the function of KCA in plant growth, plants that carried a T-DNA insertion in intron 10 of *KCA1* and exon 1 of *KCA2* were identified. Both single and double mutant were investigated. Molecular characterization of the mutant alleles showed that *KCA2* transcript was absent from mutant plants. Despite of the T-DNA insertion in *KCA1* mutants, *KCA1* transcripts of full-length size and a shorter fragment were detected. Western blotting using an antibody that recognizes both *KCA1* and *KCA2*, revealed the absence of KCA proteins in double mutants, but not in single insertion mutants. KCA mutants were phenotypically characterized and compared to plants mutated in the genes that encode for the *KCA1* interaction partners katanin and AtTPS1. Processes related to cell division and cell expansion were not perturbed in the *kca* mutants under the conditions tested. It is possible that the T-DNA insertion in the *KCA1* gene is not a knock out and that functional *KCA1* protein is still produced. Alternatively, other kinesins or parallel mechanisms can take over KCA activity. It is also possible that phenotypes were too subtle and growth conditions not apt to uncover phenotypic aberrations.

Introduction

Plant cells are unique in that they build three MT structures that are absent in other eukaryotes. The cortical array is typical for interphase cells and directs cell expansion. Dividing cells produce different configurations that contribute to cell division. The PPB and the phragmoplast are implicated in the alignment and construction of the cell plate during cytokinesis (Wasteneys, 2002). Consistent with this, plant specific MAPs, both structural MAPs and kinesins, associate with these MT structures and disruption of their respective genes affects MT organization leading to altered growth morphologies (Torresruiz and Jurgens, 1994; Traas et al., 1995; Oppenheimer et al., 1997; Furutani et al., 2000; Nishihama et al., 2002; Strompen et al., 2002; Yang et al., 2003; Muller et al., 2004).

In plants, kinesins function in intracellular transport of vesicles and organelles and MT organization during interphase and mitosis (Lee and Liu, 2004). The minus-end directed kinesin KCBP is involved in trichome morphogenesis in Arabidopsis, probably by organizing the cortical MTs in these specialized cell types (Oppenheimer et al., 1997; Mathur and Chua, 2000). In addition, KCBP plays a role during cell division. It localizes to all mitotic MT arrays and a function in spindle pole formation has been proposed based on antibody microinjection experiments (Bowser and Reddy, 1997; Vos et al., 2000). Arabidopsis plants that are mutated in the kinesin genes *ATK1* or *ATK5* have broad spindle poles, suggesting that other minus-end directed kinesins are also implicated in spindle pole formation (Chen et al., 2002; Marcus et al., 2002; Marcus et al., 2003; Ambrose et al., 2005). In addition, *ATK1* functions in the construction of the bipolar spindle as *atk1* mutant spindles displayed a reduced bipolarity. Probably, *ATK1* plays antagonistic roles to BimC/Kinesin-5 like kinesins in spindle formation. The tobacco TKRP125 is a BimC like kinesin that has been localized to the PPB, spindle and phragmoplast. Antibodies raised against the motor domain of this kinesin inhibit sliding of phragmoplast MTs in BY-2 cells, indicating that TKRP125 functions in phragmoplast MT organization (Asada et al., 1997). Several plant specific kinesins play distinct roles during cytokinesis. *AtPAKRP1* and its homologue *AtPAKRP1L* localize to the midzone of the phragmoplast (Lee and Liu, 2000; Pan et al., 2004). It was proposed that they function in the maintenance of the bipolar phragmoplast structure, once it is constructed. *AtPAKRP2* also localizes to the phragmoplast midline, but in a Brefeldin A dependent punctate manner. This kinesin is membrane associated and is a good candidate to deliver Golgi-derived vesicles to the phragmoplast midline (Lee et al., 2001). *NACK1/HIK* and *NACK2/TES* are essential to respectively mitotic and meiotic cytokinesis (Hulskamp et al., 1997; Nishihama et al., 2002; Yang et al., 2003). MT reorganization during phragmoplast expansion was impaired in *hik* mutants, indicating that they function in MT dynamics leading to cell plate expansion (Strompen et al., 2002).

The KCA motor proteins are strongly related proteins. Based on homology within the motor domain, they were classified in a distinct subclass with the kinesin KCBP in the C-terminal/Kinesin-14 subfamily (Dagenbach and Endow, 2004; Lawrence et al., 2004). Homologues of the KCA proteins are restricted to the plant kingdom, suggesting that they play a role in MT based processes that are

unique to plants. Expression and immunofluorescence data suggested that the KCA proteins function in both interphase and mitosis (Kong and Hanley-Bowdoin, 2002; Vanstraelen et al., 2004). A function in cell division is supported by the interaction with the cell cycle kinase CDKA;1 and the differential localization of KCA1 during cell division (Chapter 3 and 4). In addition, KCA1 marks the division site throughout cell division, pointing to a role for KCA1 in cell plate guidance (Chapter 4). Two hybrid assays identified several binding partners of KCA1 (De Veylder et al., 1997; Kong and Hanley-Bowdoin, 2002; Bouquin et al., 2003). KCA1 was identified as an interaction partner of the katanin p60 subunit, AtKSS (Bouquin et al., 2003). Arabidopsis mutants of the katanin are affected in cell elongation leading to anisotropic growth. In addition, misaligned cell plates were observed in certain tissues (Bichet et al., 2001; Burk et al., 2001; Webb et al., 2002; Bouquin et al., 2003). More recently, the trehalose phosphate synthase AtTPS1 was found to interact with KCA1, CDKA;1 and β -tubulin (Chapter 5). AtTPS1 mutant plants are embryo lethal. Rescue of the mutation by temporal expression of wild type gene until seed maturation resulted in plants with impaired flowering induction, indicating a role in plant development (Eastmond et al., 2002; van Dijken et al., 2004).

To unravel the function of the KCA proteins in plant growth, we inspected KCA T-DNA mutants for phenotypes that fit with the molecular data and phenotypes of the AtKSS and the AtTPS1 mutants.

Results

Isolation and molecular characterization of KCA T-DNA insertion mutants

The Salk collection of Arabidopsis T-DNA insertion lines was searched for mutants in the *KCA* genes. Two independent mutant lines were identified for *KCA1*, with insertions respectively in the 5' UTR (*kca1-1*) and in intron 10 (*kca1-2*; stalk domain) (Fig. 6.1A). A single mutant was identified for the *KCA2* gene with an insertion in exon 1 (*kca2-1*; N-terminal region preceding the motor domain) (Fig. 6.1A).

Plants homozygous for these T-DNA insertions were identified by PCR analysis. Genomic right border (RB) and left border (LB) primers flanking the T-DNA insertions were designed to amplify wild type (WT) *KCA1* and *KCA2* alleles. In WT samples, bands of 957 and 954 base pairs (bp) were observed with primers specific for respectively *KCA1* and *KCA2* (Fig. 6.1B). These bands were absent from respectively *kca1-2* and *kca2-1* samples, confirming the absence of wild type genomic sequences for these genes. Next, the RB primer was used in combination with the LBB1 primer to identify the presence of the T-DNA in the target genes. PCR products of respectively 907 and 609 bp were observed in *kca1-2* and *kca2-1* samples and not in WT samples (Fig. 6.1B). *Kca1-2* and *kca2-1* lines homozygous for the respective T-DNA insertions were therefore identified.

Semi-quantitative RT-PCR was performed on two weeks old seedlings to analyse *KCA1* and *KCA2* transcripts in the mutant lines. cDNA specific primers were designed for *KCA1* and *KCA2* that flanked the T-DNA insertion site. Two bands were detected in *kca1-2* lines when *KCA1* specific

primers were used (Fig. 6.1C). Sequence inspection indicated that the T-DNA insert in the *KCA1* gene was located in intron 10. The higher MW band was similar in size to the full length *KCA1* transcript. The abundance of this PCR product was lower relative to reaction products obtained with WT samples. The two cDNA fragments were cloned and the sequence determined. The sequence of the higher MW band matched with the endogenous *KCA1* full-length cDNA sequence. Sequencing of the lower MW band revealed a deletion of 650 bp at nucleotide position 766-1416 bp corresponding to the amino acids 255-472. The deletion resulted in the loss of exons 7-10 and part of exon 6 that together encode for the major part of the *KCA1* motor domain (bp 420-1386 or aa 140-462). Thus, the T-DNA caused aberrant splicing by which a coding region upstream of the insertion and the insertion itself were removed. The *KCA2* T-DNA insertion mutant showed a less complex transcriptional pattern (Fig. 6.1C). No *KCA2* transcript was detected in *kca2-1* samples using cDNA primers that flanked the *kca2-1* T-DNA insertion site. *Kca1-1* homozygous lines with a T-DNA in the 5'UTR of *KCA1* were also identified and subjected to RT-PCR (data not shown). As there was no change in *KCA1* transcript levels in the *kca1-1* lines compared to WT plants (data not shown), further analysis was restricted to *kca1-2* and *kca2-1* mutants.

KCA protein levels were assessed in WT and mutant plants using an antibody raised against the motor domain of *KCA2*, anti-*KCA2*;motor. Specificity of the antibody was tested against bacterial extracts containing either His tagged *KCA1* or *KCA2*. The anti-*KCA1*;motor serum detected a 143 kDa band in His-*KCA1* and His-*KCA2* extracts, indicating that the antiserum could not discriminate between *KCA1* and *KCA2* (data not shown). The anti-*KCA2*;motor serum cross-reacted with a protein band of similar size in WT plant extracts (Fig. 6.1D). Addition of a 6 x His tag increases the MW with 2 kDa, a difference that is difficult to detect on protein acrylamide gel electrophoresis (PAGE). In *kca1-2* and *kca2-1* extracts, a similar band was observed. Because the antiserum lacks specificity, this protein could represent either of the two homologous kinesins.

A first inspection of the *kca1-2* and *kca2-1* plants did not reveal gross morphological defects that are expected when cell division or expansion is drastically affected. Mutant seedlings and soil grown plants were similar in size to WT plants (Fig. 6.2, A and B). Organ growth and morphology was followed throughout plant development. Stems, cauline and rosette leaves, flowers, siliques appeared simultaneously in WT and mutant plants and the morphology was comparable.

Other strategies to affect the protein level of *KCA1* and *KCA2* were undertaken. These included the construction of hairpin constructs and overexpression vectors to respectively down regulate or increase the expression of *KCA1* and/or *KCA2* (Karimi et al., 2002). Expression of hairpin constructs results in the formation of double stranded RNA that specifically triggers high-level PTGS of homologous sequences (Waterhouse et al., 1998; Smith et al., 2000). In that way, we anticipated down-regulation of both *KCA1* and *KCA2* simultaneously. However, *KCA* protein was detected by the anti-*KCA2*:motor serum (data not shown). Overexpression of either *KCA1* or *KCA2* did not result in an increase of *KCA* protein level, indicating that the expression level of *KCA1* and 2 is strictly regulated and limited to a given threshold. Consistent with this, plant morphology and development was similar between RNAi, overexpression and WT plants (data not shown).

To down regulate both *KCA* genes, single homozygous *kca* mutants were crossed and the selfed progeny was screened for double homozygous *kca1-2/kca2-1* plants using the primer sets indicated above (Fig. 6.1B). PCR reactions using the LB-RB primers for *KCA1* and *KCA2* gave no PCR product, confirming the absence of WT genomic sequences for these genes in the *kca1-2/kca2-1* plants (Fig. 6.1B). The presence of T-DNA insertions in the *KCA* genes was studied by PCR, using the LBb1 primer in combination with the respective RB primers. This yielded PCR products of respectively 907 and 609 bp, showing that *kca1-2/kca2-1* plants were homozygous for both insertions (Fig. 6.1B).

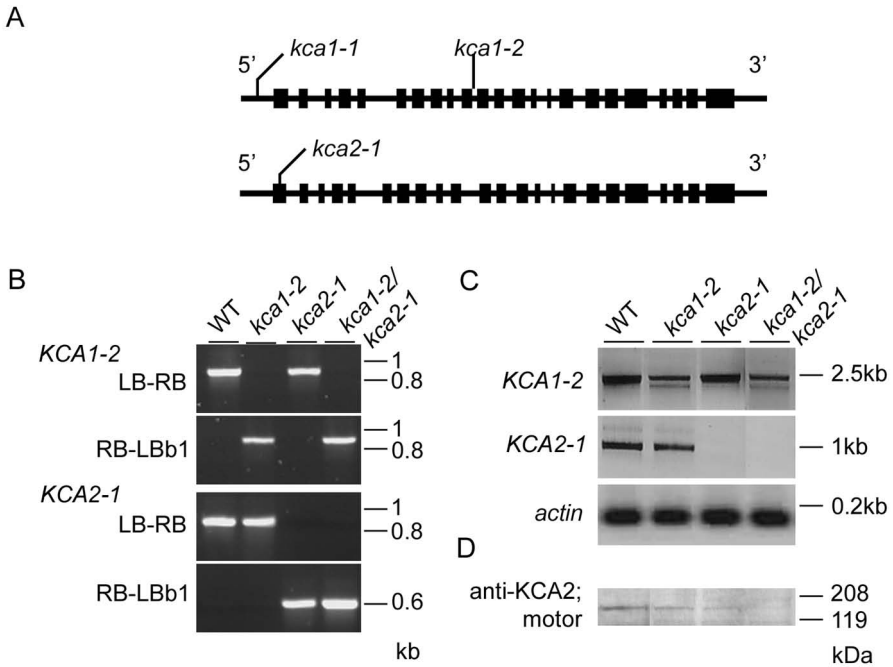


Figure 6.1 Structure of the *KCA1* and *KCA2* genes and molecular characterization of the *kca* mutant alleles. A, Exon and intron organization of the *KCA* genes. The positions and lengths of exons and introns are indicated by closed rectangles and lines, respectively. The positions of T-DNA inserts associated with *kca1-1*, *kca1-2* and *kca2-1* alleles are shown above the gene diagrams. B, PCR identification of single and double mutants for the *kca1-2* and *kca2-1* alleles. PCR primers specific to *KCA1* (LB-RB; 957bp) and *KCA2* (LB-RB; 954bp) that flank the respective T-DNAs were used to amplify WT alleles. The T-DNA specific primer (LBb1) was used in combination with the gene specific primer RB from respectively *KCA1* (RB-LBb1; 907bp) and *KCA2* (RB-LBb1; 609bp) to amplify the T-DNA insertion site. C, Expression of the *KCA* genes. RT-PCR analysis shows *KCA1* mRNA accumulation (2.5 kb) in WT and mutant plants. The lower band in *kca1-2* and *kca1-2/kca2-1* probably represents aberrant splicing events. *KCA2* mRNA (995 bp) is present in WT and *kca1-2*, but absent from *kca2-1* and *kca1-2/kca2-1* plants. Gene specific primers for the *ACT7* gene were used as a control (138bp). D, *KCA* protein levels in *kca* plants. Western blot analysis using the non discriminative anti-KCA2;motor antibody shows the presence of the *KCA* protein (141 kDa) in WT and single mutant plants. *KCA* protein is not detected in double mutant plants.

To analyse *KCA* transcripts in the double mutant *kca1-2/kca2-1* lines, semi-quantitative RT-PCR was performed as described for the single mutants (Fig. 6.1C). *KCA1* related mRNA doublet was present as observed in the single *kca1-2* plants. No transcripts were detected for *KCA2* in the samples using cDNA primers that flanked the *kca2-1* T-DNA insertion site. To check whether the residual *KCA1* mRNA was translated into protein, the anti-*KCA2*;motor serum was tested against protein extracts from double homozygous *kca* plants. The 141 kDa protein band was not detected in these extracts (Fig. 6.1D). This indicates that *KCA1* transcripts are not translated into protein, or the recombinant *KCA1* protein is less stable. Alternatively, the residual amount of *KCA1* transcripts in the *kca1-2/kca2-1* mutant was too low for detection with the anti-*KCA2*;motor serum. The absence of the 141 kDa band confirms non-discriminative binding of the serum to *KCA1* and *KCA2* and further identifies the respective band as *KCA* proteins.

Investigating a role for *KCA* in cell expansion

KCA1 was previously shown to interact with AtKSS, the MT severing p60 subunit of katanin (Bouquin et al., 2003). Arabidopsis mutants that carry mutations in the *AtKSS* gene exhibit a delayed transition of cortical MTs in a transverse orientation in elongating cells. Accordingly, cell elongation is impaired resulting in isotropic cell growth, shorter and thicker organs and smaller plants (Bichet et al., 2001; Burk et al., 2001; Webb et al., 2002; Bouquin et al., 2003). Therefore, we analysed cell elongation and growth abnormalities that were previously correlated with the AtKSS protein.

To this end WT and mutant lines were germinated on MS agar and transferred to soil. Aerial parts of the plants were screened for smaller plants with a general reduction in organ length as shown for the katanin mutants (Bichet et al., 2001; Burk et al., 2001; Bouquin et al., 2003). Inflorescence stems, rosette leaves, flowers and siliques in single and double *kca1-2/kca2* plants all appeared normal with sizes comparable to WT plants (Fig. 6.2A).

Semi-quantitative RT-PCR analysis revealed that *KCA1* is highly expressed in roots where *KCA2* is also abundantly present (Vanstraelen et al., 2004). As increase in root length is mainly determined by cell expansion in the elongation zone, we compared root sizes between WT plants and *kca* mutant lines. Wild type plants, single and double *kca1-2* and *kca2-1* lines were grown on tilted agar plates under continuous light. Fig. 6.2B shows that root length was comparable between WT and mutant plants. Root length was measured 7 days after transfer of agar plates to the growth chambers. WT plants had an average root length of 6.53 cm (n=30) and *kca1-2*, *kca2-1* and double mutant roots were respectively 6.11cm, 6.47 cm and 6.50 cm in length (n=30) (Fig. 6.2C). Statistical analysis (ANOVA tests) indicated that the minor differences in root length were not significant to separate WT plants from mutant lines. Cell expansion leading to root growth was therefore not impaired in *kca* single and double mutants.

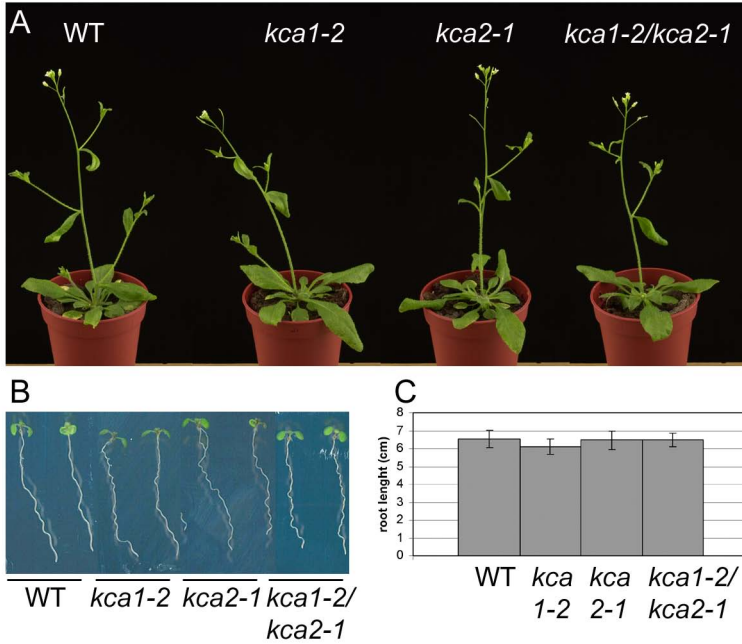


Figure 6.2 Growth of the *kca* mutant plants. A, The general morphology of four week old single and double *kca* plants is not altered compared to WT plants. B, 5 day old seedlings of WT and mutant plants have comparative root lengths when grown on tilted agar plates. C, Mean root length of 30 seedlings, grown 7 days on tilted agar under continuous light of WT and *kca* mutant plants.

Investigating a role for *KCA* in cell expansion upon hormone treatment

The katanin mutant *lue1* was initially isolated in a screen for genes involved in gibberellin (GA) responses. Hormonal responses to GA were impaired such that stem elongation and leaf length were insensitive to GA treatment, whereas flowering induction remained sensitive similar to WT plants (Bouquin et al., 2003). To assess whether *kca* mutants showed altered GA sensitivity, the GA related responses flowering time and stem elongation, were compared with GA-treated WT plants under long day conditions. Flowering time was induced 18.0 days (n=50) after transfer of WT seedlings to soil (Fig. 6.3A). In *kca1-2* and *kca2-1* single and double mutants, flowering induction was achieved after respectively 19.0, 19.4 and 19.0 days (n=50). Stem length was measured at the time of flowering induction (Fig. 6.3B). WT stems measured 68.6 mm, *kca1-2* plants 70.8 mm, *kca2-1* plants 70.9 mm and double *kca* mutants 72.9 mm (n=50). Other GA related responses, like length of rosette leaves (both petiole and blade) were also comparable between *kca* mutants and WT (data not shown). The results indicate that, in contrast to the katanin *lue1* mutant, *kca* alleles are not impaired in their response to GA.

Hypocotyl length is often considered as a standard test in elongation and cell expansion studies (Tanimoto et al., 1995; Ramirez-Parra et al., 2004; Yang et al., 2005). We therefore measured hypocotyls of *kca* and WT plants, grown in the dark. Ethylene is a determinative element in this process (Kieber, 1997). In addition, *leu1* mutants reveal impaired hypocotyl hook formation upon ACC treatment (Bouquin et al., 2003). Therefore we included the ethylene precursor ACC in the analysis. WT and *kca* seeds were plated on MS with or without 50 μ M ACC and allowed to germinate in the dark. After 3, 4, 5 and 6 days, agar plates were retained from the dark and inspected. In a pilot experiment, very few seeds germinated under these conditions, for both WT and *kca*. However, from the few seeds that germinated it was clear that hypocotyl elongation occurred normally in *kca* single and double mutants (Fig. 6.3C). Both WT and *kca* seedlings exhibited a typical hook that could be increased upon ACC treatment. Other ethylene induced morphological changes were also unchanged in *kca* mutants, including hypocotyl thickening, and hypocotyl and root shortening. Because the pilot experiment did not indicate impaired plant responses in the *kca* mutants, no further analysis were undertaken.

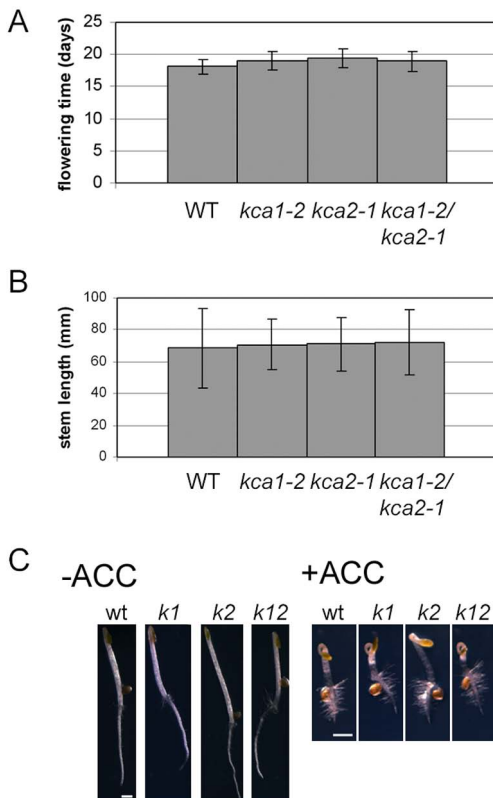


Figure 6.3 *Kca* responses to GA3 and ACC treatments. A, Flowering time (expressed in days) of WT and *kca* plants sprayed with 10 μ M GA3 every 4 days until bolting. B, WT and *kca* stem elongation (expressed in mm) upon GA3 treatment was measured at bolting. C, WT and mutant seedlings were grown in the dark on MS plates with (+) or without (-) 50 μ M ACC. After 4 days, hypocotyl elongation in absence of ACC and hook formation upon ACC treatment were similar for WT and mutant plants. Wt: WT plants, *k1*: *kca1-2*, *k2*: *kca2-1* and *k12*: *kca1-2/kca2-1*. Bar = 1mm.

KCA and cell plate alignment in Arabidopsis root tips

The potential role for *KCA1* in marking the division site in dividing BY-2 cells (Chapter 4), prompted us to investigate cell wall organization in *kca* mutants. The katanin mutants, *erh3* and *bot1* contained misaligned cell plates in root tips and *fra1* has irregular placed cell division planes in parenchyma cells of pith and petioles (Bichet et al., 2001; Burk et al., 2001; Webb et al., 2002). Therefore, we inspected root tips of 2 days old WT and mutant seedlings for the occurrence of misaligned cell plates. Compressed 3D images of mutant roots showed that the general architecture at the tip was similar to WT root tips (Fig. 6.4). Longitudinal sections taken at the centre or epidermis of the root tip showed that the majority of the walls are aligned either transverse or longitudinal to the root axis. Higher magnifications of cells in cytokinesis showed that cell plates were formed with a normal appearance and alignment (data not shown). In conclusion, no apparent dysfunction in cell plate alignment in *kca* mutants could be observed in the root tips. In *botero1*, the occurrence of misaligned cell plates was explained as a result of the altered cell volume and/or geometry. In the different allelic katanin mutants, defects in cell elongation are accompanied with an increased radial swelling of the cells. The absence of a cell elongation phenotype in the *kca* mutants can explain why aberrant cell plates were not observed.

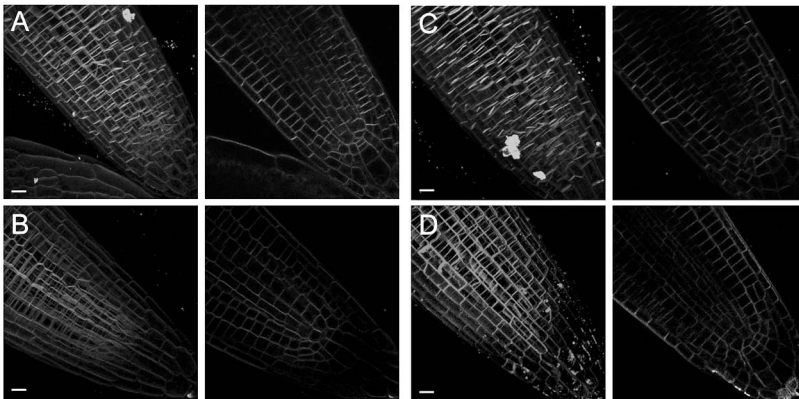


Figure 6.4 Root architecture of WT and *kca* plants. Root tips of 2 days old seedlings of WT (A), *kca1-2* (B), *kca2-1* (C) and *kca1-2/kca2-1* (D) plants were stained with FM4-64 and imaged by confocal microscopy. Compressed 3D images (left column) and a 2D section in the middle of the root (right column) are shown. Bar = 10 μ m.

KCA and AtTPS1

In Chapter 4, we demonstrated that KCA1 interacts with AtTPS1 and show evidence that both occur in a complex together with CDKA;1 and β -tubulin. To investigate a possible role for this interaction in Arabidopsis plants, we analysed the *kca1-2/kca2-1* mutants for phenotypes observed in the AtTPS1 mutant alleles *tps1-1* and *tps1-2*.

Homozygous *tps1* mutants are embryo lethal and embryo development was arrested beyond the heart stage. Segregating seed batches display a wrinkled seed phenotype in the ratio of 3:1 and in developing *TPS1/tps1-1* siliques arrested embryos were recognizable as pale seeds among the green colored heterozygous *tps1-1* mutants and WT (Eastmond et al., 2002). *Kca* single and double mutants were not embryo lethal. Nevertheless we checked seed pods of single and double homozygous *kca* plants for aberrant appearance of seeds and embryos. Dry seed batches did not contain wrinkled seeds, nor did we observe other malformed embryonic structures. This observation is in agreement with the fact that the *KCA* genes are poorly expressed in embryos (<https://www.genevestigator.ethz.ch/>). In contrast, *AtTPS1* is highly expressed in developing embryos (van Dijken et al., 2004).

The *tps1* embryonic defect could be rescued by dexamethasone (DEX) induced expression of the *AtTPS1* gene. In this way, viable homozygous *tps1-2* plants were generated that produced seeds that germinated and developed into fertile plants without further DEX induction of WT *AtTPS1* gene. When seeds were germinated on MS without DEX and sugars, *tps1* seedlings displayed a short root compared to WT accompanied with a reduction in length of the meristematic region at the root tip (van Dijken et al., 2004). In the *kca* single and double mutants, growth of seedlings on MS without sugar did not result in shorter roots (data not shown). Furthermore, plants generated from rescued *tps1-2* seeds revealed an overall growth delay in absence of DEX induction and produced small rosettes. In addition, flowering induction was inhibited resulting in plants consisting of only a rosette and no stem or flowers. Although both *AtTPS1* and *KCA2* were strongly expressed upon the appearance of the inflorescence stem (<https://www.genevestigator.ethz.ch/>), no phenotype correlated with floral transition or rosette morphology was observed in the single or double *kca* mutants under normal growth conditions (Fig. 6.2A).

Discussion

For more than a decade, Arabidopsis mutants have been used to characterize the molecular bases of development in flowering plants, and several mutants impaired in cytoskeletal organization resulting in defects in cell expansion and cell division have been isolated. To address the question whether the kinesins KCA1 and KCA2 play a role in plant growth, we isolated single and double *kca* mutants that carried T-DNA insertions in the respective genes. RT-PCR confirmed absence of *KCA2* transcript. In contrast, the mutant plants produced *KCA1* transcripts of full length size and an

aberrant truncated transcript was detected. Sequencing identified both transcripts as *KCA1*, indicating that *kca1-2* single and double mutants still produce *KCA1* transcript.

On western blot, anti-KCA2;motor detected KCA proteins in WT and single *kca* mutant plants. The serum recognized both *KCA1* and *KCA2* in bacterial extracts expressing either His tagged *KCA1* or *KCA2*, suggesting that the high MW proteins in the single mutants represent the homologous kinesin. No KCA proteins were detected in double *kca* mutants. This confirms the identity of the high MW protein band as KCA proteins. In contrast, RT-PCR indicated that *KCA1* full length transcripts are still present. The truncated *KCA1* transcript contains a deletion of exon 6-10 and probably results from an aberrant splicing event due to the T-DNA in intron 10. The novel transcript had a major part of the *KCA1* motor domain deleted. As the anti-KCA2;motor antibody was raised against the KCA motor domain, truncated *KCA1* proteins were not detected on western blot.

To investigate the significance of the interaction of *KCA1* with the katanin or AtTPS1 we analysed *kca* mutants for phenotypes observed in plants mutated in the genes encoding the interaction partners of KCA. Mutations that affected the interactors resulted in cell division and elongation phenotypes. Katanin p60 mutants are stunted plants with a general reduction in organ size as a result of defects in cell elongation (Bouquin et al., 2003). In addition misalignment of cell division planes was observed in certain tissues (Bichet et al., 2001; Burk et al., 2001; Webb et al., 2002). *Tps1* mutants are embryo lethal and temporal rescue of the phenotype to mature seeds results in a generation of plants with impaired flower induction (Eastmond et al., 2002; Schlupe et al., 2003; van Dijken et al., 2004). A first inspection of *kca* mutants showed no gross defects. Growth conditions that alter cell elongation (GA, growth in dark) did not reveal an impaired response in cell expansion when compared to WT plants. In addition, cell plate positioning in root tips was normal. The *kca* mutants are not embryo lethal and plants produced flowers simultaneously with WT plants. The KCA proteins share 89% similarity and have similar domain organization. They behave similarly in terms of subcellular localization, conformational changes and interaction with CDKA;1 and are expressed in the same plant organs (Vanstraelen et al., 2004). These data suggest that the KCA proteins are functionally redundant. Unfortunately, double *kca* mutants did not reveal a phenotype. Either there exist other kinesins or proteins that can take over the KCA activity. It is also possible that our growth conditions did not reveal a need for normal activity of the KCA protein. As no phenotypes were observed under *in vitro* conditions or in green house grown plants, it seems more likely that the T-DNA insertion in *KCA1* is not a true knock out and functional *KCA1* protein may still be produced. Indeed, the T-DNA in *KCA1* appeared to be spliced out in *kca1-2* plants, resulting in a *KCA1* transcript that may suffice for production of KCA protein not detected in western analysis. We also analyzed the insertion in the 5'UTR of *KCA1* (data not shown). RT-PCR analysis revealed no decrease in *KCA1* transcript. No T-DNA insertions are currently available in the *KCA1* coding sequence that could knock out *KCA1*.

Till now, 13 of the 61 Arabidopsis kinesins have been characterized (Table 6.1). Phenotypic studies of several of these kinesins show that only 2 kinesins reveal strong defects in plant development and morphology (Strompen et al., 2002; Zhong et al., 2002). Abnormalities in 6 other kinesins are

restricted to specialized tissues, like pollen grains or trichomes (Oppenheimer et al., 1997; Chen et al., 2002; Yang et al., 2003; Lu et al., 2005) or reveal abnormalities in MT arrays during mitotic cell division (Vos et al., 2000; Marcus et al., 2003; Ambrose et al., 2005). The fact that the latter defects do not affect plant growth or development suggests the existence of an error correcting mechanism. The Arabidopsis genome contains 61 kinesins of which 21 belong to the C-terminal subfamily. Phylogenetic analyses of the motor domains of these kinesins also indicate that they are more closely related to each other than to other Arabidopsis kinesins. Additionally, their functions seem to be involving aspects of cell division, suggesting functional redundancy. Thus other minus-end directed kinesins could act as a functional substitute of KCA. Another error correcting mechanism has been proposed by Marcus et al. (2003). They observed that plants defective in the ATK1 kinesin have an abnormal spindle morphology leading to defective male meiosis, whilst mitosis in the vegetative parts of the plant was unaffected. The authors proposed that in mitosis, abnormalities in the spindle are targeted for depolymerization or severing possibly by katanin proteins. If the interaction between KCA and the katanin is significant in such a process, then *kca* mutants should be crossed into other MT defective mutants, like ATK1, in order to check whether a stronger phenotype is revealed due to a defective error correcting system.

The presence of KCA transcript throughout the plant suggests that the KCA proteins have functions both in dividing and non dividing tissues. To unravel the function of the KCA proteins in better detail, it might be necessary to study the kinetics of cell division in the *kca* mutants with more precision. Defects in MT organization or cell plate formation, which do not affect cell morphology or organ architecture, can be visualized using GFP markers. We therefore crossed *kca* mutants with MT GFP markers (work in progress). On the other hand, it might be necessary to find other strategies to affect the KCA proteins than overexpression or knock down. For instance, the kinesin KCBP localizes to the spindle and phragmoplast, suggesting a function in cell division (Bowser and Reddy, 1997). However, mutant plants (Zwichel) have defects in trichome branching as a results of MT disorganisation (Oppenheimer et al., 1997). Using an antibody that constitutively activates the KCBP protein, defects in spindle and phragmoplast formation were revealed (Vos et al., 2000). Phosphorylation mutants for KCA that mimic a constitutive activation by CDKA;1 are under construction and might help to tackle the KCA functional analysis.

Table 6.1 Characterized kinesins in Arabidopsis

| Nr | Kinesin (species) | Subfamily | Intracellular localization | Mutant name | Mutant phenotype | Predicted cellular function | References |
|----|----------------------------|---------------------------|--|-----------------|--|---|---|
| 1 | KatA/ATK1 | C-terminal/ Kinesin-14 | PPB, spindle (concentrated near the midzone), phragmoplast | <i>atk1-1</i> | Reduced male fertility, abnormal spindle organization during microsporogenesis and somatic mitose, broad unfocused spindle poles | MT bundling at spindle poles, formation of bipolar spindle | (Liu et al., 1996; Chen et al., 2002; Marcus et al., 2003) |
| 2 | ATK5 | C-terminal/ Kinesin-14 | Interphase array (preferentially plus-ends), midzone of spindle and phragmoplast | <i>atk5-1</i> | Abnormal broadened spindle poles | Cross-link and align overlapping MTs of the spindle midzone | (Ambrose et al., 2005) |
| 3 | KCBP/ Zwichel | C-terminal/ Kinesin-14 | Cortical MT (in cotton fibers), PPB, perinuclear region in prophase, spindle, phragmoplast | <i>zwichel</i> | Reduction of branch formation in leaf trichomes | Microtubule stabilization to induce trichome branching Spindle pole formation during mitosis | (Bowser and Reddy, 1997; Oppenheimer et al., 1997; Preuss et al., 2003) |
| 4 | AtPAKRP1/ AtKinesin-12A | Kinesin-12 | Midline of the spindle (from anaphase), midzone of the phragmoplast | <i>pakrp1-1</i> | none | Maintenance of mirror shaped phragmoplast | (Lee and Liu, 2000; Pan et al., 2004) |
| 5 | AtPAKRP1/ AtKinesin-12B | Kinesin-12 | Midline of the phragmoplast | <i>pakrp1-1</i> | none | | (Pan et al., 2004) |
| 6 | AtPAKRP2 | Orphan Kinesins | Punctuate pattern at midzone late anaphase spindle and phragmoplast midline | ND | ND | Delivery of Golgi derived vesicles to the phragmoplast midline | (Lee et al., 2001) |

| Nr | Kinesin (species) | Subfamily | Intracellular localization | Mutant name | Mutant phenotype | Predicted cellular function | References |
|----|-------------------|---|--|----------------------------------|--|---|--|
| 7 | AtNACK1/HIK | ungrouped | Midline of phragmoplast | <i>Hinkel</i> <i>Nack1</i> | seedling lethal, incomplete cell walls during vegetative cytokinesis ceased growth at vegetative stage, incomplete cell walls | Phragmoplast/cell plate expansion Active transporter of NPK1 | (Nishihama et al., 2002; Strompen et al., 2002; Tanaka et al., 2004) |
| 8 | AtNACK2/ ACTES | ungrouped | ND | <i>tes</i> | Failure of male meiotic cytokinesis | Tetrad formation in male gametogenesis, establishment of radial MT array prior to cytokinesis | (Yang et al., 2003) |
| 9 | AtFRA1 | Chromokinesi / Kinesin-4 Ungrouped | Periphery of the cytoplasm in Arabidopsis roots | <i>fra1</i> | Altered cellulose microfibril orientation | MT control of cellulose deposition in the cell wall | (Zhong et al., 2002) |
| 10 | MKRPL/2 | Ungrouped | mitochondria | ND | ND | Segregation of mitochondria | (Itoh et al., 2001) |
| 11 | AtKinesin13A | MCAK/ Kinesin-13 | Golgi stacks | <i>kinesin13a</i> <i>-1/2</i> | Additional branching events in leaf trichomes, aggregation of Golgi stacks | Distribution of Golgi stacks with a role in trichome morphogenesis | (Lu et al., 2004) |
| 12 | KCA1/ AtGRIMP | C-terminal/ Kinesin-14 | Plasma membrane (except at division site during mitosis), cell plate | <i>kca1-2</i> | none | | (Kong and Hanley-Bowdoin, 2002; Vanstraelen et al., 2004) |
| 13 | KCA2 | C-terminal/ Kinesin-14 | Plasma membrane (except at division site during mitosis), cell plate | <i>kca2-1</i> | none | | (Vanstraelen et al., 2004) |

Material and methods

Plant growth and treatments

Arabidopsis thaliana (Columbia) seedlings were grown on MS medium supplemented with 1% sucrose, 0.5% MES, 0.1% myo-inositol and 0.8% agar and transferred to soil under 18h-6h day/night in growth chambers at 21°C. For root measurements, seeds were plated on the medium described above, vernalized for 3 days in the dark and then grown under continuous light at 21°C on plates tilted backwards for about 5°. For gibberellin treatments, 1-week-old seedlings were transferred to soil and grown under long day conditions. Plants were sprayed twice a week with 10 µM GA3 (Sigma-Aldrich) until bolting. Sensitivity to ethylene in the dark was investigated by plating WT and *kca* mutant seeds on MS medium supplied with 0.7% agar, 1% sucrose with or without 50 µM ACC (Sigma-Aldrich). Plates were incubated vertically at 21°C in the dark. Seedlings were photographed after 4 days of incubation.

FM4-64 staining

2 day old WT and mutant seedlings were stained for 10 minutes in a solution of 0.33 mM FM4-64 (Molecular Probes, Leiden, The Netherlands) in liquid MS medium on ice (to prevent endocytosis). Then, seedlings were washed three times in MS medium and immediately analysed by confocal microscopy. Red fluorescence from FM4-64 was imaged with 543 nm light for excitation and emission fluorescence was captured via a 560 nm cut-off filter.

Genotyping

T-DNA insertional mutants were identified in the Salk collection (La Jolla, CA). Salk_036411 (T-DNA insertion in the 5' UTR of *kca1*) and Salk_014609 (T-DNA insertion at intron 10 of *kca1*) were designated *kca1-1* and *kca1-2* respectively. Salk_099639 (T-DNA insertion at exon 1 of *kca2*) was named *kca2-1*. Genotyping was performed in two separate PCR reactions. The following gene specific primers were used to amplify WT *KCA* alleles; KCA1-LB AACTTTCCACGCTCTCTGC and KCA2-LB TTTTATCAGCCAGAACACCT as forward primers and KCA1-RB TGTGCTTGAATACCTCCTCG and KCA2-RB CCGAACAAATGAACTGAAATC as reverse primers. To identify the presence of the T-DNA, the RB primers were used in combination with the LbB1 primer GCGTGGACCGCTTGCTGCAACT in a separate PCR reaction.

RNA analysis

RNA was extracted with TRIzol reagent from WT and *kca* seedlings. To this end, grinded plant tissue was homogenized in 1 mL TRIzol and samples were incubated 2 minutes on ice after addition

of 200 μ L chloroform. After centrifugation at 11000 rpm in an Eppendorf centrifuge 5417 for 15 minutes at 4 $^{\circ}$, the aqueous phase was transferred to an Rnase free tube and RNA was precipitated by adding 500 μ L isopropanol. After incubation for 10 minutes, samples were centrifuged at 11000 rpm at 4 $^{\circ}$ for 10 minutes. The RNA pellet was washed with 1 mL 75% ethanol and centrifuged at 11000 rpm for 5 minutes at 4 $^{\circ}$ C.

1 μ g of RNA was used as a template for the SuperScript first-strand synthesis system for RT-PCR (Invitrogen). RT-PCR was performed by combining gene-specific primers salkTH65-RTPCRF AATAGATGGAAGTGGGAGGT as forward primer and AtKLP2-9F2 TGGATCTGCGTATCAAGATATCGAA as reverse primer for KCA1; AtKLP1-33R3 GGGTCACAGTAGACTTTGATTATCATTC as forward primer and S9-RT-PCR-F ATGGCGGAGCAGAAGAGTAC as reverse primer for KCA2; and ACT2-FW TTGACTACGAGCAGGAGATGG and ACT2-REV ACAAACGAGGGCTGGAACAAG for ACT2. In total, 28 cycles were run for to amplify KCA and actin2 RNA.

Protein Gel-Blot Analysis

Crude extracts of one week old were grinded in liquid nitrogen with a mortar and pestle and homogenized in ice cold P10 buffer (25 mM Tris-HCl, pH 7.6, 15 mM ethyleneglycol-bis(β -aminoethyl)tetra-acetate, 1 mM dithiothreitol, 15 mM MgCl₂, 85 mM NaCl, 15 mM pNO₂PhePO₄, 60 mM glycerol phosphate, 0.1% NP40, 1 mM NaF, 0.1 mM Na₃VO₄, and 100 μ l protease inhibitor cocktail; Sigma-Aldrich). The homogenate was centrifuged twice at 10,000 g for 10 min in an Eppendorf centrifuge 5417 at 4 $^{\circ}$ C to remove cell debris. The supernatant was then centrifuged at 14,000 g for 10 min. Loading buffer (Laemmli, 1970) was added and the samples were heated for 10 min at 95 $^{\circ}$ C. After centrifugation at 14,000 g for 4 min, samples were separated on a 12% gel and blotted onto nitrocellulose membranes (Hybond-C super; Amersham Biosciences) in 190 mM glycine and 25 mM Tris with a liquid mini-blotting system (Bio-Rad, Hercules, CA) for 1 h. Membranes were blocked overnight at 4 $^{\circ}$ C in phosphate buffer with 0.1% Tween-20 and 5% skin milk (BD Difco; Becton Dickinson, Franklin Lakes, NJ). For immunodetection, anti-KCA2;motor was applied in the blocking buffer at a dilution of 1:1000 and anti-rabbit Ig horseradish peroxidase from donkey (Amersham Biosciences) was used as a second antibody at a dilution of 1:10000. Proteins were detected by the chemiluminescence procedure (Bio-Rad).

References

- Ambrose JC, Li W, Marcus A, Ma H, Cyr R** (2005) A Minus-End Directed Kinesin with +TIP Activity Is Involved in Spindle Morphogenesis. *Mol Biol Cell*
- Asada T, Kuriyama R, Shibaoka H** (1997) TKRP125, a kinesin-related protein involved in the centrosome-independent organization of the cytokinetic apparatus in tobacco BY-2 cells. *Journal of Cell Science* **110**: 179-189
- Bichet A, Desnos T, Turner S, Grandjean O, Hofte H** (2001) BOTERO1 is required for normal orientation of cortical microtubules and anisotropic cell expansion in Arabidopsis. *Plant J* **25**: 137-148
- Bouquin T, Mattsson O, Naested H, Foster R, Mundy J** (2003) The Arabidopsis lue1 mutant defines a katanin p60 ortholog involved in hormonal control of microtubule orientation during cell growth. *J Cell Sci* **116**: 791-801
- Bowser J, Reddy AS** (1997) Localization of a kinesin-like calmodulin-binding protein in dividing cells of Arabidopsis and tobacco. *Plant J* **12**: 1429-1437
- Burk DH, Liu B, Zhong R, Morrison WH, Ye ZH** (2001) A katanin-like protein regulates normal cell wall biosynthesis and cell elongation. *Plant Cell* **13**: 807-827
- Chen C, Marcus A, Li W, Hu Y, Calzada JP, Grossniklaus U, Cyr RJ, Ma H** (2002) The Arabidopsis ATK1 gene is required for spindle morphogenesis in male meiosis. *Development* **129**: 2401-2409
- Dagenbach EM, Endow SA** (2004) A new kinesin tree. *Journal of Cell Science* **117**: 3-7
- De Veylder L, Segers G, Glab N, Van Montagu M, Inzé D** (1997) Identification of proteins interacting with the Arabidopsis Cdc2aAt protein. *J Exp Bot* **48**: 2113-2114
- Eastmond PJ, van Dijken AJH, Spielman M, Kerr A, Tissier AF, Dickinson HG, Jones JDG, Smeekens SC, Graham IA** (2002) Trehalose-6-phosphate synthase 1, which catalyses the first step in trehalose synthesis, is essential for Arabidopsis embryo maturation. *Plant Journal* **29**: 225-235
- Furutani I, Watanabe Y, Prieto R, Masukawa M, Suzuki K, Naoi K, Thitamadee S, Shikanai T, Hashimoto T** (2000) The SPIRAL genes are required for directional control of cell elongation in Arabidopsis thaliana. *Development* **127**: 4443-4453
- Hulskamp M, Parekh NS, Grini P, Schneitz K, Zimmermann I, Lolle SJ, Pruitt RE** (1997) The STUD gene is required for male-specific cytokinesis after telophase II of meiosis in Arabidopsis thaliana. *Developmental Biology* **187**: 114-124
- Karimi M, Inze D, Depicker A** (2002) GATEWAY vectors for Agrobacterium-mediated plant transformation. *Trends Plant Sci* **7**: 193-195
- Kieber JJ** (1997) The ethylene response pathway in arabidopsis. *Annual Review of Plant Physiology and Plant Molecular Biology* **48**: 277-296
- Kong LJ, Hanley-Bowdoin L** (2002) A geminivirus replication protein interacts with a protein kinase and a motor protein that display different expression patterns during plant development and infection. *Plant Cell* **14**: 1817-1832
- Laemmli UK** (1970) Cleavage of structural proteins during the assembly of the head of bacteriophage T4. *Nature (London)* **227**: 680-685
- Lawrence CJ, Dawe RK, Christie KR, Cleveland DW, Dawson SC, Endow SA, Goldstein LSB, Goodson HV, Hirokawa N, Howard J, Malmberg RL, McIntosh JR, Miki H, Mitchison TJ, Okada Y, Reddy ASN, Saxton WM, Schliwa M, Scholey JM, Vale RD, Walczak CE, Wordeman L** (2004) A standardized kinesin nomenclature. *Journal of Cell Biology* **167**: 19-22
- Lee YR, Giang HM, Liu B** (2001) A novel plant kinesin-related protein specifically associates with the phragmoplast organelles. *Plant Cell* **13**: 2427-2439
- Lee YR, Liu B** (2000) Identification of a phragmoplast-associated kinesin-related protein in higher plants. *Curr Biol* **10**: 797-800
- Lee YR, Liu B** (2004) Cytoskeletal motors in Arabidopsis. Sixty-one kinesins and seventeen myosins. *Plant Physiol* **136**: 3877-3883
- Lu L, Lee YR, Pan R, Maloof JN, Liu B** (2005) An internal motor Kinesin is associated with the Golgi apparatus and plays a role in trichome morphogenesis in Arabidopsis. *Mol Biol Cell* **16**: 811-823
- Marcus AI, Ambrose JC, Blickley L, Hancock WO, Cyr RJ** (2002) Arabidopsis thaliana protein, ATK1, is a minus-end directed kinesin that exhibits non-processive movement. *Cell Motil Cytoskeleton* **52**: 144-150

- Marcus AI, Li W, Ma H, Cyr RJ** (2003) A kinesin mutant with an atypical bipolar spindle undergoes normal mitosis. *Mol Biol Cell* **14**: 1717-1726
- Mathur J, Chua NH** (2000) Microtubule stabilization leads to growth reorientation in *Arabidopsis* trichomes. *Plant Cell* **12**: 465-477
- Muller S, Smertenko A, Wagner V, Heinrich M, Hussey PJ, Hauser MT** (2004) The plant microtubule-associated protein AtMAP65-3/PLE is essential for cytokinetic phragmoplast function. *Curr Biol* **14**: 412-417
- Nishihama R, Soyano T, Ishikawa M, Araki S, Tanaka H, Asada T, Irie K, Ito M, Terada M, Banno H, Yamazaki Y, Machida Y** (2002) Expansion of the cell plate in plant cytokinesis requires a kinesin-like protein/MAPKKK complex. *Cell* **109**: 87-99
- Oppenheimer DG, Pollock MA, Vacik J, Szymanski DB, Ericson B, Feldmann K, Marks MD** (1997) Essential role of a kinesin-like protein in *Arabidopsis* trichome morphogenesis. *Proc Natl Acad Sci U S A* **94**: 6261-6266
- Pan R, Lee YR, Liu B** (2004) Localization of two homologous *Arabidopsis* kinesin-related proteins in the phragmoplast. *Planta* **220**: 156-164
- Ramirez-Parra E, Lopez-Matas MA, Frundt C, Gutierrez C** (2004) Role of an atypical E2F transcription factor in the control of *Arabidopsis* cell growth and differentiation. *Plant Cell* **16**: 2350-2363
- Schluepmann H, Pellny T, van Dijken A, Smeekens S, Paul M** (2003) Trehalose 6-phosphate is indispensable for carbohydrate utilization and growth in *Arabidopsis thaliana*. *Proc Natl Acad Sci U S A* **100**: 6849-6854
- Smith NA, Singh SP, Wang MB, Stoutjesdijk PA, Green AG, Waterhouse PM** (2000) Gene expression - Total silencing by intron-spliced hairpin RNAs. *Nature* **407**: 319-320
- Strompen G, El Kasmi F, Richter S, Lukowitz W, Assaad FF, Jurgens G, Mayer U** (2002) The *Arabidopsis* HINKEL gene encodes a kinesin-related protein involved in cytokinesis and is expressed in a cell cycle-dependent manner. *Curr Biol* **12**: 153-158
- Tanimoto M, Roberts K, Dolan L** (1995) Ethylene is a positive regulator of root hair development in *Arabidopsis thaliana*. *Plant J* **8**: 943-948
- Torresruiz RA, Jurgens G** (1994) Mutations in the FASS Gene Uncouple Pattern-Formation and Morphogenesis in *Arabidopsis* Development. *Development* **120**: 2967-2978
- Traas J, Bellini C, Nacry P, Kronenberger J, Bouchez D, Caboche M** (1995) Normal Differentiation Patterns in Plants Lacking Microtubular Preprophase Bands. *Nature* **375**: 676-677
- van Dijken AJ, Schlupepmann H, Smeekens SC** (2004) *Arabidopsis* trehalose-6-phosphate synthase 1 is essential for normal vegetative growth and transition to flowering. *Plant Physiol* **135**: 969-977
- Vanstraelen M, Torres Acosta JA, De Veylder L, Inze D, Geelen D** (2004) A plant-specific subclass of C-terminal kinesins contains a conserved a-type cyclin-dependent kinase site implicated in folding and dimerization. *Plant Physiol* **135**: 1417-1429
- Vos JW, Safadi F, Reddy AS, Hepler PK** (2000) The kinesin-like calmodulin binding protein is differentially involved in cell division. *Plant Cell* **12**: 979-990
- Wasteneys GO** (2002) Microtubule organization in the green kingdom: chaos or self-order? *J Cell Sci* **115**: 1345-1354
- Waterhouse PM, Graham HW, Wang MB** (1998) Virus resistance and gene silencing in plants can be induced by simultaneous expression of sense and antisense RNA. *Proceedings of the National Academy of Sciences of the United States of America* **95**: 13959-13964
- Webb M, Jouannic S, Foreman J, Linstead P, Dolan L** (2002) Cell specification in the *Arabidopsis* root epidermis requires the activity of ECTOPIC ROOT HAIR 3--a katanin-p60 protein. *Development* **129**: 123-131
- Yang CY, Spielman M, Coles JP, Li Y, Ghelani S, Bourdon V, Brown RC, Lemmon BE, Scott RJ, Dickinson HG** (2003) TETRASPORE encodes a kinesin required for male meiotic cytokinesis in *Arabidopsis*. *Plant J* **34**: 229-240
- Yang XH, Xu ZH, Xue HW** (2005) *Arabidopsis* membrane steroid binding protein 1 is involved in inhibition of cell elongation. *Plant Cell* **17**: 116-131
- Zhong R, Burk DH, Morrison WH, 3rd, Ye ZH** (2002) A kinesin-like protein is essential for oriented deposition of cellulose microfibrils and cell wall strength. *Plant Cell* **14**: 3101-3117

The background of the entire page is a microscopic image of cells expressing a red fluorescent marker. The cells are scattered across the field of view, showing various shapes and sizes. In the upper-left quadrant, there is a smaller, more densely packed inset image of similar red fluorescent cells.

Chapter 7

Conclusions and further perspectives

Chapter page: *Arabidopsis thaliana* seed coat, imaged using confocal microscopy (GFP filter settings).

The complexity and dynamics of the plant MT cytoskeleton and the presence of plant specific MT structures require the cooperation of many MAPs of which some are specific to plants. The goal of this research was to characterize kinesins that function in plant specific MT related processes during cell division. Initially, KCA1 was identified as a CDKA₁ interacting protein in a yeast two hybrid screen (De Veylder et al., 1997) and later, evidence for CDK dependent phosphorylation was provided in insect cells (Kong and Hanley-Bowdoin, 2002). KCA1 and its homolog are plant specific kinesins that belong to the C-terminal/Kinesin-14 subfamily of kinesins, members of which have functions related to cell division (Moore and Endow, 1996; Dagenbach and Endow, 2004). For these reasons we anticipated that KCA1 and KCA2 were potential candidates to function in MT related processes during plant cell division.

The KCA proteins are strongly related to each other, sharing 81% identity and 89% similarity. Based on homology within the motor domain, they were classified in a distinct subclass with the kinesin KCBP within the C-terminal/Kinesin-14 subfamily (Dagenbach and Endow, 2004). Homologues of the KCA proteins and KCBP are restricted to the plant kingdom, suggesting that they play a role in MT based processes unique to plants. KCBP is unique among all known kinesins in having a CaM binding domain that regulates the MT binding capacity of the motor domain (Song et al., 1997). In addition, KCBP contains a region that is also present in some members of myosin-like proteins (Reddy and Reddy, 1999). Myosins are motor proteins that exert transport activities along the actin filaments. The N-terminal tail of KCBP contains a MyTH4 domain and the talin-like domain. Thus KCBP is a molecular hybrid consisting of a motor domain from MT based motors and a tail region of actin-based motors. The KCA proteins do not contain a MyTH4 or talin-like domain; however, the N-terminal part of the KCA tail domain interacts with a tropomyosin and a myosin-like protein in yeast two hybrid and co-immunoprecipitation assays (Torres-Acosta, De Veylder and Inzé, unpublished data). The significance of myosin-like domains in KCBP or the interaction of the KCA proteins with putative actin binding proteins is not known at this time. It is possible that they function in cross-bridging the MT and actin cytoskeleton or they facilitate cargo exchange between two types of motors. On the other hand, KCA1 is associated to membranes of the cell plate and the plasma membrane (Chapter 3 and 4). Thus, interaction between KCA and the tropomyosin and the myosin-like protein may be required for anchoring actin filaments to the plasma membrane.

The founding member of the C-terminal/Kinesin-14 family is Ncd that moves towards the minus-end of MTs. Minus-end directed movement has been demonstrated *in vitro* for three plant members of this subfamily, including KCBP. They typically carry the motor domain at the C-terminal side of the peptide, just like it is for Ncd. Arabidopsis has 21 C-terminal/Kinesin-14 members, of which 11 have internal motors and five have N-terminal motors. The latter includes KCA1 and KCA2. Direction of movement has not been tested for these motors yet, but all contain a neck sequence typical for minus-end directed motors (Reddy and Day, 2001). This neck domain is located N-terminal to the motor domain and contains the conserved GN residues at the neck/motor core junction (Endow and Waligora, 1998), suggesting that they move towards the minus-end of MTs. Interestingly, at least one coiled coil domain precedes the motor domain in 7 out of 11 internal and in 3 out of 5 N-

terminal positioned motors of the C-terminal subfamily. This N-terminal placed coiled coil might be implicated in the motility of minus-end directed motors. Plus-end directed kinesins do not contain a coiled coil N-terminally to the motor domain. Therefore it is possible that this coiled coil in combination with the neck domain functions as the stalk/neck of minus-end directed motors, which is essential for minus-end directed movement (Endow and Waligora, 1998). Another peculiarity in the KCA1 and KCA2 sequence is a divergence from other kinesins in the nucleotide flanking site, switch I (respectively FNVTH and STVTH instead of SSRSH). The switch I site communicates the nucleotide state to the motor domain, and thus translates the chemical energy of ATP into mechanical energy, which is essential for kinesin movement (Klumpp et al., 2003). It is thus possible that the KCA proteins cannot transfer the ATP hydrolysis status to the motor domain with the consequence that they will never take a walk. From this point of view, KCA might act more as an anchor protein than as a motor protein.

During cytokinesis, KCBP, KCA1 and KCA2 (data not shown) localize to the phragmoplast. In contrast to KCBP, which associates to the phragmoplast MTs, KCA labeled the phragmoplast midline and expansion of GFP-KCA1 signal followed the leading edges of the phragmoplast MTs. Several plant kinesins have been shown to localize at the phragmoplast midline during cytokinesis (Lee and Liu, 2000; Lee et al., 2001; Nishihama et al., 2002; Pan et al., 2004). These motors were proposed to function in the organization and dynamics of phragmoplast MTs or the delivery of membrane material to the midline. Unlike these motors, KCA1 remains associated with the cell plate where MTs have depolymerized, suggesting a different function for KCA during cytokinesis.

In plants and animals, motor proteins drive the transport of a wide variety of organelles and vesicular cargoes (Goldstein and Yang, 2000; Lee and Liu, 2004). However, this is the first report on the localization of a kinesin at the plasma membrane. Immunogold labeling with an antibody directed against the stalk domain of KCA confirmed the association of KCA to the cell plate and plasma membrane. GFP-KCA1 accumulation at the plasma membrane or cell plate does not involve the MT binding motor domain. On the other hand, the stalk domain of KCA1 was essential to plasma membrane association and the N-terminal tail was a prerequisite for label at the cell plate. These domains are implicated in respectively dimerization and folding of the KCA proteins, suggesting that different folding conformations determine the localization of KCA. When GFP was fused to the C-terminus of KCA1, yet another subcellular localization was revealed, showing accumulation at the ER. EM images however did not affirm an enrichment of endogenous KCA protein at these membranes. Possibly, the presence of GFP at the C-terminus of KCA interfered with the correct folding of KCA, resulting in mistargeting of the protein. Because GFP-KCA1 travels to the cell plate on Golgi-derived vesicles, it could also be that KCA1 is loaded onto ER membranes for its distribution, and that the C-terminal KCA1-GFP fusion is hindered in its path to move to the Golgi, resulting in accumulation at the ER. Upon deletion of a small C-terminal part of the KCA1 tail domain, cell plate and plasma membrane localization was lost, suggesting that this part of KCA1 contains sequences essential for membrane association. Signal peptides for secretion were absent from the C terminus or elsewhere in the protein. Moreover, there are no transmembrane regions,

suggesting that KCA1 is a soluble protein. Membrane association is therefore likely to occur indirectly via other proteins.

Based on transcriptional levels throughout the cell cycle, KCA and KCBP were not recognized as mitotic motors (chapter 2). Indeed, disruption of the KCBP gene results in aberrant trichome morphogenesis, which is attributed to defects in MT organization in trichomes (Oppenheimer et al., 1997; Mathur and Chua, 2000). However, KCBP protein accumulates during mitosis, suggesting an additional role for KCBP in cell division (Bowser and Reddy, 1997). KCBP localizes to the mitotic spindle and microinjection experiments suggest that KCBP functions in spindle pole formation during nuclear envelope breakdown and anaphase (Vos et al., 2000). KCA protein levels have not been studied throughout cell cycle. KCA mRNA is present throughout the cell cycle and in all plant organs (Chapter 3). Immunofluorescence located the KCA proteins both in meristematic tissues and in young and mature leaves (Kong and Hanley-Bowdoin, 2002), suggesting that the KCA proteins play a role in both interphase and mitosis. This is also supported by several observations within this study. Firstly, KCA interacts with the cell cycle dependent kinase CDKA;1. KCA1 and KCA2 share two CDKA;1 phosphorylation sites in the N-terminal portion of the tail domain and CDK dependent phosphorylation has been demonstrated within insect cells (Kong and Hanley-Bowdoin, 2002). In addition, mutagenesis and inhibitor studies pointed to a role for CDKA;1 phosphorylation in the conformational changes of the KCA molecules. Phosphorylation prevented tail folding and favored the accumulation of KCA dimers, suggesting that CDKA;1 phosphorylation drives KCA dimerization, that is known to trigger MT mobility of certain kinesins (chapter 3).

Secondly, at the start of mitosis, GFP-KCA1 fluorescence accumulated at the plasma membrane and simultaneously a region depleted of GFP-KCA1 fluorescence (KDZ) was formed at the division site (chapter 4). This suggests that localization of GFP-KCA1 is dependent on mitosis specific signals. Later, during cytokinesis, KCA1 accumulated at the forming cell plate. Localization at the cell plate and plasma membrane and the formation of a KDZ was also observed for KCA2 (data not shown). Thirdly, different peptide domains of KCA1 were responsible for cell plate targeting and KDZ formation, suggesting that two separate targeting mechanisms control the localization of the KCA1 protein. The dimerization domain was a prerequisite for the accumulation of the protein at the plasma membrane and the complete tail domain has been shown to be involved in cell plate targeting. Two hybrid assays indicated that the tail domain could fold onto itself and that CDKA;1 was unable to bind to the tail domain as a separate unit. Therefore, it is conceivable that CDKA;1 only binds unfolded KCA and that subsequent phosphorylation prevents tail folding and allows KCA dimerization. At the start of mitosis, this would lead to different conformations of KCA molecules that result in different intracellular localizations with distinct purposes. Phosphorylation mutants of KCA1 are under construction to determine whether CDK phosphorylation is required for the accumulation of KCA1 molecules at the plasma membrane during cell division.

KCA1 has been identified in two hybrid assays as an interactor of CDKA;1 (De Veylder, 1997), the geminivirus protein AL1 (Kong and Hanley-Bowdoin, 2002), the MT severing katanin AtKSS

(Bouquin et al., 2003), the trehalose-6-phosphate synthase AtTPS1 (chapter 4) and a tropomyosin and myosin-like protein (Torres Acosta, De Veylder and Inzé, unpublished data).

Geminiviruses are a group of DNA viruses that rely on host factors to support their replication. Because they infect terminally differentiated cells, they first have to induce their plant hosts to express the replication machinery. The viral protein AL1 is essential for viral DNA replication and interacts with the retinoblastoma host protein RBR1 in plants (Kong et al., 2000). This disrupts E2F/RBR1 regulation, allowing G1/S transition (Egelkrout et al., 2001). As a consequence viral and chromosomal DNA are replicated, but cells do not proceed to complete mitosis (Nagar et al., 1995). The premature inhibition of mitosis is somewhat reminiscent to endoreduplication, the onset of which is correlated with the inhibition of M-phase-associated CDK activity (Grafi and Larkins, 1995; Joubes et al., 1999). In light of the interaction between AL1 and KCA1, the following model is proposed (Fig. 7.1A). During virus infection, AL1 interacts with RBR1, thereby allowing E2F to drive G1/S transition and replication of viral and chromosomal DNA (Egelkrout et al., 2001). Cells pass through S phase, but are arrested in early prophase. Perhaps AL1 binds KCA1, thereby preventing

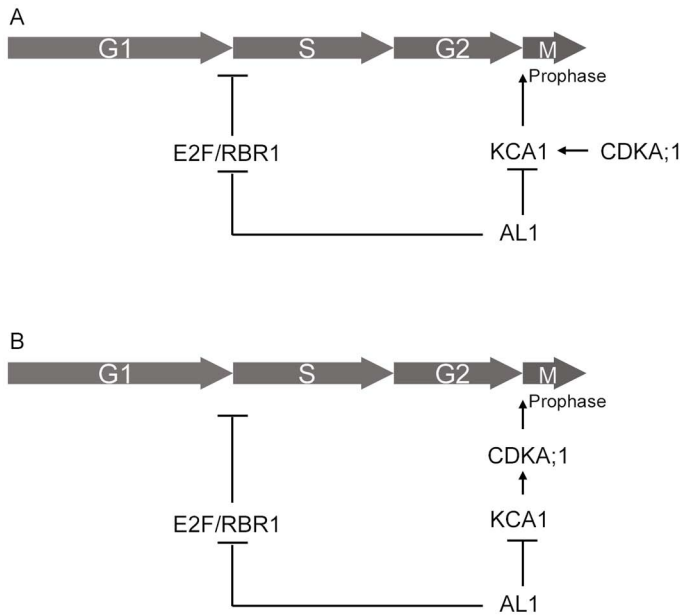


Figure 7.1 Putative model for KCA1 action upon geminivirus infection. A, Upon geminivirus infection, AL1 interacts with RBR1. This allows E2F to drive G1/S transition and infected cells to enter S-phase, resulting in the replication of viral and chromosomal DNA. AL1 also binds KCA1. This interaction could prevent CDKA;1 phosphorylation of KCA1, which might prevent KCA1 molecules to accumulate at the plasma membrane. If KCA1 would be involved in the reorganization of the cytoskeleton at the start of mitosis, binding of AL1 to KCA1 prevents cells to reorganize their cytoskeleton. B, Alternatively, if the action of KCA1 were to stimulate M-phase associated CDKA;1 activity, then AL1 may block the CDK mitotic checkpoint by binding KCA1 and preventing KCA1 from activating M-phase associated CDKA;1 activity.

its phosphorylation by CDKA;1. Progression throughout mitosis requires the reorganization of the cytoskeleton into different MT arrays. The binding of AL1 and block of CDK phosphorylation of KCA1 might prevent KCA1 molecules to accumulate at the plasma membrane. As a result, cortical MTs are not reorganized into mitotic arrays upon virus infection. It is therefore worthwhile investigating whether KCA1 still accumulates at the plasma membrane in infected cells that have re-entered the cell cycle. In an alternative scenario, the AL1 protein may control the progression through cell cycle by preventing M-phase associated CDKA;1 activation (Fig. 7.1B). If the action of KCA1 were to stimulate CDKA;1 activity, than its association with AL1 may block the mitotic progression. This mechanism would place KCA1 upstream of the CDK mitotic checkpoint. Progression of cytokinesis is controlled by a similar mechanism, involving the kinesin NACK1. NACK1 targets a MAPK signaling cascade to the phragmoplast, which is required for expansion of the cell plate (Nishihama et al., 2002). As virus infection had no apparent effect on KCA1 protein level in mature Arabidopsis leaves, the function of KCA1 is most likely not restricted to viral infected cells (Kong and Hanley-Bowdoin, 2002).

A function for KCA1 to control mitosis has also been suggested in chapter 5. Here, a protein complex was proposed consisting of AtTPS1, KCA1, CDKA;1 and tubulin. This interaction may provide a link between sugar availability and control over cell division. Tubulin was immunopurified with AtTPS1 antibody from plant extracts, suggesting a link with the MT cytoskeleton. CDKA;1 binds MTs both during interphase and mitosis (Stals et al., 1997; Hemsley et al., 2001; Weingartner et al., 2001). Thus, control of carbon availability over cell division with regards to the proposed protein complex, is likely to occur at the level of MT organization. Colocalisation experiments of AtTPS1 and KCA1 suggested that the largest overlap in distribution occurs at prophase, when AtTPS1 and KCA1 mainly reside in the cytoplasm. Thus, when sufficient carbon sources support the process of cell division, AtTPS1 might direct CDKA;1-activated KCA1 to the cell cortex to induce reorganization of the cortical MTs, which is required to support successful mitosis. On the other hand, AtTPS1 is a stress molecule and might be activated when carbon sources are insufficient. It then prevents cells from entering the cell division by interaction with CDKA;1 and KCA1. This model is opposite to the former hypothesis and experimental data should be gathered to gain further insight in this issue. Probably, the interaction between AtTPS1 and KCA1 is restricted to the beginning of cell division as KCA1 but not AtTPS1 accumulates at the plasma membrane and cell plate during M-phase progression.

During the course of mitosis, GFP-KCA1 accumulated at the plasma membrane and simultaneously, a region depleted of GFP-KCA1 appeared at the division site, consequently termed the KDZ (KCA depleted zone). Later, during cytokinesis GFP-KCA1 was associated to the entire length of the cell plate, which was guided towards the KDZ. This localization pattern was also observed for KCA2 (data not shown). The data suggests a function for KCA in cell plate guidance. During mitosis, actin filaments remain present at the cell cortex during mitosis except at the division site (Cleary et al., 1992). At the cell plate, actin filaments parallel the organization of the phragmoplast MTs. During expansion, they remain associated with the central parts of the cell plate where MTs have

depolymerized. Thus, the distribution of KCA during cytokinesis resembles that of actin filaments. However, actin depolymerizing drugs did not alter the association of KCA1 at the plasma membrane or cell plate. Yeast two hybrid experiments revealed an interaction of the tail domain of KCA1 and KCA2 with a tropomyosin and a myosin-like protein (Torres Acosta, De Veylder and Inzé, unpublished data). The myosin-like protein does not contain a myosin motor domain but could be a subunit of a myosin complex or function as an actin binding protein. Therefore, KCA could act as an anchor protein between myosin-actin complexes and membranes of the cell plate and plasma membrane. In other words, KCA operates as a template for the localization of actin filaments along the cell cortex and cell plate during cell division (Fig. 7.2). It has been hypothesized that actin filaments link the cell plate edges with the cell cortex and guide the cell plate towards the plasma membrane. KCA1 is absent from the division site, allowing actin filaments to create a balance of pulling forces that guides the cell plate towards the division site (Wick, 1991; Smith, 1999; Sylvester, 2000). The necessity for a KDZ in cell plate guidance was supported by drug application. The MT depolymerizing drug propyzamide occasionally prevented the formation of the KDZ, which resulted in misguidance of the cell plate. As KCA might function as an anchor for actin filament distribution during cell division, it might be interesting to look at actin filaments in dividing cells of plants that do not contain the KCA proteins.

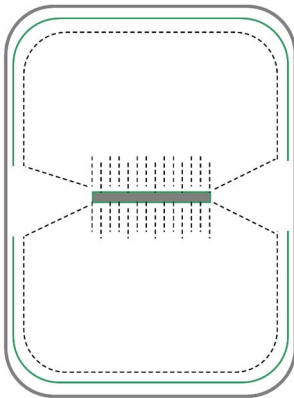


Figure 7.2 Model for KCA1 as a scaffold for actin filament organization during cell division.

The sketch represents a plant cell in cytokinesis with a cell plate at the centre of the cell. GFP-KCA1 (green) is located along the cell plate and at the plasma membrane and serves as a template for the distribution of actin filaments (dotted lines) along these membranes. At the plasma membrane, KCA1 is absent from the division site. As a result, actin filaments are depleted from this region too (ADZ). At the rim of the actin depleted zone, actin filaments dive into the cytoplasm and connect with the leading edges of the expanding cell plate. During cell plate expansion, a balance of actin pulling forces from either side of the division site leads to guidance of the cell plate to the division site.

The requirement of PPB MTs to create the KDZ provides a clear link with the MT cytoskeleton. Despite the intrinsic capacity of the KCA1 protein to bind MTs, neither the GFP tagged full-length or immunolocalization provided evidence for the association of KCA with the MT cytoskeleton. The

motor domain as a separate GFP fusion did label MTs in BY-2 cells. Deletion of a small C-terminal sequence from the full-length KCA1 protein prevented membrane association, but did not allow MT binding. This indicates that membrane association does not inhibit MT binding and that conformational changes of the stalk and tail domain would be required for MT association.

Finally, an interaction of KCA1 with the katanin P60 subunit AtKSS has been reported (Bouquin et al., 2003). Katanins form a family of MAPs that regulate MT dynamics and organization by MT severing. In animal cells, they consist of a catalytic p60 subunit that binds and severs MTs and a regulatory p80 subunit (Sedbrook et al., 2004). Both subunits are present in Arabidopsis and MT severing has been demonstrated *in vitro* for AtKSS (Stoppin-Mellet et al., 2002). Arabidopsis mutants have been characterized that carry mutations in the *AtKSS* gene; *leu1*, *botero1*, *ectopic root hair 3 (erh3)* and *fragile fiber 2 (fraz)* (Bichet et al., 2001; Burk et al., 2001; Webb et al., 2002; Bouquin et al., 2003). AtKSS mutants exhibit a delayed transition of cortical MTs in a transverse orientation in cells that exit mitosis. In accordance, cell elongation is impaired resulting in isotropic cell growth, shorter and thicker organs and smaller plants. In animal cells, katanin is responsible for the majority of M-phase severing activity (McNally and Thomas, 1998). In addition, MT-severing is activated by cyclin B/CDK during M-phase, although katanin itself is not directly activated by cyclinB/cdc2 (McNally and Thomas, 1998). In Arabidopsis, evidence that katanin is controlled by CDKA;1 is missing. However, CDKA;1 interacts with KCA1 and phosphorylation induces conformational changes that favor the dimeric form of KCA1 over the monomeric form. As KCA1 binds AtKSS, the latter might be indirectly controlled by CDKA;1. At the onset of mitosis, KCA1 accumulates at the plasma membrane. Both CDKA;1 and AtKSS associate with the cortical MTs (Hemsley et al., 2001; Bouquin et al., 2003). In addition AtKSS and KCA1 are absent from the PPB and the KDZ is formed during PPB formation (McClinton et al., 2001). To situate the relationship between KCA1 and AtKSS, we propose the following model. At the onset of mitosis, CDKA;1 phosphorylates KCA1, resulting in the accumulation of KCA1 dimers. These gather at the plasma membrane and direct the katanin AtKSS to the cortical MTs resulting in controlled MT severing and breakdown of the cortical array. KCA1 may therefore acts as a scaffold for proteins that accumulate at the cortex. As KCA1 accumulates at the cortex during the G2/M transition, katanin mutants could be delayed in the reorganization of MTs at the start of mitosis. As a result, katanin mutants would show reduced growth, that at least in part accounts for their smaller growth phenotype.

After cell division, AtKSS mutants exhibit a delayed transition of cortical MTs in a transverse orientation in elongating cells. At this time, CDKA;1 activity is inhibited and less dimeric KCA1 molecules accumulate at the plasma membrane. Instead of driving depolymerization of cortical MTs, KCA1 might function in the organization of cortical MTs into a transverse array. Acting as a sensor between the cell wall microfibrils and the cortical MTs, KCA1 could direct AtKSS towards MTs that are not co-aligned with transverse microfibers in the cell wall. In this way, the KCA1-AtKSS complex contributes to the transverse alignment of cortical MTs leading to cell elongation.

In conclusion, it appears that KCA interacts with several proteins through the stalk domain and N-terminal part of the tail domain (Fig. 7.3). These domains are proposed to be involved in

dimerization and folding. The fact that several proteins can independently bind to this central part of KCA, together with the differential subcellular localization and the different folding conformations of KCA, suggest that different regulatory pathways converge onto KCA1 and that this protein therefore may operate as a landing site for mitosis-related processes.

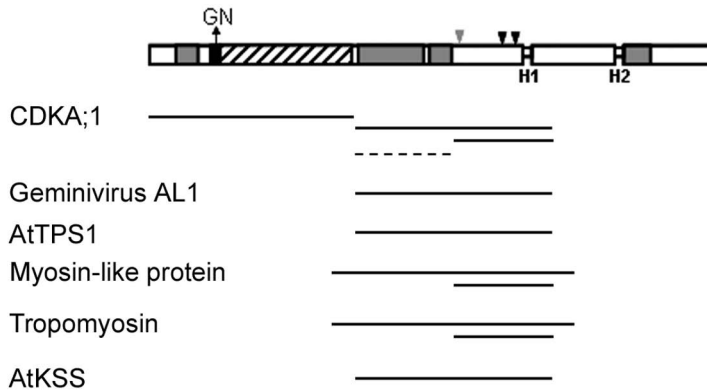


Figure 7.3 Interaction of KCA1 with its binding partners. Secondary structure and domain organization of KCA1. Neck with conserved GN motif for putative minus-end directed motility; black box, motor domain; dashed box, coiled coils; grey boxes, conserved CDKA;1 phosphorylation sites; black arrowheads and hinge regions, H1 and H2. KCA1 interacts with several proteins that bind to the central part of the KCA1 protein consisting of the dimerization domain and the N-terminal tail domain. Bars indicate the site of interaction with KCA1. Interaction with CDKA;1 was also tested for the stalk domain of KCA2 as a separate unit (dotted bar).

References

- Bichet A, Desnos T, Turner S, Grandjean O, Hofte H** (2001) BOTERO1 is required for normal orientation of cortical microtubules and anisotropic cell expansion in Arabidopsis. *Plant J* **25**: 137-148
- Bouquin T, Mattsson O, Naested H, Foster R, Mundy J** (2003) The Arabidopsis lue1 mutant defines a katanin p60 ortholog involved in hormonal control of microtubule orientation during cell growth. *J Cell Sci* **116**: 791-801
- Bowser J, Reddy AS** (1997) Localization of a kinesin-like calmodulin-binding protein in dividing cells of Arabidopsis and tobacco. *Plant J* **12**: 1429-1437
- Burk DH, Liu B, Zhong R, Morrison WH, Ye ZH** (2001) A katanin-like protein regulates normal cell wall biosynthesis and cell elongation. *Plant Cell* **13**: 807-827
- Cleary AL, Gunning BES, Wasteneys GO, Hepler PK** (1992) Microtubule and F-Actin Dynamics at the Division Site in Living Tradescantia Stamen Hair-Cells. *Journal of Cell Science* **103**: 977-988
- Dagenbach EM, Endow SA** (2004) A new kinesin tree. *Journal of Cell Science* **117**: 3-7
- Dagenbach EM, Endow SA** (2004) A new kinesin tree. *J Cell Sci* **117**: 3-7
- De Veylder L, Segers G, Glab N, Van Montagu M, Inzé D** (1997) Identification of proteins interacting with the Arabidopsis Cdc2aAt protein. *J Exp Bot* **48**: 2113-2114
- Egelkrout EM, Robertson D, Hanley-Bowdoin L** (2001) Proliferating cell nuclear antigen transcription is repressed through an E2F consensus element and activated by geminivirus infection in mature leaves. *Plant Cell* **13**: 1437-1452
- Endow SA, Waligora KW** (1998) Determinants of kinesin motor polarity. *Science* **281**: 1200-1202
- Goldstein LS, Yang Z** (2000) Microtubule-based transport systems in neurons: the roles of kinesins and dyneins. *Annu Rev Neurosci* **23**: 39-71
- Graf G, Larkins BA** (1995) Endoreduplication in Maize Endosperm - Involvement of M-Phase-Promoting Factor Inhibition and Induction of S-Phase-Related Kinases. *Science* **269**: 1262-1264
- Hemsley R, McCutcheon S, Doonan J, Lloyd C** (2001) P34(cdc2) kinase is associated with cortical microtubules from higher plant protoplasts. *FEBS Lett* **508**: 157-161
- Joubes J, Phan TH, Just D, Rothan C, Bergounioux C, Raymond P, Chevalier C** (1999) Molecular and biochemical characterization of the involvement of cyclin-dependent kinase A during the early development of tomato fruit. *Plant Physiology* **121**: 857-869
- Klump LM, Mackey AT, Farrell CM, Rosenberg JM, Gilbert SP** (2003) A kinesin switch I arginine to lysine mutation rescues microtubule function. *J Biol Chem* **278**: 39059-39067
- Kong LJ, Hanley-Bowdoin L** (2002) A geminivirus replication protein interacts with a protein kinase and a motor protein that display different expression patterns during plant development and infection. *Plant Cell* **14**: 1817-1832
- Kong LJ, Orozco BM, Roe JL, Nagar S, Ou S, Feiler HS, Durfee T, Miller AB, Grissem W, Robertson D, Hanley-Bowdoin L** (2000) A geminivirus replication protein interacts with the retinoblastoma protein through a novel domain to determine symptoms and tissue specificity of infection in plants. *Embo Journal* **19**: 3485-3495
- Lee YR, Giang HM, Liu B** (2001) A novel plant kinesin-related protein specifically associates with the phragmoplast organelles. *Plant Cell* **13**: 2427-2439
- Lee YR, Liu B** (2000) Identification of a phragmoplast-associated kinesin-related protein in higher plants. *Curr Biol* **10**: 797-800
- Lee YR, Liu B** (2004) Cytoskeletal motors in Arabidopsis. Sixty-one kinesins and seventeen myosins. *Plant Physiol* **136**: 3877-3883
- Mathur J, Chua NH** (2000) Microtubule stabilization leads to growth reorientation in Arabidopsis trichomes. *Plant Cell* **12**: 465-477
- McClinton RS, Chandler JS, Callis J** (2001) cDNA isolation, characterization, and protein intracellular localization of a katanin-like p60 subunit from Arabidopsis thaliana. *Protoplasma* **216**: 181-190
- McNally FJ, Thomas S** (1998) Katanin is responsible for the M-phase microtubule-severing activity in *Xenopus* eggs. *Mol Biol Cell* **9**: 1847-1861
- Moore JD, Endow SA** (1996) Kinesin proteins: A phylum of motors for microtubule-based motility. *Bioessays* **18**: 207-219

- Nagar S, Pedersen TJ, Carrick KM, Hanleybowdoin L, Robertson D** (1995) A Geminivirus Induces Expression of a Host DNA-Synthesis Protein in Terminally Differentiated Plant-Cells. *Plant Cell* **7**: 705-719
- Nishihama R, Soyano T, Ishikawa M, Araki S, Tanaka H, Asada T, Irie K, Ito M, Terada M, Banno H, Yamazaki Y, Machida Y** (2002) Expansion of the cell plate in plant cytokinesis requires a kinesin-like protein/MAPKKK complex. *Cell* **109**: 87-99
- Oppenheimer DG, Pollock MA, Vacik J, Szymanski DB, Ericson B, Feldmann K, Marks MD** (1997) Essential role of a kinesin-like protein in Arabidopsis trichome morphogenesis. *Proc Natl Acad Sci U S A* **94**: 6261-6266
- Pan R, Lee YR, Liu B** (2004) Localization of two homologous Arabidopsis kinesin-related proteins in the phragmoplast. *Planta* **220**: 156-164
- Reddy AS, Day IS** (2001) Kinesins in the Arabidopsis genome: a comparative analysis among eukaryotes. *BMC Genomics* **2**: 2
- Reddy VS, Reddy AS** (1999) A plant calmodulin-binding motor is part kinesin and part myosin. *Bioinformatics* **15**: 1055-1057
- Sedbrook JC, Ehrhardt DW, Fisher SE, Scheible WR, Somerville CR** (2004) The Arabidopsis sku6/spiral1 gene encodes a plus end-localized microtubule-interacting protein involved in directional cell expansion. *Plant Cell* **16**: 1506-1520
- Smith LG** (1999) Divide and conquer: cytokinesis in plant cells. *Curr Opin Plant Biol* **2**: 447-453
- Song H, Golovkin M, Reddy ASN, Endow SA** (1997) In vitro motility of AtKCBP, a calmodulin-binding kinesin protein of Arabidopsis. *Proceedings of the National Academy of Sciences of the United States of America* **94**: 322-327
- Stals H, Bauwens S, Traas J, Van Montagu M, Engler G, Inze D** (1997) Plant CDC2 is not only targeted to the pre-prophase band, but also co-localizes with the spindle, phragmoplast, and chromosomes. *FEBS Lett* **418**: 229-234
- Stoppin-Mellet V, Gaillard J, Vantard M** (2002) Functional evidence for in vitro microtubule severing by the plant katanin homologue. *Biochem J* **365**: 337-342
- Sylvester AW** (2000) Division decisions and the spatial regulation of cytokinesis. *Curr Opin Plant Biol* **3**: 58-66
- Vos JW, Safadi F, Reddy AS, Hepler PK** (2000) The kinesin-like calmodulin binding protein is differentially involved in cell division. *Plant Cell* **12**: 979-990
- Webb M, Jouannic S, Foreman J, Linstead P, Dolan L** (2002) Cell specification in the Arabidopsis root epidermis requires the activity of ECTOPIC ROOT HAIR 3--a katanin-p60 protein. *Development* **129**: 123-131
- Weingartner M, Binarova P, Drykova D, Schweighofer A, David JP, Heberle-Bors E, Doonan J, Bogre L** (2001) Dynamic recruitment of Cdc2 to specific microtubule structures during mitosis. *Plant Cell* **13**: 1929-1943
- Wick SM** (1991) Spatial aspects of cytokinesis in plant cells. *Curr Opin Cell Biol* **3**: 253-260



**Summary/
Samenvatting**

Chapter page: Leaf epidermal cells of an *Arabidopsis thaliana* seedling expressing GFP fused to a peroxisomal targeting signal. Cells were stained with FM4-64 and imaged using confocal microscopy (GFP/RFP filter settings). In the centre of the picture are two stomatal cells.

Summary

Plant cells are encased by a rigid cell wall that provides mechanical support for each cell and the whole plant body. It also renders plant cells immobile and this fixed nature of plant cells requires that morphological and developmental diversity in plants is determined by the strict regulation of the division plane alignment and the direction of cell expansion. The microtubule (MT) cytoskeleton organizes into various arrays to govern these processes. MT-associated proteins (MAP) associate with MTs and cooperate to organize them into different structures throughout the cell cycle.

During cell division, plant cells make unique MT structures such as the preprophase band (PPB) and the phragmoplast that contribute to aspects of division orientation and cytokinesis. MAPs play an important role in regulating MT behavior to establish these plant specific MT arrays. In **Chapter 2**, we searched for kinesins in the Arabidopsis genome that are cell cycle controlled. In the publicly available Affymetrix microarray data of synchronized Arabidopsis tissue culture cells (Menges et al., 2003), 22 kinesin genes were found that show increased expression during mitosis (Table 2.1). The presence of putative phosphorylation sites, protein degradation boxes and regulatory promoter elements support a function for these motors in cell division. A comparison between kinesins from plants, animal, yeast and fungi kinesins suggests that functions for kinesins in establishing spindle bipolarity are conserved between eukaryotes. Some homologues of animal kinesins that function in chromosome movement play unrelated roles in plant cells and appear to be involved in processes during interphase. The highest number of mitotic kinesins belongs to the C-terminal subfamily. Because C-terminal kinesins typically show minus-end directed movement, one can assume that some of their functions relate to that of dyneins for which no homologues are found in plants (Lawrence et al., 2001). Also, plants lack centrosomes at spindle poles where MT minus-ends congregate and therefore may require specially adapted kinesins. Finally, nine kinesins that are transcriptionally up-regulated during mitosis may be plant specific. Some of these were shown to function in phragmoplast dynamics during cytokinesis. The analysis of uncharacterized plant specific kinesins with a mitotic expression profile may shed light on the function of motor proteins in PPB formation, a structure that is not very well understood.

Cyclin-dependent kinases (CDKs) control cell cycle progression through timely coordinated phosphorylation events. CDKA;1 associates with MTs both in dividing and interphase cells and regulates MT organization by phosphorylation of MT-associated proteins (Stals et al., 1997; Cassimeris, 1999; Andersen, 2000; Hemsley et al., 2001; Weingartner et al., 2001). Two kinesins that interact with CDKA;1 were previously identified (De Veylder et al., 1997) and were designated KCA1 and KCA2. These kinesins were chosen for this study because they carry a potential phosphorylation site, interact with CDKA;1 and are plant specific, suggesting that they function in MT processes during plant cell division. The KCA kinesins are classified into the C-terminal/Kinesin-14 subfamily and carry a typical neck sequence for minus-end directed kinesins. The KCA proteins are 81% identical and have a similar three-partite domain organization, consisting of a motor, stalk and tail domain. A green fluorescent protein (GFP) fusion of the N-terminal domain of KCA1 containing the N-

Summary

terminal motor domain decorated MTs in BY-2 cells, demonstrating MT-binding activity (**chapter 3**). During cytokinesis the full-length GFP-fusion protein accumulated at the midline of cylindrical and ring-like phragmoplasts. Two-hybrid analysis and co-immunoprecipitation experiments showed that coiled-coil structures of the central stalk were responsible for homo- and heterodimerization of KCA1 and KCA2. By Western blot analysis, high molecular weight KCA molecules were detected in extracts from BY-2 cells overproducing the full-length GFP fusion. Treatment of these cultures with the phosphatase inhibitor vanadate caused an accumulation of these KCA molecules. In addition to dimerization, interactions within the C-terminally located tail domain were revealed, indicating that the tail could fold onto itself. The tail domains of KCA1 and KCA2 contained two adjacent putative CDKA;1 phosphorylation sites one of which is conserved in KCA homologues from other plant species. Site-directed mutagenesis of the conserved phosphorylation sites in KCA1 resulted in a reduced binding to CDKA;1 and abolished intramolecular tail interactions. The data highlight that phosphorylation of the CDKA;1 site provokes a conformational change in the structure of KCA with implications in folding and dimerization.

Using GFP-KCA1 markers, we found remarkable localization patterns that support the complexity of KCA protein configurations. First (chapter 3), we demonstrated that the kinesin KCA1 associates with the developing cell plate at the midline of the phragmoplast in BY-2 cells. In addition, KCA1 was targeted to the plasma membrane (**chapter 4**). Cell plate and plasma membrane accumulation was independent of the MT-binding motor domain. In contrast, this domain, fused to GFP labeled MTs in BY-2 cells, suggesting that the conformation of the full length GFP-KCA1 prevented MT association. The KCA1 stalk and tail domains were required for respectively plasma membrane and cell plate targeting. Thus two separate targeting mechanisms seem to control the localization of the KCA1 protein. As these domains are implicated in respectively dimerization and folding of the KCA proteins, localization of GFP-KCA1 to the different subcellular compartments likely involves different conformations of the KCA proteins. Brefeldin A prevented association to both the cell plate and the plasma membrane, indicating that a Golgi derived vesicle traffic route was required. The same result was obtained when a small C-terminal part of KCA1 was deleted, suggesting that this domain is essential for membrane association.

Surrounded by a rigid cell wall plant cells are stationary and require a strict regulation of the division plane to control the direction of growth and the spatial organization of their organs (Traas et al., 1995). The underlying mechanisms of division plane establishment are poorly understood (Smith, 1999). Using GFP-KCA1, we demonstrate in **chapter 4** that a region within the plasma membrane predicts the division site before cytokinesis. At the onset of mitosis, GFP-KCA1 associated fluorescence increased at the plasma membrane. Simultaneously, a region depleted in GFP-KCA1 fluorescence appeared at the plasma membrane corresponding to the site of the PPB. We designated this plasma membrane domain the KCA1 depleted zone or KDZ. Throughout mitosis, the KDZ marked the division site and served as guide for phragmoplast and cell plate expansion. The KDZ was formed at preprophase and this required the presence of PPB MTs. However, later during mitosis, MTs or actin filaments did not support the preservation of the KDZ at the plasma

membrane. The KDZ was further characterized by the appearance of strong connections between the cell wall and plasma membrane upon plasmolysis. In conclusion, the data show that KCA1 reveals a subdomain of the plasma membrane that defines the division site in plant cells.

Kinesin motor proteins often associate with kinesin light chains, kinesin associated proteins (KAP), regulatory proteins and other proteins, to regulate their activity and cargo binding (Reilein et al., 2001). Using trehalose-6-phosphate synthase AtTPS1 as bait in yeast two hybrid experiments, KCA1 was identified (**chapter 5**). AtTPS1 catalyzes the first step of trehalose formation from UDP-glucose and is involved in the regulation of the sugar metabolism. Plants produce low levels of trehalose (Vogel et al., 2001), suggesting that AtTPS1 is likely to play a regulatory role. Indeed, knocking out the AtTPS1 gene in Arabidopsis causes an embryo lethal phenotype and demonstrates the importance for trehalose in plant development (Eastmond et al., 2002). AtTPS1 forms a protein complex in yeast of a 600-800 kDa particle in FPLC separated extracts. We found evidence that a complex is also formed in Arabidopsis, albeit that the contributing components may be different. The Arabidopsis AtTPS1 co-migrated with the cell cycle kinase CDKA;1 and tubulin. In two hybrid experiments, AtTPS1 interacted with CDKA;1 and the CDKA;1 interacting protein KCA1. The AtTPS1 domain responsible for the interaction with KCA1 and CDKA;1 was mapped to an N-terminal extension of the AtTPS1 protein that controls the trehalose synthase enzymatic activity. AtTPS1 co-precipitated with CDKA;1 affinity beads indicating that it is part of a protein complex that contains KCA1 and tubulin. The data presented in this chapter provided the first physical link between control of cell division and sugar metabolism.

KCA1 interacts with AtTPS1 (Chapter 5) and the katanin p60 subunit AtKSS (Bouquin et al., 2003), two genes that are implicated in development and morphology of Arabidopsis. To study the function of KCA in plant growth, plants were identified that carried a T-DNA insertion within intron 10 of *KCA1* and exon 1 of *KCA2* (**Chapter 6**). Molecular characterization of the mutant alleles showed that *KCA2* transcript was absent from the mutant plants. Despite of the T-DNA insertion in *KCA1* mutants, *KCA1* transcripts of both full length size and a shorter fragment were detected. Western blotting using an antibody that recognizes both KCA1 and KCA2, revealed the absence of KCA proteins in double mutants, but not in single insertion mutants. KCA mutants were phenotypically characterized and compared to plants mutated in the genes that encode for the KCA1 interaction partners AtKSS and AtTPS1. Processes related to cell division and cell expansion were not perturbed in the *kca* mutants under the conditions tested. It is possible that the T-DNA insertion in the KCA1 gene is not a knock out and that functional KCA1 protein is still produced. Alternatively, other kinesins or parallel mechanisms can take over KCA activity. It is also possible that phenotypes were too subtle and growth conditions not apt to uncover phenotypic aberrations.

Samenvatting

Plantencellen zijn omgeven door een stevige celwand die mechanische ondersteuning biedt aan elke cel en aan de plant in zijn geheel. Het maakt dat plantencellen tevens onbeweeglijk zijn. De morfologie en de ontwikkeling van planten wordt bepaald door de stricte regulatie van het delingsvlak en de richting van expansie. Het microtubulair (MT) cytoskelet wordt georganiseerd in verschillende structuren om deze processen te coördineren. De organisatie van deze MT structuren vereist de samenwerking van MT geassocieerde proteïnen (MAP).

De unieke MT structuren die planten maken tijdens de celdeling zijn de preprophase band (PPB) en de fragmoplast. Ze dragen bij tot de orientatie van het celdelingsvlak en de cytokinese. MAPs spelen een belangrijke rol in de organisatie van deze plant specifieke MT structuren. **Hoofdstuk 2** beschrijft de zoektocht in het genoom van *Arabidopsis* naar kinesines die celcyclus gecontroleerd zijn. In de publiek beschikbare Affymetrix microarray data van gesynchroniseerde *Arabidopsis* cel culturen (Menges et al., 2003), werden 22 kinesines gevonden met een verhoogde expressie tijdens de mitose (Table 2.1). De aanwezigheid van mogelijke fosforylatieplaatsen, proteïne-degradatie boxen en regulatorische promoter elementen ondersteunt een functie voor deze motor proteïnen tijdens celdeling. Een vergelijking tussen kinesines van planten, dieren, gist en fungi veronderstelt dat functies voor kinesines in de opbouw van de bipolariteit van de spoelfiguur geconserveerd zijn bij eukaryoten. Sommige homologen van dierlijke kinesines, die betrokken zijn in chromosomale bewegingen tijdens de mitose, spelen klaarblijkelijk een andere rol tijdens de interfase in planten cellen. Het grootste aantal mitotische kinesines behoort tot de C-terminale subfamilie. Omdat dergelijke kinesines typisch naar het min-uiteinde van de MT bewegen, is het mogelijk dat sommige hiervan functies uitoefenen die gerelateerd zijn aan dat van dyneïnes, waarvan er geen homologen bestaan in *Arabidopsis* (Lawrence et al., 2001). Daarenboven zijn er in planten geen centrosomen. In dierlijke cellen verankeren de centrosomen de min-uiteinden van MT met de polen van de spoelfiguur en dus kunnen speciaal aangepaste kinesines een vervanging hiervoor vormen in planten. Negen kinesines, die transcriptioneel opgereguleerd zijn tijdens mitose, blijken specifiek te zijn voor planten. Voor sommige hiervan werd er een functie aangetoond in de dynamiek van de fragmoplast MT tijdens de cytokinese. De analyse van de tot nog toe ongekaracteriseerde plant specifieke kinesines met een mitotisch expressie profiel zou een tipje van de sluier kunnen oplichten in verband met de functie van motor proteïnen bij de vorming van de PPB.

Cycline-afhankelijke kinasen (CDK) controleren de progressie doorheen de celcyclus via gecoördineerde fosforylatie van doeleiwitten. CDKA;1 associeert met MT in delende en interfase cellen en reguleert de organisatie van MT door fosforylatie van MAPs, zoals kinesines (Stals et al., 1997; Cassimeris, 1999; Andersen, 2000; Hemsley et al., 2001; Weingartner et al., 2001). Twee kinesines die interageren met CDKA;1 werden voordien geïdentificeerd (De Veylder, 1997) en werden KCA1 en KCA2 genoemd. Deze kinesines werden gekozen voor deze studie omdat ze een potentiële fosforylatieplaats dragen, interageren met CDKA;1 en plant specifiek zijn, hetgeen veronderstelt dat ze betrokken zijn in de celdeling bij planten. De KCA kinesines behoren tot de C-

terminale/Kinesine-14 subfamilie en dragen een neksequentie die typisch voorkomt bij kinesines die naar het min-uiteinde bewegen. KCA1 en KCA2 zijn 81% identisch en hebben een gelijkaardige drie-delige domein organisatie, bestaande uit een motor-, steel- en staartdomein. Een proteïnefusie bestaande uit het groen fluorescerend proteïne (GFP) en het N-terminaal domein van KCA1, dat het N-terminale motor domein bevat, kleurde MT in BY-2 cellen, waardoor het MT bindend karakter van dit domein aangetoond werd (**hoofdstuk 3**). Tijdens de cytokinese accumuleerde het volledige KCA1 eiwit, gefusioneerd aan GFP (GFP-KCA1), ter hoogte van de middellijn van de cilindrische en ring-vormige fragmoplast. Twee-hybride analyse en co-immunoprecipitatie experimenten toonden aan dat coiled coils in het centraal gelegen steel domein verantwoordelijk zijn voor homo- of heterodimerizatie van KCA1 en KCA2. In western blots werden hoog moleculaire gewicht KCA moleculen gedetecteerd in BY-2 extracten die GFP-KCA1 bevatten. Behandeling van deze cellen met de fosfataseinhibitor vanadaat, veroorzaakte een accumulatie van deze KCA moleculen. Naast dimerizatie werden tevens interacties vastgesteld tussen onderdelen van het C-terminaal geplaatste staartdomein, hetgeen suggereert dat het staartdomein kan dichtvouwen. De staartdomeinen van KCA1 en KCA2 bevatten twee naast elkaar geplaatste potentiële CDKA₁ fosforylatieplaatsen, waarvan er één geconserveerd bij ander KCA homologen in andere plantensoorten. Plaats-gerichte mutagenese van de geconserveerde fosforylatieplaatsen KCA1 resulteerde in een verlaagde binding met CDKA₁ en verhinderde de intramoleculaire staartinteracties. De resultaten tonen dat fosforylatie van de CDKA₁ plaats een conformationele verandering teweegbrengt in de structuur van KCA met gevolgen voor de opvouwing en dimerizatie.

Aan de hand van GFP-KCA1 merkers werden opmerkelijke lokalisatiepatronen verkregen die de complexiteit van conformationele opvouwing van de KCA kinesines weerspiegelt. Voordien (**hoofdstuk 3**) werd aangetoond dat het kinesine KCA1 associëerde met de ontwikkelende celplaat ter hoogte van de middellijn van de fragmoplast in BY-2 cellen. Daarenboven lokalizeert KCA1 ook op de plasmamembraan (**hoofdstuk 4**). Celplaat en plasmamembraan accumulatie gebeurde onafhankelijk van het MT bindende motordomein. Dit motordomein, gefusioneerd aan GFP, kleurde MT in BY-2 cellen, hetgeen suggereert dat de opvouwing van het intacte KCA1 kinesine associatie met MT verhindert. De KCA1 steel- en staartdomeinen waren essentieel voor lokalizatie ter hoogte van de plasmamembraan en de celplaat respectievelijk. Dus twee verschillende mechanismen controleren de lokalizatie van de KCA proteïnen. Vermits deze domeinen betrokken zijn in respectievelijk de dimerizatie en opvouwing van KCA, weerspiegelt de lokalizatie van GFP-KCA1 ter hoogte van deze verschillende subcellulaire compartimenten waarschijnlijk de verschillende conformationele vouwingen van de KCA proteïnen. Brefeldine A verhinderde associatie met zowel de celplaat als de plasma membraan, hetgeen aanduidt dat KCA1 via een Golgi afhankelijke transportroute deze compartimenten bereikt. Hetzelfde resultaat werd verkregen wanneer een korte C-terminale sequentie werd verwijderd van de GFP-KCA1 fusie, wat aantoont dat deze sequentie essentieel is voor membraanassociatie.

Het immobiele karakter van planten cellen vereist een stricte regulatie van het celdelingsvlak om zo de groeirichting en ruimtelijke organisatie van de plant onderdelen te controleren (Traas et al.,

1995). De mechanismen die het celdelingsvlak bepalen zijn tot heden grotendeels ongekend (Smith, 1999). Aan de hand van GFP-KCA1 tonen we in **hoofdstuk 4** aan dat een regio binnen de plasmamembraan de delingszone voorspelt alvorens cytokinese aanvangt. Bij de aanvang van de mitose accumuleerde GFP-KCA1 ter hoogte van de plasmamembraan. Gelijktijdig werd een plasmamembraan regio, vrij van GFP-KCA1 fluorescentie, zichtbaar ter hoogte van de PPB. Dit domein werd de 'KCA1 depleted zone' of KDZ genoemd. Doorheen mitose duidde de KDZ de delingszone aan en opeerde als een leidraad voor fragmoplast- en celplaatexpansie. De KDZ werd gevormd tijdens preprofase en hiervoor was de aanwezigheid van PPB MT noodzakelijk. Later tijdens de mitose waren MT en actine filamenten niet essentieel voor het behoud van de KDZ in de plasmamembraan. Verder werd de KDZ nog gekarakteriseerd door een sterke hechting tussen de plasmamembraan en de celwand die zichtbaar werden na plasmolyse. Als conclusie kunnen we stellen dat KCA1 een subdomein van de plasma membraan afbakent dat overeenstemt met de delingszone in plantencellen.

In het algemeen associëren kinesines met kinesine lichte ketens, kinesine geassocieerde proteïnen, regulatorische proteïnen en andere, welke de activiteit en interactie met de te transporteren vracht controleren. In twee-hybride testen waarbij het trehalose-6-fosfaat syntase AtTPS1 gebruikt werd als aas, werd KCA1 geïdentificeerd (**hoofdstuk 5**). AtTPS1 katalyseert de eerste stap van trehalosevorming uitgaande van UDP-glucose en is betrokken in de regulatie van het suiker metabolisme. Planten produceren kleine hoeveelheden trehalose (Vogel et al., 2001), en dus speelt AtTPS1 waarschijnlijk eerder een regulatorische rol. Inderdaad, de uitschakeling van het AtTPS1 gen in Arabidopsis is lethaal voor het embryo. Dit demonstreert het belang van trehalose in de ontwikkeling van planten (Eastmond et al., 2002). AtTPS1 vormt een 600-800 kDa proteïne complex in gist extracten gescheiden via FPLC. In dit hoofdstuk werd bewijs gevonden voor een AtTPS1 complex in Arabidopsis, waarvan de componenten kunnen verschillen. Het Arabidopsis AtTPS1 co-migreerde met het celcyclus kinase CDKA;1 en tubuline. In twee-hybride experimenten interageerde AtTPS1 met CDKA;1 en het CDKA;1 interagerende proteïne KCA1. De N-terminale extensie van AtTPS1, dat de enzymatische activiteit controleert van AtTPS1, was verantwoordelijk voor de interactie met KCA1 en CDKA;1. AtTPS1 werd met CDKA;1 affiniteits korrels geprecipiteerd, wat duidt op zijn aanwezigheid in een proteïne complex dat tevens KCA1 en tubuline bevat. De resultaten van dit hoofdstuk verschaffen het eerste fysische verband tussen suiker metabolisme en controle over celdeling.

KCA1 interageert met AtTPS1 (hoofdstuk 5) en de katanine p60 onderdeel AtKSS, twee genen die essentieel zijn voor de ontwikkeling en morfologie van Arabidopsis. Om de functie van KCA in planten te bestuderen, werden planten geïdentificeerd welke een T-DNA insertie dragen in intron 10 van KCA1 en exon 1 van KCA2 (**hoofdstuk 6**). Moleculaire karakterisatie van de mutante allelen toonde aan dat KCA2 transcript afwezig was in de KCA2 mutante planten. Ondanks de T-DNA insertie in KCA1 mutanten, waren transcripten van volledige lengte en een korter fragment aanwezig. Via western blot analyse met een antilichaam dat geen onderscheid maakt tussen KCA1 en KCA2, werd aangetoond dat KCA proteïnen afwezig waren in de dubbele mutanten, maar niet in

Samenvatting

de enkelvoudige mutanten. KCA mutante planten werden fenotypisch gekarakteriseerd en vergeleken met planten die gemuteerd zijn in de genen die coderen voor de KCA1 interactiepartners. Processen die verband houden met celdeling en celexpansie waren niet verstoord in de *kca* mutanten onder de geteste condities. Het is mogelijk dat de T-DNA insertie in het KCA1 gen geen 'knock out' is en dat functioneel KCA1 proteïne nog steeds geproduceerd wordt. Het is tevens mogelijk dat andere kinesines of parallele mechanismen de activiteit van KCA overnemen. Mogelijks waren de fenotypes te subtiel en de groei condities niet geschikt om fenotypische abnormaliteiten aan het licht te brengen.

References

- Andersen SS** (2000) Spindle assembly and the art of regulating microtubule dynamics by MAPs and Stathmin/Op18. *Trends Cell Biol* **10**: 261-267
- Cassimeris L** (1999) Accessory protein regulation of microtubule dynamics throughout the cell cycle. *Curr Opin Cell Biol* **11**: 134-141
- Eastmond PJ, van Dijken AJH, Spielman M, Kerr A, Tissier AF, Dickinson HG, Jones JDG, Smeekens SC, Graham IA** (2002) Trehalose-6-phosphate synthase 1, which catalyses the first step in trehalose synthesis, is essential for Arabidopsis embryo maturation. *Plant Journal* **29**: 225-235
- Hemsley R, McCutcheon S, Doonan J, Lloyd C** (2001) P34(cdc2) kinase is associated with cortical microtubules from higher plant protoplasts. *FEBS Lett* **508**: 157-161
- Lawrence CJ, Morris NR, Meagher RB, Dawe RK** (2001) Dyneins have run their course in plant lineage. *Traffic* **2**: 362-363
- Menges M, Hennig L, Gruissem W, Murray JA** (2003) Genome-wide gene expression in an Arabidopsis cell suspension. *Plant Mol Biol* **53**: 423-442
- Smith LG** (1999) Divide and conquer: cytokinesis in plant cells. *Curr Opin Plant Biol* **2**: 447-453
- Stals H, Bauwens S, Traas J, Van Montagu M, Engler G, Inze D** (1997) Plant CDC2 is not only targeted to the pre-prophase band, but also co-localizes with the spindle, phragmoplast, and chromosomes. *FEBS Lett* **418**: 229-234
- Traas J, Bellini C, Nacry P, Kronenberger J, Bouchez D, Caboche M** (1995) Normal Differentiation Patterns in Plants Lacking Microtubular Preprophase Bands. *Nature* **375**: 676-677
- Vogel G, Fiehn O, Jean-Richard-dit-Bressel L, Boller T, Wiemken A, Aeschbacher RA, Wingler A** (2001) Trehalose metabolism in Arabidopsis: occurrence of trehalose and molecular cloning and characterization of trehalose-6-phosphate synthase homologues. *Journal of Experimental Botany* **52**: 1817-1826
- Weingartner M, Binarova P, Drykova D, Schweighofer A, David JP, Heberle-Bors E, Doonan J, Bogre L** (2001) Dynamic recruitment of Cdc2 to specific microtubule structures during mitosis. *Plant Cell* **13**: 1929-1943

Nawoord

De laatste kleine aanpassingen zijn gebeurd, het is 's ochtends vroeg en er rest me 'enkel' nog woorden van dank uit te spreken naar een hele hoop mensen toe die dit, op verschillende nivo's, mogelijk hebben gemaakt. Ik herinner me nog de dag dat ik, kakelvers afgestudeerd, met mijn diploma binnenstapte in het labo Genetica op de Ledeganckstraat (via mijn bijen-thesis had ik vernomen dat daar vooral onderzoek werd verricht op 'cucaracha's ☺) om te kijken of er daar ergens een plaats voor me was om een doctoraat te beginnen. Zo kwam ik bij **Danny Geelen** terecht. Jouw enthousiasme had me snel overtuigd en de daaropvolgende 4 jaar heb ik uren onder de confocale naar BY-2 cellekes gekeken (of keken zij naar mij?). Je stond steeds open voor nieuwe ideeën en vond altijd wel de tijd om deze kritisch en met kennis van zaken te bepreken. Bedankt om me doorheen dit werk te loodsen.

Ik wil ook graag **Dirk Inzé** bedanken om me de mogelijkheid te bieden in dit labo mijn onderzoek te kunnen starten. Dankzij deze kans heb ik de complexe en (soms on-)vatbare wereld van de wetenschap kunnen exploreren, in al haar aspecten. Ook mijn dank aan het IWT dat mijn onderzoek financieel mogelijk maakte.

De reis begon eerst in de Ledeganckstraat, op de vijfde verdieping. Mijn thesis startte daar in de microscopie groep met **Gilbert, Rosa, Riet, Janice, Ruth, Marleen B., Kris** en **Danny**. Na heel wat dynamiek is hieruit de cell biology groep ontstaan met **Daniel** (ik heb altijd genoten van onze kleine discussies, jammer dat we niet de kans hadden om wat meer samen te werken), **Silvie** (wat ik enorm waardaar is je enthousiasme waarmee je studenten begeleidt. Keep on doing that!) en **Kris**. You and (Professor) **Mansour** were two partners in crime, a dangerous combination in one room (especially in the setting of the Ledeganck). Anyway, you learned me all about making little explosives and I'm sure you enjoyed scaring me to death once and a while. **Bartel**, jouw specialisatie in RNA extractie breide zich wel eens uit van nematode spit naar 'cucaracha's. Het was steeds leuk een stille (alhoewel; Ramstein) venoot te hebben 's avonds en in het weekend. Dan was er natuurlijk ook mijn buurvrouwje **Eva**, die nu de plantjes vaarwel heeft gezegd om zebra visjes te bestuderen in Boston en sinds kort ook de ontwikkeling van de mens. **Manu**, ik heb je wat laat leren waarderen, maar ik weet nu dat er achter dat groot bakkes ne goeie gast zit.

Daarnaast waren er natuurlijk een heleboel mensen die steeds vol enthousiasme bereid waren een handje toe te steken. **Wilson**, you managed to make sequence analysis actually a fun part of research. Your smile and of course the Spanish radio cheered me up when sequences were not so nice. Thanks for all the help, you're a good friend. **Rebecca**, bedankt voor die honderden prepjes. Het zijn 'kleine' dingen zoals deze die zware periodes steeds een beetje lichter maakten. Ook iedereen die instaat voor het draaiende houden van het labo (**Jackie, Nancy, Ann, Jacques, Christine, Diane, Hilde, Nico...**), bedankt. **Martine** en **Karel**, zonder jullie zouden er geen papers zijn, high impact of niet. Merci! Ook **Nino** en **Blancheke** wil ik bedanken voor het in stand houden van exotische dialecten...

De gezelligheid (eufimisme voor het wereldrecord materiaal proppen in een gang) van de Ledeganck nodigde wekelijks uit tot een feestje. Vaste afspraak, vrijdagavond in het Petunia kot. Discolichtjes, kleuren plakband, een oude stereo keten, pintjes en de attributen van Jan's bureau waren vaste ingrediënten voor weer een avondje lol op het labo. Vaste 'tooghangers' waren **Zetje, Michiel** (& **Suzanne** later), **Griet, Ward** en **Wivel**. Jan en Michiel, ik mis jullie allebei hoor, maar ik denk dat we elkaar gaan blijven zien en dat het steeds weer even leuk zal zijn. Griet, je bent er ook bijna. Het zal wel hard werken worden, maar ik ben er zeker van dat je het schitterend zal doen. **Vince**, your famous laugh and English ('raiver') were contagious and I hope to enjoy it again this summer in Argenton. De Bio-informatici vrienden **Jeroen** (je bambi ogen en continue smile blijven in het geheugen gegrift) en **Stephane** (California here we come!) brachten het dry-lab een beetje dichterbij.

Door de jaren heen is er heel wat veranderd, veel mensen zijn weggegaan en nieuwe zijn gekomen. De verhuis naar Zwijnaarde (ondertussen wereldberoemd als 'Pig-earth', de officiële e-mail signature met 'Ghent' heeft dit niet kunnen verhinderen...) leek eerst een beetje het sociaal contact te bekoelen, maar we bleven werken aan een terugbeweging. **Ryan**, I'm very happy to have met you. You have become not only a great colleague, but also a great friend. I look very much forward to explore Australia together with you and Willem and of course to surf on those great waves you always tell us about. **Delphine**, we only really met last autumn, but since then many things have happened. I know you went through a hard time, but you did well and I am really happy that things are better (great) for you now. Een dikke knipoog naar de Plant Microbes, die er altijd waren met een luisterend oor, sciencewise of niet. **Juperke**, you and your lovely wife **Sofie** brought salsa in our lives. I really hope you can continue working on that fantastic project in our lab. **Paul** was always there to provide us with shocking e-mails. I heard you're having a good time in London, but don't miss out on your plans to go to Sydney. **Tom**, jij bracht Holland terug in het labo. Bedankt voor de vele schouderklopjes tijdens de lange uren in de bib. Ook in onze groep veranderde de samenstelling. **Evelien**, bedankt om zo door te zetten met het KCA werk. Ook al stond ik niet steeds open voor discussie deze laatste maanden, ik waardeer je doorzettingsvermogen enorm. **Bertje** (Bibber), mijn favoriete thesis studentje, je slaagde erin je weg te vinden in mijn chaotisch begeleiding. Je hebt dat goed gedaan, but don't spell the word PNAS anymore when you're drunk... Sinds Zwijnaarde deelden we ons lab met de '**Roots**'. Het was altijd gezellig met jullie erbij en **Ives**, keep on wearing those white socks, I adore them!

De laatste maanden is de PSB bib mijn vaste stek geworden. Mits wat eigen decoratie en stapels artikels ben ik erin geslaagd een van de bureautjes te kolonialisieren. Bedankt aan iedereen die af eens langskwam om te checken of het wel ging of me wegsleurde voor een kopje thee. **Hendrik**, duizend maal dank om mij steeds uit de nood te redden wanneer mijn labtopke weer eens zijn kuren had. **Mo**, ik vond het heel geestig dat jij hier ook regelmatig zat. Onze kleine gesprekjes doorbraken 's avonds de lange uren.

Aan mijn tijd in Gent als doctoraatstudent zijn eerst heel wat wilde jaren vooraf gegaan. **Katleen**, die tijden dat we Limburg, Italië, Zwitserland en Frankrijk afschuimden, op zoek naar avontuur zijn onvergetelijk. We hebben elkaar een beetje uit het oog verloren later, en ik vind het fantastisch dat we elkaar weer tegengekomen zijn, al waren de omstandigheden niet altijd de beste. We spreken binnenkort weer af. In Diepenbeek werkte ik mijn kandidaturen Biologie af. Ik denk dan vooral terug aan al mijn vrienden in kot Miezerik en kot Bère en dan vooral aan **Kerlijne, JP** en **Katrien**, de realiteit bleek ver, ver weg en dat was heerlijk. Ook in de studentenvereniging heb ik snel mijn weg gevonden. **Totter, Pirre, Sara, Sigrid** en **Annick**, jullie hebben van mijn Diepenbeek jaren een feest gemaakt (afgezien van die examenperiodes tijdens de welke ik wel eens van de aardbol leek verdwenen). Annick en Sigrid, jullie zijn twee prachtvriendinnen. Ik weet dat ik jullie veel te weinig heb opgezocht de laatste tijd. Jullie vriendschap is onvoorwaardelijk en betekent erg veel voor me. Binnenkort, als dit hier voorbij is gaan we ne keer goe profiteren.

Na twee jaar Diepenbeek kwam Gent. Na de lesuren werd er vast afgesproken in de Sala, waar Rita steeds weer met evenveel plezier de pintjes tapt. Met **Patje, Katrien, Seppe, Dries, Jordi**, en **Ivan** heb ik veel toogverhalen gedeeld. Patje, you're one of the good guys! Ik ben blij dat we elkaar nog regelmatig tegenkomen. **Ivan** en **Sas**, binnenkort gaan jullie trouwen en met deze wens ik jullie alle geluk toe! Ook buiten het unief heb ik mensen ontmoet. **Steven** en **Thierry**, jullie zijn twee echte vrienden geworden van me. Ik waardeer enorm het goede evenwicht tussen spelen en ernst bij jullie. Steven, binnen een dik half jaar is't aan u! Nymfette of niet, ik sta 100% achter je. **Eli, Tom en Lea**, het was zalig om bij jullie in Waregem te komen relaxen na een lange werkdag, laat de zomer maar komen! **Matthias** en **Janniek**, bedankt voor de vriendschappelijke warmte.

Mama en **papa**, jullie zijn twee fantastische ouders. Bedankt om me doorheen al die jaren te steunen en in me blijven te geloven. Een groot deel van deze thesis is dankzij jullie tot stand gekomen en dat besef ik heel goed. **Filip**, na alle kuren tijdens onze kinderjaren zijn we goeie vriendjes geworden. Je bent mijn grote broer en ik zie je heel graag.

En dan mijn **schattie**. Hoe moet ik nu zeggen wat er allemaal door me heen gaat? Je bent mijn liefje, mijn soulmaatje, mijn reisvriendje en zoveel meer. Binnenkort gaan we samen de wereld verkennen en ik voel gewoon dat het goed zit.

Ik denk dat ik het echte einde bereikt heb...

Bedankt iedereen en een dikke kus,

Marleen(tje)

Curriculum vitae

Marleen Vanstraelen
Department of Plant Systems Biology (VIB)
Laboratory of Molecular Genetics (Ugent)
Ghent University
Technologiepark 927
B-9052 Ghent
Belgium
Tel: +32 9 331 39 34
Fax: +32 9 331 38 09
E-mail: mastr@psb.ugent.be
www.psb.ugent.be

UNDERGRADUATE STUDIES

01.10.1997 – 05.07.2000

Master in Biological Sciences
obtained on the 5th of July 2000 with great distinction
Ghent University, Belgium

Undergraduate Thesis:

'The use of biochemical and biotechnological detection techniques for the development of *Melissococcus plutonius* diagnose in the honey bee (*Apis mellifera*).'

Promotor: Prof. Dr. F. Jacobs

Department of Biochemistry, Physiology and Microbiology,
Ghent University, Belgium

POSTGRADUATE STUDIES

01.10.2000 – 27.05.2005

PhD in Biotechnology, Department of Plant Systems Biology (VIB), Laboratory of Molecular Genetics, University of Ghent, Belgium

Promotor: Dir. Prof. D. Inzé and Co-Promotor: Dr. D. Geelen

Title of the thesis; 'Walking with plant specific kinesins during cell division'

PROFESSIONAL EXPERIENCE

01.10.2000-30.09.2004

Predocorial fellowship from the IWT (Vlaams Instituut voor de bevordering van het Wetenschappelijk-Technologisch Onderzoek in de Industrie) at the Department of Plant Systems Biology (VIB)/ Laboratory of Molecular Genetics (Ugent), Ghent University, Belgium (Dir. Prof. D. Inzé)

01.10.2004-31.03.2005

Full-time scientific collaborator at the Department of Plant Systems Biology (VIB)/ Laboratory of Molecular Genetics, Ghent University, Belgium (Dir. Prof. D. Inzé)

FELLOWSHIPS

01.10.2000 – 30.09.2004 IWT fellowship, Flemish Government
Title project: 'Walking with plant specific kinesins during cell division'
Department of Plant Systems Biology (VIB)/Laboratory of Molecular Genetics (Ugent), Ghent University, Belgium (Dir. Prof. D. Inzé)

EDUCATIONAL CONTRIBUTIONS

Supervision of students during the preparation of an undergraduate thesis

Helene Mertens, student at the Erasmus Hoger School, Brussels, Belgium. (Academic year 2001-2002): 'Expression of GFP-fusion proteins in transformed BY-2 calli'

Brecht Yserbit, master in Biotechnology, University of Ghent, Belgium. (Academic year 2002-2003): 'The BY-2 tobacco cell suspension culture as a model system to study cell division and for mathematical analysis of nuclear and cell size'

Bert Devriendt, master in Biotechnology, University of Ghent, Belgium. (Academic year 2003-2004): 'Molecular characterization of plant specific motor proteins: the Arabidopsis kinesins KCA1 and KCA2'

Supervision of students during practical courses

Practical courses Genetics, Licentiate Biology and Biotechnology (Prof. Dr. A. Depicker, Ghent University), Academic years 2000-2001; 2001-2002; 2002-2003; 2003-2005

ABSTRACT AND POSTER PRESENTATION AT INTERNATIONAL MEETINGS

XIII International Conference on Arabidopsis Research, Sevilla, Spain. June 28- July 2, 2002.
'CDKA;1 interacting motor proteins implicated in cell division'

Vanstraelen M, Torres Acosta J-A, De Veylder L, Inzé D, and Geelen D

Plant and Fungal Cytoskeleton, Gordon Research Conference, Andover New Hampshire. US. August 11-16, 2002.

'Localization and functional analysis of a collection of mitotic genes implicated in cell plate positioning and cytokinesis'

Geelen D, Van Damme D, **Vanstraelen M**, Bouget F-Y, and Inzé D

XIV International Conference on Arabidopsis Research, Madison Wisconsin, US. June 20-24, 2003.

'GFP-fluorescence profiling of plant cell division related proteins'

Geelen D, Van Damme D, **Vanstraelen M**, Coutuer S, Bouget F-Y, and Inzé D

Membrane trafficking in plants, SEB Congress (Society for Experimental Biology), Glasgow, UK. August 23-26, 2003.

'The kinesin KCA1 is associated with the vesicle traffic machinery and is involved in cytokinesis'

Vanstraelen M, Inzé D, and Geelen D

Gordon Research Conference on Plant and Fungal Cytoskeleton, Andover, New Hampshire, US. August 15-20, 2004.

'A plant-specific subclass of C-terminal, phragmoplast localized kinesins contains a conserved A-type cyclin-dependent kinase site implicated in folding and dimerization'

Vanstraelen M, Torres Acosta J-A, De Veylder L, Inzé D, and Geelen D

International workshop; Cell and Molecular Biology of Tobacco BY-2 cells, Yokohama, Japan. September 14-16, 2004

'Molecular dissection of plant cytokinesis and phragmoplast structure'

Geelen D, Van Damme D, **Vanstraelen M**, Coutuer S, Van Poucke K, Bouget FY and Inzé D

ABSTRACT AND POSTER PRESENTATION AT NATIONAL MEETINGS

VIB Congress, Blankenberge, Belgium. March 14-15, 2002.

'Two Arabidopsis kinesin motor proteins implicated in cell division'

Vanstraelen M, Torres Acosta J-A, De Veylder L, Inzé D, and Geelen D

VIB Congress, Blankenberge, Belgium. March 13-14, 2003.

'The kinesin KCA1 associates with the vesicle traffic machinery and is involved in cytokinesis'

Vanstraelen M, Inzé D, and Geelen D

PUBLICATIONS

Vanstraelen M, Torres Acosta J-A, De Veylder L, Inzé D, Geelen D (2004). A plant-specific subclass of C-terminal kinesins contains a conserved a-type cyclin-dependent kinase site implicated in folding and dimerization. *Plant Physiology*, 135(3):1417-1429

Vanstraelen M, De Rycke R, Inzé D, and Geelen D. A plasma membrane domain defines the division site in plant cells. Manuscript in preparation.

Vanstraelen M, Inzé D, and Geelen D. Mitotic kinesins in Arabidopsis. Manuscript in preparation.

Geelen D, Royackers K, **Vanstraelen M**, De Bus M, Inzé D, Van Dijck P, Thevelein J-M and Leyman, B. Arabidopsis trehalose-6-P synthase *AtTPS1* forms a high molecular weight protein complex, together with cell cycle proteins CDKA;1 and the kinesin KCA1. Manuscript in preparation.

